The role of climate legacies in shaping extinction risk throughout Earth's history

DISSERTATION

zur Erlangung des akademischen Grades eines
Doktors der Naturwissenschaften (Dr. rer. nat.)
an der Fakultät für Biologie, Chemie und Geowissenschaften
der Universität Bayreuth

vorgelegt von

Gregor Mathes
aus *Erlangen*
Bayreuth, 2022

Die vorliegende Arbeit wurde in der Zeit von Oktober 2019 bis September 2022 in Bayreuth am Lehrstuhl Sportökologie unter Betreuung von Herrn Professor Dr. Manuel Steinbauer angefertigt.

Vollständiger Abdruck der von der Fakultät für Biologie, Chemie und Geowissenschaften der Universität Bayreuth genehmigten Dissertation zur Erlangung des akademischen Grades eines Doktors der Naturwissenschaften (Dr. rer. nat.).

Dissertation eingereicht am: 31.08.2022

Zulassung durch die Promotionskommission: 21.09.2022

Wissenschaftliches Kolloquium: 02.02.2023

Amtierender Dekan: Prof. Dr. Benedikt Westermann

Prüfungsausschuss:

Prof. Dr. Manuel Steinbauer (Gutachter)
Prof. Dr. Axel Munnecke (Gutachter)
Prof. Dr. Bettina Engelbrecht (Vorsitz)
JProf. Dr. Lisa Hülsmann

Table of Content

1. Summary

1.1 Graphical abstract

1.2 German summary

Die heutige Biodiversität ist durch den menschengemachten Klimawandel stark gefährdet. Eines der Kernziele der ökologischen Forschung zum Schutz der Biodiversität ist es daher, das zugrundeliegende Verständnis der Prozesse zu verbessern, die zum Artensterben führen können. Das Vorhandensein von non-linearen Dynamiken, multiplen Gleichgewichten, Schwellenwerten und internen Rückkopplungen in ökologischen und klimatischen Systemen erschwert jedoch oft ein mechanistisches Verständnis.

Eines dieser grundlegenden Probleme für Studien die sich mit Aussterbeereignissen und Klimawandel beschäftigen ist, dass aktuelle Ereignisse immer von vergangenen Bedingungen abhängen. In der Ökologie wird diese Abhängigkeit von aktuellen Biodiversitätsdynamik vom vergangenen Klima allgemein als „Climate Legacy“, respektive Klimavermächtnisse, bezeichnet. Diese Klimavermächtnisse können aus einer Vielzahl von ökologischen Prozessen entstehen. Als Folge der dynamischen Natur ökologischer Muster und Prozesse kann außerdem davon ausgegangen werden, dass Klimavermächtnisse in allen Ökosystemen vorhanden sind. Wenn sie nicht berücksichtigt werden, können Klimavermächtnisse die Messung und Quantifizierung echter ökologischer Reaktionen auf den Klimawandel behindern oder sogar verhindern. Allerdings beziehen nur wenige Studien, die sich mit Aussterbeereignissen und Klimawandel beschäftigen, diese Klimavermächtnisse mit ein. Noch weniger Studien gehen über die bloße Diskussion möglicher Auswirkungen von Klimavermächtnissen hinaus und beziehen sie in ihren empirischen Rahmen ein. Diejenigen Studien, in denen Klimavermächtnisse einbezogen und quantifiziert wurden, fanden einen großen Einfluss dieser Klimavermächtnissen auf Aussterbeereignisse.

In dieser Dissertation stelle ich einen methodischen Rahmen für die Quantifizierung von Effekten vor, die sich aus Klimavermächtnissen in biotischen Systemen jeder zeitlichen Größenordnung ergeben. Ich führe zunächst das Konzept der “Climate Interactions”, respektive Klimawechselwirkungen ein, die die potenzielle Abhängigkeit des Aussterberisikos vom vorhergenden klimatischen Kontext beschreiben und quantifizieren. Klimawechselwirkungen entstehen aus Klimavermächtnissen, die über Tage bis Millionen von Jahren wirken, und könnten ein charakteristisches Muster in Aussterbeereignissen erzeugen. Sie bieten daher einen einheitlichen Rahmen für die Untersuchung der Folgen von Klimavermächtnissen in Ökosystemen. Das erwartete charakteristische Muster besteht aus einem höheren Aussterberisiko, wenn klimatische Veränderungen vorangegangene Trends verstärken (z. B. wenn ein Temperaturanstieg das Klima vorangegangener Erwärmungen weiter erwärmt). Es wird die Hypothese aufgestellt, dass diese synergistischen Klimawechselwirkungen zunächst zu Umweltbedingungen führen, die sich zunehmend von anfänglichen Anpassungen von Arten unterscheiden, was dann zu einem höheren Aussterberisiko für diese Arten führt. Eine antagonistische Klimawechselwirkung, bei der ein kurzfristiger Klimawandel einen früheren langfristigen Trend umkehrt (z. B. wenn auf eine lange andauernde Erwärmung eine kurzzeitige Eiszeit folgt), könnte zu einem allgemein geringeren Aussterberisiko führen, da klimatische Bedingungen dann mehr den bevorzugten klimatischen Bedingungen der untersuchten Arten entsprechen.

Dieser vorgeschlagene methodische Rahmen der Klimawechselwirkungen wird im Folgenden auf eine Vielzahl von marinen und terrestrischen Ökosystemen angewendet, wobei ich insbesondere die Entstehung der erwarteten Muster teste. Da klimabedingte Aussterbeereignisse in heutigen Ökosystemen selten sind, verwende ich hierzu die Informationen über vergangene Reaktionen von Organismen auf Klimaveränderungen, die Fossilien bereitstellen. Vier Manuskripte dieser Dissertation testen die mithilfe der Klimawechselwirkungen entwickelte Hypothese und liefern Evidenzen für die erwarteten Auswirkungen bei Aussterbe- und Evolutionsereignissen während des Phanerozoikums, bei Migrationsdynamiken während des Quartärs, und bei Vegetationsdynamiken während des Holozäns. Ein weiteres Manuskript liefert dringend benötigte Klimadaten für das katastrophalste Massensterben in der Erdgeschichte, und ein anderes Manuskript diskutiert im Zuge der Klimawechselwirkungen, wie man Rückschlüsse auf zeitgenössische ökologische Dynamiken mit paläoökologischen Perspektiven in einem transdisziplinären Rahmen kombinieren kann.

Die sechs Manuskripte dieser Dissertation liefern daher methodologische, empirische und theoretische Beiträge, die darauf abzielen, das mechanistische Verständnis von Klimavermächtnissen und den resultierenden Mustern im Laufe der Erdgeschichte zu verbessern, insbesondere durch die Anwendung des Konzeptes der Klimawechselwirkungen. Basierend auf den Ergebnissen wird eine synergistische Klimawechselwirkung, definiert als klimatische Veränderung welche vorangegangene Trends verstärkt, negative Auswirkungen auf die Artenvielfalt haben. Der aktuelle monotone Erwärmungstrend des menschengemachten Klimawandels erhöht die Wahrscheinlichkeit des Auftretens synergistischer Klimawechselwirkungen mit potenziell schwerwiegenden Auswirkungen auf die Biodiversität in der Zukunft. Die Zusammenführung der Ergebnisse der einzelnen Forschungsprojekte dieser Arbeit mit ihren Erkenntnissen über biotische Reaktionen auf Klimaänderungen ermöglicht ein verbessertes Verständnis der Auswirkungen des zukünftigen menschengemachten Klimawandels auf die Biosphäre.

1.3 English summary

Biodiversity is critically endangered by anthropogenic climate change. One of the core goals of ecological research and conservation science is therefore to enhance the mechanistic understanding of the processes that cause species to go extinct, particularly in light of anthropogenic climate change. However, the presence of non-linearities, multiple equilibria, thresholds, and internal feedbacks within ecological and climatic systems often impedes a mechanistic comprehension.

One fundamental issue for extinction studies using contemporary data is that this data is always dependent on past conditions. Within ecology, the dependence of contemporary biodiversity dynamics on past climate is generally termed “climate legacy”. Climate legacies can arise from a multitude of ecological processes, such as time lags, niche conservatism, physiological thresholds, or cascading effects. Further, climate legacies can be assumed to be present in all ecological systems as a consequence of the dynamic nature of ecological patterns and processes. If not accounted for, climate legacies can hinder or even prevent the detection of true ecological responses to climate change. However, few studies on the relationship between extinction dynamics and climate include these climate legacies. Even less studies reach beyond merely discussing potential impacts of climate legacies and include them in their empirical framework. Those studies where climate legacies were included and quantified found a large impact of these legacy effects on extinction dynamics.

In this thesis, I introduce a methodical framework for the quantification of effects arising from climate legacies in biotic systems of any temporal scale. I first introduce the concept of climate interactions, which describe and quantify the potential dependence of extinction risk on the long-term climatic context. Climate interactions might create a characteristic pattern in extinction dynamics and can arise from climate legacies acting over days to millions of years. They therefore provide a unifying framework for studying the consequences of climate legacies in ecosystems. The expected characteristic pattern consists of higher extinction risk, or related measures, when climatic changes add to previous trends in the same direction (such as a short-term warming adding to a long-term warming trend). It is hypothesised that these synergistic climate interactions first lead to environmental conditions increasingly different from initial adaptations of taxa, which then result in a higher extinction risk for these taxa. An antagonistic climate interaction, where a short-term climate change reverses a previous long-term trend (such as short-term cooling adding to a long-term warming trend), might result in a generally lower extinction risk through climatic conditions being more similar to initial adaptations of taxa.

This methodical framework of climate interaction is then applied to a variety of ecosystems, both marine and terrestrial, where I test the emergence of expected patterns. As climate-induced extinction events are rare in contemporary ecosystems, I take advantage of the fossil record with its rich information of past responses of organisms to climatic changes. Four manuscripts of this thesis test the hypothesis developed under climate interactions, and provide evidence for the expected effect in extinction and origination events throughout the Phanerozoic, in migration dynamics throughout the Quaternary, and in compositional turnover of plant assemblages throughout the Holocene. One additional manuscript provides crucially needed climatic data for the most catastrophic mass extinction event in Earth’s history, and another manuscript discusses how to combine inferences about contemporary ecological dynamics with palaeoecological perspectives in a transdisciplinary framework.

The six manuscripts of this thesis therefore provide methodological, empirical, and theoretical contributions that aim to enhance the mechanistic understanding of climate legacies and their emerging patterns throughout Earth's history, particularly through the application of the climate interaction framework. Based on the findings, a synergistic climate interaction, defined as a short-term climate change adding to a long-term trend in the same direction, will have more deleterious impacts on biodiversity. The current monotonic warming trend of anthropogenic climate change increases the occurrence probability of synergistic climate interactions, with potentially severe implications for biodiversity in the future. Bringing together the findings of the individual research projects of this thesis, with their insights about biotic responses to climatic changes, yields the chance to increase our ability to correctly assess the impact of future anthropogenic climate change on the biosphere.

2. Introduction

"Don't panic."

– Douglas Adams

2.1. Motivation

Biodiversity is critically endangered by current climate change (Pecl et al., 2017). The potential to predict the impact of future climate change on the biosphere is strongly dependent on our understanding of underlying mechanisms and interactions (Brook & Alroy, 2017; Kerr et al., 2007; Stigall, 2013). Enhancing our understanding of the mechanisms that drive taxa into extinction or extirpation is hence among the most fundamental objectives of ecological research and conservation science.

While there has been enormous progress in the general understanding of the current state of the climate (Masson-Delmotte et al., 2021), the presence of non-linearities, multiple equilibria, thresholds, and internal feedbacks often impedes a mechanistic comprehension. Similarly, the biosphere comprises a multitude of complex adaptive systems that display multiple alternating states and can shift from one to another in abrupt ways (Solé & Levin, 2022). Studying the intersection between the climate system and the biosphere is therefore a highly complex task but simultaneously offers the potential to provide insights into one of the most pressing questions of the 21st Century: How can we mitigate the impact of anthropogenic climate change?

2.2. Structure of this thesis

My thesis starts with examining general patterns of extinction dynamics arising from climate change throughout Earth's history. It subsequently introduces the concept of climate legacy, a process that might explain how extinction patterns emerge from climate change. Ecological mechanisms through which climate legacies can act are thereafter shortly summarised. This is followed by a comprehensive meta-analysis, aiming to answer (i) how many studies covering extinction and climate change have incorporated or discussed climate legacies and (ii) what the effect of climate legacies on extinction risk was when included in the focal study. Based on the results of this meta-analysis, I identify gaps in the literature and I develop a novel research hypothesis extending the concept of climate legacy. The findings of the six manuscripts of this thesis, which test and extend the above mentioned hypothesis, are then shortly summarised and my contribution to them is clarified. Lastly, I provide an outlook on how these findings might be used to mitigate the effects of a changing climate on the biosphere in the future.

I have included citations from Douglas Adams in this thesis, as it is my belief that science is best served with dry humour. His book on a variety of endangered species ("*Last Chance To See"*) sparked my interest in conservation science when I was a teenager, and his writing, particularly on the intersection of evolution and computer science, still provides me with inspiration for my scientific endeavours to this day.

2.3. The role of temperature in extinction dynamics

> **“There is a theory which states that if ever anyone discovers exactly what the Universe is for and why it is here, it will instantly disappear and be replaced by something even more bizarre and inexplicable.**
> **There is another theory which states that this has already happened.”**
> *– Douglas Adams*

Anthropogenic climate change has already caused substantial damages in terrestrial, freshwater, and marine ecosystems (Pörtner et al., 2022). Reliable assessments of extinction risk arising from climate change are thus crucial for the effective protection of the biosphere (Mathes, van Dijk, et al., 2021; Pecl et al., 2017). While a wave of extinctions is predicted for the near future (Urban, 2015), only few global species extinctions are thought to have been caused by anthropogenic climate change (Cahill et al., 2013; IUCN, 2022). The low amount of recent extinctions attributable to climate change renders it difficult to study the relationship between climate and extinction dynamics. However, the rich information on past biotic responses to climate change provided by the fossil record can fill this crucial information gap (Calosi et al., 2019; Finnegan et al., 2015; Harnik, Lotze, et al., 2012). Palaeontological records, together with palaeoclimatic data, comprise the potential to understand how the biosphere has responded to past climate changes, as well as to quantify the adaptive capacity and vulnerability of ecosystems (Pörtner et al., 2022).

Palaeontologically informed models have demonstrated a strong link between temperature stress and extinction risk (Bond & Grasby, 2017; Penn et al., 2018; Reddin et al., 2022). The extinction risk in fossil taxa increases with distance from the climatic conditions they are adapted to (Beaugrand, 2015; Lord et al., 2017; Wiens & Graham, 2005), indicating that extinction risk is dependent on both the rate and magnitude of climate change. Studies on the fossil record also deepened our understanding of intrinsic thresholds of the biosphere: Mass extinctions, events with an extinction rate significantly above the background rate, occurred when the magnitude of temperature change exceeded 5.2°C (Song et al., 2021).

Throughout Earth’s history, various events of abrupt climate warming occurred (Foster et al., 2018). These so-called hyperthermal events are characterised by rapid warming of >1°C, and may coincide with severe mass extinctions (Benton, 2018; Bond & Grasby, 2017). Particularly the rapid but long lasting climatic changes during the end of the Permian period (~ 252 million years ago, Ma) resulted in devastating biotic responses, with 81% of marine animal species and 70% of terrestrial tetrapod species going extinct (Stanley, 2016). Other examples include the rapid global warming at the end-Cretaceous period (~ 66 Ma), where around 75% of species were wiped out (Bond & Grasby, 2017). However, some hyperthermals did not result in profound extinctions, despite their high rate of warming. The Palaeocene-Eocene Thermal Maximum (~ 56 Ma), together with other hyperthermal events during the Quaternary, showed fewer extinction events as would be expected from the rate of warming during these times (Botkin et al., 2007; Foster et al., 2018). This incongruence in the relationship between climate change and extinction risk is noted as a big “conundrum” of modern science (Botkin et al., 2007). Solving this conundrum holds the potential to provide crucial information for conserving Earth’s biodiversity under anthropogenic climate change.

2.4. Climate legacies in biotic systems

> **“Time is an illusion. Lunchtime doubly so.”**
>
> *– Douglas Adams*

Data in environmental and (palaeo-)ecological studies typically consist of a sequence of observations collected over time (Bence, 1995). In these so-called time series, the value of an observation at time *t* is to some degree dependent on the value of the previous observation at *t-1*. This effect is termed “autocorrelation”, and treating the time series as observations would be independent (i.e. ignoring autocorrelation) can lead to severe misinterpretation of the data at hand (Hurlbert, 1984). One consequence arising from autocorrelation in time series is a moment of inertia: The effect of a parameter α on a dependant variable β at time *t* is influenced by the previous values of α (Figure 1). However, when studying the effect of climate change on the biosphere, this moment of inertia is often ignored, potentially leading to a misinterpretation of the apparent relationship (Mathes, van Dijk, et al., 2021; Ogle et al., 2015).

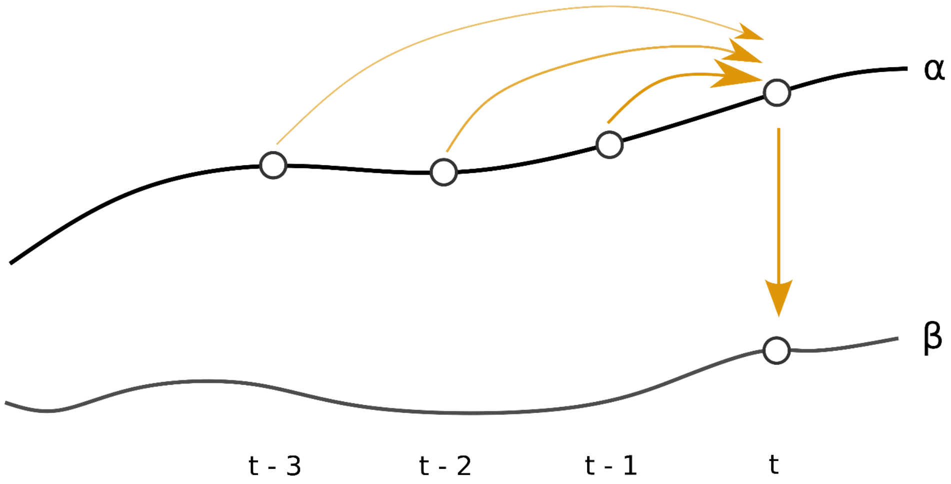

Figure 1: The effect of a parameter α on a dependent variable β at time t is influenced by the previous values of α through temporal autocorrelation. This effect is termed “climate legacy” when the effect of a climate parameter on an ecological dependent variable is measured.

Within ecology, the dependence of biodiversity patterns on climate dynamics and their autocorrelation is generally termed “climate legacy” (Svenning et al., 2015). While the theoretical mechanisms of these legacy effects in ecological and environmental studies are well known, only a few studies have incorporated them in their methodological framework until recently (Ogle et al., 2015; Svenning et al., 2015). This is particularly intriguing, as climate legacy can be assumed to be present in all ecological systems as a consequence of the ubiquitous autocorrelation in climatic and ecological systems and the dynamic nature of ecological patterns and processes (Chave, 2013). While the magnitude of these climate legacies might be strongly scale dependent, the general presence of climate legacies can arise from any length of time in the past (Svenning et al., 2015). Climate legacies can manifest through a multitude of ecological processes but the main mechanisms through which past climate can act on the biosphere and on the extinction risk of taxa within largely reflect four categories: (i) time lags, (ii) niche conservatism, (ii) physiological thresholds, and (iv) cascading effects. While cascading effects can occur on any temporal scale, it is likely that the remaining categories act on different timescales and durations (Svenning et al., 2015). While time lags and in particular migration lags are likely to dominate over timescales of hundred to a few thousand years, niche conservatism may be more important on coarser timescales covering millions of years. Physiological thresholds, on the contrary, may lead to severe climate legacies over seconds to years. Understanding these mechanisms and their complex interactions is crucial when studying the effect of climatic changes on ecosystems, particularly in light of the ongoing anthropogenic climate change and the predicted biodiversity crisis.

2.4.1. Time lags

Time lags comprise the amount of time between an extrinsic perturbation to a system and the return to a state of equilibrium (Hastings, 2004). In ecological systems, these time lags constitute a frequent phenomenon and can have severe ecological consequences (Svenning & Sandel, 2013). Extinction debt, the delay between extinction or extirpation of a species following habitat loss or degradation, is one prominent example of an ecological time lag (Kuussaari et al., 2009). Similarly, climate induced extinctions can lead to long-lasting legacy effects determining the susceptibility to climatic changes of the remaining species within an ecosystem (Calosi et al., 2019). Non-random species loss as a consequence of climate change hereby determines the ability of the remaining species to respond to future climate change. This has been exemplary shown for tree community dynamics (García‑Valdés et al., 2018) but is also well known from the fossil record (Svenning et al., 2015). In general, climate shows a strong selective pressure on functional traits (Wright et al., 2005), shaping the susceptibility of an assemblage to future climate change (Couvreur et al., 2015).

Ecosystem functioning in recent ecosystems is strongly driven by time lags as well. Past climate conditions can leave biophysical legacies, resulting in lagged effects into the future (Bunting et al., 2017). For example, wet and dry climatic regimes of the previous year determine the ecosystem dynamics of forests (Anderegg et al., 2013; Lenihan et al., 2003), grasslands (Kuneš et al., 2015), and shrubland ecosystems (Bunting et al., 2017). Precipitation and temperature patterns of past months, seasons, or years can also impact ecosystem productivity

(Coops et al., 2007; Leuning et al., 2005; Reichmann et al., 2013; Sala et al., 2012). Predictions for ecosystems under future climate change similarly show lagged dynamics (Chapin & Starfield, 1997; Normand et al., 2013; Svenning et al., 2015).

Species adapted to a particular climate niche can follow this niche as it shifts with climate change by migrating along the latitudinal temperature gradient. However, climate changes as fast as those of ice age cycles may cause migration lags (Stephens et al., 2019; Svenning & Skov, 2004), potentially resulting in extinctions (Normand et al., 2011). These migration lags are related to the migration capacity of species (Normand et al., 2011), but biotic interactions may also have a significant impact. (Dormann et al., 2018). Particularly priority effects, defined as the process that earlier arriving species have on establishment success of later arriving species (Chase, 2003), may significantly slow down or even prohibit the establishment of species in a suitable habitat on both ecological (Fukami, 2015) and geological time scales (Schueth et al., 2015). Through time lags, such priority effects consequently determine transient dynamics of ecological systems (Fukami & Nakajima, 2011).

Time lags are thought to have influenced patterns in species richness and composition of ecosystems. As known from the fossil record (Bond & Grasby, 2017; Mathes, Kiessling, et al., 2021; Penn et al., 2018), speciation and extinction rates may depend mechanistically on climate. Under the assumption of higher speciation and lower extinction rates in high-energy climates, past climate could have shaped the modern-day latitudinal diversity gradient (Mittelbach et al., 2007). Tree species richness within recent biomes is more correlated to environmental conditions of the past than to recent environmental conditions (Fine & Ree, 2006). Similarly, the recent species richness of the four major terrestrial vertebrate groups is best determined by past climate (Jetz & Fine, 2012). All this indicates that recent patterns of biodiversity contain a strong signal of the past, with time lags providing a mechanistic explanation on how these patterns emerged.

2.4.2. Niche conservatism

Niche conservatism, which is the relative stability of a lineage's niche during evolutionary change (Hopkins et al., 2014; Wiens & Graham, 2005), can generate long-lasting climate legacies in ecological systems (Mathes, van Dijk, et al., 2021; Svenning et al., 2015). In these ecological systems, a clear signature of evolutionary rescue (i.e. rapid evolutionary adaptations to climatic changes) is rare (Carlson et al., 2014). Fossil studies have similarly shown that the preference of taxa for a particular niche stays constant through time (Antell et al., 2021; Lieberman & Saupe, 2016). If taxa do not adapt to climate changes over evolutionary timescales, then these changes will successively move taxa out of their adaptation space (Mathes, van Dijk, et al., 2021). Taxa that have experienced climatic changes are consequently expected to show different susceptibility to new climatic changes compared to taxa that are in full equilibrium with their adaptation space.

Additionally, niche conservatism might generate climate legacies through phylogenetic clustering in novel climates (Hawkins et al., 2014; Miller et al., 2013). Under this hypothesis, niche conservatism determines the phylogenetic structure and composition of regional species pools, thereby impacting how these assemblages respond to future climatic changes. Niche conservatism and climatic lags arising from it might further explain recent patterns of biodiversity, such as the latitudinal diversity gradient. For example, many groups of organisms are globally widespread in tropical regions, but have not successfully invaded or radiated in temperate regions, potentially due to niche conservatism (Wiens & Donoghue, 2004). This tropical niche conservatism might have led to a disparity in species richness over time, and consequently a higher species richness in low latitudinal zones (Wiens & Donoghue, 2004; Wiens & Graham, 2005).

2.4.3. Physiological thresholds

Physiological mechanisms are thought to underlie differential ability of species to tolerate stress and differential extinction of species under climate change. This has been shown in various experimental settings as well as for extinction events in the fossil record (Reddin et al., 2020). The ability of taxa to respond to climatic changes is therefore dependent on their physiological tolerances of such changes (Calosi et al., 2019). Past climatic changes may have already impacted the fitness of individual taxa, shaping their tolerance to future climate changes. Crossing physiological thresholds is therefore more likely if previous climatic changes have impacted taxa negatively. These climate legacies arising from general physiological limitations are thought to act over finer temporal scales (Svenning et al., 2015) but can add up to be detectable in large scale fossil systems (Reddin et al., 2022). Interacting with time lags, they can hamper the identification of areas or groups most relevant for conservation efforts (Ogle et al., 2015).

Besides these endogenic physiological thresholds, climate legacies can be generated from exogenic processes affecting the limitations to performance. For example, legacies of land use history affect the representation of traits related to plant performance of peanut plants (Li et al., 2019) and past pollution still determines the performance of aquatic organisms years after (Johnson et al., 2013). Despite a limited understanding of mechanisms underpinning the tolerance of taxa to climate change as a function of physiology (Hofmann & Todgham, 2010; Somero, 2012), inferences from physiological limitations and their interactions with climate legacies will likely increase the capacity to identify sensitive and tolerant taxa under anthropogenic climate change (Calosi et al., 2019).

2.4.4. Cascading effects

A fourth and less concrete mechanism that may generate climate legacies are cascading effects and tipping points (Beaugrand, 2015; Holling, 1973; Lord et al., 2017). The biosphere consists of complex adaptive systems that display multiple alternating states, which can shift from one to another in abrupt ways (Solé & Levin, 2022). Exceeding certain temperature thresholds under climate change might trigger unforeseen reinforcing processes that cause significant changes in the Earth system (Friedlingstein et al., 2001; Ren & Leslie, 2011). Crossing critical thresholds could hereby cause ecosystems to switch from one state to another

(Beaugrand, 2015; Rocha et al., 2015). Since effects differ between trophic levels (Thackeray et al., 2010), it is likely that even resilient species will be impacted by changes on other trophic levels. While identifying the exact mechanisms causing such changes is challenging, it is undisputed that past climate, and hence climate legacies, strongly influences whether or not ecosystems reach critical thresholds (Ogle et al., 2015). For example, if a period of warming adds to a previous period of warming, ecological systems are more likely to reach a trigger point for major system changes than if the warming just reverses a previous cooling (Mathes, van Dijk, et al., 2021).

2.5. Systematic review and meta-analysis of the published literature

> **“It can be very dangerous to see things from somebody else's point of view without the proper training.”**
>
> *– Douglas Adams*

2.5.1. Systematic review

I have conducted a systematic review of the published literature on extinction risk arising from climate legacies, aiming to answer (i) how many studies covering extinction and climate change have incorporated or discussed climate legacies and (ii) what the effect of climate legacies on extinction risk was when included in the focal study. For this, I searched for published studies on the 6th of April 2022 on Web of Science citation database (www.webofknowledge.com) and the Scopus (www.scopus.com) citation database with keywords as follows: “(TI=((‘extinct*’ OR ‘extirpat*’) AND (‘climate change’ OR ‘changing climate’ OR ‘temperature’))) AND DT=(Article)” for the Web of Science (288 results); “TITLE(("extinct*" OR "extirpat*") AND ("climate change" OR "changing climate" OR "temperature")) AND DOCTYPE(ar)” for Scopus (313 results). This corresponds to a literature search for studies which have either extinction or extirpation in combination with climate change in their title. I then used the R programming software (R Core Team, 2021) to find duplicate entries, using R version v.4.1.2. After removing duplicates, the data set contained 351 publications. All code and data can be accessed on github (https://github.com/Ischi94/lit_review_past_climate). I then manually checked the abstract of the remaining publications for relevance, i.e. whether the study covers the effect of climate changes on extinction risk of organisms or a related measure. 144 publications were removed in this step, resulting in 207 remaining publications. I then went through each of the 207 publications and recorded the following meta-data wherever possible: year of publication, biotic unit of the studied taxa (e.g. species, population, …), the kingdom of the studied taxa, the temporal scale of the climate change, the methodology used to assess the impact of climatic changes on taxa, whether climate legacies were included, whether these climate legacies where quantified, the assumed ecological mechanism of the climate legacy, the temporal scale of the climate legacy, and the effect size of the climate legacy.

2.5.2. Meta-analysis

Based on the data retrieved from the systematic review, I have conducted a meta-analysis using the R programming software and the tidyverse consortium of R packages (Wickham et al., 2019). Effect sizes of the focal climate legacy were transformed to the Cohen’s d effect size metric using common formulas in meta-analyses (Lipsey & Wilson, 2001), to present the magnitude of the reported effects in a standardised, scale-independent metric. I conducted the meta-analysis via partial pooling through a linear mixed effect model (Bolker et al., 2009), whereby studies were used as a random effect and the variance of each study was incorporated via a variance function structure. I further tested for a trend in the inclusion of climate legacies through time via a logistic regression. All code and data can be accessed on github (https://github.com/lschi94/lit_review_past_climate).

2.5.3. Results

Most studies covered either animals (137) or plants (56), with a few studies on fungi (2), protozoans (2), or chromista (2). The most common biotic unit was on species-level (118), followed by population (32) and genus (11), and a few studies with even higher resolution up to tribes (1) or individuals (1). Five studies were using simulated biotic units (meta-species or meta-populations). The temporal scale of the focal climate change hereby ranged from days to millions of years (Figure 2).

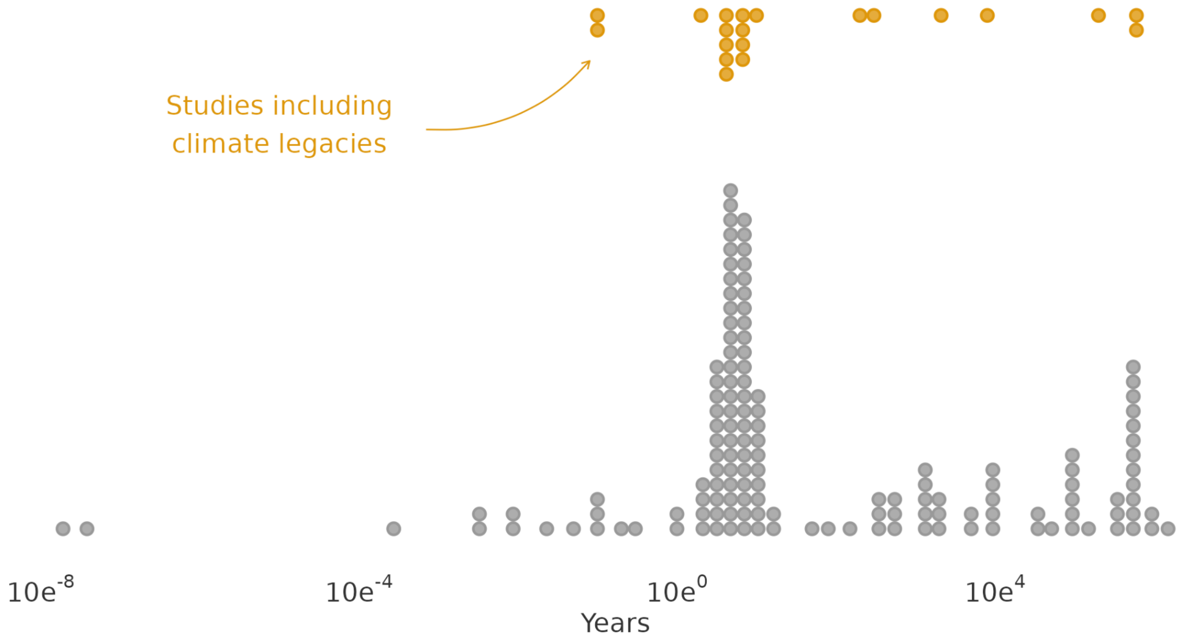

Figure 2: The temporal scale of each study of the systematic literature review on extinction risk and climate change. Studies that do not include climate legacies, neither in their methodological framework nor in their discussion, are shown in grey. Studies including climate legacies are shown in yellow.

Out of 193 studies, only 14 included climate legacies either in their methodological framework or discussed them in text (Figure 2). 7 of these 14 studies were quantifying the effect of the climate legacy measure on the extinction parameter, whereas the remaining 7 discussed the effect of climate legacies qualitatively. From the 7 studies quantifying the focal effect, 6 were reporting sufficient information to convert the effect size into the Cohen's d effect size metric and were subsequently used in the meta-analysis. There is a modest trend in the inclusion of climate legacies in studies covering extinction risk and climate change through time (Figure 3). With each year, the probability that a study is including climate legacies either in their methodological framework or in their discussion is growing, on average, by 2.3% (95% Confidence Interval (CI) [-3%, 10%]). Based on this, a randomly selected study from 1980, for example, would have a probability of including climate legacies of 5.2% (95% CI [0%, 16.6%]. Whereas a study that is going to be published next year, in 2023, would have a probability of 13% (95% CI [4.9%, 21%]) of including climate legacies, based on the estimated relationship. The general probability that a study would include climate legacies was therefore low but slightly growing with time.

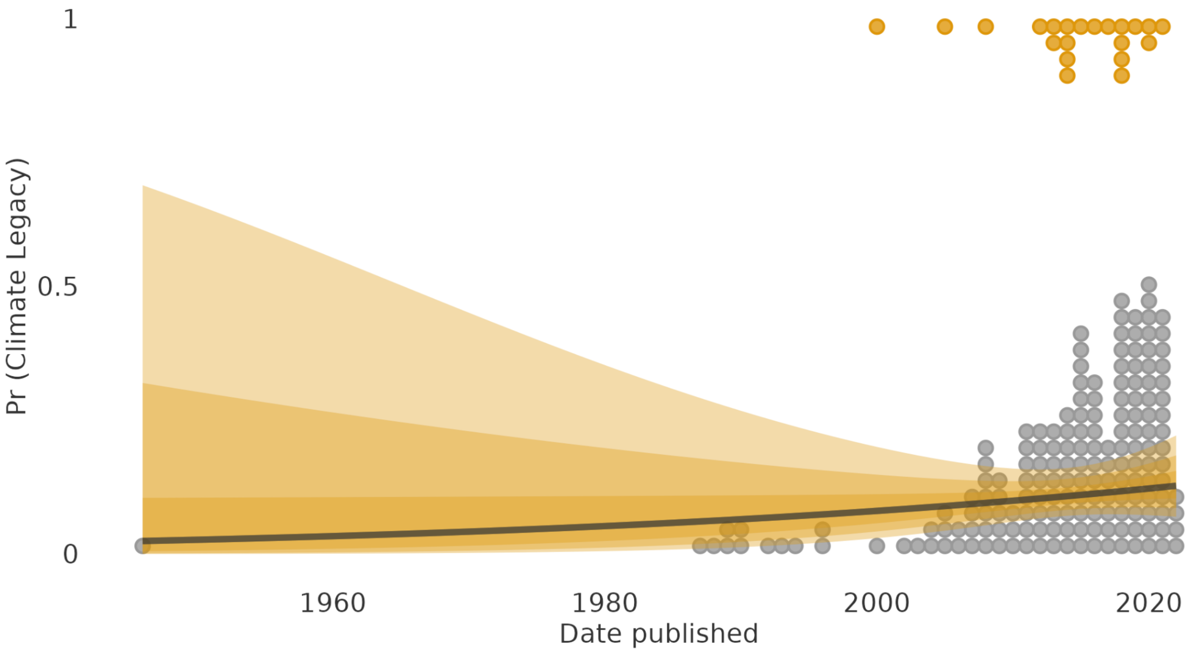

Figure 3: The temporal trend of the inclusion of climate legacies in studies on extinction risk and climate change. The y-axis shows the probability of climate legacies being included as a function of time. The trend was estimated by a logistic regression, whereby grey points indicate studies not including climate legacies, and yellow points indicate studies including climate legacies. The grey line shows the mean trend, with the yellow shaded areas depicting the 50%, 80%, and 95% confidence intervals around this trend.

The discussed mechanisms through which climate legacies could affect extinction risk were highly diverse. The most common mechanisms discussed were migration lags (Lunney et al., 2014; Sax et al., 2013; Wiens et al., 2019; Yalcin & Leroux, 2018). Other studies included time lags in their methodological framework but did not discuss the underlying ecological rationale for doing so (Mayhew et al., 2008; Saltré et al., 2016; Xenopoulos et al., 2005). Contrarily, Keith et al. (2014) discussed the presence of time lags in a variety of population metrics but did not include them in the methodological risk assessment.

Baseline conditions were the second most common mechanisms discussed, particularly how they shape susceptibility to climate change and how they serve as a potential trigger for cascading effects. Riquelme et al. (2020), for example, discussed a secular effect of long-term warming on the carrying capacities of populations. In a forest succession model, García-Valdés et al. (2018) showed how climate change-driven extinctions of tree species affect forest functioning more than random extinctions, with the remaining community being more susceptible to future climatic changes. Similarly, climatic induced removal of individuals in Ginseng populations was found to be associated with changes in reproductive rates and inbreeding, shaping population functioning (Souther & McGraw, 2014). Urban et al. (2012) found a cascading dynamic in the response of species to climate change, with competition creating range lags, and those range lags subsequently modifying the ability of the community to respond to further climatic changes. On a coarser temporal scale ranging from 21 thousand years to 2 million years, baseline climatic conditions were discussed to affect the ability of taxa to respond to environmental perturbations, such as during the Late Quaternary mammalian extinctions (Varela et al., 2015), the Cretaceous-Paleogene mass extinction (Zhang et al., 2018), or the end-Triassic mass extinction (Petryshyn et al., 2020).

Physiological thresholds were commonly discussed to create climate legacies. Sinervo et al. (2018) looked at pre-existing thermoregulatory adaptations to climate, whereas other physiological thresholds arising from initial adaptations to climate included juvenile recruitment (Butler et al., 2017), susceptibility to drought conditions (Pomara et al., 2014), reproductive success as a function of snow-free grounds in the previous year (Imperio et al., 2013), and growth and reproduction influenced by autocorrelated temperature (Griebeler & Gottschalk, 2000). A mechanism closely related to physiological thresholds, niche conservatism, was discussed as well (Mathes, van Dijk, et al., 2021).

Those six studies directly incorporating and quantifying climate legacies in their methodological framework found a large impact of the focal climate legacy on the extinction risk metric (Figure 4). The overall effect size, as estimated by the meta-analysis and expressed as Cohen’s d, was 1.02 (95% CI [0.49, 1.56]), and can be interpreted as large (Sawilowsky, 2009). The individual studies showed similarly large effect sizes, with their corresponding confidence intervals ranging from medium to very large effect sizes. I found this to be independent of the temporal scale the assessed climate legacy was covering, with studies showing large effect sizes from climate legacies covering years (Butler et al., 2017; Griebeler & Gottschalk, 2000; Imperio et al., 2013), thousands of years (Varela et al., 2015), or millions of years (Mathes, van Dijk, et al., 2021; Mayhew et al., 2008). The meta-analysis indicates that once climate legacies are methodically included in the study and quantified, large impacts of those legacies are found on extinction risk and its corresponding metrics. While it is possible and probable that positive and large effect sizes from climate legacy are more likely to be reported, the overall agreement of the studies and the comprehensiveness of the systematic literature review point towards a large relevance of climate legacies in extinction studies.

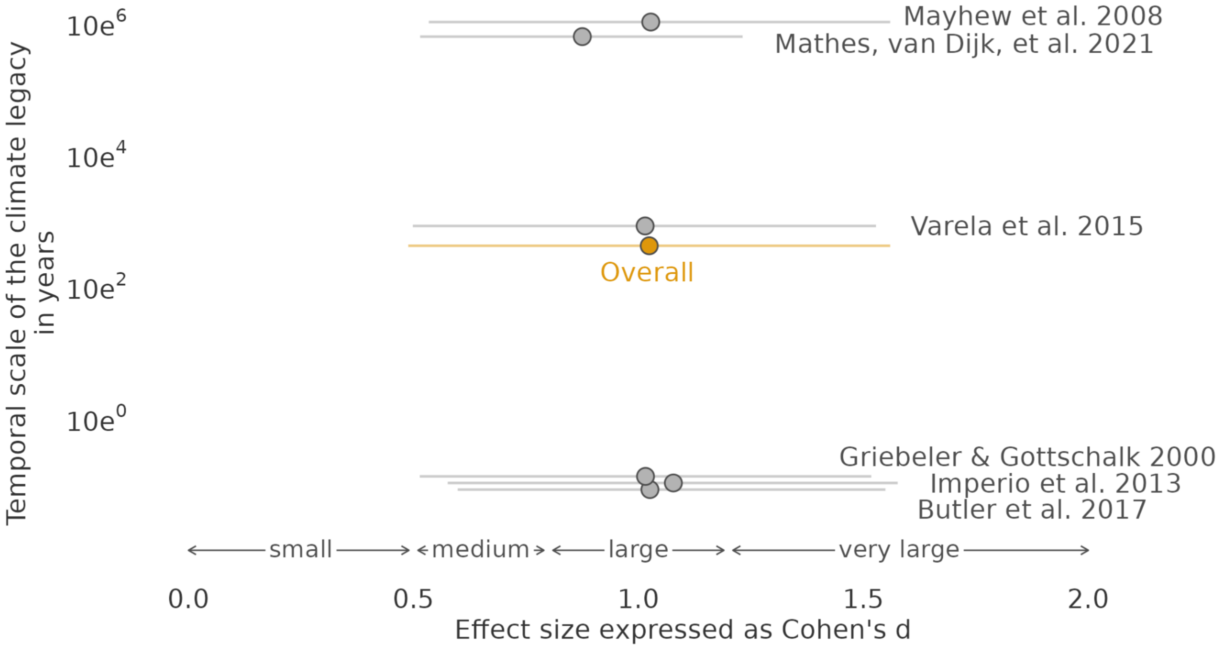

Figure 4: Results of the meta-analysis. The temporal scale of the focal climate legacy studied as a function of the absolute effect size of each individual study quantifying the impact of climate legacies on extinction dynamics. Points show the mean estimate per study and the lines the corresponding 95% confidence interval. The interpretation of the absolute Cohen's d effect sizes, ranging from small to very large, follows general recommendations (Sawilowsky, 2009). The yellow point and line indicates the overall effect size, averaged across studies through partial pooling.

2.6. Climate interactions as a unifying framework

> **“We demand rigidly defined areas of doubt and uncertainty!”**
>
> *– Douglas Adams*

2.6.1. Differential extinction risk resulting from long-term climate changes

As the systematic review and meta-analysis has shown, only a few studies on the relationship between extinction dynamics and climate included climate legacies (Figure 2 and 3), but those who did found large effect sizes (Figure 4). This estimated large effect size was present across a wide range of temporal scales and hypothesised mechanisms. Individually, these mechanisms are well-known and studied (Svenning et al., 2015) but a solid understanding of their interactions and feedbacks is currently lacking (Ogle et al., 2015). In light of anthropogenic climate change, analytical frameworks summarising the patterns arising from those interactions and feedbacks, while simultaneously quantifying the ecological consequences of climate legacies, are needed.

One crucial, yet largely unstudied, framework consists of climate interactions, which describe and quantify the potential dependence of extinction risk on the long-term climatic context (Mathes, van Dijk, et al., 2021). Climate interactions might create a characteristic pattern in extinction dynamics and can arise from any of the above mentioned climate legacies such as niche conservatism, time lags, physiological thresholds, or cascading effects. They therefore provide a unifying framework for studying the consequences of climate legacies in ecosystems. The expected characteristic pattern consists of higher extinction risk, or related measures, when climatic changes add to previous trends in the same direction (e.g. a short-term warming adding to a secular warming trend, Figure 5). These synergistic interactions might create environmental conditions increasingly different from previous adaptations of taxa, leading to a high extinction risk. On the contrary, climatic change might be less deleterious for species when added to a long-term temperature trend in the opposite direction (e.g. a short-term warming following a prolonged cooling trend, Figure 5). These antagonistic interactions might create environmental conditions more similar to initial adaptations of taxa, resulting in a generally lower extinction risk.

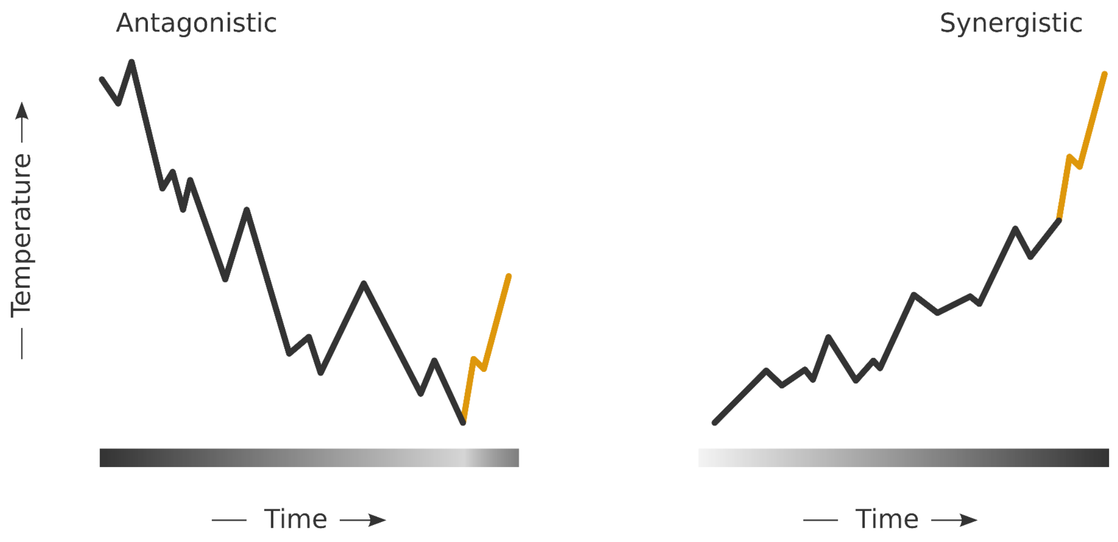

Figure 5: A similar temperature increase, illustrated in yellow, might have differential effects on biota, depending on if it follows after a period of long-term cooling (antagonistic interaction) or warming (synergistic interaction). Environmental conditions, illustrated by the grey bar, are more similar to initial conditions after antagonistic climate interactions, whereas environmental conditions are increasingly different from previous adaptations under synergistic climate interactions.

The differential extinction risk resulting from climate interactions can arise from at least four known mechanisms, potentially interacting with each other. Over very long timescales, such as millions of years, the relative stability of lineage's niches during evolutionary change (Hopkins et al., 2014; Wiens & Graham, 2005) might determine the response of taxa to climate change, depending on the preceding long-term climatic changes. If taxa show a strong preference for a particular climatic niche through time, then the probability that the adaptive evolutionary potential cannot keep up with the selective pressure imposed by synergistic climate interactions increases. On the contrary, environmental conditions might be more similar to the preferred climatic niche of taxa under antagonistic climate interaction, where a short-term temperature change cancels out the environmental changes of a previous long-term change. Some taxa might therefore be able to return to the centre of their initial adaptation under antagonistic climate interaction, but are potentially moved out of their adaptation space under synergistic climate interaction. There is growing evidence for these ecological consequences arising from niche conservatism - for example the past niche evolution of species has been shown to determine susceptibility to climate changes (Lavergne et al., 2013). Additionally, consequences of niche conservatism have been described over various temporal scales, ranging from months and decades (Peterson, 2011), through millenia (Antell et al., 2021), to millions of years (Hopkins et al., 2014; Stigall, 2014).

A differential response of taxa to climate changes, depending on the preceding long-term changes, might also arise from accumulated migration lags. The ability to keep pace with shifting habitats under climate change is a key determinant of extinction risk (Reddin et al., 2018). Migration lags can hereby occur from reduced migration capacity of species (Normand et al., 2011), biotic interactions (Dormann et al., 2018), a delayed ecological response (Ogle et al., 2015), or migration barriers (Dullinger et al., 2012). Under antagonistic climate interactions, species can overcome migration lags by persisting in climate refugia (Gavin et al., 2014). This has been prominently shown for range dynamics in response to cyclical warming and cooling of Quaternary ice age dynamics (Tzedakis et al., 2002). Contrarily, suitable climatic conditions will not return under synergistic climate interactions and climate refugia will therefore no longer facilitate survival. The current monotonic warming trend of anthropogenic climate change is one example for this (Keppel et al., 2012). Accumulated migration lags might hence lead to more severe extinction responses when a climate change follows a long-term trend in the same direction (synergistic interaction), compared to when the same climate change opposes the direction of the previous long-term trend (antagonistic interaction).

While migration lags are presumably most important over timescales of hundred to a few thousand years (Svenning et al., 2015), physiological thresholds might create differential extinction responses from climate interactions over seconds to years. It is more likely that lineages approach physiological limits under synergistic climate interactions, as monotonic climatic changes might create unsuitable environmental conditions. Once physiological thresholds are reached, escaping environmental pressure is only feasible through major innovations in the genepool (Merilä, 2012). These events, however, are rare (Carlson et al., 2014). Reaching physiological thresholds faster under synergistic climate interactions may therefore increase the extinction risk of taxa, in strong contrast to antagonistic interaction where preferred conditions are retained.

Significant cascading effects in biotic systems can be expected under synergistic climate interactions, as they lead to increasingly different environmental conditions compared to initial adaptations. These cascading effects can arise from all previously described ecological mechanisms, such as retained niche preferences, accumulated migration lags, or crossed physiological thresholds, as well as from interactions and feedbacks between these mechanisms. The quantitative assessment of ecological consequences from climate interactions is complicated by these interactions and feedbacks (Kinzig et al., 2006), but it is more important than ever given the potential harm to biodiversity and ecosystems (Murphy et al., 2020; Parmesan, 2006). A theoretical framework identifying the patterns and quantifying the consequences arising from climate interactions is therefore needed. Chapter 2.6.2. of this thesis is aiming to fill this research gap through the development and description of a novel methodological framework. The remaining chapters will then illustrate applications of this framework and will provide further implications of my findings.

2.6.2. Quantification of climate interactions

As climate interactions can arise from any of the above mentioned ecological mechanisms, acting over timescales ranging from seconds to millions of years (see Chapter 2.4.), a scale-independent framework is needed to quantify the consequences arising from climate interactions. For this, I developed a flexible analytical approach for evaluating the influence of climate interactions in ecosystems, allowing for the quantification of the length, temporal pattern, and magnitude of patterns arising from climate legacies. The approach consists of four steps, each described in detail in the following and visually explained by Figure 6.

The first step consists of the preparation of environmental data for the analysis. This environmental data could describe temperature, precipitation, soil water estimates or any environmental parameter of interest, as long as it is available in the form of a time series spanning the time range relevant for the focal study. As climate interactions are based on directional changes of these environmental parameters, the time series of observational values needs to be transformed into a time series of trends. This means quantifying the specific rate of change from one observation to the previous observation, in the following named Δ_{change}. If, for example, the temperature at *t-1* is 10°C, and at *t* 14°C, and the time span between the two observations spans one year, then Δ_{change} is 4°C per year. The calculation of Δ_{change} can either be done by subtracting the environmental value at *t-1* from the value at *t*, or by using the slope of a linear regression of these two observations. After calculating Δ_{change} for all observations of the environmental parameter, the preceding long-term trends need to be quantified. These long-term trends will be named Δ_{trend} in the following. Δ_{trend} similarly consists of the rate of change between two values, but instead of calculating the change between *t* and *t-1*, the change between preceding values and *t-1* is used. Δ_{trend} therefore quantifies the rate of change in environmental parameters before Δ_{change}, enabling the independent calculation of the climate interactions. Δ_{trend} can be computed by using the slope of a linear regression between two observations and subsequently dividing the slope estimate by the time span between the two observations. While the length of Δ_{change} is determined by the temporal resolution of the environmental parameters, Δ_{trend} can span any arbitrary length in a successively growing way, such as the change between *t-2* and *t-1*, *t-3* and *t-1*, *t-4* and *t-1* …, *t-n* and *t-1*. The appropriate length of Δ_{trend} can be assessed by means of model comparison, which is incorporated in the third step succeeding the model fitting procedure explained in the following paragraph. At the end of the first step, all observations of the environmental parameter have an associated value for Δ_{change} and various values for Δ_{trend}.

In a second step, the change and trend estimates for the environmental parameters are combined with the response variable in a model setting. The response variable should consist of a time series with the same resolution as the environmental time series, and can comprise any metric appropriate for the measure of extinction risk in ecological systems, such as, for example, direct extinction events, change in population size, or change in geographical range. The additive and multiplicative effects of climate interactions, defined as the interacting effects of Δ_{change} and Δ_{trend} , on the response variable, can then be estimated in a modelling framework in the form:

Response Variable ~ $\Delta_{change} : \Delta_{trend}$ + *random structure*.

The random structure variable in the model should be used to account for any intrinsic correlation of the response variable, such as dependence of observations in time series or phylogenetic relationship between taxonomic groups. This can be done by using random effects within a mixed effect model framework (Bolker et al., 2009). The likelihood and link-function of the mixed effect model should be chosen based on the distribution of the response variable. For example, for a response variable that measures when taxa went extinct versus when they survived, a binomial likelihood with a logit link might be most suitable. While these mixed effect models can be fitted in a Frequentist modelling framework, Bayesian models should be preferred as they can ensure an appropriate model fitting even under a highly complex random structure of the response variable (McElreath, 2020). The model fitting procedure should be done for every calculated length of Δ_{trend}.

The third step consists of quantifying temporal memory of the models, which corresponds to quantifying the best performing length of Δ_{trend}. By calculating one model for each long-term temperature trend (Δ_{trend}), it is possible to choose the trend explaining the most variation of extinction risk in interaction with short-term change. This can be done by means of model comparison, which consists of comparing the model performance of each model to models with a different length of Δ_{trend}. The model performance can be assessed through any measure of goodness of fit of the model, such as the Akaike information criterion (Burnham, 1998) in a Frequentist setting or Pareto smoothed importance sampling (Vehtari et al., 2017) in a Bayesian modelling framework. This model comparison should not result in the removal of all models with a worse performance than the model with the best performing Δ_{trend} (i.e. model selection), but instead the following inference should be based on all models weighed by their importance. This can either be done by doing the following step four for every individual model, or by averaging inference estimates across models (i.e. model averaging).

In step four, the fitted models are used to estimate the effect of a short-term change (Δ_{change}) on the response variable, depending on the preceding long-term trend (Δ_{trend}). For this, a grid of equally spaced short-term changes with equally spaced long-term trends can be created. The range of the grid should capture the vast majority of environmental changes and trends observed in the actual data. For example, a study on the temperature change in the glacial cycles of the past 700 thousand years should use a grid of values between -2°C and 2°C, as this range captures most of the observed temperature changes. Models can then be used to predict values over this grid, meaning that the estimated relationship of the climate interaction within a model is used to predict the response variable across all combinations of Δ_{change} and Δ_{trend} of the grid. By doing so, one can for example estimate the effect of a 1°C warming on the response variable, and can compare this estimated effect between a scenario where a long-term cooling preceded the warming and a scenario where a long-term warming preceded the warming. This procedure further ensures capturing a range of potential long-term trends and short-term changes while having the same amount of observations per climate interaction.

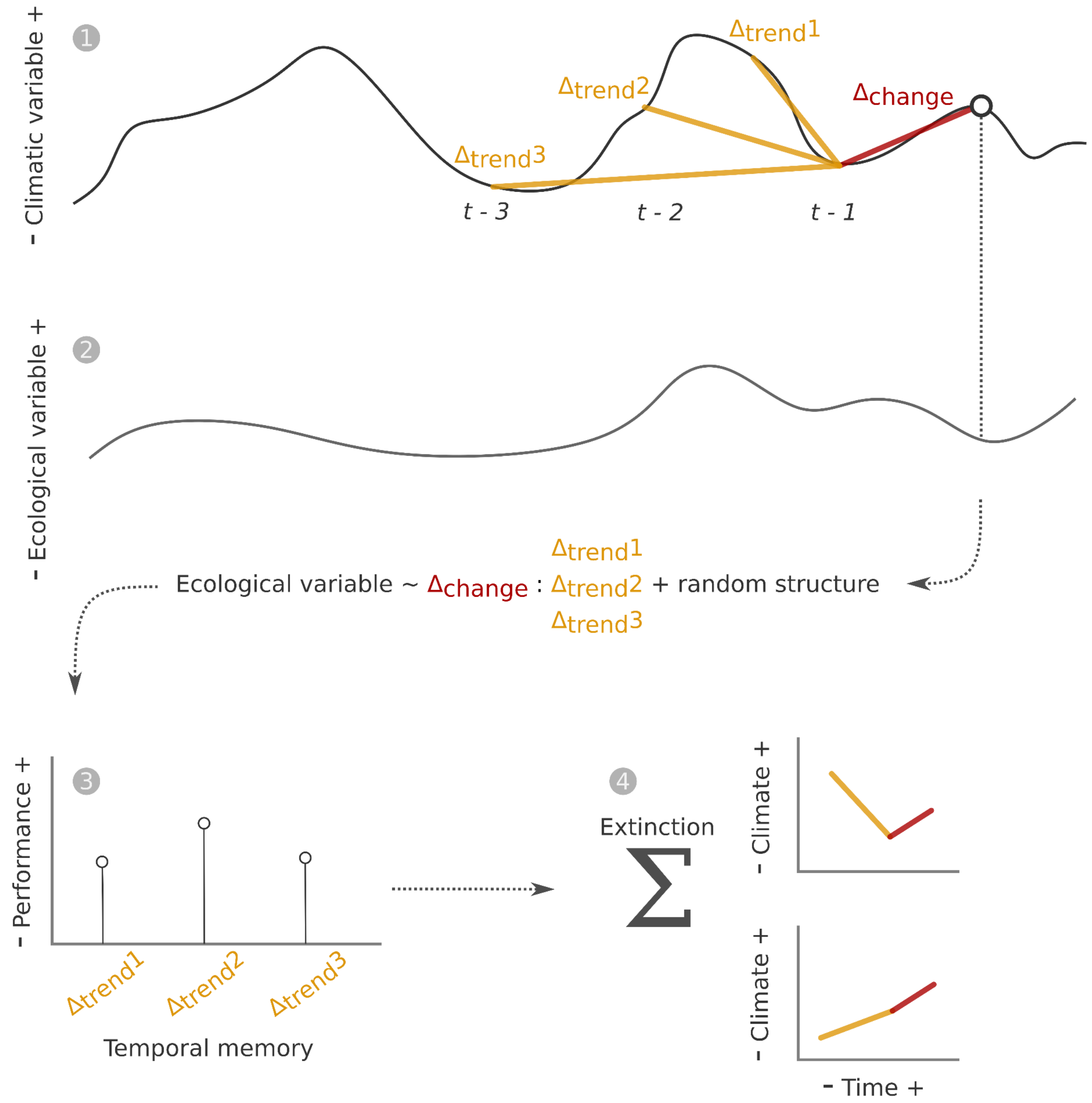

Figure 6: Methodological framework for the quantification of extinction risk from climate legacies in ecological systems through climate interactions. In the first step, short-term changes (Δ_{change}*) and long-term trends (*Δ_{trend}*) for the climatic variable of interest are calculated. The second step consists of combining those changes and trends with the ecological response variable of interest in an interaction model. Each long-term trend is hereby included through an individual model. In the third step, temporal memory of each model gets quantified, which corresponds to identifying the best performing length of *Δ_{trend}*. This performance measure can then be used to weigh estimates from each model in the fourth step. In this last step, the effect of each climate interaction on the ecological variable is estimated through an extinction risk assessment. For*

this, the effect of a short-term change in the climatic variable on the ecological variable can be estimated through the models, and this estimated effect can be compared between a scenario where a long-term decrease in the climatic variable preceded the short-term change and a scenario where a long-term increase preceded the short-term change. The figure illustrates the concept for one time slice shown by the dotted line. The final models, however, integrate across all time slices. Modified after Mathes, van Dijk et al. (2021).

The proposed analytical approach can be used for ecological and environmental data on any scale, and has the advantage of quantifying consequences of climate legacies without having to disentangle underlying processes. It further allows for the quantification of the temporal pattern of climate legacies (i.e. temporal memory) and can be used to estimate ecological consequences of climate legacies under future climate change, by taking advantage of the estimated relationship between the response variable and climate changes within each model. The overall modelling framework aims to provide a flexible analytical tool to evaluate the role of climate legacies in shaping extinction risk throughout Earth's history. I designed the framework to be useful in revealing novel insights throughout a wide variety of biotic systems. In the following chapter, I will illustrate this through a set of studies covering timescales from the geological deep time up to modern ecosystems, with examples from marine and terrestrial fossil extinction events, evolutionary bursts, range dynamics, and compositional change within ecosystems.

3. Synopsis

“I may not have gone where I intended to go, but I think I have ended up where I needed to be.”

– Douglas Adams

The identification and comprehension of basic patterns or regularities that appear at certain scales or may even be scale-independent is one of ecology's primary objectives (Rosenzweig, 1995; Steinbauer, 2013). Within the introduction, I provided a general overview of patterns and regularities arising from climate legacies in extinction dynamics. I further developed a heuristic framework that unifies these patterns, which can be used in any ecological setting irregardless of the temporal scale. In the following, I will briefly illustrate applications of this framework in six manuscripts with different degrees of complexity and varying timescales (Figure 7). The manuscripts of this thesis all deal with environmental parameters and how they are associated with ecological dynamics in time. Combining the findings from these studies allows for a detailed examination and discussion of how climate legacies shaped extinction risk throughout Earth’s history.

Manuscript 1 provides a comprehensive application of the climate interaction framework to fossil extinction events. It is shown that the majority of taxa known for their good fossil record exhibit substantially increased extinction rates after they experienced synergistic climate interactions (i.e. a short-term temperature change on top of a long-term trend in the same direction). The effect size of palaeoclimate interaction is hereby similar to other key drivers of extinction risk. The results illustrate that without explicit integration, palaeoclimate interaction could blur or even reverse apparent extinction patterns and prevent useful predictions for future scenarios.

To be able to study the relationship between extinction dynamics and climate, high resolution time series of climate data are needed. **Manuscript 2** provides this high resolution climate data for a period of the largest biological crisis in Earth’s history, the end-Permian mass extinction. Additionally, intricate feedback mechanisms of weathering processes are discussed, providing crucial insights into the global carbon cycle.

Manuscript 3 assesses the relationship between deep-time evolutionary processes and climate by means of the climate interaction framework. Biodiversity is determined by both extinction and origination dynamics. While Manuscript 1 revealed that extinction dynamics are substantially driven by climate interactions, Manuscript 3 illustrates the same for origination rates. Using the marine fossil record, it is shown that origination probability substantially increases when a short-term climate cooling adds to a long-term cooling trend. The discussed mechanisms for this effect include niche conservatism and time lags such as migration or range lags.

Manuscript 4 examines the dynamics of migration and range lags through time and how climate interactions might explain arising patterns. Using the exceptional fossil record of planktonic foraminifera hereby allowed for a view into the composition of marine assemblages in the past with an extraordinary temporal and spatial resolution. It is demonstrated that high magnitudes of temperature changes led to large and often irreversible compositional changes, pointing towards the presence of critical tipping points within these marine assemblages.

As climate interactions can arise from processes acting over timescales from the geological deep time up to modern ecosystems, transdisciplinary research is needed to correctly estimate the effect of climate interactions in biotic systems. **Manuscript 5** discusses opportunities and benefits of an interdisciplinary integration between macroecology and palaeoecology, and how scales can be bridged using this approach. It is in particular demonstrated that climate legacies can only be identified and quantified when both macroecological and palaeoecological perspectives are combined within a holistic framework.

Manuscript 6 shows the prevalence of climate interactions in global vegetation dynamics over previously unassessed timescales. It is shown that vegetation change through space and time is substantially greater after synergistic climate interactions. While Manuscript 1 and 3 quantify the impact of climate interactions in deep-time biotic systems (millions of years), and Manuscript 4 in Cenozoic ecosystems (several hundred thousand years), Manuscript 6 covers ecological timescales (centuries to millennia). This high temporal resolution allows for a prediction of global vegetation dynamics under anthropogenic climate change, where I show that terrestrial plant assemblages are likely to shift into rates of change unprecedented throughout the previous 21 thousand years.

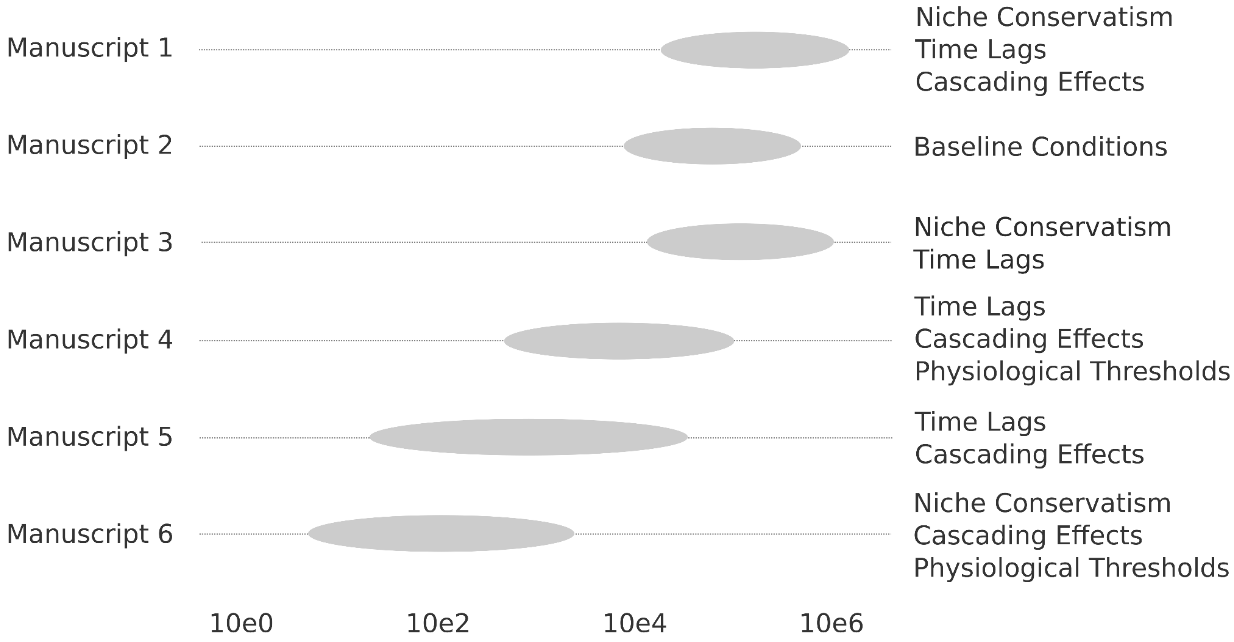

Figure 7: Temporal scale of each manuscript of this thesis, along with the discussed sources of climate legacies.

3.1. Climate interactions in the geological deep-time

Palaeontological records, together with palaeoclimatic data, comprise the potential to understand how the biosphere has adapted to previous climate shifts, as well as to measure the adaptability and fragility of ecosystems (Pörtner et al., 2022). Using the rich information on past biotic responses to climate change provided by the fossil record can shed light on the general impact of climate legacies in the biosphere (Svenning et al., 2015), and can help to predict biotic responses under anthropogenic climate change (Dietl & Flessa, 2011). The following three manuscripts cover evolutionary and climatic dynamics in the geological deep-time across the Phanerozoic. The main goals of this chapter of my thesis on the geological deep-time are to (i) test the hypothesis developed under the climate interaction framework that synergistic interactions have a more deleterious impact on the biosphere compared to antagonistic interactions, (ii) to describe general climatic processes related to mass extinction events, and (iii) to study the effects of climate interactions on origination and speciation processes.

3.1.1. Manuscript 1

Mathes GH, van Dijk J, Kiessling W, Steinbauer MJ (2021) Extinction risk controlled by interaction of long-term and short-term climate change, ***Nature Ecology & Evolution***, doi: https://doi.org/10.1038/s41559-020-01377-w

Assessing extinction risk from climate drivers is a major goal of conservation science (Barnosky et al., 2011; Brook & Alroy, 2017). Biotic responses to climatic changes are, however, mediated by past conditions (Ogle et al., 2015). Ignoring this dependency on the past can potentially lead to a misinterpretation of the apparent relationship between climate and extinction dynamics (Svenning et al., 2015). Here I tested the hypothesis that a temperature change leads to more extinction events when it follows on a preceding long-term temperature trend in the same direction (synergistic interaction), as compared to when the preceding long-term trends was in the opposite direction (antagonistic interaction). For this, I analysed the extinction dynamics of eight fossil clades (arthropods, bivalves, cnidarians, echinoderms, foraminifera, gastropods, mammals, and reptiles) across the past 485 million years. By combining these groups known for their good fossil record (Reddin et al., 2018) with reconstructed temperature changes, I was able to show that synergistic climate interactions can significantly elevate the temperature-related extinction risk of both marine and terrestrial organisms. The effect size of palaeoclimate interaction was hereby similar to other key drivers of extinction risk such as geographic range (Finnegan et al., 2015; Foote et al., 2008; Harnik, Lotze, et al., 2012), abundance (Harnik, 2011; Payne et al., 2011), or clade membership (Harnik, Simpson, et al., 2012; McKinney, 1997).

The temporal memory of this climate legacy effect, the length over which preceding long-term trends still had an effect on extinction dynamics, was up to 60 million years long. This might have implications for the predicted biodiversity crisis under anthropogenic climate warming, where a short-term warming is preceded by a long-term cooling trend during the Paleogene and Neogene. If this antagonistic climate interaction is not incorporated in assessments of extinction risk under future warming, predictions may overestimate the apparent risk. However, this direct projection of the studied climate interactions into the near-time future is hampered by the temporal resolution of the study, calling for the need of quantifying consequences of climate interactions in biotic systems with a finer temporal resolution.

Three different climate legacy concepts are discussed to cause the increase in extinction risk after synergistic climate interaction. Niche conservatism (Hopkins et al., 2014; Wiens & Graham, 2005), migration lags (Normand et al., 2011; Svenning & Skov, 2004), and cascading effects (Beaugrand, 2015; Lord et al., 2017) are all based on the concept of niche stability over geological time scales and imply that synergistic temperature changes successively move taxa out of their adaptation space. This mismatch with existing climate could then lead to a higher extinction risk.

In conclusion, this study was the first to show that extinction dynamics can be explained by the proposed climate interaction framework. While the effect on extinction dynamics was found to be large, insights arising from climate interactions for anthropogenic climate change need to be verified in biotic systems with a finer temporal resolution.

3.1.2. Manuscript 2

Joachimski MM, Müller J, Gallagher TM, Mathes GH, Chu DL, Mouraviev F, Silantiev V, Yadong DS, Tong JN (2022) Five million years of high atmospheric CO_2 in the aftermath of the Permian-Triassic mass extinction. ***Geology***, doi: https://doi.org/10.1130/G49714.1

To deduce general extinction patterns from climate legacies, high-resolution data for environmental data during extinction events are needed. The most catastrophic mass extinction event in the Phanerozoic occurred during the Permian-Triassic transition (Sepkoski, 1981). The extinction event was accompanied by 8°C to 10°C low latitudinal warming and extensive global ocean anoxia (Joachimski et al., 2020; Sun et al., 2012), representing a fossil analogue to anthropogenic climate warming (Payne & Clapham, 2012). One of the main drivers of extinction selectivity during this period was arguably hypercapnic stress from elevated pCO_2 (Knoll et al., 2007; Payne & Clapham, 2012). However, there has been so far no empirical study approach that investigated atmospheric CO_2 dynamics of the late Permian to Early Triassic hothouse period.

In this study, atmospheric CO_2 history throughout the late Permian and Early Triassic was reconstructed by using the paleosol pCO_2 proxy record. A fourfold increase in atmospheric pCO_2 across the Permian-Triassic boundary to high and intermediate CO_2 levels in the Early Triassic was found, which is in line with documented greenhouse warming and hot Early Triassic oceans. These elevated pCO_2 values persisted for more than five million years, suggesting that silicate weathering failed to draw down CO_2 until the latest Early Triassic. These findings may enhance the mechanistic understanding of biotic responses to extreme climatic changes, and add crucially needed data and insights to one of the most important analogues for anthropogenic climate warming.

3.1.3. Manuscript 3

Mathes GH, Kiessling W, Steinbauer MJ (2021) Deep-time climate legacies affect origination rates of marine genera, ***PNAS***, doi: https://doi.org/10.1073/pnas.2105769118

While previous analysis has shown that climate interactions control extinction risk throughout the Phanerozoic (Mathes, van Dijk, et al., 2021), the effect of these climate legacies on deep-time origination is largely unknown. Due to niche conservatism (Hopkins et al., 2014; Wiens & Graham, 2005), synergistic climate interactions might lead to taxa having less adaptations to the climatic situation than under antagonistic climate interactions. This lack of adaptation to climatic conditions might result in ecological releases, bottleneck, and subsequent founder effects (Button, 2017; Gilman et al., 2010; Raup, 1979), which are known to influence rates of evolution and speciation (Templeton, 2008; Wahl et al., 2002).

Building on these ecological mechanisms, I hypothesised and showed that climate interaction was a strong determinant of origination rates in the deep-time fossil record. I analysed how global trajectories of past climate can affect the origination probabilities of twelve marine fossil phyla (Annelida, Arthropoda, Brachiopoda, Bryozoa, Chordata, Cnidaria, Echinodermata, Foraminifera, Hemichordata, Hyolitha, Mollusca, and Porifera) throughout the last 485 million years. The results showed a substantial increase in origination rates when a short-term cooling added to a long-term cooling. This increase in origination rates might occur through increased habitat fragmentation. Cooling–cooling climate interaction might therefore cause a drop in eustatic sea level due to glaciation, leading to reduced continental shelf area and emerging barriers in this main habitat of the majority of the studied fossil groups. Increased habitat fragmentation might then lead to higher allopatric speciation through vicariance (Mayr, 1963; Peters, 2005), explaining the observed increase in origination rates.

In conclusion, this study showed that the effect of climate interaction on evolutionary dynamics is not restricted to extinction patterns, but seems to determine origination probability as well. While the underlying ecological mechanisms such as niche conservatism and time lags might be the same as in extinction events, the emerging patterns of increased allopatric speciation through vicariance provided novel insights into the relationship of temperature and biodiversity in Earth’s history.

3.2. Climate interactions throughout the Quaternary

The effect of climate change on spatio-temporal patterns in assemblages on a global scale is poorly understood (García Molinos et al., 2016). The majority of research focuses on individual species rather than examining changes in assemblages. (Dornelas et al., 2014). Due to its unique capacity to record how animals responded to a wide variety of climatic changes, the fossil record offers the opportunity to bridge this crucial knowledge gap of changes within assemblages. However, most studies taking advantage of the fossil record are either limited to single historical timesteps (Greenstein & Pandolfi, 2008; Kiessling et al., 2012) or cover scales of 10^6 to 10^7 years (Kocsis et al., 2018; Martin-Garin et al., 2012; Reddin et al., 2018), which are considerably above timescales relevant for modern ecosystems. The high resolution fossil record of microfossil and pollen assemblages provide an excellent opportunity to fill this research gap and to study the effect of climate interactions of finer temporal scales within the Quaternary. The main goals of this chapter of my thesis on the Quaternary are to (i) to test whether climate interaction remains a strong determinant of extinction dynamics over finer temporal scales than covered by previous analysis, and (ii) to provide and describe a holistic framework that allows to study the effect of climatic interactions across different temporal scales through transdisciplinary research.

3.2.1. Manuscript 4

Mathes GH, Reddin CJ, Kiessling W, Antell GS, Saupe EE, Steinbauer MJ (2022) Nowhere to run: Lagged responses of tropical and polar planktonic foraminifera over 700,000 years of climate change, ***Global Ecology and Biogeography***, *in submission*

One key response of marine assemblages exposed to a changing climate is by tracking climatic niches in space via distribution shifts (Chen et al., 2011; Pinsky et al., 2013; Poloczanska et al., 2013). However, if marine organisms can fully adapt to climatic changes via dispersal remains uncertain (García Molinos et al., 2016; Munday et al., 2013). While individual marine ectotherm species are projected to closely follow their thermal limitations (Sunday et al., 2012), assemblages are unlikely to travel cohesively (Graham et al., 1996; Reddin et al., 2018; Walther et al., 2002), resulting in a disequilibrium or lag that causes a mismatch between ambient temperatures and those preferred by assemblages (Devictor et al., 2012; Menéndez et al., 2006; Svenning & Sandel, 2013).

In this study, I investigated these disequilibrium dynamics over the past 700,000 years of glacial-interglacial cycles at a 8 thousand year resolution, using the theoretical framework of climate interactions. For this, I used the exceptional fossil record of planktonic foraminifera (Protista), which are primary components of marine food webs and biogeochemical cycles, in combination with a coupled Atmosphere–Ocean Generalised Circulation Model. Results showed that assemblages were not able to move ranges fast enough to track shifts in suitable climates when climatic changes were high, pointing towards the presence of critical tipping points within these marine assemblages.

How well assemblages were able to react to climatic changes was mediated by the long-term climatic context, illustrating the importance of climate interactions at timescales of millennia to hundred thousand years. Overall, these findings indicate that the vulnerability of marine assemblages to climate change is potentially more extensive than previously anticipated.

3.2.2. Manuscript 5

Flantua SGA, Mottl O, Felde VA, Giesecke T, Hooghiemstra H, Irl S, Lenoir J, Mathes GH, McMichael C, Seddon A, Steinbauer MJ, Tovar C, Vetaas O, Birks HJB, Grytnes JA (2022) The joint world of macroecology and terrestrial palaeoecology, ***Global Ecology and Biogeography***, *in review*

A fundamental issue for studying ecosystem processes from contemporary data is that assemblages and observed metrics are always dependent on past conditions (Svenning et al., 2015). This issue can only be overcome by incorporating knowledge and data about preceding ecological dynamics (Ogle et al., 2015), and by developing solid approaches to assess temporal processes by means of time series (Sugihara et al., 2012). In this study, a conceptual synthesis is developed to combine inferences about contemporary ecological dynamics with palaeoecological perspectives. Key research topics which can benefit from transdisciplinary research between macroecology and palaeoecology are highlighted, and a conceptual framework for the successful integration of these two research fields is provided.

It is in particular demonstrated that climate legacies can only be identified and quantified when both macroecological and palaeoecological perspectives are combined within such a holistic framework. The processes and timescales over which climate interactions act can only be determined through transdisciplinary research. Both research fields have ample opportunities to contribute to this transdisciplinary research, and these potential contributions are identified and described throughout the manuscript.

3.3. Climate interactions throughout the Holocene

While previous analyses (Manuscript 1, 3 and 4) have shown that climate interactions are an important determinant of evolutionary dynamics in both deep-time biotic systems and Cenozoic ecosystems, the legacy effects arising from climate interactions have not yet been quantified for modern global ecosystems (Benito et al., 2020). Under anthropogenic climate change, the ecological consequences from climate interaction might even be further exacerbated by the increased occurrence of climate extremes and compound climatic hazards (AghaKouchak et al., 2020). The last chapter of my thesis therefore aims to test whether climate interaction remains a strong determinant of extinction dynamics over timescales with direct relevance to the current anthropogenic climate change.

3.3.1. Manuscript 6

Mathes GH, Kiessling W, Mottl O, Flantua SGA, Birks HJB, Grytnes JA, Steinbauer MJ (2022) Climate legacies accelerated global rates of change in plant assemblages over the last 21000 years, ***Nature Communications***, *in review*

A major obstacle for conserving biodiversity and the diverse services that terrestrial ecosystems provide lies in understanding how terrestrial organisms will adapt to climate change (Jump & Peñuelas, 2005; Urban, 2015; Warren et al., 2013). Responses of plant assemblages to a wide variety of climate changes are preserved through palynological proxies (Giesecke et al., 2017; Williams et al., 2004), offering the potential to study the relationship between assemblage turnover and climate change through time, particularly within the framework of climate interactions.

Here I tested the hypothesis that a temperature change leads to more assemblage turnover when it follows on a preceding long-term temperature trend in the same direction (synergistic interaction), as compared to when the preceding long-term trends was in the opposite direction (antagonistic interaction). For this, I was using a global database of pollen sequences, recording the responses of plant assemblages to climatic changes of the past 21,000 years. The high-resolution record of pollen sequences allowed for the quantification of effects arising from climate interactions over previously unassessed timescales, with short-term temperature change capturing a period of 100 years. Results were similar to assessments of climate interaction throughout the Quaternary and the geological deep-time, with synergistic climate interactions resulting in a substantial increase of turnover in plant assemblages. The temporal memory of this effect ranged from 100 to 1,000 years. This allowed me to estimate the response of plant assemblages to future climate change, by using the temperature trajectories of the last 1,000 years together with different climate change scenarios under various shared socioeconomic pathways. Under these scenarios, I predict an unprecedented turnover of plant assemblages as compared to a pre-human baseline.

In conclusion, climate interactions were indeed a major determinant of turnover in plant assemblages, which can be interpreted as a proxy for extinction and extirpation risk of individual taxa within those assemblages. The temporal scale of this study allowed for quantifying potential ecological responses to climate interactions under future climate change scenarios, which has been called for in Manuscript 1, 3, and 4. Climate legacies, and the arising patterns captured in the heuristic framework of climate interactions, might therefore be a crucial concept for the conservation of biodiversity under the accelerating warming trend of anthropogenic climate change.

4. Author contributions

Manuscript 1:

Authors: Mathes GH, van Dijk J, Kiessling W, Steinbauer MJ
Title: **Extinction risk controlled by interaction of long-term and short-term climate change**
Journal and status: ***Nature Ecology & Evolution***, 5, 304-310 (2021)
Own contribution: conceptualization: 50%, formal analysis: 90%, visualisation: 100%, writing: 80%, corresponding author

Manuscript 2:

Authors: Joachimski MM, Müller J, Gallagher TM, Mathes GH, Chu DL, Mouraviev F, Silantiev V, Yadong DS, Tong JN
Title: **Five million years of high atmospheric CO2 in the aftermath of the Permian-Triassic mass extinction**
Journal and status: ***Geology***, 50, 650-654 (2022)
Own contribution: statistical data processing: 100%, writing: 20%

Manuscript 3:

Authors: Mathes GH, Kiessling W, Steinbauer MJ
Title: **Deep-time climate legacies affect origination rates of marine genera**
Journal and status: ***Proceedings of the National Academy of Sciences***, 118, e2105769118 (2021)
Own contribution: conceptualization: 80%, formal analysis: 95%, visualisation: 100%, writing: 85%, corresponding author

Manuscript 4:

Authors: Mathes GH, Reddin CJ, Kiessling W, Antell GS, Saupe EE, Steinbauer MJ
Title: **Nowhere to run: Lagged responses of tropical and polar planktonic foraminifera over 700,000 years of climate change**
Journal and status: ***Global Ecology and Biogeography***, in submission
Own contribution: conceptualization: 90%, formal analysis: 95%, visualisation: 100%, writing: 80%, corresponding author

Manuscript 5:

Authors: Flantua SGA, Mottl O, Felde VA, Giesecke T, Hooghiemstra H, Irl S; Lenoir J, Mathes GH, McMichael C, Seddon A, Steinbauer MJ, Tovar C, Vetaas O, Birks HJB, Grytnes JA
Title: **The joint world of macroecology and terrestrial palaeoecology**
Journal and status: ***Global Ecology and Biogeography***, in review
Own contribution: visualisation: 40%, writing: 30%

Manuscript 6:

Authors: Mathes GH, Kiessling W, Mottl O, Flantua SGA, Birks HJB, Grytnes JA, Steinbauer MJ
Title: **Climate legacies accelerated global rates of change in plant assemblages over the last 21000 years**
Journal and status: ***Nature Communications***, in review
Own contribution: conceptualization: 90%, formal analysis: 95%, visualisation: 100%, writing: 85%, corresponding author

5. Main research

Manuscript 1

Extinction risk controlled by interaction of long-term and short-term climate change

***Nature Ecology & Evolution* 5 (2021) DOI: https://doi.org/10.1038/s41559-020-01377-w**

Gregor H. Mathes[1,2*] , Jeroen van Dijk[1] , Wolfgang Kiessling[1], Manuel J. Steinbauer[2,3]

[1] Department of Geography and Geosciences, GeoZentrum Nordbayern, Friedrich-Alexander University Erlangen-Nürnberg (FAU), Erlangen, Germany.
[2] Bayreuth Center of Ecology and Environmental Research (BayCEER), University of Bayreuth, Bayreuth, Germany.
[3] Department of Biological Sciences, University of Bergen, Bergen, Norway.
* Corresponding author: gregor.mathes@uni-bayreuth.de

ABSTRACT

Assessing extinction risk from climate drivers is a major goal of conservation science. Few studies, however, include a long-term perspective of climate change. Without explicit integration, such long-term temperature trends and their interactions with short-term climate change may be so dominant that they blur or even reverse the apparent direct relationship between climate change and extinction. Here we evaluate how observed genus-level extinctions of arthropods, bivalves, cnidarians, echinoderms, foraminifera, gastropods, mammals and reptiles in the geological past can be predicted from the interaction of long-term temperature trends with short-term climate change. We compare synergistic palaeoclimate interaction (a short-term change on top of a long-term trend in the same direction) to antagonistic palaeoclimate interaction such as long-term cooling followed by short-term warming. Synergistic palaeoclimate interaction increases extinction risk by up to 40%. The memory of palaeoclimate interaction including the climate history experienced by ancestral lineages can be up to 60 Myr long. The effect size of palaeoclimate interaction is similar to other key factors such as geographic range, abundance or clade membership. Insights arising from this previously unknown driver of extinction risk might attenuate recent predictions of climate change-induced biodiversity loss.

INTRODUCTION

Biodiversity and ecosystems are critically endangered by current climate change(García Molinos et al., 2016; Pecl et al., 2017). Reliable assessments of extinction risk are thus essential for the effective protection of biodiversity (Barnosky et al., 2011; Brook & Alroy, 2017). Whereas several assessments categorize extinction risk from climate change (Urban, 2015, 2015), relatively few studies make use of the rich information on past biotic responses to climate changes provided by the fossil record (Collins et al., 2018; Finnegan et al., 2015; van Woesik et al., 2012). Palaeontologically informed models have proven to be powerful in discerning biotic factors that determine future extinction vulnerability (Calosi et al., 2019; Harnik, Lotze, et al., 2012; Kiessling & Kocsis, 2016). Numerous reports demonstrate that the impact of climatic changes increases with distance from the climatic conditions species are adapted to (Beaugrand, 2015; Lord et al., 2017; Wiens & Graham, 2005). Additionally, a strong link between temperature stress and extinction risk is also known from the fossil record (Bond & Grasby, 2017; Penn et al., 2018; Reddin et al., 2020). However, one potentially crucial factor of extinction dynamics, the interaction of long-term temperature trends with short-term temperature change, has not been investigated until now.

Here, we quantify how the interaction of long-term temperature trends with short-term temperature change can affect temperature-related extinction probabilities. We expect temperature change to be more critical when it adds to previous trends in the same direction (synergistic interactions) because taxa then face conditions increasingly different from previous adaptations. To the contrary, current anthropogenic warming occurs after a 40-Myr cooling trend, raising the possibility that many modern clades are increasingly exposed to climates they experienced during their origination. Such change may be less harmful. Understanding the effect of this palaeoclimate interaction could hence provide crucial insights into extinction mechanisms and lead to improved mitigation efforts for biodiversity under current climate change.

We analysed eight fossil clades, both marine and terrestrial, each containing more than 400 genera. We implemented generalized linear mixed effect models with binomial family error (GLMMs) (Bolker et al., 2009) to explain how survival and extinction on genus level is affected by palaeoclimate interaction (Fig. 1). Besides quantifying effect size, we also estimated the temporal memory of this effect. We then compared these models containing information about both long-term temperature trends and short-term changes to models including short-term temperature changes only using model selection (Burnham, 1998).

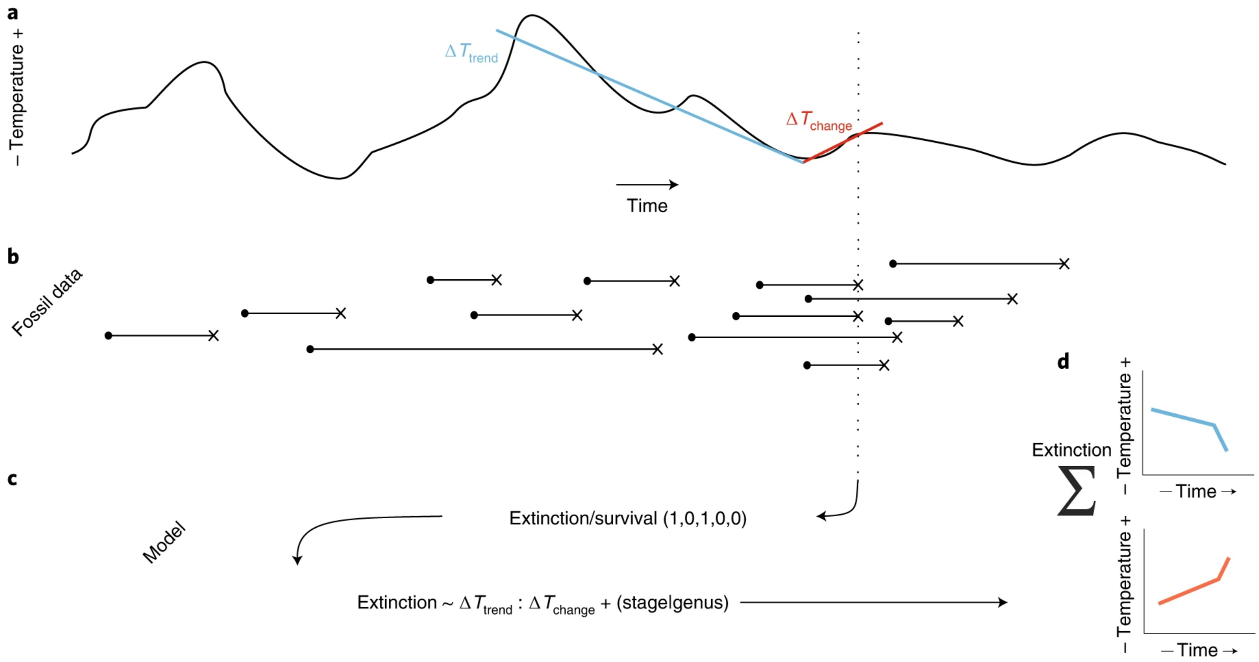

Figure 1: Schematic of analytical protocol. ***a****, For each geological stage, we calculated the magnitude in temperature change compared to the previous stage (ΔT_{change}) and long-term temperature trends with varying duration (ΔT_{trend}).* ***b,c****, The extinction/survival signal from fossil range data* ***(b)****, where 1 depicts the extinction of a genus, was combined with the palaeotemperature information using generalized linear mixed effect models* ***(c)****. The figure illustrates this for one time slice shown by the dotted line. The implemented mixed effect models, however, integrate all time slices in one joint model.* ***d,*** *In a last step, we quantified the effect of palaeoclimate interaction on intrinsic extinction risk for each palaeoclimate interaction using the results of our models. We subsequently applied the same model structure to simulated fossil data and compared them to our results for statistical inference.*

RESULTS

Palaeoclimate interactions improved model performance in seven out of eight clades when compared to models including short-term temperature changes only on the basis of Akaike's Information Criterion (AIC) (Fig. 2). Only mammals showed a deteriorating model performance for short-term cooling when palaeoclimate interaction was included.

Short-term climate change adding to a previous temperature trend in the same direction (synergistic palaeoclimate interaction) increased extinction risk in all significant models (Fig. 3 and Extended Data Fig. 1). Model predictions showed an increase in extinction risk between 10 and 40% after such a synergistic palaeoclimate interaction for arthropods, bivalves, foraminifera, mammals and reptiles. The synergistic interaction of long-term cooling with short-term cooling yielded the most severe impact on extinction risk with a 40% increase for mammals and 33% for foraminifera.

We observe a negative relationship between extinction risk predicted by the interaction models and the duration of genera (Fig. 4). The effect of palaeoclimate interaction on extinction is strongest for clades with short-duration genera, whereas clades with greater durations of genera experienced a lower change in extinction risk. The climatic history of each genus accounted for 37% variation of median and 40% of mean duration (adjusted R^2; based on F statistics).

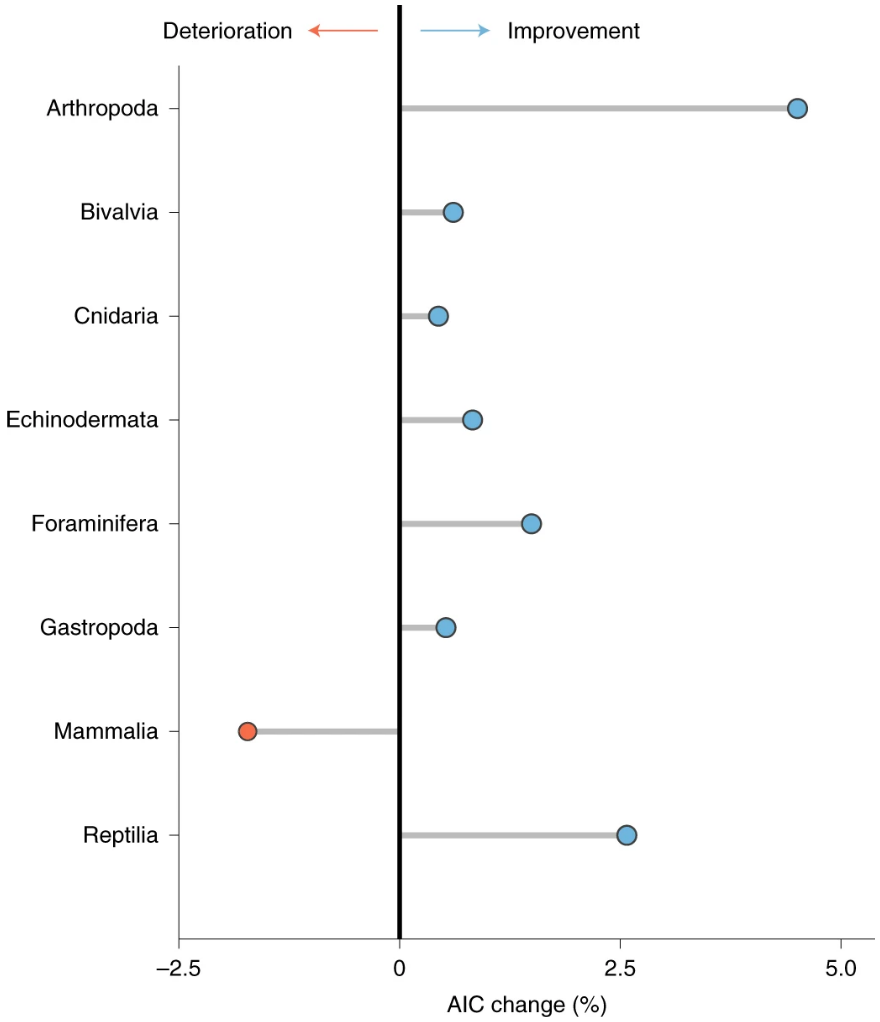

Figure 2: Model comparison. Model performance of traditional models (change only) was compared to model performance taking palaeoclimate interaction into account (change and trend). Model performance was evaluated using AIC. The figure shows the proportional change in AIC of the traditional model compared to the performance of the model including palaeoclimate interactions, for each individual clade. Values above zero (blue points) show a model improvement for palaeoclimate interactions and values below zero (red point) a model deterioration.

The extinction risk of marine and terrestrial taxa is dependent on temperature trends extending over a period of 5 to 60 Myr or up to ten geological stages. For each genus within a clade, we calculated up to ten long-term temperature trends interacting with short-term temperature change. We subsequently determined the period of time where the interaction resulted in the strongest change in intrinsic extinction risk (that is, temporal memory; Extended Data Fig. 2).

Some clades such as arthropods, foraminifera and reptiles are more responsive to temperature changes with geologically short durations (5 to 24 Myr), while bivalves, cnidarians, echinoderms, gastropods and mammals respond more strongly to interactions with geologically long climate trends (24–60 Myr). The temporal memory of the interaction effect was independent from the durations of genera (Extended Data Fig. 3).

Null models of temperature-independent extinction/survival processes were used to test the robustness of our analytical results (Extended Data Fig. 4; Methods). These simulations resulted in negligible changes of intrinsic extinction risk suggesting that we reveal biologically meaningful patterns.

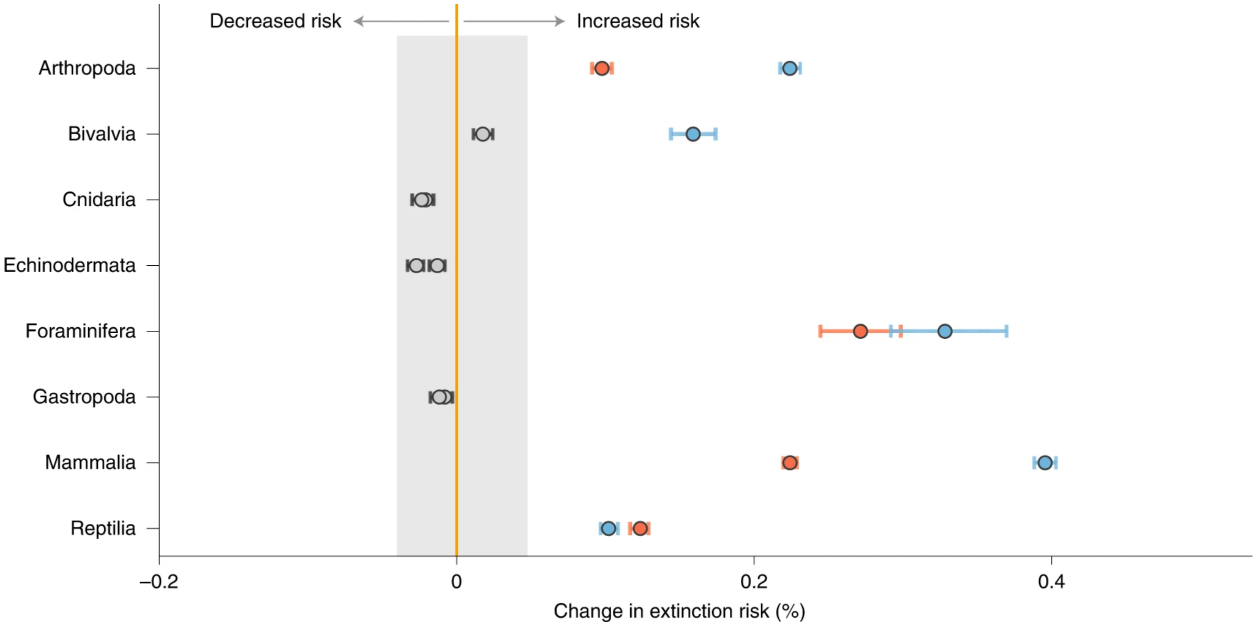

Figure 3: Change in extinction risk due to palaeoclimate interaction of all studied fossil clades. Red data points show change in extinction risk of fossil taxa after warming–warming palaeoclimate interaction compared to all antagonistic interactions of short-term warming. Blue points show change in extinction risk after cooling–cooling interaction compared to antagonistic interactions of short-term cooling. Points are placed at the median of results and error bars denote 95% Wald confidence intervals as estimated by Wilcoxon rank sum tests (Methods). Grey points and confidence intervals demarcate insignificant results based on simulated null models and F statistics, and the grey-shaded rectangle shows the range of simulated null models (Methods).

DISCUSSION

We show that palaeoclimatic interactions can significantly elevate the temperature-related extinction risk of organisms and that this increase is negatively linked to the durations of fossil genera. Our results are consistent with previous findings, revealing profound impacts of temperature change on extinction risk (Bond & Grasby, 2017; Penn et al., 2018; Reddin et al., 2020). However, the effect of palaeoclimate interaction is so strong, that both neontological and palaeontological studies may either overestimate or underestimate the impact of short-term temperature change when ignoring the interaction with long-term trends. Incorporating long-term temperature trends and thus climate history, generally improves model performance and can increase inferred extinction risk by up to 40% when compared to antagonistic palaeoclimate interaction. Considering the vast amount of additional biotic and abiotic factors that contribute to extinction risk (McKinney, 1997), the explanatory power of palaeoclimate interaction compared to traditional models is remarkable. Our results indicate that the effect size of palaeoclimate interaction is on par with other key factors such as geographic range (Finnegan et al., 2015; Foote et al., 2008; Kiessling & Kocsis, 2016), abundance (Harnik, 2011; Payne et al., 2011) or clade membership (Collins et al., 2018; Harnik, Simpson, et al., 2012; McKinney, 1997).

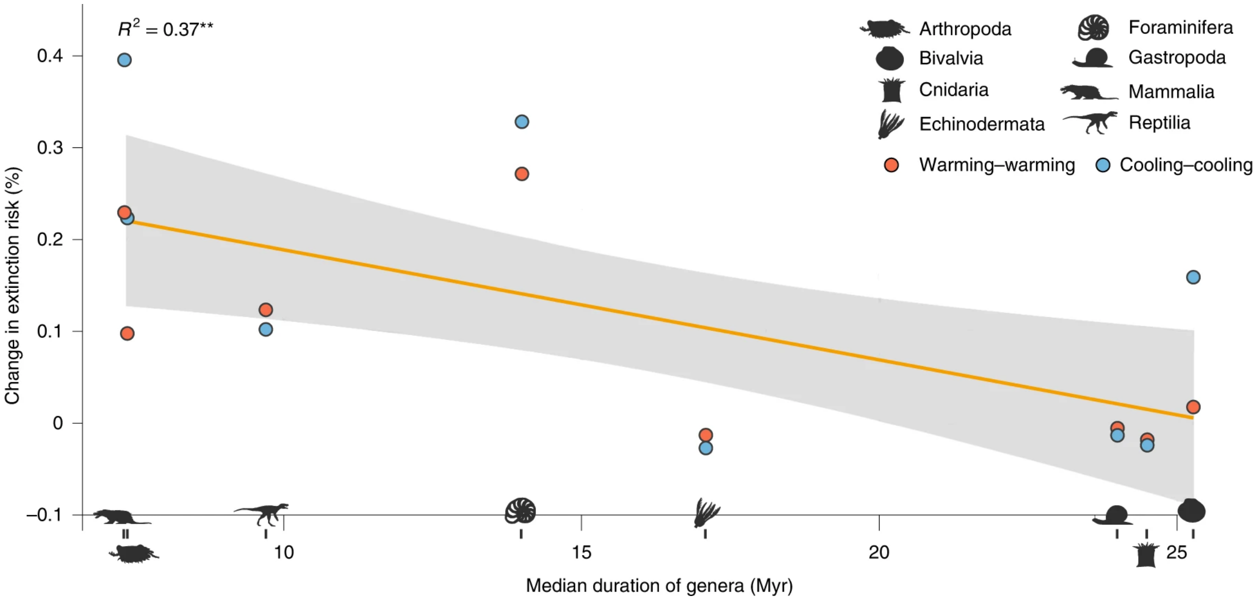

Figure 4: Change in extinction risk of fossil clades related to median duration. Red points show change in extinction risk of fossil taxa with warming–warming palaeoclimate interaction. Blue points show change in extinction risk with cooling–cooling interaction. Grey area depicts the 95% confidence interval of the regression slope. Trend line and R2 value are based on univariate linear regression across all points and significance, indicated by the asterisks ($P < 0.01$), is based on F statistics.

Hypothetically, the effect of synergistic temperature change on extinction risk can be caused by three (or potentially more) ecological mechanisms: niche conservatism (Hopkins et al., 2014; Wiens & Graham, 2005), migration lags (Normand et al., 2011; Svenning & Skov, 2004) and cascading effects (Beaugrand, 2015; Lord et al., 2017). All three mechanisms are based on the concept of niche stability over geological timescales and imply that synergistic temperature changes successively move taxa out of their adaptation space. An additional short-term perturbation in the same direction as the trend is thus expected to increase extinction risk. Although variable among major clades, evidence for niche stability abounds in the fossil record (Hopkins et al., 2014; Stigall, 2014).

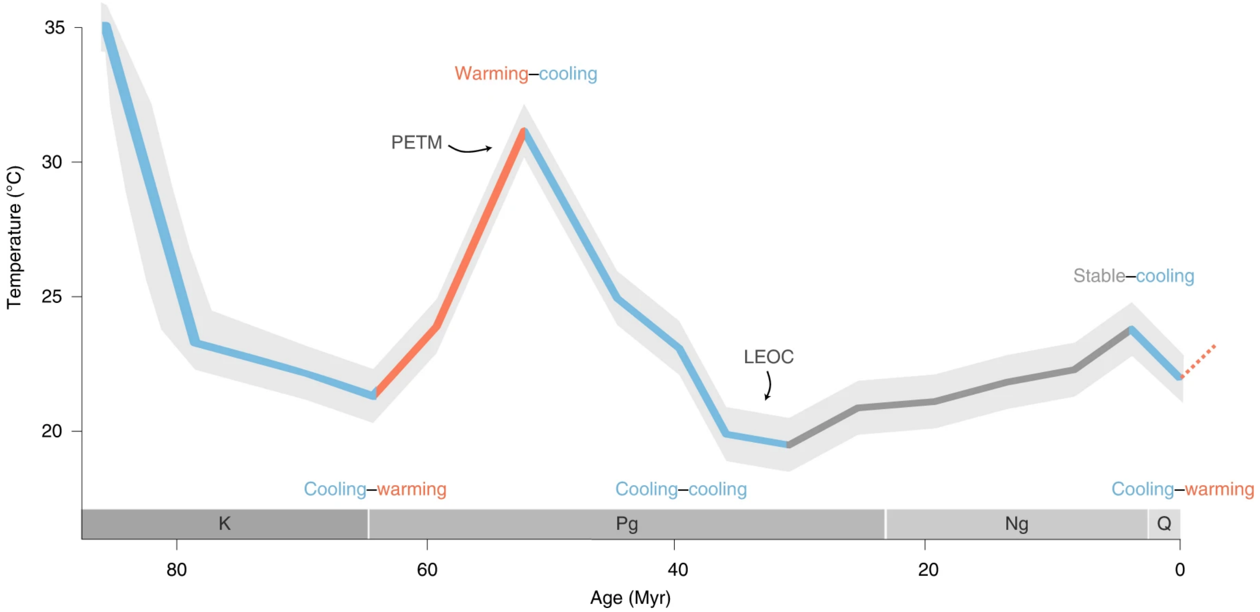

Figure 5: Palaeoclimate interactions through the Late Cretaceous and Cenozoic and potential implications for future climate changes. Moderate extinction rates during the PETM hyperthermal could be explained by a long-term cooling trend throughout the Late Cretaceous, as cooling–warming interaction potentially mitigates extinction risk. Contrarily, high extinction rates throughout the Late Eocene–Oligocene Cooling (LEOC) could be explained by a previous long-term cooling trend, reinforcing extinction risk. Current palaeontologically informed models did not consider long-term climate trends, which potentially overestimates extinction risk of modern taxa due to current climate change (cooling–warming interaction). Future temperature predictions are taken from the IPCC for surface air temperature (Masson-Delmotte et al., 2018) and illustrated by the dotted line. Colours show the direction of temperature trends for both long-term trajectories and short-term change, where red illustrates warming and blue cooling. K, Cretaceous; Pg, Palaeogene; Ng, Neogene; Q, Quaternary.

Understanding the mechanisms of palaeoclimate interaction is particularly relevant for palaeontologically informed models to assess extinction risk under current climate change. Previous models (Collins et al., 2018; Finnegan et al., 2015; van Woesik et al., 2012) were calibrated in a trend of long-term cooling during the Palaeogene and Neogene. Within this nearly monotonic long-term cooling, only two types of palaeoclimate interactions can occur: antagonistic short-term warming on top of a cooling trend and synergistic short-term cooling on top of a cooling trend, with the latter being more common. On the basis of our results, previous predictions may overestimate the extinction risk of modern taxa under current climate change (Fig. 5).

Directly projecting palaeoclimate interactions into the near-time future is hampered by insufficient knowledge of underlying mechanisms and potential scaling effects. Our analysis covers long geological time spans and does not take short-scale climatic variations into account. Hence, assessing the effect of palaeoclimate interaction on extinction risk over shorter timescales (millennia or even centuries) should be the focus of future research. We show that the effect of palaeoclimate interaction can prevail over millions of years. However, niche stability has been ascertained over different spatial and temporal scales, as well as taxonomical hierarchies (Hopkins et al., 2014; Steinbauer et al., 2016; Wiens & Graham, 2005). Likewise, our proposal that synergistic temperature changes successively move taxa out of their adaptation space and hence increase their extinction risk remains valid over ecological time spans such as centuries (Beaugrand, 2015; Lord et al., 2017; Normand et al., 2011; Svenning & Skov, 2004; Wiens & Graham, 2005). We thus expect palaeoclimate interaction to be a key mechanism of extinction risk over shorter timescales as well. Besides contributing to improved baseline estimates of vulnerability for the future, our findings also provide insights into the past. As the palaeoclimatic history a clade has experienced is a strong determinant of its fate, studies about extreme climate change events in the geological past should take climatic developments before such an event into account. Hyperthermal events represent natural examples of abrupt climate changes (Foster et al., 2018). These abrupt climate changes may coincide with severe mass extinctions (Barnosky et al., 2011; Leckie et al., 2002) but not necessarily so. The Palaeocene–Eocene Thermal Maximum (PETM), for example, was not associated with profound extinctions (Foster et al., 2018). The effect of palaeoclimate interaction could provide an explanation for this conundrum, as short-term warming in the PETM follows a general long-term cooling trend in the Late Cretaceous (Fig. 5). This is particularly important, as the PETM is often used as an analogue of anthropogenic climate change and for testing climate models (Foster et al., 2018). Major biotic turnovers during short-term cooling at the Eocene–Oligocene boundary (Coxall & Pearson, 2007), on the other hand, were potentially amplified by a previous long-term cooling trend throughout the Palaeogene (Fig. 5).

By providing insights into an understudied key mechanism of extinction processes, our findings may hence facilitate the interpretation of temperature-driven extinction events. Without explicit integration, palaeoclimate interaction could blur or even reverse apparent extinction patterns and prevent useful predictions for future scenarios, as has been shown for other complex ecological interactions (Ritterbush & Foote, 2017; Stigall, 2013). Current assessments of extinction vulnerability under future climate change include neither palaeoclimatic interactions nor a long-term temperature history of the studied taxa. Given the long-term cooling that most living taxa have experienced in their duration, extinction risk under future warming might be less severe than these assessments predict.

METHODS

Fossil data

Occurrences of post-Cambrian arthropods, bivalves, gastropods, reptiles (including birds and dinosaurs), cnidarians and echinoderms were downloaded from the Paleobiology Database (PaleoDB, paleobiodb.org) on 21 September 2020. We further downloaded occurrence data for Cenozoic mammals from the New and Old Worlds Database (NOW, www.helsinki.fi/science/now/) on 23 September 2020. We favoured NOW over the PaleoDB for mammal data, as mammal occurrences are continuously controlled and revised by NOW advisory board members. Stratigraphic range data for post-Cambrian large benthic foraminifera were compiled from a comprehensive reference work on larger foraminifera (Boudaugher-Fadel, 2018) and merged with occurrence data downloaded for planktonic foraminifera from the

Neptune Database (nsb-mfn-berlin.de) accessed on 23 September 2020. For each download, we included all occurrences with current latitude and longitude, the actual taxonomic name by which the occurrence was identified and additional information about the taxonomic classification.

We included marine invertebrate clades (cnidarians, gastropods, bivalves, echinoderms, foraminifera and arthropods) known for their good fossil record (Reddin et al., 2018) in our analysis and added terrestrial vertebrate animals (reptiles and mammals) to ensure coverage of all possible lifestyles and habitats. Each clade contained >400 genera, adding up to >14,900 analysed genera after applying our cleaning protocol (Extended Data Fig. 5).

All analyses were conducted at the genus level. This taxonomic level is a compromise between uncertainty in the species-level taxonomy of fossils and data loss at coarser taxonomic resolutions (Valentine, 1974). To ensure uniformity of datasets, we applied a standardized cleaning protocol to all of them including removal of genera ranging to the recent, uncertain taxonomical ranks, duplicates in bins, single-collection and single-reference taxa as well as missing higher-level taxonomy. We then transformed occurrence data into ranges congruent to a time series with one single origination and extinction event for each genus using the R package divDyn (Kocsis et al., 2019).

We subsequently binned the data into one of 80 geological stages (Gradstein et al., 2012), ranging from the Ordovician to the Pleistocene. The Holocene was excluded from the analysis. Additionally, taxa confined to a single stage (singletons) were excluded for all datasets as they tend to produce undesirable distortions of the fossil record (Foote, 2000).

Climate proxy data

To reconstruct temperature change over time, we used the tropical whole surface water (mixed layers <300 m deep) oxygen isotope dataset from a compilation of marine carbonate isotopes (Veizer & Prokoph, 2015). The $\delta^{18}O$ values of well-preserved calcareous shells are often considered as the best available temperature proxy for the fossil record (Song et al., 2019).To reduce bias while calculating palaeotemperature from the raw $\delta^{18}O$ values, we followed the data processing of Reddin et al. (2018). This includes adjustments for the secular trend in oxygen isotopic composition of seawater using the equation: $\delta^{18}O_{pw}$ (‰) = t2 + 0.0046‰ t, with pw being Phanerozoic seawater in standard mean ocean water and t being age in million years ago, as well as averaging of tropical and subtropical records. We subsequently binned temperature data on the basis of isotope values to geological stages to provide global mean temperature for each of the 80 stages. We emphasize that the interpretation of $\delta^{18}O$ values in deep time is a subject of considerable debate (Grossman, 2012; Henkes et al., 2018; Ryb, 2018; Song et al., 2019; Veizer & Prokoph, 2015). Throughout our data processing, we follow the argumentation of Veizer and Prokoph (Veizer & Prokoph, 2015), inferring a secular increase in seawater $\delta^{18}O$ values due to changes in how surficial oxygen reservoirs are exchanged with the vastly larger oxygen reservoir in crust and mantle silicates.

Generalized linear mixed effect models

All analyses were carried out in R (R Core Team, 2021) using R v.4.0.2. We used the lme4 package (Bates et al., 2015) to perform the analysis and the ggplot2 package (Wickham et al., 2019) to visualize results.

We quantified the effect of temperature change interacting with past temperature trends on extinction risk using generalized linear mixed effect models with a binomial family error (GLMMs, Fig. 1) (Bolker et al., 2009; Malik et al., 2020; Quené & van den Bergh, 2008). The additive and multiplicative effects of cumulative temperature change were tested against the probability of extinction in each time interval in the form: glm (extinct ~ΔTtrend: ΔTchange + (stage|genus), family = binomial).

In a first step, we aligned the climate proxy data with the fossil data. Each genus was hence represented as a time series of repeated survivals followed by one extinction event. Each observation within this time series was associated with a specific magnitude in temperature change compared to the previous observation (ΔT_{change}), assessed by using the slope of a linear regression of these two observations. Additionally, we computed long-term temperature trends (ΔT_{trend}). Each of these long-term trends was evaluated by the slope of a linear regression across temperature estimates of 1–10 time intervals before a focal interval. In this way, ΔT_{change}, defined as the change in temperature compared to the previous stage, was excluded from ΔT_{trend}, enabling the independent calculation of palaeoclimate interaction. Each of the trends covered a successively growing time of temperature history: trend.st1 ranged one stage back, trend.st2 two stages, …, trend.st10 ten stages (Fig. 1).

We controlled for the fact that observations on the same genus are non-independent by including genus identity as a random effect. By also setting stage as a random effect, we allowed for a random slope of each stage within each genus with correlated intercept, accounting for the temporal structure of the data (Bolker et al., 2009; Zuur et al., 2009). For each fossil clade, we calculated up to ten GLMMs for cooling–cooling and warming–warming interaction, respectively. Within these models, ΔT_{change} was fixed as the short-term temperature change leading up to the extinction event of a genus. The value ΔT_{trend} varied for each model on the basis of long-term trends.

The model performance of GLMMs with different long-term trends were compared using AIC (Burnham, 1998) and for each group one final model was selected on the basis of AIC for further analytical evaluation. Results remained the same when using Bayesian Information Criteria for model performance. We additionally determined the significance of palaeoclimate interaction on extinction risk for each model using maximum likelihood.

Model comparison

Palaeontological studies on temperature-related extinctions usually rely on the temperature change from the previous geological stage to the focal stage, defined here as short-term change. To test if models improve when long-term temperature trends are included, we compared GLMMs including short-term change only to GLMMs including the palaeoclimatic interaction of short-term change with long-term trends. For models taking only short-term change into account, we used the same data processing as aforementioned but excluded long-term trends from the final model: glm (extinct ~ΔTchange + (stage|genus), family = binomial).

Quantifying change in intrinsic extinction risk

We extracted the results of each final GLMM using the predict() function. To quantify the effect of cumulative temperature change on extinction risk, we transformed the results from odds ratio to probability. We compared the effect of cooling–cooling interaction on extinction risk with every other possible interaction of short-term cooling and vice versa the effect of warming–warming interaction with every other possible interaction of short-term warming (Extended Data Fig. 1). To do so, we used Wilcoxon rank sum tests with continuity correction to compare effect sizes. Results were recorded including 95% Wald confidence intervals derived from the Wilcoxon rank sum tests.

Finally, we compared these results to the simulated effect range of null models to test if results could be produced by a random structure (Null models below). This significance testing approach was implemented with Wilcoxon rank sum tests with continuity correction comparing simulated distributions with results based on observed data.

Assessing temporal memory of past climate change effects

By calculating one GLMM model for each long-term temperature trend (ΔT_{trend}), we were able to choose the trend explaining the most variation of extinction risk in interaction with short-term change. The model with the lowest AIC also showed the highest effect of past temperature change on extinction risk. Effect size decreased with increasing AIC of the remaining models, enabling determination of the temporal memory of the effect on the basis of the AIC (Extended Data Fig. 2).

Null models

Estimating the parameters of a statistical model is a key step in statistical analyses. However, fitting fixed-effect parameters of a GLMM can lead to biased statistical inference (Bolker et al., 2009). To avoid this bias, we applied our model structure to randomly generated data (Extended Data Fig. 4). We then used the results of these ‘random’ models as a distribution to compare with empirical results. This approach enabled the determination of type I error rates of our models and the probability of obtaining results as strong as those observed from a random structure with intrinsic biases of non-fossil data, such as serial autocorrelation of climate proxy data. Incorporating this two-tailed null hypothesis testing in addition to the maximum likelihood framework renders our statistical inference highly robust and reliable (Fox et al., 2015). This multiple testing approach is conservative at the cost of increased type II error rates (Lieberman & Cunningham, 2009). Our analysis therefore tends to discard palaeoclimate interactions with moderate intensity as insignificant, even when these interactions had a measurable effect on extinction risk.

Null models started with generating first appearance datums (FAD) using a random number generator. We generated 3,000 FADs from a uniform distribution. Last appearance datums (LAD) were assigned by drawing a number from the durations of all genera with replacement from our observed data and subtracting it from the FAD. Distributions of the generated datasets therefore simulated observed conditions (a log-normal distribution). For each of these genus ranges, we generated higher taxonomic ranks applying the same simulation approach as for genera and subsequently merged these two datasets. Again, we imitated the number of higher taxonomical ranks from observed data. Each observation in the generated dataset was then binned to one of 80 geological stages. We subsequently applied the same data processing to the simulated ranges as for the observed data including the calculation of short-term and long-term temperature trends for each genus on the basis of our climate proxy data.

Our simulations thus had random (independent from temperature) LADs and FADs but non-random numbers of higher taxonomic ranks and durations and were linked to our climate proxy data. Finally, we extracted 900 datasets with number of observations ranging from 1,000 to 30,000 by sampling from the simulated dataset with 3,000 observations (with replacement). We then applied the GLMMs to these datasets and stored the results. For each dataset, we calculated ten models. Subsequently, we quantified the change in intrinsic extinction risk of each model on the basis of the simulated extinction signal and observed climate proxy data. We repeated this step 100 times for each dataset. The simulations hence captured intrinsic biases of both climate proxy data and our applied model structure. We then used the range of variation for the simulated models for significance testing (Fig. 3).

Robustness testing

Our simulations have shown that a minimum number of 1,000 observations is needed to produce statistically robust results (Extended Data Fig. 4). We therefore did not apply any subsampling method or sampling standardization to the observed data, as reducing the number of observations used in our analysis could increase type II errors. Further, GLMMs do not depend on perfect time continuous data record (Bolker et al., 2009) and are thus suitable for the imperfect nature of deep-time biotic data used in our analysis. Subsampling all our data would hence only increase statistical uncertainty without improving our analysis. Nevertheless, we tested for a systematic bias in our results by applying two subsampling methods to two fossil clades which had a sufficient number of genera (bivalves and reptiles). Subsampling did not alter results for these two clades, as model comparisons for subsampled data still indicated an improved model performance when a long-term temperature perspective is included (Extended Data Fig. 6). As expected, subsampling increased statistical uncertainty resulting in lower differences between AIC values.

We further tested if autocorrelation between the extinction signal and climate proxy data could bias our results (Extended Data Fig. 7). For this, we generated autocorrelated random time series for both extinction and climate proxy data and grouped them in a similar structure as our empirical data. We then processed these autocorrelated datasets using the same cleaning protocol as for our empirical data and applied our GLMM model structure to extract the simulated change in extinction risk for autocorrelated data. We did this for 900 datasets with directly correlated extinction/climate time series (red noise) and for 900 datasets with inversely correlated time series (blue noise). The intensity of autocorrelation for both red and blue noise differed for each simulated dataset. Results are within the same range as our null model with a mean change in extinction risk of 0 for red noise and 0.001 for blue noise (mean change of null model = −0.001). This shows that our model framework accounts for autocorrelation of the underlying data and that our null model simulation is appropriate to evaluate the probability of obtaining values as extreme as our empirical models. Additional to this, we tested for serial autocorrelation within each final empirical model. We simulated residuals for each model and calculated the Durbin–Watson statistic for temporal autocorrelation (Durbin & Watson, 1971). No model showed values below 1 or above 3 for the Durbin–Watson statistic, indicating low serial autocorrelation throughout our analysis (Extended Data Fig. 7).

Further robustness testing included assessing the impact of mass extinctions on the observed effect. We fitted GLMMs on all fossil groups and all stages and compared these with models excluding stages where the big five mass extinctions occurred (End-Ordovician, Late Devonian, End-Permian, End-Triassic and End-Cretaceous). Model comparison was based on the conditional coefficient for determination (pseudo-R2) for GLMMs (Nakagawa et al., 2017). Models without mass extinctions showed a slightly increased pseudo-R^2, indicating that the effect of palaeoclimate interactions on extinction risk is more severe during background extinction events (Extended Data Fig. 8).

Data availability

All data used to conduct analyses are available at https://github.com/Ischi94/pal-int-extinction.

Code availability

All scripts used to conduct analyses are available at https://github.com/Ischi94/pal-int-extinction.

Acknowledgements

This work was supported by the Deutsche Forschungsgemeinschaft (KI 806/16–1 and STE 2360/2-1) and is embedded in the Research Unit TERSANE (FOR 2332: Temperature-related stressors as a unifying principle in ancient extinctions). M.J.S. acknowledges support by European Research Council grant no. 741413 Humans on Planet Earth (HOPE).

Contributions

M.J.S. was responsible for conceptualization and supervision. G.H.M. undertook formal analysis, investigation and visualization. J.v.D. designed the methodology. W.K. secured resources. W.K. and M.J.S. were responsible for funding acquisition. G.H.M. wrote the original draft and the other authors were involved in reviewing and editing the final manuscript.

Competing interests

The authors declare no competing interests.

Additional information

Peer review information Nature Ecology & Evolution thanks Michael Benton, Noel Heim and the other, anonymous, reviewer(s) for their contribution to the peer review of this work. Peer reviewer reports are available.

References

Barnosky, A. D., Matzke, N., Tomiya, S., Wogan, G. O., Swartz, B., Quental, T. B., Marshall, C., McGuire, J. L., Lindsey, E. L., & Maguire, K. C. (2011). Has the Earth's sixth mass extinction already arrived? *Nature*, *471*(7336), 51–57.

Bates, D., Mächler, M., Bolker, B., & Walker, S. (2015). Fitting linear mixed-effects models using lme4. *Journal of Statistical Software*, 1–48. https://doi.org/10.18637/jss.v067.i01

Beaugrand, G. (2015). Theoretical basis for predicting climate-induced abrupt shifts in the oceans. *Philosophical Transactions of the Royal Society B: Biological Sciences*, *370*(1659), 20130264.

Bolker, B. M., Brooks, M. E., Clark, C. J., Geange, S. W., Poulsen, J. R., Stevens, M. H. H., & White, J.-S. S. (2009). Generalized linear mixed models: A practical guide for ecology and evolution. *Trends in Ecology & Evolution*, *24*(3), 127–135.

Bond, D. P., & Grasby, S. E. (2017). On the causes of mass extinctions. *Palaeogeography, Palaeoclimatology, Palaeoecology*, *478*, 3–29.

Boudaugher-Fadel, M. K. (2018). *Evolution and Geological Significance of Larger Benthic Foraminifera, Second Edition*. UCL Press.

Brook, B. W., & Alroy, J. (2017). Pattern, process, inference and prediction in extinction biology. In *Biology letters* (Vol. 13, Issue 1, p. 20160828). The Royal Society.

Burnham, K. P. (1998). Model selection and multimodel inference. *A Practical Information-Theoretic Approach*.

Calosi, P., Putnam, H. M., Twitchett, R. J., & Vermandele, F. (2019). Marine metazoan modern mass extinction: Improving predictions by integrating fossil, modern, and physiological data. *Annual Review of Marine Science*, *11*, 369–390.

Collins, K. S., Edie, S. M., Hunt, G., Roy, K., & Jablonski, D. (2018). Extinction risk in extant marine species integrating palaeontological and biodistributional data. *Proceedings of the Royal Society B: Biological Sciences*, *285*(1887), 20181698.

Coxall, H. K., & Pearson, P. N. (2007). The Eocene-Oligocene transition. *Deep Time Perspectives on Climate Change: Marrying the Signal from Computer Models and Biological Proxies*, 351–387.

Durbin, J., & Watson, G. S. (1971). Testing for serial correlation in least squares regression.III. *Biometrika*, *58*(1), 1–19. https://doi.org/10.1093/biomet/58.1.1

Finnegan, S., Anderson, S. C., Harnik, P. G., Simpson, C., Tittensor, D. P., Byrnes, J. E., Finkel, Z. V., Lindberg, D. R., Liow, L. H., & Lockwood, R. (2015). Paleontological baselines for evaluating extinction risk in the modern oceans. *Science*, *348*(6234), 567–570.

Foote, M. (2000). Origination and extinction components of taxonomic diversity: General problems. *Paleobiology*, *26*(sp4), 74–102.

Foote, M., Crampton, J. S., Beu, A. G., & Cooper, R. A. (2008). On the bidirectional relationship between geographic range and taxonomic duration. *Paleobiology*, *34*(4), 421–433.

Foster, G. L., Hull, P., Lunt, D. J., & Zachos, J. C. (2018). Placing our current 'hyperthermal'in the context of rapid climate change in our geological past. *Philosophical Transactions of the Royal Society A: Mathematical, Physical and Engineering Sciences*, *376*(2130), 20170086.

Fox, G. A., Negrete-Yankelevich, S., & Sosa, V. J. (2015). *Ecological Statistics: Contemporary Theory and Application*. Oxford University Press.

García Molinos, J., Halpern, B. S., Schoeman, D. S., Brown, C. J., Kiessling, W., Moore, P. J., Pandolfi, J. M., Poloczanska, E. S., Richardson, A. J., & Burrows, M. T. (2016). Climate velocity and the future global redistribution of marine biodiversity. *Nature Climate Change*, *6*(1), 83–88. https://doi.org/10.1038/nclimate2769

Gradstein, F. M., Ogg, J. G., Schmitz, M., & Ogg, G. (2012). *The Geologic Time Scale 2012*. Elsevier.

Grossman, E. L. (2012). Applying Oxygen Isotope Paleothermometry in Deep Time. *The*

Paleontological Society Papers, *18*, 39–68. https://doi.org/10.1017/S1089332600002540

Harnik, P. G. (2011). Direct and indirect effects of biological factors on extinction risk in fossil bivalves. *Proceedings of the National Academy of Sciences*, *108*(33), 13594–13599.

Harnik, P. G., Lotze, H. K., Anderson, S. C., Finkel, Z. V., Finnegan, S., Lindberg, D. R., Liow, L. H., Lockwood, R., McClain, C. R., & McGuire, J. L. (2012). Extinctions in ancient and modern seas. *Trends in Ecology & Evolution*, *27*(11), 608–617.

Harnik, P. G., Simpson, C., & Payne, J. L. (2012). Long-term differences in extinction risk among the seven forms of rarity. *Proceedings of the Royal Society B: Biological Sciences*, *279*(1749), 4969–4976.

Henkes, G. A., Passey, B. H., Grossman, E. L., Shenton, B. J., Yancey, T. E., & Pérez-Huerta, A. (2018). Temperature evolution and the oxygen isotope composition of Phanerozoic oceans from carbonate clumped isotope thermometry. *Earth and Planetary Science Letters*, *490*, 40–50. https://doi.org/10.1016/j.epsl.2018.02.001

Hopkins, M. J., Simpson, C., & Kiessling, W. (2014). Differential niche dynamics among major marine invertebrate clades. *Ecology Letters*, *17*(3), 314–323. https://doi.org/10.1111/ele.12232

Kiessling, W., & Kocsis, Á. T. (2016). Adding fossil occupancy trajectories to the assessment of modern extinction risk. *Biology Letters*, *12*(10), 20150813.

Kocsis, À. T., Reddin, C. J., Alroy, J., & Kiessling, W. (2019). The R package divDyn for quantifying diversity dynamics using fossil sampling data. *Methods in Ecology and Evolution*, *10*(5), 735–743.

Leckie, R. M., Bralower, T. J., & Cashman, R. (2002). Oceanic anoxic events and plankton evolution: Biotic response to tectonic forcing during the mid-Cretaceous: OCEANIC ANOXIC EVENTS AND PLANKTON EVOLUTION. *Paleoceanography*, *17*(3), 13-1-13–29. https://doi.org/10.1029/2001PA000623

Lieberman, M. D., & Cunningham, W. A. (2009). Type I and Type II error concerns in fMRI research: Re-balancing the scale. *Social Cognitive and Affective Neuroscience*, *4*(4), 423–428. https://doi.org/10.1093/scan/nsp052

Lord, J. P., Barry, J. P., & Graves, D. (2017). Impact of climate change on direct and indirect species interactions. *Marine Ecology Progress Series*, *571*, 1–11.

Malik, W. A., Marco-Llorca, C., Berendzen, K., & Piepho, H.-P. (2020). Choice of link and variance function for generalized linear mixed models: A case study with binomial response in proteomics. *Communications in Statistics - Theory and Methods*, *49*(17), 4313–4332. https://doi.org/10.1080/03610926.2019.1599021

Masson-Delmotte, V., Pörtner, H.-O., Skea, J., Zhai, P., Roberts, D., Shukla, P. R., Pirani, A., Pidcock, R., Chen, Y., Lonnoy, E., Moufouma-Okia, W., Péan, C., Connors, S., Matthews, J. B. R., Zhou, X., Gomis, M. I., Maycock, T., Tignor, M., & Waterfield, T. (2018). *An IPCC Special Report on the impacts of global warming of 1.5°C above pre-industrial levels and related global greenhouse gas emission pathways, in the context of strengthening the global response to the threat of climate change, sustainable development, and efforts to eradicate poverty*. 630.

McKinney, M. L. (1997). Extinction vulnerability and selectivity: Combining ecological and paleontological views. *Annual Review of Ecology and Systematics*, 495–516.

Nakagawa, S., Johnson, P. C. D., & Schielzeth, H. (2017). *The coefficient of determination R2 and intra-class correlation coefficient from generalized linear mixed-effects models revisited and expanded | Journal of The Royal Society Interface*. https://royalsocietypublishing.org/doi/full/10.1098/rsif.2017.0213

Normand, S., Ricklefs, R. E., Skov, F., Bladt, J., Tackenberg, O., & Svenning, J.-C. (2011). Postglacial migration supplements climate in determining plant species ranges in Europe. *Proceedings of the Royal Society B: Biological Sciences*, *278*(1725), 3644–3653.

Payne, J. L., Truebe, S., Nützel, A., & Chang, E. T. (2011). Local and global abundance associated with extinction risk in late Paleozoic and early Mesozoic gastropods. *Paleobiology*, *37*(4), 616–632.

Pecl, G. T., Araújo, M. B., Bell, J. D., Blanchard, J., Bonebrake, T. C., Chen, I.-C., Clark, T. D., Colwell, R. K., Danielsen, F., & Evengård, B. (2017). Biodiversity redistribution under climate change: Impacts on ecosystems and human well-being. *Science*, *355*(6332), eaai9214.

Penn, J. L., Deutsch, C., Payne, J. L., & Sperling, E. A. (2018). Temperature-dependent hypoxia explains biogeography and severity of end-Permian marine mass extinction. *Science*, *362*(6419), eaat1327.

Quené, H., & van den Bergh, H. (2008). Examples of mixed-effects modeling with crossed random effects and with binomial data. *Journal of Memory and Language*, *59*(4), 413–425. https://doi.org/10.1016/j.jml.2008.02.002

R Core Team. (2021). *R: A Language and Environment for Statistical Computing* (4.1.2) [R]. R Foundation for Statistical Computing. https://www.R-project.org/

Reddin, C. J., Kocsis, Á. T., & Kiessling, W. (2018). Marine invertebrate migrations trace climate change over 450 million years. *Global Ecology and Biogeography*, *27*(6), 704–713. https://doi.org/10.1111/geb.12732

Reddin, C. J., Nätscher, P. S., Kocsis, Á. T., Pörtner, H.-O., & Kiessling, W. (2020). Marine clade sensitivities to climate change conform across timescales. *Nature Climate Change*, *10*(3), 249–253. https://doi.org/10.1038/s41558-020-0690-7

Ritterbush, K. A., & Foote, M. (2017). Association between geographic range and initial survival of Mesozoic marine animal genera: Circumventing the confounding effects of temporal and taxonomic heterogeneity. *Paleobiology*, *43*(2), 209–223. https://doi.org/10.1017/pab.2016.25

Ryb, U. (2018). *Oxygen isotope composition of the Phanerozoic ocean and a possible solution to the dolomite problem | PNAS*. https://www.pnas.org/doi/abs/10.1073/pnas.1719681115

Song, H., Wignall, P. B., Song, H., Dai, X., & Chu, D. (2019). Seawater temperature and dissolved oxygen over the past 500 million years. *Journal of Earth Science*, *30*(2), 236–243.

Steinbauer, M. J., Field, R., Fernández‐Palacios, J. M., Irl, S. D. H., Otto, R., Schaefer, H., Beierkuhnlein, C., & Santos, A. M. C. (2016). Biogeographic ranges do not support niche theory in radiating C anary I sland plant clades. *Global Ecology and Biogeography*, *25*(7), 792–804. https://doi.org/10.1111/geb.12425

Stigall, A. L. (2013). Analysing links between biogeography, niche stability and speciation: The impact of complex feedbacks on macroevolutionary patterns: Biotic and environmental impacts on speciation. *Palaeontology*, *56*(6), 1225–1238. https://doi.org/10.1111/pala.12003

Stigall, A. L. (2014). When and how do species achieve niche stability over long time scales? *Ecography*, *37*(11), 1123–1132. https://doi.org/10.1111/ecog.00719

Svenning, J.-C., & Skov, F. (2004). Limited filling of the potential range in European tree species. *Ecology Letters*, *7*(7), 565–573.

Urban, M. C. (2015). Accelerating extinction risk from climate change. *Science*, *348*(6234), 571–573. https://doi.org/10.1126/science.aaa4984

Valentine, J. W. (1974). Temporal bias in extinctions among taxonomic categories. *Journal of Paleontology*, 549–552.

van Woesik, R., Franklin, E. C., O'Leary, J., McClanahan, T. R., Klaus, J. S., & Budd, A. F. (2012). Hosts of the Plio-Pleistocene past reflect modern-day coral vulnerability. *Proceedings of the Royal Society B: Biological Sciences*, *279*(1737), 2448–2456.

Veizer, J., & Prokoph, A. (2015). Temperatures and oxygen isotopic composition of Phanerozoic oceans. *Earth-Science Reviews*, *146*, 92–104.

Wickham, H., Averick, M., Bryan, J., Chang, W., McGowan, L. D., François, R., Grolemund, G., Hayes, A., Henry, L., & Hester, J. (2019). Welcome to the Tidyverse. *Journal of Open Source Software*, *4*(43), 1686.

Wiens, J. J., & Graham, C. H. (2005). Niche conservatism: Integrating evolution, ecology, and conservation biology. *Annual Review of Ecology, Evolution, and Systematics*, *36*(1), 519–539. https://doi.org/10.1146/annurev.ecolsys.36.102803.095431

Zuur, A. F., Ieno, E. N., Walker, N. J., Saveliev, A. A., & Smith, G. M. (2009). Mixed Effects Modelling for Nested Data. In A. F. Zuur, E. N. Ieno, N. Walker, A. A. Saveliev, & G. M. Smith (Eds.), *Mixed effects models and extensions in ecology with R* (pp. 101–142). Springer. https://doi.org/10.1007/978-0-387-87458-6_5

Extended Data

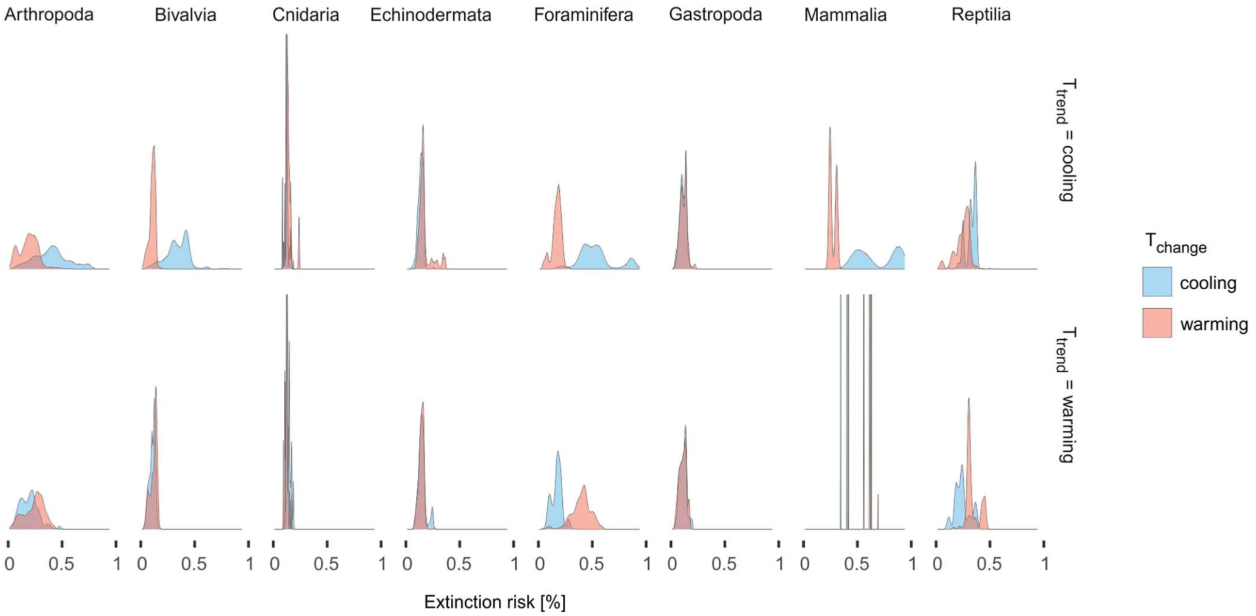

Extended Data Fig. 1: Density distribution of GLMM results. The difference in distributions were used to assess change in extinction probability of taxa due to paleoclimate interaction. Upper row blue areas show distributions of extinction risk subsequent to cooling–cooling interaction. Upper row red area cooling–warming interaction. Lower row blue area warming-cooling interaction. Lower row red area warming–warming interact

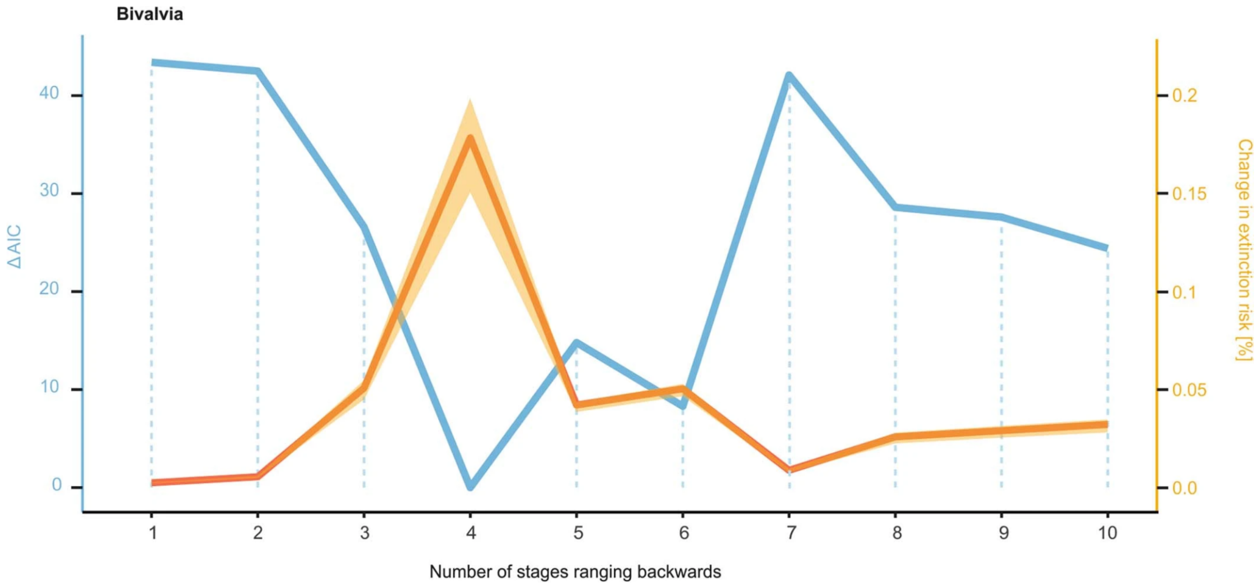

Extended Data Fig. 2: Temporal memory of the effect of paleoclimate interaction compared to the intensity of the effect. The model with the lowest ∆AIC (here representatively shown for cooling–cooling of bivalvia) universally showed the highest effect of past temperature change on extinction risk. Effect intensity decreased with increasing AIC of the remaining models, enabling determination of the temporal memory of the effect. Trends one to ten covered a successively growing time of temperature history: Trend1 ranged one stage back, trend2 two stages, …, trend10 ten stages (methods)

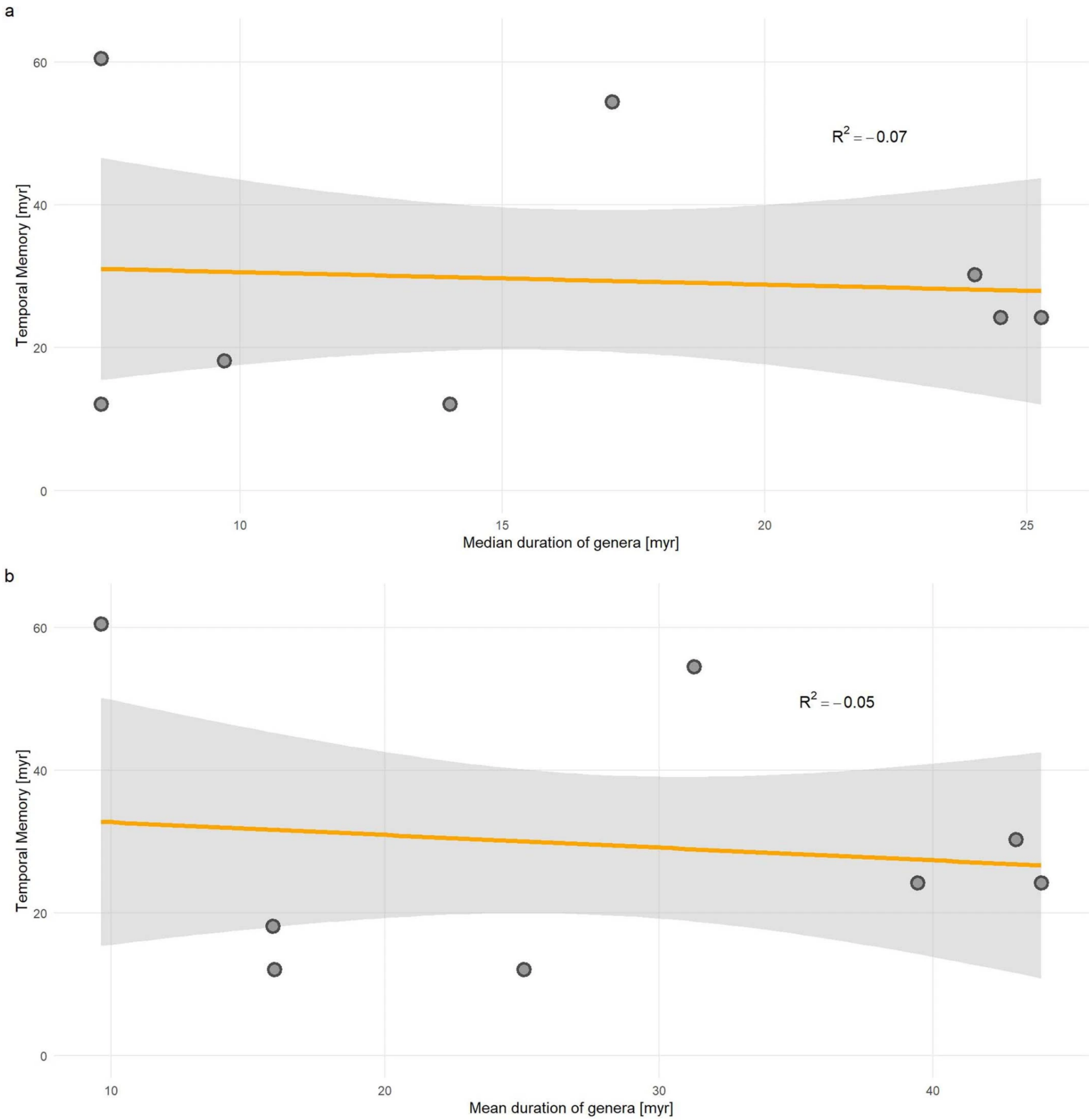

Extended Data Fig. 3: Temporal memory of paleoclimate interaction for fossil clades related to genus duration. ***a,*** *Temporal memory versus median durations of fossil clades and* ***(b)*** *mean durations. Grey area depicts the 95 % confidence interval of the regression slope. Trend line and R2 value are based on univariate linear regression and are not significant (p-value for median duration = 0.79 and for mean duration = 0.63).*

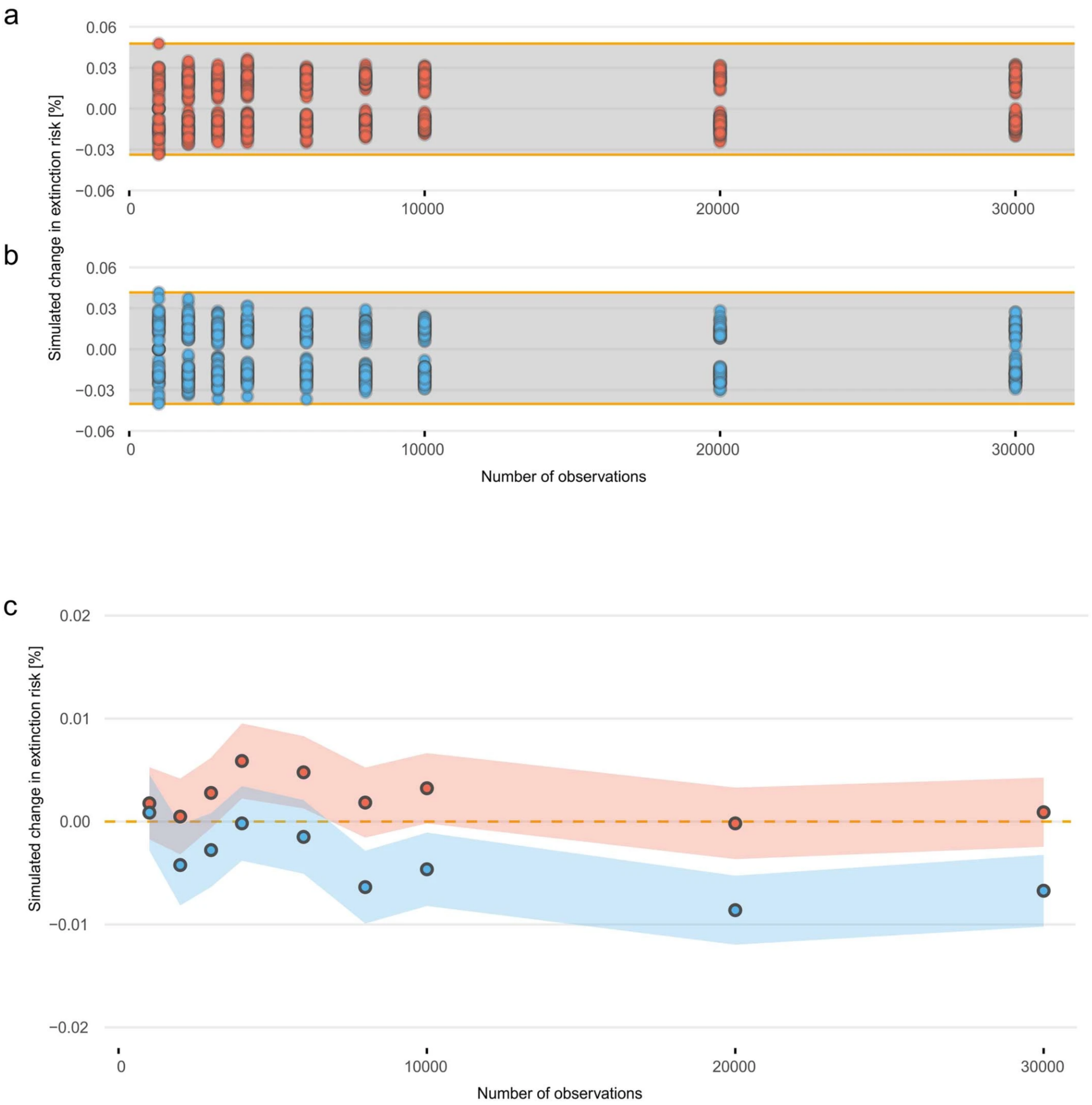

Extended Data Fig. 4: Results of simulations for null model. Change of extinction risk of null models based on simulated data for datasets with varying sizes for warming–warming palaeoclimate interaction is shown in (a), and for cooling–cooling interaction in (b). We simulated datasets with increasing number of observations and calculated 100 GLMM's for each to determine Type I Error rate of models used in our analysis. The shaded area shows the distribution of all 100 model results for warming–warming and cooling–cooling interaction respectively. The mean for each number of observations and its corresponding 95 % Wald Confidence Interval is shown in (c), where the red points and shaded intervals show the simulated response to warming–warming palaeclimate interaction, and blue points and shaded intervals to cooling–cooling.

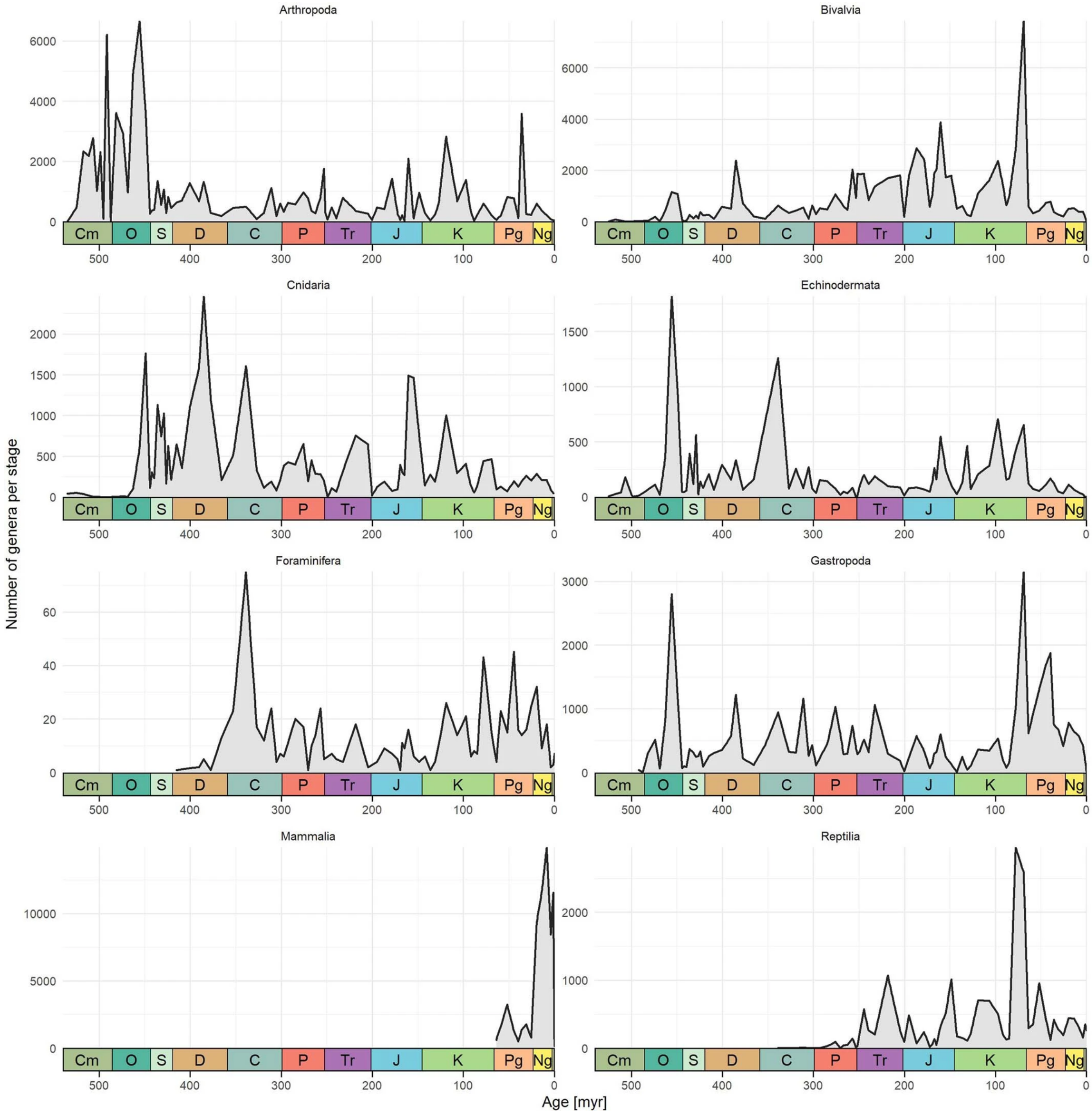

Extended Data Fig. 5: Number of fossil genera within datasets. The number of genera is shown for each fossil clade and for each stage. This is based on raw data (before filtering and processing of data).

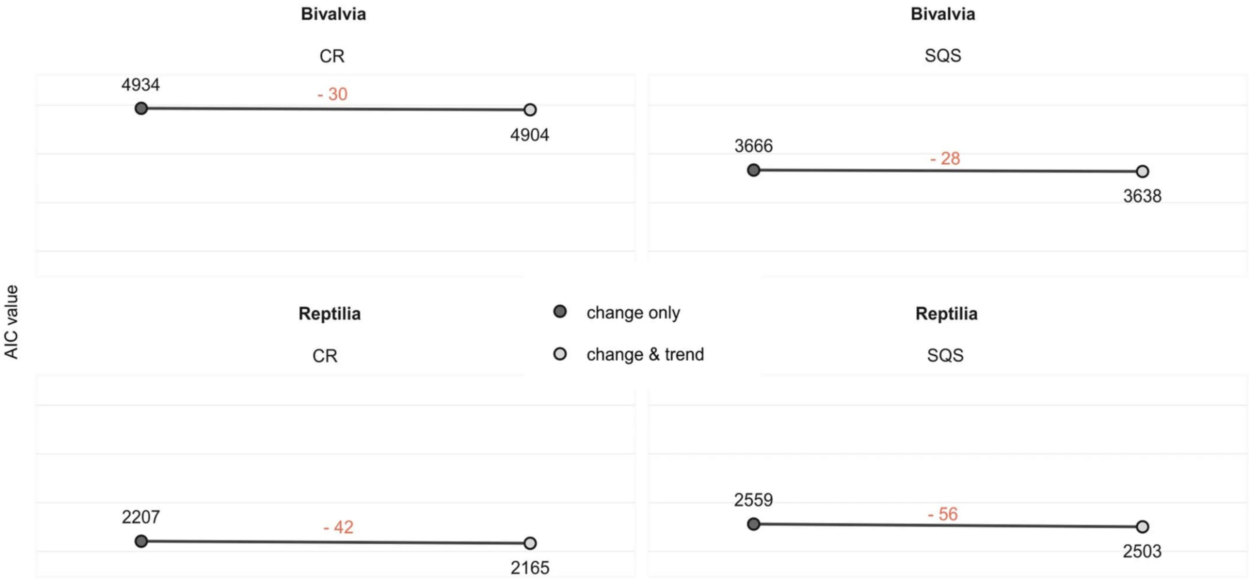

Extended Data Fig. 6: Model comparison of subsampled data for robustness testing for bivalves and reptiles. Values show AIC values after shareholder quorum subsampling (SQS) and classical rarefaction (CR). After subsampling, model quality of traditional models (change only) is compared to quality of models taking palaeoclimate interaction into account (change & trend), to test if models improve when long-term temperature trends are included. Red text indicates an improved model performance when palaeoclimate interactions are included. We used a shareholder quorum of 0.4 and classical rarefaction with 50 occurrences.

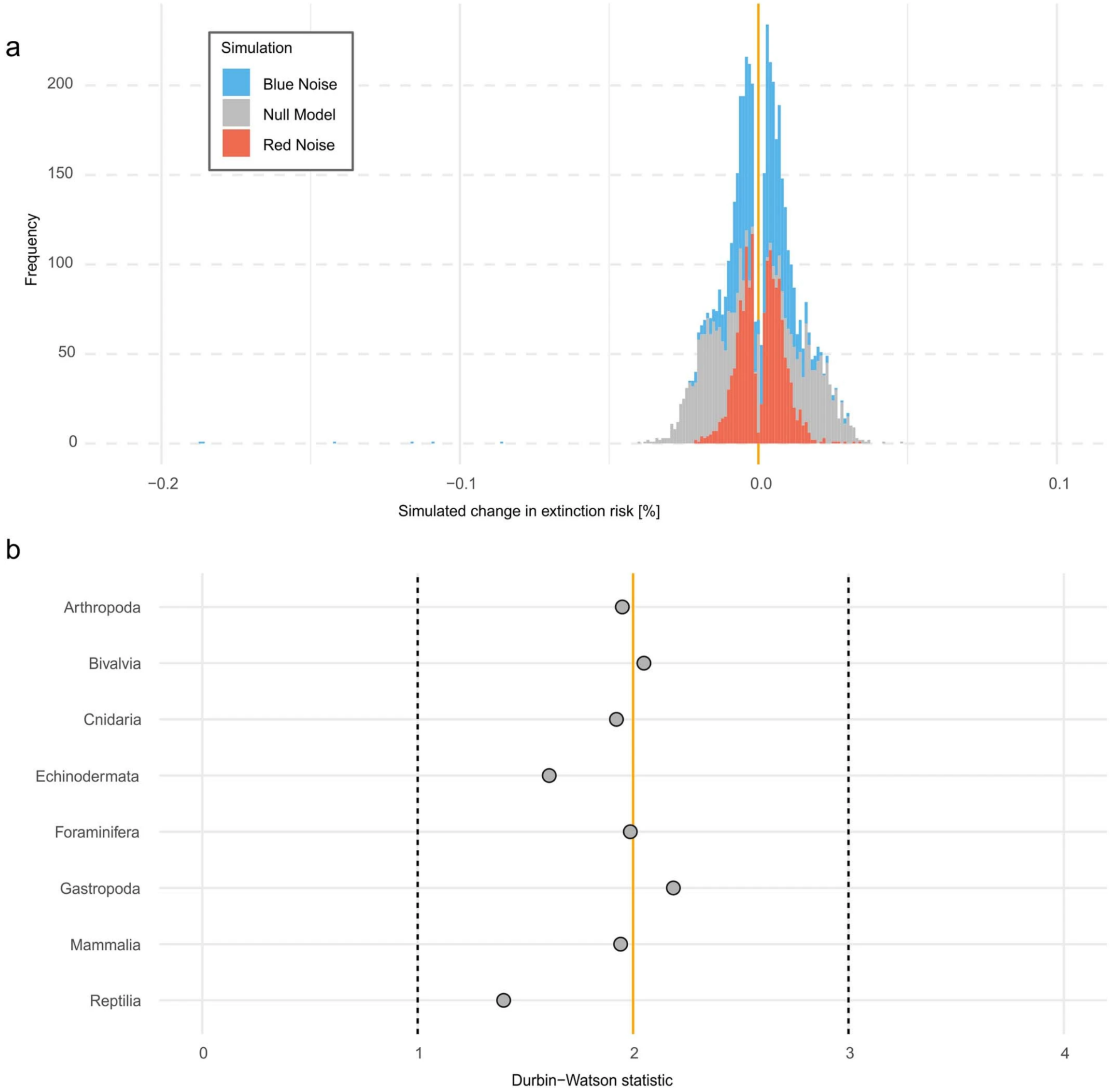

Extended Data Fig. 7: Simulations for potential autocorrelation bias. **a,** Simulations were used to test if autocorrelation between the extinction signal and climate proxy data could bias our results. The results from these simulations show that the simulated extinction risk for both blue (inversely correlated) and red noise (positively correlated) is within the range of the null models, indicating that autocorrelation does not bias our results. **b,** We additionally tested for serial autocorrelation of the final GLMMs. No model shows indication for a strong serial autocorrelation. Durbin–Watson statistic values below 1 generally indicate a strong positive autocorrelation, values above 3 a strong negative autocorrelation and values around 2 no autocorrelation.

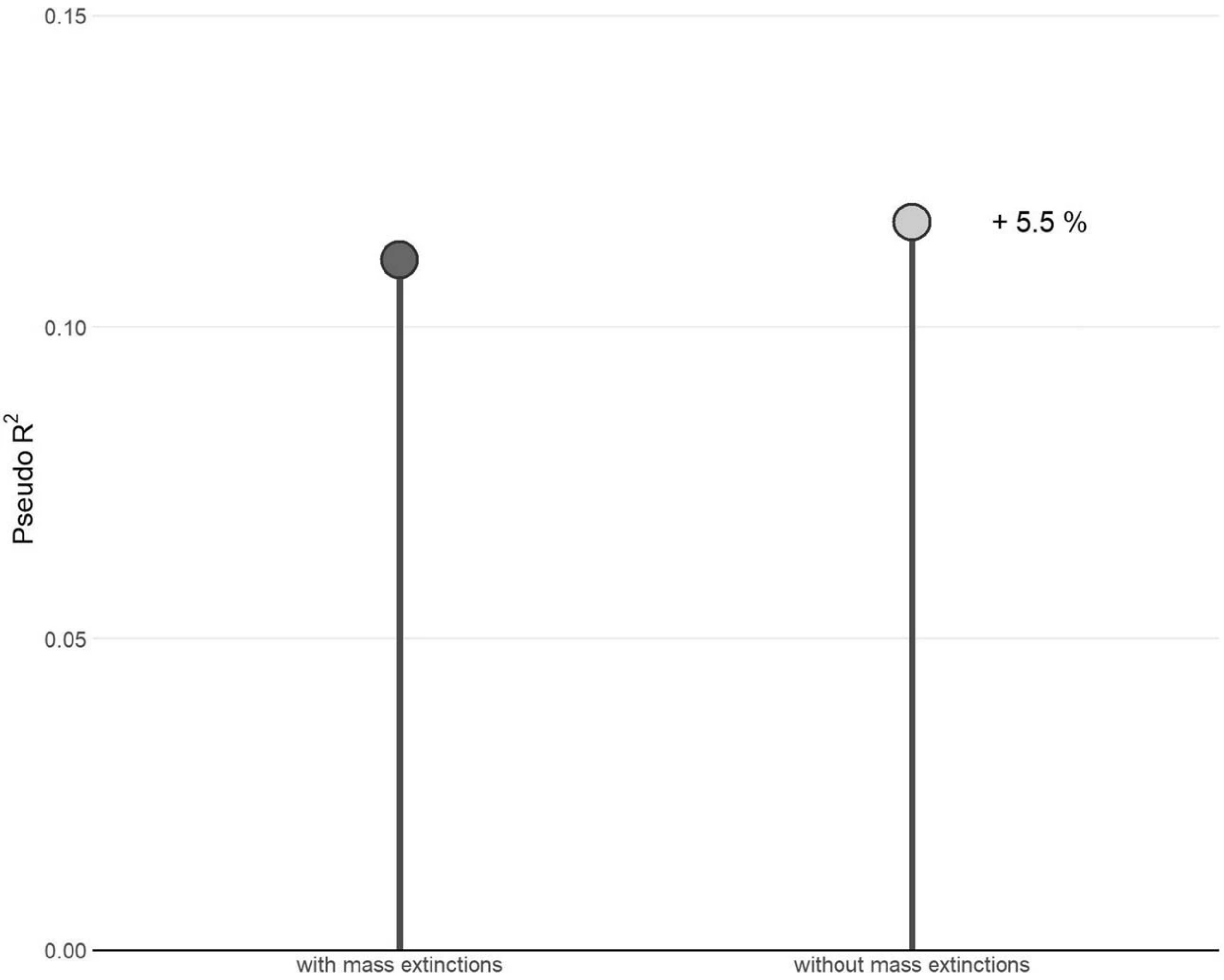

Extended Data Fig. 8: The effect of mass extinctions on the observed effect. Models fitted on all fossil groups and all stages were compared to models excluding stages where the big five mass extinctions occurred (End-Ordovician, Late Devonian, End-Permian, End-Triassic and End-Cretaceous). For each model, the proportion of the variance using the conditional coefficient for determination (pseudo-R2) was quantified.

Manuscript 2

Five million years of high atmospheric CO2 in the aftermath of the Permian-Triassic mass extinction

***Geology* 50 (2022) DOI: https://doi.org/10.1130/G49714.1**

Michael M. Joachimski[1*], Johann Müller[1], Timothy M. Gallagher[2], Gregor H. Mathes[3], Daoliang L. Chu[4], Fedor Mouraviev[5], Vladimir Silantiev[5], Yadong D. Sun[1], Jinnan N. Tong[4]

[1]GeoZentrum Nordbayern, Friedrich-Alexander Universität Erlangen-Nürnberg (FAU), Erlangen 91054, Germany.
[2]Department of Geology, Kent State University, Kent, Ohio 44240, USA.
[3]Department of Sport Science & Bayreuth Center of Ecology and Environmental Research (BayCEER), Universität Bayreuth, Bayreuth 95447, Germany.
[4]State Key Laboratory of Biogeology and Environmental Geology, School of Earth Sciences, China University of Geosciences, Wuhan 430074, China.
[5]Geology and Petroleum Technologies, Kazan Federal University, 420008 Kazan, Russia.
* Corresponding author: michael.joachimski@fau.de

ABSTRACT

The end-Permian mass extinction, the largest biological crisis in Earth history, is currently understood in the context of Siberian Traps volcanism introducing large quantities of greenhouse gases to the atmosphere, culminating in the Early Triassic hothouse. In our study, the late Permian and Early Triassic atmospheric CO^2 history was reconstructed by applying the paleosol $p\mathrm{CO}^2$ barometer. Atmospheric $p\mathrm{CO}^2$ shows an approximate 4× increase from mean concentrations of 412–919 ppmv in the late Permian (Changhsingian) to maximum levels between 2181 and 2610 ppmv in the Early Triassic (late Griesbachian). Mean CO^2 estimates for the later Early Triassic are between 1261–1936 ppmv (Dienerian) and 1063–1757 ppmv (Spathian). Significantly lower concentrations ranging from 343 to 634 ppmv are reconstructed for the latest Early to Middle Triassic (Anisian). The 5 m.y. episode of elevated $p\mathrm{CO}^2$ suggests that negative feedback mechanisms such as silicate weathering were not effective enough to reduce atmospheric $p\mathrm{CO}^2$ to precrisis levels and that marine authigenic clay formation (i.e., reverse weathering) may have been an important component of the global carbon cycle keeping atmospheric $p\mathrm{CO}^2$ at elevated levels.

INTRODUCTION

The end-Permian mass extinction (ca. 252 Ma) coincided with the onset of intrusive Siberian Traps volcanism, which was likely responsible for outgassing of large quantities of CO_2, CH4, and halogens by thermogenic heating of volatile-rich sediments (Courtillot and Renne, 2003; Svensen et al., 2009; Burgess and Bowring, 2015). The inferred increase in greenhouse gas concentrations has been interpreted to have resulted in a dramatic 8–10 °C increase in low-latitude sea-surface temperature (SST), with high ocean temperatures persisting into the Early Triassic (e.g., Sun et al., 2012; Joachimski et al., 2020). However, a proxy record for atmospheric pCO_2 has yet to be established for the late Permian to Early Triassic.

We reconstructed the late Permian to Middle Triassic atmospheric CO_2 record by applying the carbonate paleosol pCO_2 barometer to soil carbonates from sections in northwest China (Xinjiang Province), north China (Henan and Shanxi Provinces), Russia (South Ural foreland basin), South Africa (Karoo Basin), and the United Kingdom (Dorset) (Fig. 1; Table S1 in the Supplemental Material1). Stratigraphically, the samples cover the Changhsingian (late Permian) to earliest Griesbachian, late Griesbachian to Dienerian, and Spathian to Anisian (Early to Middle Triassic). Reconstructed atmospheric CO_2 levels suggest an approximate 4-fold increase in pCO_2 from the latest Permian to Early Triassic, high to intermediate CO_2 levels in the Early Triassic, and a decline to precrisis levels in the latest Early Triassic.

Paleosol *p*CO^2 barometer

We calculated atmospheric CO_2 concentrations from the carbon isotopic composition of microsampled micritic soil carbonate precipitated in the well-drained soils by applying a two-component carbon isotope mixing model, given that soil CO_2 is a mixture of two isotopically different CO_2 sources (soil-respired CO_2 and atmospheric CO_2; Cerling, 1991):

$$[\mathrm{CO_2}]_{\mathrm{atm}} = S(\mathrm{z}) \times \frac{(\delta^{13}\mathrm{C_s} - 1.0044 \times \delta^{13}\mathrm{C_{resp}} - 4.4)}{\delta^{13}\mathrm{C_{atm}} - \delta^{13}\mathrm{C_s}}. \qquad (1)$$

Here, S(z) is the soil-derived (respired) component of total soil CO_2, and $\delta^{13}C_s$, $\delta^{13}C_{resp}$, and $\delta^{13}C_{atm}$ represent the carbon isotopic compositions of total soil CO_2, soil-respired CO_2, and atmospheric CO_2, respectively. The $\delta^{13}C_s$, $\delta^{13}C_{resp}$, and $\delta^{13}C_{atm}$ values were calculated from the measured $\delta^{13}C$ value of pedogenic carbonate, soil organic matter (SOM) occluded in the carbonate nodules, and marine carbonate, respectively.

The soil-derived contribution of CO_2, S(z), and the soil temperature must be assumed, presenting the main uncertainties for paleo-pCO_2 reconstructions. While earlier studies used high S(z) values of 5000 ppmv (e.g., Ekart et al., 1999), representing soil CO_2 concentrations of the mean growing season, later studies observed that pedogenic carbonate precipitation mainly occurs during warm and dry periods characterized by a relatively low soil pCO_2 due to moisture-limited soil respiration (Breecker et al., 2009). We assumed S(z) values between 500 and 1500 ppmV following Montañez (2013), who used the $\delta^{13}C$ difference between modern soil carbonate and SOM ($\Delta_{carb\text{-}org}$) to constrain S(z) for different soil orders (see the Supplemental Material for details).

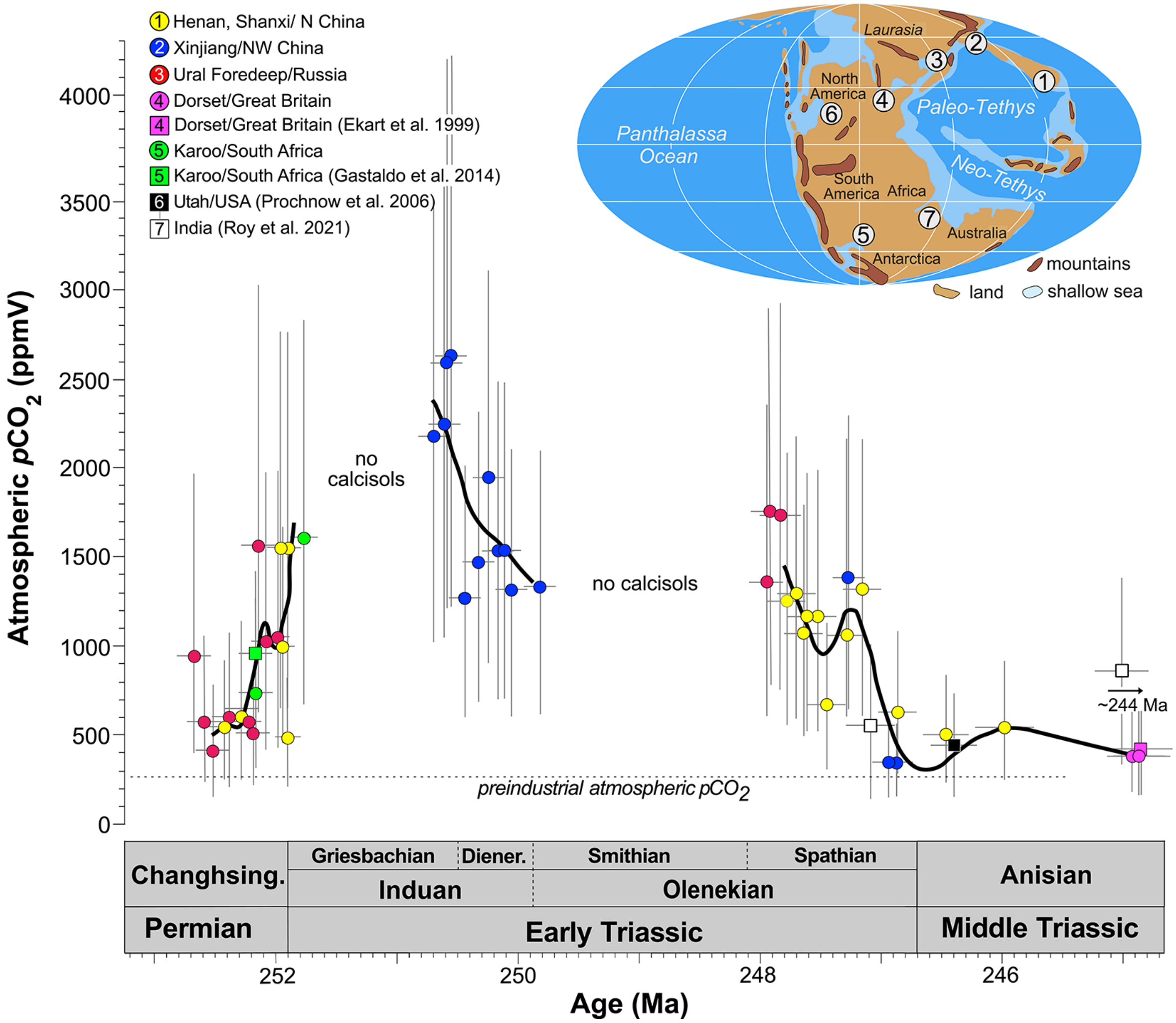

Figure 1: The Permian-Triassic atmospheric CO_2 *record. Symbols represent mean values of atmospheric* pCO_2 *calculated based on the distribution of all possible values by varying soil temperature (T), soil-respired* CO_2 *concentration [S(z)], and* $\delta^{13}C$ *of atmospheric* CO_2*. Vertical bars are 95% credible intervals for each estimate, calculated using quantile intervals of distribution of all possible values of each sample. Horizontal bars give sample age uncertainties. Trend line represents the Locfit (https://cran.r-project.org/web/packages/locfit/index.html) regression (α = 0.6). Stratigraphic scheme and absolute ages are according the Geological Time Scale 2020 (Ogg and Chen, 2020). Permian-Triassic paleogeographic reconstruction with study locations after Scotese and Moore (2014). Changhsing—Changhsingian; Diener—Dienerian.*

Soil temperature has to be estimated in order to calculate δ^{13}Cresp from the δ^{13}C value of pedogenic carbonate, utilizing the temperature-dependent carbon isotope fractionation between CO_2 and CO_3^{2-} (Romanek et al., 1992). Soil temperatures for the calcisols formed at various paleolatitudes were estimated using low-latitude SSTs (Sun et al., 2012; Joachimski et al., 2020), a low-latitudinal temperature gradient for warm climatic conditions (0.2 °C per 1° latitude; Zhang et al., 2019), air temperatures 3 °C lower than SSTs (Zhang et al., 2019), and 2–4 °C warmer soil temperatures compared to atmospheric temperatures (Hu and Feng, 2003; Table S2).

Atmospheric pCO$_2$ was calculated for each possible combination of S(z), soil temperature (Table S2), and δ^{13}C of atmospheric CO$_2$ (Table S3) by varying S(z) from 500 to 1500 ppmv in 100 ppm steps, increasing soil temperature in 1 °C steps (using a ±5 °C temperature range around estimated average soil temperature), and δ^{13}C of atmospheric CO$_2$ in 0.1‰ steps. Mean atmospheric CO$_2$ concentrations for each sample were then calculated based on the distribution of all possible values. The 95% credible interval (CI) for each estimate and sample was calculated using the quantile intervals (95% CI [lower quantile, upper quantile]) of the distribution of all possible values of each sample (Table S4).

RESULTS

Studied paleosols

All studied paleosols were classified as Calcisols because they are characterized by rare to common carbonate nodules (up to several centimeters in size; stage II nodules) or layers with stacked carbonate nodules and rhizocretions (stage II; Fig. S1). Of a total of 105 pedogenic carbonate samples, 46 carbonates showed characteristic pedogenic features (Fig. S2) as well as carbon isotope values indicative of carbonate precipitation under the influence of atmospheric CO$_2$, and these were accepted as having formed in the nonsaturated zone and used for atmospheric pCO$_2$ reconstruction (see the Supplemental Material).

Permian–Triassic Atmospheric pCO$_2$

Mean atmospheric pCO$_2$ showed a significant increase from the latest Permian (Changhsingian) to Early Triassic, with elevated pCO$_2$ persisting until the latest Early Triassic (Fig. 1). Late Changhsingian mean atmospheric pCO$_2$ estimates derived from Russian, North China, and Karoo samples are generally between 412 (95% CI [162, 688]) and 949 ppmv (95% CI [400, 1743]; n = 9). Atmospheric CO$_2$ started to increase before the Permian-Triassic boundary (PTB) to levels between 1031 ppmv (95% CI [419, 1966]) and 1558 ppmv (95% CI [676, 2789]; n = 6). Sample PY2 (north China) yielded a lower atmospheric CO$_2$ content of 483 ppmv (95% CI [214, 833]). In the earliest Griesbachian, the mean pCO$_2$ was at 1606 ppmv (95% CI [689, 2919]). Atmospheric pCO$_2$ in the late Griesbachian (Xinjiang) ranged from 2181 (95% CI [1025, 3516]) to 2610 ppmv (95% CI [1224, 4226]; n = 4), being on average 4× higher than Changhsingian background levels. Estimates for the Dienerian (Xinjiang) are between 1261 (95% CI [596, 2009]) and 1936 ppmv (95% CI [921, 3104]; n = 6), while estimates for the Spathian paleosols (Russia, North China, and Xinjiang) range from 1063 (95% CI [490, 1765]) to 1757 ppmv (95% CI [792, 2994]; n = 11), except sample DYLY, which yielded a CO$_2$ concentration of 671 ppmv (95% CI [306, 1124]). Terminal hothouse (latest Spathian and Anisian) pCO$_2$ estimates based on paleosols from Xinjiang, North China, and the United Kingdom are between 343 (95% CI [155, 575]) and 634 ppmv (95% CI [285, 1067]; n = 6), i.e., considerably lower than most Early Triassic *p*CO_2 estimates but comparable to Changhsingian CO_2 levels.

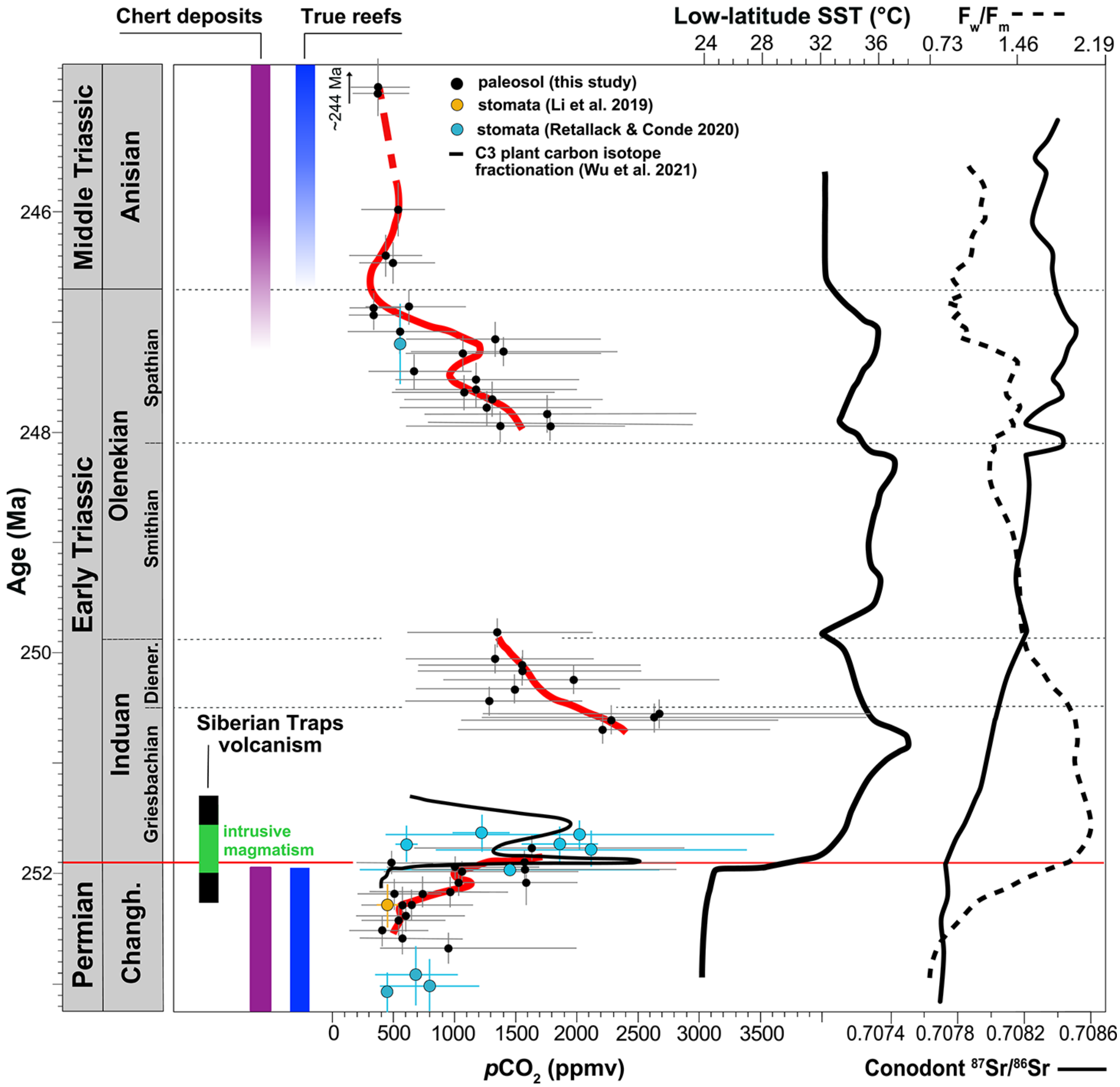

Figure 2: Comparison of Permian-Triassic atmospheric pCO2 estimates, low-latitude sea-surface temperature (SST; Sun et al., 2012; Joachimski et al., 2020), conodont $^{87}Sr/^{86}Sr$, and modeled ratio of terrestrial Sr (Fw) versus mantle Sr (Fm) flux (Song et al., 2015). Red trend line represents the Locfit (https://cran.r-project.org/web/packages/locfit/index.html) regression (α = 0.6) for mean paleosol pCO_2 estimates. Note the relatively good correspondence among pCO_2, SST, and modeled Fw/Fm, suggesting that although continental weathering increased, atmospheric pCO_2 and SSTs stayed at high levels. Siberian Traps volcanism is from Burgess and Bowring (2015). Changh—Changhsingian; Diener—Dienerian. Chert and reef record modified after Chen and Benton (2012).

DISCUSSION

The atmospheric pCO_2 estimates are in good agreement with published pCO_2 reconstructions from paleosol nodules (Karoo Basin—Gastaldo et al., 2014; India—Roy et al., 2021), stomatal index data (Li et al., 2019; Retallack and Conde, 2020), and in part with estimates based on C_3 plant carbon isotope fractionation (Wu et al., 2021; Fig. 2). However, the reliability of this latter method is controversial (e.g., Lomax et al., 2019). This could explain the significant drop in pCO_2 above the PTB reconstructed by Wu et al. (2021), which is at odds with increasing low-latitude SSTs as well as high Dienerian and Spathian pCO_2 values (this study; Fig. 2). Published Anisian paleosol pCO_2 estimates were recalculated (Fig. 1), as they had originally been calculated with S(z) of up to 5000 ppmv (Ekart et al. 1999; Prochnow et al. 2006). Most importantly, the generally good agreement among pCO_2 estimates reconstructed from time-equivalent paleosols from distant sites (this study; Fig. 1) and the comparable estimates derived from other CO_2 proxies (Fig. 2) underline the validity of the atmospheric CO_2 record presented here. However, the evolution of atmospheric pCO_2 during most of the Griesbachian and the Smithian remains unresolved because no suitable pedogenic carbonates have been found for these periods.

Early Triassic Greenhouse

Siberian Traps volcanism is interpreted as a proximate cause of the 4× increase in atmospheric CO_2 from the latest Permian (Changhsingian) to Early Triassic (late Griesbachian). The onset of Siberian effusive volcanism has been dated prior to 252.2 ± 0.1 Ma (Burgess and Bowring, 2015), ~300 k.y. before the end-Permian mass extinction. Subsequent intrusive magmatism starting at 251.9 ± 0.067 Ma probably produced >100.000 GT of CO_2 and CH_4 by thermogenic heating of sediments around large sill intrusions (Svensen et al., 2009; Augland et al., 2019). This massive emission of greenhouse gases (depleted in ^{13}C) has been suggested as the main cause of dramatic global warming, as well as of the negative carbon isotope excursion recorded globally in the latest Changhsingian to early Griesbachian (Fig. 2).

Parallel to the reconstructed rise in atmospheric pCO_2 from 412–949 ppmv in the latest Changhsingian to 2181–2610 ppmv in the late Griesbachian, low-latitude SSTs calculated from oxygen isotopes measured on conodont apatite (Fig. 2) increased by 7–10 °C, from 25–28 °C to >35 °C (Joachimski et al., 2020). With the decrease in pCO_2 in the late Spathian to Anisian, SSTs decreased again (Sun et al., 2012; Fig. 2). Thus, pCO_2 as well as SSTs persisted at high levels for almost 5 m.y. (Fig. 2), representing an unusually long time interval. High atmospheric pCO_2 conditions could only be sustained either by continuous and massive CO_2 outgassing from Siberian Traps or by reduced CO_2 consumption by continental silicate weathering and biological uptake. The emplacement of large volumes of subvolcanic intrusions (sills and dikes) started in the latest Changhsingian but continued for only 0.5 m.y. into the Early Triassic (Augland et al., 2019; Burgess and Bowring, 2015). Although large igneous province volcanism has been reported to have been active until the end of the Middle Triassic (Ivanov, 2007), published geochronological data have large uncertainties of ~5 m.y. and cannot resolve whether contact metamorphism resulted in prolonged degassing after the initial violent pulse (Augland et al., 2019). Notably, Hg concentrations in marine carbonates argue for massive volcanic activity at the Permian-Triassic transition, in accord with the Siberian Traps record, but for reduced volcanic emissions in the later Early Triassic (Wang et al., 2018).

Early Triassic Atmospheric pCO_2 Regulated by Weathering

Assuming that the outgassing of large volumes of volcanic CO_2 faded after the initial 0.5-m.y.-long phase, atmospheric pCO_2 is expected to have been drawn down relatively fast by continental silicate weathering—the most effective mechanism by which to extract CO_2 from the atmosphere and to buffer Earth's climate. However, pCO_2 stayed at elevated levels for ~4 m.y. after the Griesbachian CO_2 maximum.

Warm temperatures, water availability, and continental plates located within the humid climatic belt are the main factors favoring silicate weathering. Weathering of freshly deposited continental flood basalts would have been particularly effective at consuming atmospheric CO_2, with weathering rates of basalts being 10 times greater compared to weathering rates of granitic continental rocks (Dessert et al., 2003). This efficiency has been documented for Late Triassic Central Atlantic Magmatic Province (CAMP) volcanism, when individual volcanic pulses resulted in a doubling of atmospheric pCO_2 followed by a striking decrease to pre-eruption levels within only ~300 k.y. (Schaller et al., 2012). While CAMP volcanism occurred in warm equatorial latitudes favorable for CO_2 consumption by silicate weathering, the Siberian Traps erupted at ~60°N, with silicate weathering potentially less efficient due to colder conditions. However, the latest Permian increase of low-latitude SSTs likely resulted in an amplified warming of higher latitudes. In conjunction with intensified higher-latitude precipitation as suggested by climate modeling (Winguth et al., 2015), weathering of freshly deposited Siberian lavas should have had the potential to consume atmospheric CO_2. In contrast, Kump (2018) argued that low continental fragmentation and high continentality in Pangea's interiors combined with minimum uplift rates depressed CO_2 uptake by silicate weathering. However, this interpretation seems to be at odds with strontium as well as osmium isotope records (Song et al., 2015; Liu et al., 2020), which indicate an increase in continental weathering, especially in the Early Triassic (Fig. 2).

Silicate weathering can be modulated by reverse weathering, whereby non-kaolinite phyllosilicates form on the seafloor, leading to consumption of dissolved silica and alkalinity sourced from weathering on land and, most important, the addition of CO_2 to the ocean-atmosphere system (Isson and Planavsky, 2018). Reverse weathering has been suggested as a mechanism to maintain high pCO_2 in the Precambrian, when oceans were probably characterized by high dissolved silica concentrations (Maliva et al., 2005) before the advent of silica-secreting organisms. Interestingly, while the Permian is known for extensive chert deposition, cherts disappeared almost completely from the rock record in the Early Triassic (Beauchamp and Baud, 2002). A low abundance of silica-secreting organisms, warm ocean temperatures (increasing silica solubility), and supply of silica from land probably led to high dissolved silica concentrations in Early Triassic oceans, which should have promoted reverse weathering. Cherts re-occurred in the Spathian and Anisian (Sperling and Ingle, 2006) in conjunction with the diversification of radiolarians (O'Dogherty et al., 2010) and the late Spathian decrease in pCO_2.

In summary, the 4× increase in atmospheric pCO_2 across the Permian-Triassic boundary to high and intermediate CO_2 levels in the Early Triassic is in agreement with low-latitude SSTs documenting greenhouse warming and hot Early Triassic oceans. Elevated atmospheric pCO_2 persisted for ~5 m.y., suggesting that warm-climate–enhanced silicate weathering, although indicated by geochemical proxies, failed to draw down CO_2 until the latest Early Triassic. This apparent contradiction may indicate that the exceptional conditions in Early Triassic oceans led to an intensification of marine authigenic clay formation and contribution of CO_2 to the ocean-atmosphere system, counteracting CO2 consumption by silicate weathering.

Acknowledgements

Financial support by the National Natural Science Foundation of China (grant 41821001) is acknowledged. V. Silantiev and F. Mouraviev were supported by a subsidy allocated to Kazan Federal University (Russia) for the state assignment 671–2020–0049 in the sphere of scientific activities and cont. no. 14.Y26.31.0029, res. no. 220 of the Government of the Russian Federation. Helpful comments by anonymous reviewers on an earlier version of this manuscript are acknowledged. This is a contribution to Deutsche Forschungsgemeinschaft (DFG) Research Unit TERSANE (FOR 2332: Temperature-related stressors as a unifying principle in ancient extinctions; project Jo 219/15–1).

References

Augland, L.E., Ryabov, V.V., Vernikovsky, V.A., Planke, S., Polozov, A.G., Callegaro, S., Jerram, D.A., and Svensen, H.H., 2019, The main pulse of the Siberian Traps expanded in size and composition: Scientific Reports , v. 9, p. 18723, https://doi.org/10.1038/s41598-019-54023-2.

Beauchamp, B., and Baud, A., 2002, Growth and demise of Permian biogenic chert along northwest Pangea: Evidence for end-Permian collapse of thermohaline circulation: Palaeogeography, Palaeoclimatology, Palaeoecology , v. 184, p. 37–63, https://doi.org/10.1016/S0031-0182(02)00245-6.

Breecker, D.O., Sharp, Z.D., and McFadden, L.D., 2009, Seasonal bias in the formation and stable isotopic composition of pedogenic carbonate in modern soils from central New Mexico, USA: Geological Society of America Bulletin , v. 121, p. 630–640, https://doi.org/10.1130/B26413.1.

Burgess, S.D., and Bowring, S.A., 2015, High-precision geochronology confirms voluminous magmatism before, during, and after Earth's most severe extinction: Science Advances , v. 1, e1500470, https://doi.org/10.1126/sciadv.1500470.

Cerling, T.E., 1991, Carbon dioxide in the atmosphere: Evidence from Cenozoic and Mesozoic paleosols: American Journal of Science , v. 291, p. 377–400, https://doi.org/10.2475/ajs.291.4.377.

Chen, Z.-Q., and Benton, M.J., 2012, The timing and pattern of biotic recovery following the end-Permian mass extinction: Nature Geoscience , v. 5, p. 375–383, https://doi.org/10.1038/ngeo1475.

Courtillot, V.E., and Renne, P.R., 2003, On the ages of flood basalt events: Comptes Rendus Geoscience , v. 335, p. 113–140, https://doi.org/10.1016/S1631-0713(03)00006-3.

Dessert, C., Dupré, B., Gaillardet, J., François, L.M., and Allègre, C.J., 2003, Basalt weathering laws and the impact of basalt weathering on the global carbon cycle: Chemical Geology , v. 202, p. 257–273, https://doi.org/10.1016/j.chemgeo.2002.10.001.

Ekart, D.D., Cerling, T.E., Montanez, I.P., and Tabor, N.J., 1999, A 400 million year carbon isotope record of pedogenic carbonate: Implications for paleoatmospheric carbon dioxide: American Journal of Science , v. 299, p. 805–827, https://doi.org/10.2475/ajs.299.10.805.

Gastaldo, R.A., Knight, C.L., Neveling, J., and Tabor, N.J., 2014, Latest Permian paleosols from Wapadsberg Pass, South Africa: Implications for Changhsingian climate: Geological Society of America Bulletin , v. 126, p. 665–679, https://doi.org/10.1130/B30887.1.

Hu, Q., and Feng, S., 2003, A daily soil temperature dataset and soil temperature climatology of the contiguous United States: Journal of Applied Meteorology , v. 42, p. 1139–1156, https://doi.org/10.1175/1520-0450(2003)042<1139:ADSTDA>2.0.CO;2.

Isson, T.T., and Planavsky, N.J., 2018, Reverse weathering as a long-term stabilizer of marine pH and planetary climate: Nature , v. 560, p. 471–475, https://doi.org/10.1038/s41586-018-0408-4.

Ivanov, A.V., 2007, Evaluation of different models for the origin of the Siberian Traps, in Foulger, G.R., and Jurdy, D.M., eds., Plates, Plumes, and Planetary Processes: Geological Society of America Special Paper 430 , p. 669–691, https://doi.org/10.1130/2007.2430(31).

Joachimski, M.M., Alekseev, A.S., Grigoryan, A., and Gatovsky, Yu.A., 2020, Siberian Trap volcanism, global warming and the Permian-Triassic mass extinction: New insights from Armenian Permian-Triassic sections: Geological Society of America Bulletin , v. 132, p. 427–443, https://doi.org/10.1130/B35108.1.

Kump, L.R., 2018, Prolonged late Permian–Early Triassic hyperthermal: Failure of climate regulation: Philosophical Transactions Royal Society, series A , v. 376, p. 20170078, https://doi.org/10.1098/rsta.2017.0078.

Li, H., Yu, J., McElwain, J.C., Yiotis, C., and Chen, Z.Q., 2019, Reconstruction of atmospheric CO2 concentration during the late Changhsingian based on fossil conifers from the Dalong Formation in South China: Palaeogeography, Palaeoclimatology, Palaeoecology , v. 519, p. 37–48, https://doi.org/10.1016/j.palaeo.2018.09.006.

Liu, Z., Selby, D., Zhang, H., and Shen, S.-Z., 2020, Evidence for volcanism and weathering during the Permian-Triassic mass extinction from Meishan (South China) osmium isotope record: Palaeogeography, Palaeoclimatology, Palaeoecology , v. 553, p. 109790, https://doi.org/10.1016/j.palaeo.2020.109790.

Lomax, B.H., Lake, J.A., Leng, M.J., and Jardine, P.E., 2019, An experimental evaluation of the use of Δ13C as a proxy for palaeoatmospheric CO2: Geochimica et Cosmochimica Acta , v. 247, p. 162–174, https://doi.org/10.1016/j.gca.2018.12.026.

Maliva, R.G., Knoll, A.H., and Simonson, B.M., 2005, Secular change in the Precambrian silica cycle: Insights from chert petrology: Geological Society of America Bulletin , v. 117, p. 835–845, https://doi.org/10.1130/B25555.1.

Montañez, I.P., 2013, Modern soil constraints on reconstructing deep-time atmospheric CO2: Geochimica et Cosmochimica Acta , v. 101, p. 57–75, https://doi.org/10.1016/j.gca.2012.10.012.

O’Dogherty, L., Carter, E.S., Gorican, S., and Dumitricia, P., 2010, Triassic radiolarian biostratigraphy, in Lucas, S.G., ed., The Triassic Timescale: Geological Society [London] Special Publication 334 , p. 163–200, https://doi.org/10.1144/SP334.8.

Ogg, J.G., and Chen, Z.-Q., 2020, The Triassic Period, in Gradstein, F.M., et al, eds., Geological Time Scale 2020 , Volume 2: Boston, Massachusetts, Elsevier, p. 903–953, https://doi.org/10.1016/B978-0-12-824360-2.00025-5.

Prochnow, S.J., Nordt, L.C., Atchley, S.C., and Hudec, M.R., 2006, Multi-proxy paleosol evidence for Middle and Late Triassic climate trends in eastern Utah: Palaeogeography, Palaeoclimatology, Palaeoecology , v. 232, p. 53–72, https://doi.org/10.1016/j.palaeo.2005.08.011.

Retallack, G.J., and Conde, G.D., 2020, Deep time perspective on rising atmospheric CO2: Global and Planetary Change , v. 189, p. 103177, https://doi.org/10.1016/j.gloplacha.2020.103177.

Romanek, C.S., Grossman, E.L., and Morse, J.W., 1992, Carbon isotopic fractionation in synthetic aragonite and calcite: Effects of temperature and precipitation rate: Geochimica et Cosmochimica Acta , v. 56, p. 419–430, https://doi.org/10.1016/0016-7037(92)90142-6.

Roy, S., Sanyal, P., Parthasarathi, G., Bhattacharya, S.K., and Ajay, A., 2021, Atmospheric CO2 estimates based on Gondwanan (Indian) pedogenic carbonates reveal positive linkage with Mesozoic temperature variations: Palaeogeography, Palaeoclimatology, Palaeoecology , v. 582, 110638, https://doi.org/10.1016/j.palaeo.2021.110638.

Schaller, M.F., Wright, J.D., Kent, D.V., and Olsen, P.E., 2012, Rapid emplacement of the Central Atlantic Magmatic Province as a net sink for CO2: Earth and Planetary Science Letters , v. 323–324, p. 27–39, https://doi.org/10.1016/j.epsl.2011.12.028.

Scotese, C.R., and Moore, T.L., 2014, Atlas of Phanerozoic Ocean Currents and Salinity (Mollweide Projection): PALEOMAP Project PaleoAtlas for ArcGIS: Evanston, Illinois, PALEOMAP Project, 26 p.

Song, H., Wignall, P.B., Tong, J., Song, H., Chen, J., Chu, D., Tian, L., Luo, M., Zong, K., Chen, Y., Lai, X., Zhang, K., and Wang, H., 2015, Integrated Sr isotope variations and global environmental changes through the late Permian to early Late Triassic: Earth and Planetary Science Letters , v. 424, p. 140–147, https://doi.org/10.1016/j.epsl.2015.05.035.

Sperling, E.A., and Ingle, J.C., Jr., 2006, A Permian-Triassic boundary section at Quinn River Crossing, northwestern Nevada, and implications for the cause of the Early Triassic chert gap on the western Pangean margin: Geological Society of America Bulletin , v. 118, p. 733–746, https://doi.org/10.1130/B25803.1.

Sun, Y., Joachimski, M.M., Wignall, P.B., Yan, C., Chen, Y., Jiang, H., Wang, L., and Lai, X., 2012, Lethally hot temperatures during the Early Triassic greenhouse: Science , v. 338, p. 366–370, https://doi.org/10.1126/science.1224126.

Svensen, H., Planke, S., Polozov, A., Schmidbauer, N., Corfu, F., Podladchikov, Y., and Jamtveit, B., 2009, Siberian gas venting and the end-Permian environmental crisis: Earth and Planetary Science Letters , v. 277, p. 490–500, https://doi.org/10.1016/j.epsl.2008.11.015.

Wang, X., Cawood, P.A., Zhao, H., Zhao, L., Grasby, S.E., Chen, Z.Q., Wignall, P.B., Lv, Z., and Han, C., 2018, Mercury anomalies across the end-Permian mass extinction in South China from shallow and deep water depositional environments: Earth and Planetary Science Letters , v. 496, p. 159–167, https://doi.org/10.1016/j.epsl.2018.05.044.

Winguth, A.M.E., Shields, C.A., and Winguth, C., 2015, Transition into a hothouse world at the Permian-Triassic boundary—A model study: Palaeogeography, Palaeoclimatology, Palaeoecology , v. 440, p. 316–327, https://doi.org/10.1016/j.palaeo.2015.09.008.

Wu, Y., Chu, D., Tong, J., Song, H., Dal Corso, J., Wignall, P.B., Song, H., Du, Y., and, Cui, Y., 2021, Six-fold increase of atmospheric CO2 during the Permian-Triassic mass extinction: Nature Communications , v. 12, p. 2137, https://doi.org/10.1038/s41467-021-22298-7.

Zhang, L., Hay, W.W., Wang, C., and Gu, X., 2019, The evolution of latitudinal temperature gradients from the latest Cretaceous through the present: Earth-Science Reviews , v. 189, p. 147–158, https://doi.org/10.1016/j.earscirev.2019.01.025.

Supplemental material

Sample locations

Late Permian and Early to Middle Triassic pedogenic carbonate samples derive from sections in Russia (Southern Ural foreland basin), China (Shanxi, Shaanxi, Henan and Xinjiang provinces), South Africa (Karoo Basin) and the UK (Devon). Early Triassic pedogenic carbonates from Russia derive from the Southern Ural foreland basin (Orenburg area) which during Late Permian to Early Triassic times was at paleolatitudes of 30–35◦ N (Van der Voo and Torsvik, 2004; Newell et al., 1999). Late Permian overbank deposits with channeled sandstone deposits are overlain by coarse fluvial conglomerates and sandstones of Early Triassic age (Newell et al., 1999). The continental succession was dated primarily using biostratigraphy (ostracods and vertebrates) and magnetostratigraphy (Newell et al., 1999; Tverdokhlebov et al., 2005). The Late Permian and Early Triassic paleosols were studied in detail by Kearsey et al. (2012) with both calcitic and dolomitic pedogenic nodules occurring. Dolomitic paleosols are most abundant in the late Changhsingian, while Early Triassic paleosols contain no dolomite. The micro- to cryptocrystalline matrix of dolomitic nodules is composed of dolomitic rhombs of 2 to 5 µm size and shows a clotted texture, commonly associated with formation in vadose environments. The observation that secondary diagenetic carbonate in veins and open space structures is exclusively represented by calcite and never by dolomite as well as that dolomitic nodules only occur in latest Permian but not in the Early Triassic sediments has been taken as evidence that dolomite was precipitated as a primary mineral phase during pedogenesis (see Kearsey et al. (2012) for further details). Further, $p\mathrm{CO}_2$ estimates from paleosols from China and South Africa agree relatively well with pCO_2 estimates derived from the dolomitic pedogenic nodules from the Ural foredeep giving us confidence that the dolomitic nodules represent primary precipitates. The Taodonggou section (NW China, Xinjiang Province) is located in the southern foothills of the Bogda Mountains in the northwestern part of the Turpan-Jungar Basin which during the Late Permian to Early Triassic was located at around 45° N. The sedimentary environment is interpreted as fluvial and deltaic in the Late Permian and as mudflat (lake plain) and floodplain with fluvial channels in the Early Triassic (Thomas et al. 2011, Yang et al., 2010). The Permian-Triassic transition has been placed biostratigraphically (Liao et al., 1987; Liu, 2000) within a 30 m thick interval at the transition of the Guodikeng (Changhsingian) to Juicaiyuan Formation (Induan). The Late Permian and Early Triassic in North China (Henan, Shaanxi and Shanxi provinces) is represented by bioturbated fine-grained sandstones, reddish siltstones and mudstones containing Paleozoic-type plants (Sunjiagou Fm., Changhsingian) followed by mainly non-bioturbated reddish to brown-reddish fine-grained sandstones (Liujiagou Fm., Early Triassic) with the Early Triassic plant Pleuromeia occurring the upper part of the formation (Chu et al., 2017).

The sedimentary sequence in the Karoo Basin has been studied intensively for sedimentary facies and tetrapod populations (Keyser and Smith, 1978; Rubidge et al., 1995). Based on abundant tetrapod faunas, the Permian-Triassic boundary has traditionally been placed at the transition of the Daptocephalus tetrapod assemblage Zone (AZ; Late Permian) to the Lystrosaurus AZ (Early Triassic). The Daptocephalus AZ fauna occurs in greyish siltstones with intercalated ribbon sandstones and thin sand sheets of the Late Permian Balfour Fm. These sediments were deposited in a meandering fluvial setting. A change to red-coloured siltstones with an increasing frequency and thickness of intercalated sandstones characterizes the Palingkoff Mb. (Uppermost Beaufort Fm.; latest Permian to earliest Triassic). Sediments of the Palingkoff Mb. were interpreted to have been deposited in wide ephemeral streams (Smith, 1995) forming the precursors of the braidplains that characterize the depositional setting of the overlying Early Triassic sediments of the Katberg Fm. Sample NWP1 was taken from the New Wapadsberg pass section from approximately 70 m below the assumed PTB (see Gastaldo et al. (2014) for detailed description). Sample OLP4 is from the Old Lootsberg pass section and represents a carbonate nodule from a pedogenic nodule conglomerate (lag deposit) from the lower Katberg Fm. (Early Triassic; see Neveling et al. (2016)for detailed description). The Otter Sandstone Fm. exposed at the south Devon coast (Great Britain) is of lower to middle Anisian age (Hounslow and McIntosh, 2003) and is represented by aeolian and stacked fluvial channel sandstones with locally reworked calcretes in channel lags as well vertical rhizoconcretions (Purvis and Wright, 1991). Samples were collected from the coastal exposures east of Budleigh Salterton (East Devon).

Relative ages of the samples were estimated based on the position of the samples in the measured sections and the available magnetostratigraphic and biostratigraphic information by assuming constant sedimentation rate for the dated time intervals.

Classification of pedogenic nodules

A total of 105 pedogenic carbonate samples were collected from the various sections (Table S1). Most carbonate nodules were collected from 40 to 150 cm below overlying fluvial silt to sandstone beds generally cutting into the floodplain deposits. We rarely observed larger scale paleosol structures (e.g. slickensides) or distinct erosive boundaries within the 50 cm of overlying sediment. Given compaction as well as erosional removal of the topmost parts of the soil profiles, we assume that carbonate nodules formed at > 50 cm depth in the soils.

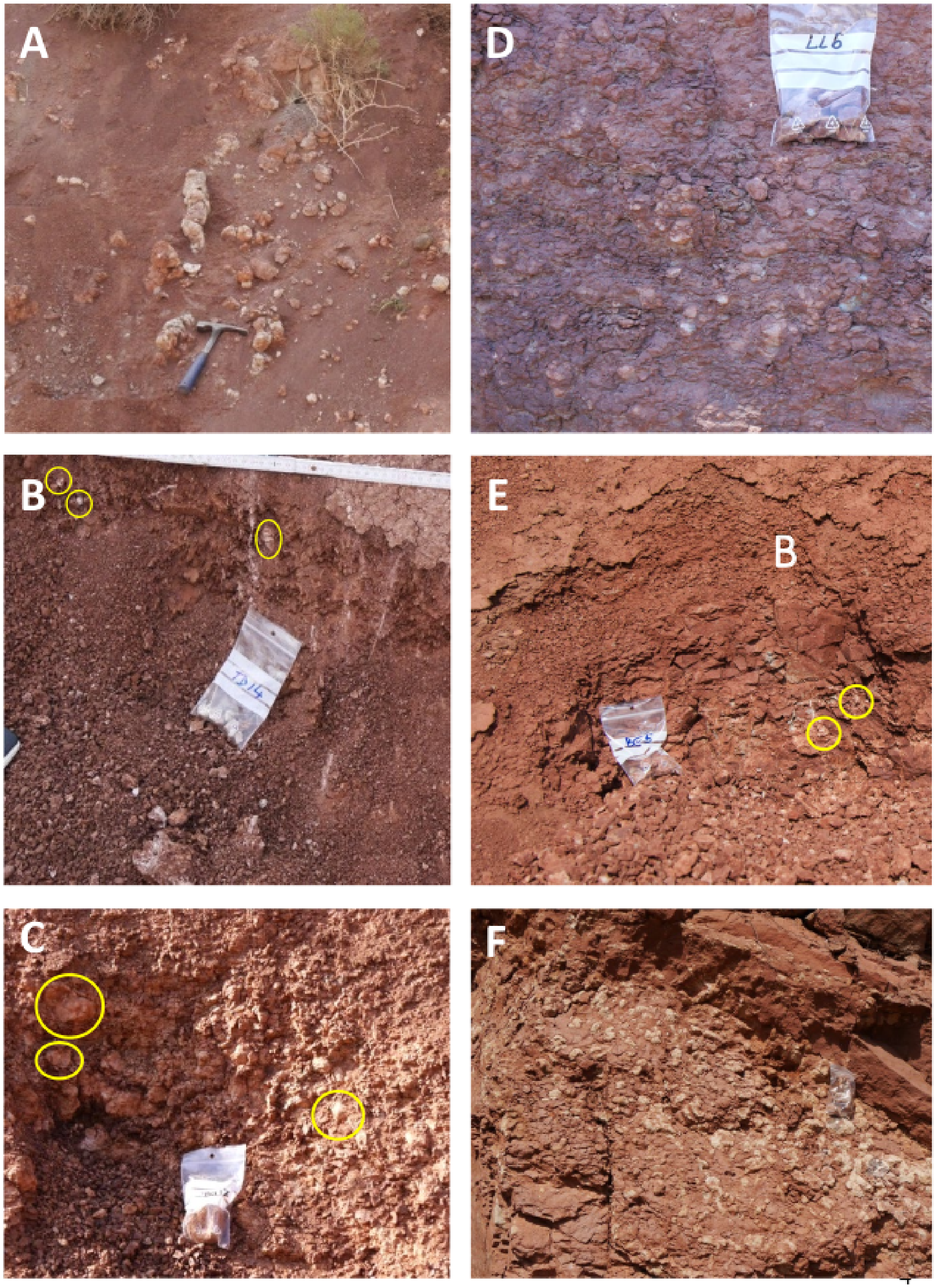

Figure S1: Calcisols (Stage II) from NW China and Russia showing rare to abundant pedogenic nodules (stage II). A - Taondonggou W Section (Xinjiang Province, Northwest China; sample TD5) showing rhizoconcretions and carbonate nodules ; B - Taondonggou W Section (Xinjiang Province, Northwest China; sample TD14); C - Boyevaya Gora section (Southern Ural foredeep, Russia; sample DYL-Z); D - Liulin Section (Shanxi Province, North China; sample LL 6); E - Boyevaya Gora Section (Southern Ural foreland basin, Russia; sample BG 5); F - Dayulin section (Henan Province, North China; sample BG12). Size of sample bags is 12 x 8 cm

All studied paleosols were classified as calcisols (Mack et al., 1993; except pedogenic nodule conglomerate from Old Lootsberg Pass/Karoo which represents a fluvial lag deposit) and are characterized by rare to common carbonate nodules (up to several cm in size; Stage II; Figure S1) or more rarely by stacked nodules and rhizocretions (Stage II). Thin sections of all samples were studied for pedogenic features in order to characterize the environment of formation (e.g. non-saturated vs. saturated soil zone; Figure S2). Based on thin section features and carbon isotope ratios (δ13Chypo, see below), 46 pedogenic carbonate samples were accepted as having formed in the non-saturated soil zone and used for atmospheric CO_2 reconstruction (Table S4). The matrix of the nodules is characterized by a crystic plasmic fabric (Brewer 1964) with patches of crystal sizes ranging from micrite to microspar with a clear dominance of micrite. Most nodules exhibit alpha-fabric (abiogenic) features as floating, etched or exploded grains, circum-granular cracking and globular structures. Beta-fabric (biogenic, mainly fungal and root related) features as rhizoliths were present as root molds and root tubules preserved as roundish voids of 0.1 to 1 mm diameter cemented by sparite. The rhizoliths either consist of relatively homogenous micrite distinctly separated from the carbonate matrix by color or grain size or show a more complex structure of concentric laminae or a cellular structure. In part, rhizoliths are encompassed by circum-granular cracks resulting from displacive carbonate growth. Alveolar septal structures (Wright 1986) were frequently observed in nodules comprising rhizoliths.

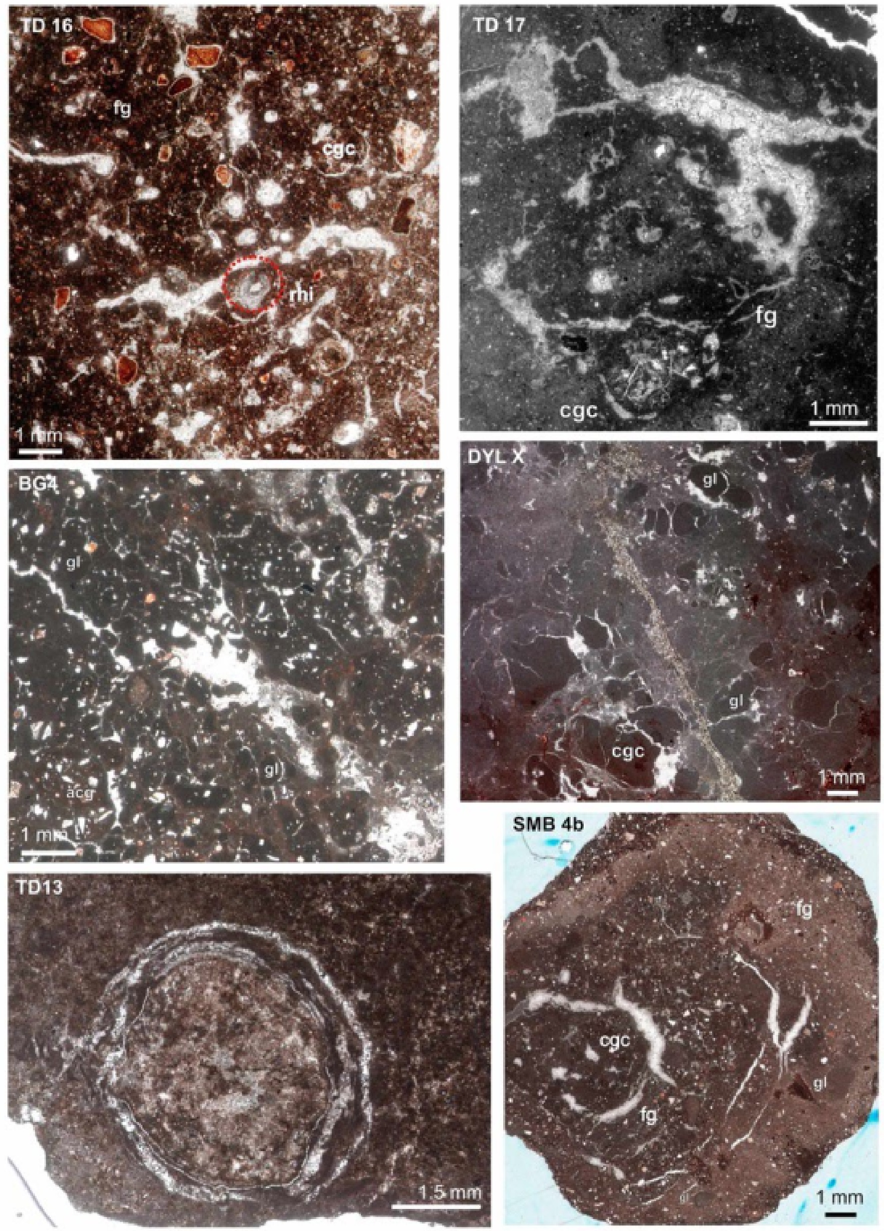

Figure S2: Thin section photomicrographs showing typical pedogenic features of abiogenic alpha and biogenic beta fabrics. TD16: well-developed floating grain (fg) fabric and circumgranular cracking (cgc), both related to displacive carbonate precipitation in soils. Structures attributed to root growth include rhizocretions (rhi) as well as irregular and roundish root molds or casts filled by sparite. TD17: fg fabric, rhizocretion and cgc. Irregular voids filled by sparite resembling root casts or molds. BG4: fg fabric and abundant and distinct glaebules (gl) or peloids surrounded by cgc. Aggregated coated grain (acg) in the lower left. DYL-X: Glaebular fabric with cgc and matrix brecciation as a result of displacive carbonate precipitation. TD 13: Rhizocretion with concentric micritic to microsparitic laminae surrounded by cgc. SMB 4b: Carbonate nodule showing pronounced fg fabric and features as cgc and gl. TD - Taodonggou section (Xinjiang/China), DYL – Dayulin B section (Henan/North China), BG - Boyevaya Gora section (South Urals/Russia), SMB – Sambullak section (South Urals/Russia).

Formation in the non-saturated zone was further evaluated by comparing the carbon isotope ratios of soil carbonate and soil organic matter. For soil carbonates precipitated under wellaerated or non-saturated conditions, total soil CO_2 is derived from microbial oxidation of soil organic matter (SOM), root respiration as well as atmospheric CO2. Instead in waterlogged soils, atmospheric CO_2 will not contribute to total soil CO_2 (Cerling, 1984; Tabor et al. 2007). Pedogenic carbonate formed under closed system conditions will be around 14.8‰ (exact value depends on soil temperature) heavier than oxidizing organic matter, while carbonates formed in open system conditions will have higher δ13C values due to the admixture of atmospheric CO_2 enriched in ^{13}C.

In order to further evaluate whether studied pedogenic carbonates were precipitated under open system conditions, the carbon isotope composition of a hypothetical carbonate ($\delta^{13}C_{hypo}$) precipitated from soil-CO_2 derived exclusively from the oxidation of SOM was calculated by applying a +4.4‰ correction to account for the more rapid diffusion of $^{12}CO_2$ relative to $^{13}CO_2$ through the soil matrix (Cerling, 1984) and the temperature dependent carbon isotope fractionation between soil CO_2 and carbonate (Romanek et al., 1992). $\delta^{13}C_{hypo}$ is in all cases lower than $\delta^{13}C$ of studied pedogenic calcites and dolomites which further supports the interpretation that the carbonates formed in open system conditions under the influence of atmospheric CO_2 (Table S4).

Material and Methods

Stable isotope analyses

Micritic areas were microsampled for carbonate carbon isotope analysis from polished rock slabs using a hand-held microdrill as micrite is considered as the most appropriate texture to ensure that pedogenic calcite preserves records of open system exchange with atmospheric CO_2 (Cerling, 1984; Tabor et al., 2007). Carbonate powders were reacted with 100% phosphoric acid at 70°C using a Gasbench II connected to a ThermoFisher Delta V Plus mass spectrometer. All values are reported in per mil relative to V-PDB ((ViennaPDB). Reproducibility and accuracy were monitored by replicate analysis of laboratory standards calibrated by assigning $\delta^{13}C$ values of +1.95‰ to NBS19 and -46.6‰ to LSVEC and $\delta^{18}O$ values of -2.20‰ to NBS19 and -23.2‰ to NBS18. Reproducibility for $\delta^{13}C$ was ±0.06‰ (1σ).

$\delta^{13}C$ of organic carbon was measured on sedimentary organic carbon (SOM) occluded in the in the pedogenic nodules. Powdered pedogenic carbonates were dissolved in 10% HCl. Insoluble residues were neutralized by washing repeatedly with de-ionized water, dried at 60°C and following homogenized and weighed for isotope analysis. Carbon isotope analyses of SOM was performed with a Flash EA 2000 elemental analyzer connected online to ThermoFisher Delta V Plus mass spectrometer. All carbon isotope values are reported in the conventional δnotation in permil relative to V-PDB. Accuracy and reproducibility of the analyses were determined by replicate analyses of laboratory standards calibrated to international standards USGS 40 and 41. Reproducibility was ±0.05‰ (1σ). The carbon isotope values of organic carbon were not corrected by -1‰ for a potential enrichment in 13C during organic carbon decomposition (e.g. Myers et al. 2016).

Paleosol pCO2 barometer

Atmospheric CO_2 concentrations were calculated from the carbon isotopic composition of soil carbonate precipitated in the well-drained soils by applying the two-component carbon isotope mixing model given that soil CO_2 is a mixture of two isotopically different CO2 sources, soil respired CO_2 and atmospheric CO_2 (Cerling, 1984;1991).

$$[CO_2]_{atm} = S(z) \cdot \frac{(\delta_s^{13}C_s - 1.0033 \cdot \delta_{resp}^{13} - 4.4}{\delta_{atm}^{13} - \delta_s^{13}C_s} \qquad (1)$$

S(z) is the soil respired CO_2 concentration, δ_{13}Cs, δ_{13}Cresp and δ_{13}Catm represent the carbon isotopic composition of total soil CO_2, soil respired CO_2 and atmospheric CO_2, respectively. $\delta^{13}C_s$, $\delta^{13}C_{resp}$ and $\delta^{13}C_{atm}$ are calculated from the measured carbon isotope composition of pedogenic carbonate, soil organic matter (SOM) and marine carbonate, respectively. We estimated S(z) following Montanez (2013) who compiled a large stable isotope dataset for Holocene soils to determine S(z) for different soil orders. The difference in $\delta^{13}C$ of modern soil carbonate and SOM ($\Delta_{carb\text{-}org}$) was used to further constrain S(z). For modern protosols and calcisols having $\Delta_{carb\text{-}org}$ of 12.2 to 15.8‰, a S(z) range of 500 to 2500 ppmV with a best S(z) estimate between 1500 and 2000 ppmv is observed (Montanez 2013). However, all studied Permian and Early Triassic calcisols show $\Delta_{carb\text{-}org}$ values > 15.8‰ (Table S4) suggesting that carbonate precipitation occurred during periods of low soil productivity and that atmospheric CO_2 was probably a large component of soil CO_2. In our study, $\Delta_{carb\text{-}org}$ is in all cases > 16‰ and for 75% of all samples > 18‰. According to Montanez (2013), $\Delta_{carb\text{-}org}$ > 16‰ is indicative of soil atmospheres ≤2000 ppmv, while for $\Delta_{carb\text{-}org}$ > 18‰ or higher, soil respired CO_2 is likely ≤1000 ppmv. Following, we argue that carbonate nodules originated from low-productivity drylands with S(z) between 500 to 1500 ppmV.

$\delta^{13}C_{resp}$ equals $\delta^{13}C$ of organic matter of the pedogenic nodules. $\delta^{13}C_a$ (Table S3) is calculated from $\delta^{13}C$ of marine carbonates utilizing the CO_2(g) - calcite fractionation factor of Romanek et al. (1992). As the carbon isotope fractionation between carbon dioxide and calcite is dependent on temperature, water temperature during precipitation of the marine carbonates has to be assessed. We use the carbon isotope record (Sun et al. 2012; Shen et al. 2013) as well oxygen isotope temperatures (Joachimski et al. 2012, Sun et al. 2012) published for South China as conodonts analyzed for oxygen isotopes derive from the same carbonates used to reconstruct the carbon isotope record. By this we make sure that reconstructed temperatures are close to water temperature during carbonate precipitation. Soil temperature and S(z) in particular are the variables that most strongly influence the calculated atmospheric CO_2 concentrations, as shown in Figure S3.

Statistical data processing

We used the Tidyverse package (Wickham et al., 2019) for data processing. Quantile intervals have been calculated according to Kruschke, J. K. (2011). All scripts used to conduct analyses are available at https://github.com/Ischi94/Joachimski.

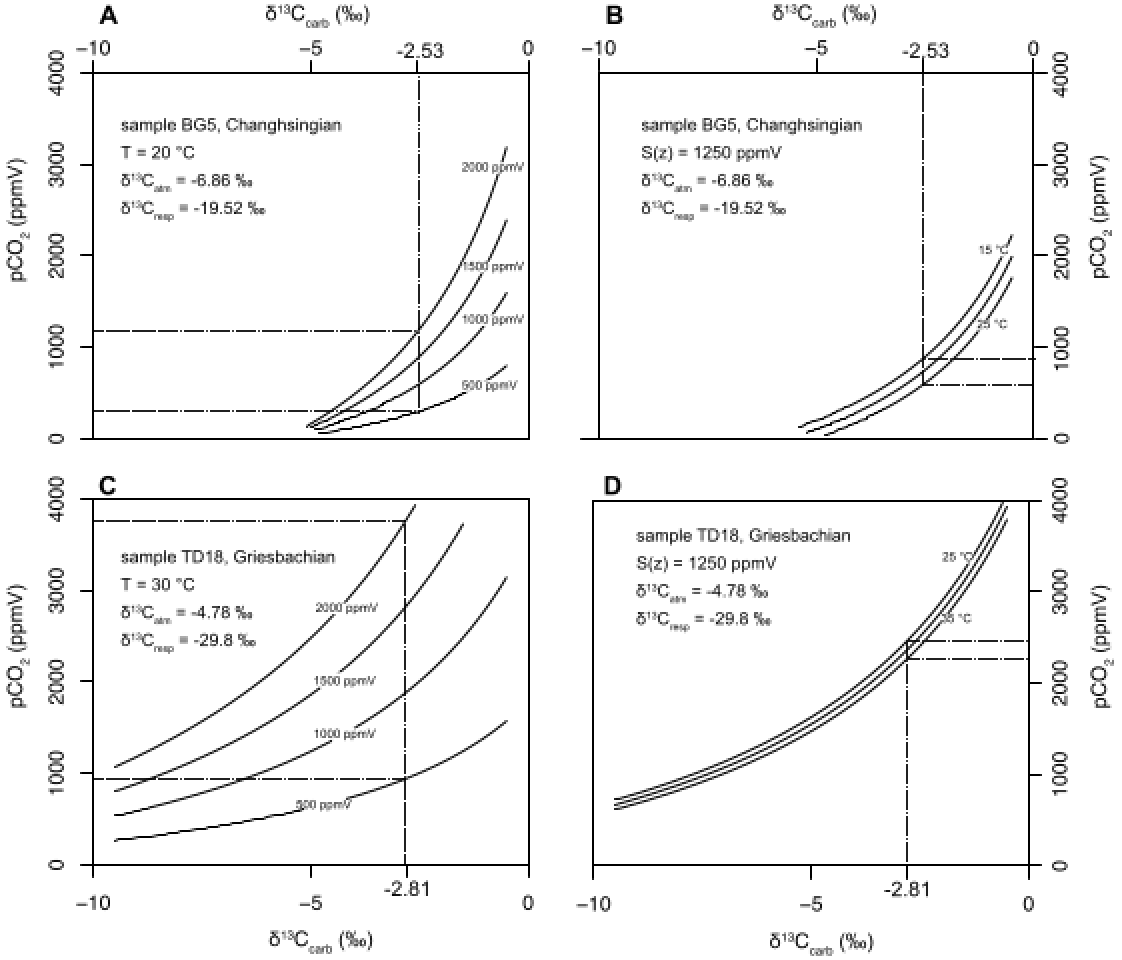

Figure S3: Effect of S(z) and soil temperature (T) on reconstructed atmospheric pCO_2 illustrated for samples BG5 (Changhsingian) and TD18 (Griesbachian): A-B) S(z) varying between 500 to 2000 ppmV, all other variables including soil temperature constant; C-D) Soil temperature varying by ± 5°C around reconstructed mean soil temperature, all other variables constant including S(z). Vertical dotted lines corresponds to measured $\delta^{13}C$ of pedogenic calcite, horizontal dotted lines give calculated minimum and maximum atmospheric pCO_2. Note significant influence of S(z) on pCO_2.

Supplemental references

Brewer, R., 1964, Fabric and mineral analysis of soils: 470 pp. John Wiley & Sons, London and New York.

Cerling T. E., 1984, The stable isotopic composition of modern soil carbonate and its relationships to climate: Earth and Planetary Science Letters, v. 71, p. 229–240.

Cerling, T.E., 1991, Carbon dioxide in the atmosphere: evidence from Cenozoic and Mesozoic paleosols: American Journal of Science, v. 291, p. 377–400.

Chu, D., Tong, J., Bottjer, D.J., Song, H., Song, H., Benton, M.J., Tian, L., and Guo, W., 2017, Microbial mats in the terrestrial Lower Triassic of North China and implications for the Permian–Triassic mass extinction: Palaeogeography, Palaeoclimatology, Palaeoecology, v. 474, p. 214-231.

Gastaldo, R.A, Knight, C.L., Neveling, J., and Tabor, N.J., 2014, Latest Permian paleosols from Wapadsberg Pass, South Africa: Implications for Changhsingian climate: Geological Society of America Bulletin, v. 126, p. 665-679.

Hounslow, M.W. and McIntosh, G., 2003, Magnetostratigraphy of the Sherwood Sandstone Group (Lower and Middle Triassic), south Devon, UK: detailed correlation of the marine and nonmarine Anisian: Palaeogeography, Palaeoclimatology, Palaeoecology, v. 193, 325-348.

Hu, Q. and Feng, S., 2013, A daily soil temperature dataset and soil temperature climatology of the contiguous United States: Journal of Applied Meterology, v. 42, p. 1139-1156.

Joachimski, M.M., Alekseev, A.S., Grigoryan, A., and Gatovsky, Yu.A., 2020, Siberian Trap volcanism, global warming and the Permian-Triassic mass extinction: new insights from Armenian Permian-Triassic sections: Geol. Soc. Am. Bull., v. 132, p. 427-443.

Kruschke, J. K., 2011, Doing Bayesian data analysis: a tutorial with R and BUGS: Burlington, MA, Academic Press/Elsevier Elsevier.

Kearsey, T., Twitchett, R.J., and Newell, A.J., 2012, The origin and significance of pedogenic dolomite from the Upper Permian of the South Urals of Russia: Geological Magazine, v. 149, p. 291-307.

Keyser, A.W. and Smith, R.H.M., 1978, Vertebrate biozonation of the Beaufort Group with special reference to the Western Karoo Basin: Annales Geological Survey, v. 12, p. 1-35.

Liao, Z. et al., 1987, Carboniferous and Permian in the western part of East Mts. Tian Mountains: Guidebook Excursion 4. 11th International Congress of Carboniferous Stratigraphy and Geology, Beijing, China.

Liu, Z., 2000, The Permo-Triassic boundary at the northern margin of Tu–Ha Basin: Journal of Stratigraphy, v. 24, p. 310–314.

Mack, G.H., James, W.C., and Monger, H.C., 1993. Classification of paleosols: Geological Society of America Bulletin, v. 105, p. 129–136.

Montanez, I.P., 2013, Modern soil constraints on reconstructing deep-time atmospheric CO2: Geochimica et Cosmochimica Acta, v. 101, p. 57-75

Myers, T.S., Tabor, N.J., Jacobs L.L., and Bussert, R., 2016, Effects of different organic-matter sources on estimates of atmospheric and soil pCO2 using pedogenic carbonate: Journal of Sedimentary Research,v. 86, p. 800-812.

Neveling, J., Gastaldo, R.A., and Geissman, J.W., 2016, The Permo-Triassic boundary in the Karoo Basin: Field trip Guide Pre3, 35th International Geological Congress, p. 1-79.

Newell, A.J., Tverdokhlebov, V.P. and Benton, M.J., 1999, Interplay of tectonics and climate on a transverse fluvial system, Upper Permian, Southern Uralian Foreland Basin, Russia: Sedimentary Geology, v. 127, p. 11–29.

Ogg, J.G., Ogg, G.M., and Gradstein, F.M., 2016, Triassic, in Ogg, J.G., Ogg, G.M., and Gradstein, F.M., eds., The Concise Geologic Time Scale 2016, Elsevier, p. 133-149.

Parton, J.W., and Logan, J.E., 1981, A model for diurnal variation in soil and air temperature: Agricultural Meterology, v. 23, p. 205-216.

Purvis, K. and Wright, P., 1991, Calcretes related to phreatophytic vegetation from the Middle Triassic Otter Sandstone of South West England: Sedimentology, v. 38, p. 539-551.

Romanek, C.S., Grossman, E.L., and Morse, J.W., 1992, Carbon isotopic fractionation in synthetic aragonite and calcite: effects of temperature and precipitation rate: Geochimica Cosmochimica Acta, v. 56, p. 419–430.

Rubidge, B.S., Johnson, M.R., Kitchinh, J.W., Smith, R.M.H., Keyer, A.W., and Groenewald, G.H., 1995, An introduction to the biozonation of the Beaufort Group, in Rubidge, B.S., ed., Biostratigraphy of the Beaufort Group (Karoo Basin). South African Committee for Stratigraphy, Biostratigraphic Series, v. 1, p. 1-2.

Shen, S.-Z., Cao, C.Q., Zhang, H., Bowring, S.A., Henderson, C.M., Payne, J.L, Davydov, V.I., Chen, B., Yuan, D.X., Zang, Y.C., Wang, W., Zheng, Q.F., 2013, High-resolution δ13Ccarb chemostratigraphy from latest Guadalupian through earliest Triassic in South China and Iran. Earth and Planetary Science Letters, v. 375, p. 156-165.

Smith, R.M.H., 1995, Changing fluvial environments across the Permian-Triassic boundary in the Karoo Basin, South Africa and possible causes of tetrapod extinctions: Palaeogeography, Palaeoclimatology, Palaeoecology, v. 116, p. 81-104.

Sun, Y., Joachimski, M.M., Wignall, P.B., Yan, C., Chen, Y., Jiang, H., Wang, L., and Lai, X., 2012, Lethally hot temperatures during the early Triassic greenhouse: Science, v. 338, p. 366–370.

Tabor, N.J., Montanez, I.P., Steiner, M.B., and Schwindt, D., 2007. δ13C values of carbonate nodules across the Permian-Triassic boundary in the Karoo Supergroup (South Africa) reflect a stinking sulfurous swamp, not atmospheric CO2: Paleogeography, Paleoclimatology, Paleoecology, v 252, p. 370-381.

Thomas, S.G., Tabor, N.J., Yang, W., Myers, T.S., Yang, Y., and Wang, D., 2011, Palaeosol stratigraphy across the Permian–Triassic boundary, Bogda Mountains, NW China: Implications for palaeoenvironmental transition through earth's largest mass extinction: Paleogeography, Paleoclimatology, Paleoecology, v.308, p. 41-64. Tverdokhlebov, V.P., Tverdokhlebova, G.I., Minikh, A.V., Surkov, M.V., and Benton, M.J., 2005, Upper Permian vertebrates and their sedimentological context in the Southern Urals, Russia: Earth Science Reviews, v. 69, p. 27–77.

Upchurch, G.R., Kiehl, J., Shields, C., Scherer, J., and Scotese, C., 2015, Latitudinal temperature gradients and high-latitude temperatures during the latest Cretaceous: congruence of geologic data and climate models: Geology, v. 43, p. 683–686.

Van der Voo, R. and Torsvik, T.H., 2004, The quality of the European Permo-Triassic paleopoles and its impact on Pangea reconstructions: Geophysical Monographs, v. 145, p. 29–42.

Wickham, H., Averick, M., Bryan, J., Chang, W., D'Agostino McGowan L., Romain, F. et al., 2019, Welcome to the Tidyverse: Journal of Open Source Software, v. 4, 1686.

Wright, V.P., 1986, The role of fungal biomineralization in the formation of Early Carboniferous soil fabrics: Sedimentology, v. 33, p. 831–838.

Yang, W., Feng, Q., Liu, Y., Tabor, N., Miggins, D., Crowley, J.L., Lin, J., and Thomas, S., 2010, Depositional environments and cyclo- and chronostratigraphy of uppermost Carboniferous– Lower Triassic fluvial–lacustrine deposits, southern Bogda Mountains, NW China — A terrestrial paleoclimatic record of mid-latitude NE Pange: Global Planetary Change, v. 73, p. 15–113.

Zhang,L., Hay, W.W., Wang, C., and Gu, X., 2019, The evolution of latitudinal temperature gradients from the latest Cretaceous through the Present: Earth-Science Reviews, v. 189, 147-158.

Manuscript 3

Deep-time climate legacies affect origination rates of marine genera

Proceedings of the National Academy of Sciences 118 (2021) DOI: https://doi.org/10.1073/pnas.2105769118

Gregor H. Mathes[1,2*], Wolfgang Kiessling[1], Manuel J. Steinbauer[2,3]

[1] Department of Geography and Geosciences, GeoZentrum Nordbayern, Friedrich-Alexander University Erlangen-Nürnberg (FAU), Erlangen, Germany.
[2] Bayreuth Center of Ecology and Environmental Research (BayCEER), University of Bayreuth, Bayreuth, Germany.
[3] Department of Biological Sciences, University of Bergen, Bergen, Norway.
* Corresponding author: gregor.mathes@uni-bayreuth.de

ABSTRACT

Biodiversity dynamics are shaped by a complex interplay between current conditions and historic legacy. The interaction of short- and long-term climate change may mask the true relationship of evolutionary responses to climate change if not specifically accounted for. These paleoclimate interactions have been demonstrated for extinction risk and biodiversity change, but their importance for origination dynamics remains untested. Here, we show that origination probability in marine fossil genera is strongly affected by paleoclimate interactions. Overall, origination probability increases by 27.8% [95% CI (27.4%, 28.3%)] when a short-term cooling adds to a long-term cooling trend. This large effect is consistent through time and all studied groups. The mechanisms of the detected effect might be manifold but are likely connected to increased allopatric speciation with eustatic sea level drop caused by sustained global cooling. We tested this potential mechanism through which paleoclimate interactions can act on origination rates by additionally examining a proxy for habitat fragmentation. This proxy, continental fragmentation, has a similar effect on origination rates as paleoclimate interactions, supporting the importance of allopatric speciation through habitat fragmentation in the deep-time fossil record. The identified complex nature of paleoclimate interactions might explain contradictory conclusions on the relationship between temperature and origination in the previous literature. Our results highlight the need to account for complex interactions in evolutionary studies both between and among biotic and abiotic factors.

INTRODUCTION

Biodiversity responses to modern climate change are dependent on past climate (Antão et al., 2020; Mathes et al., 2021; Svenning et al., 2015). Climate legacies were important drivers of both extinction and diversification dynamics in the Quaternary (Lister, 2004; Maldonado-Coelho, 2012; Postigo-Mijarra et al., 2010; Svenning et al., 2015). However, the effect of these legacies on deep-time origination dynamics is largely unknown.

The interaction of climate change with previous climate might affect origination dynamics through a variety of ecological mechanism. If short-term change adds to a long-term temperature trend in the same direction (e.g., a short-term cooling following a prolonged cooling trend), species are less likely to have adaptations to the climatic situation due to niche conservatism (Hopkins et al., 2014; Stigall, 2014; Wiens & Graham, 2005). This lack of adaptation to climatic conditions might result in bottleneck and subsequent founder effects, as well as ecological releases (Button, 2017; Gilman et al., 2010; Raup, 1979). Such ecological effects influence rates of evolution and speciation (Templeton, 2008; Wahl et al., 2002). Additionally, climate history can hypothetically drive origination rates of marine genera through global sea level changes, affecting the amount of habitat fragmentation in the continental shelf area. Habitat fragmentation and loss is correlated with the intensity of ecological interactions (Schuler et al., 2017; Tilman, 1994; Valentine, 1968) and speciation rates (Alroy, 2008; Mayr & O'Hara, 1986).

Building on these ecological concepts through which past climate might affect origination dynamics, we expect that the interaction between climate change and previous temperature trends is a strong determinant of origination rates in the deep-time fossil record. We hypothesize that origination processes are more strongly influenced by temperature change if the change adds to a previous temperature trend in the same direction (synergistic paleoclimate interaction) rather than if the focal change withdraws previous trends (antagonistic paleoclimate interaction). Among synergistic paleoclimate interactions, we expect to detect a weakened origination signal after cooling–cooling due to the "common cause" of sampling biases and biological signal that is driven by low sea levels (Peters, 2005).

Here, we analyze how the global trajectories of past climate can affect the origination probabilities of 12 marine fossil phyla in the last 485 million years (Annelida, Arthropoda, Brachiopoda, Bryozoa, Chordata, Cnidaria, Echinodermata, Foraminifera, Hemichordata, Hyolitha, Mollusca, and Porifera). We use paleoclimate interactions as explanatory variables, which are defined as the interaction of short-term temperature change with long-term temperature trends. We first apply regression models using paleo-temperature estimates and sample-standardized genus-level fossil data using a dynamic modeling framework. Dynamic implies that we let the long-term trend vary for each paleoclimate interaction and subsequently select the best performing model. We then test whether cumulative paleoclimate interactions increase the origination probability of fossil taxa. Our results show, on average, a substantial increase in origination rates when a short-term cooling adds to a long-term cooling trend. To estimate whether this increase is caused by a reduction in available habitat space subsequent to cooling–cooling paleoclimate interaction, we also analyze the effect of a proxy for shelf area habitat space on origination rates using the same modeling framework.

RESULTS

Origination probability

Cooling–cooling paleoclimate interactions concurred with an increased origination probability (Fig. 1 and SI Appendix, Table S1). We compared the origination probability for marine groups per paleoclimate interaction, based on the output of our regression models. The overall origination probability was lower after cooling–warming, warming–cooling, and warming–warming paleoclimate interactions compared to the average origination probability of 13.3% per geological stage. To the contrary, cooling–cooling paleoclimate interactions coincides with an increased mean origination probability of 15.1%, whereas the origination probability in all other cases was 11.4%.

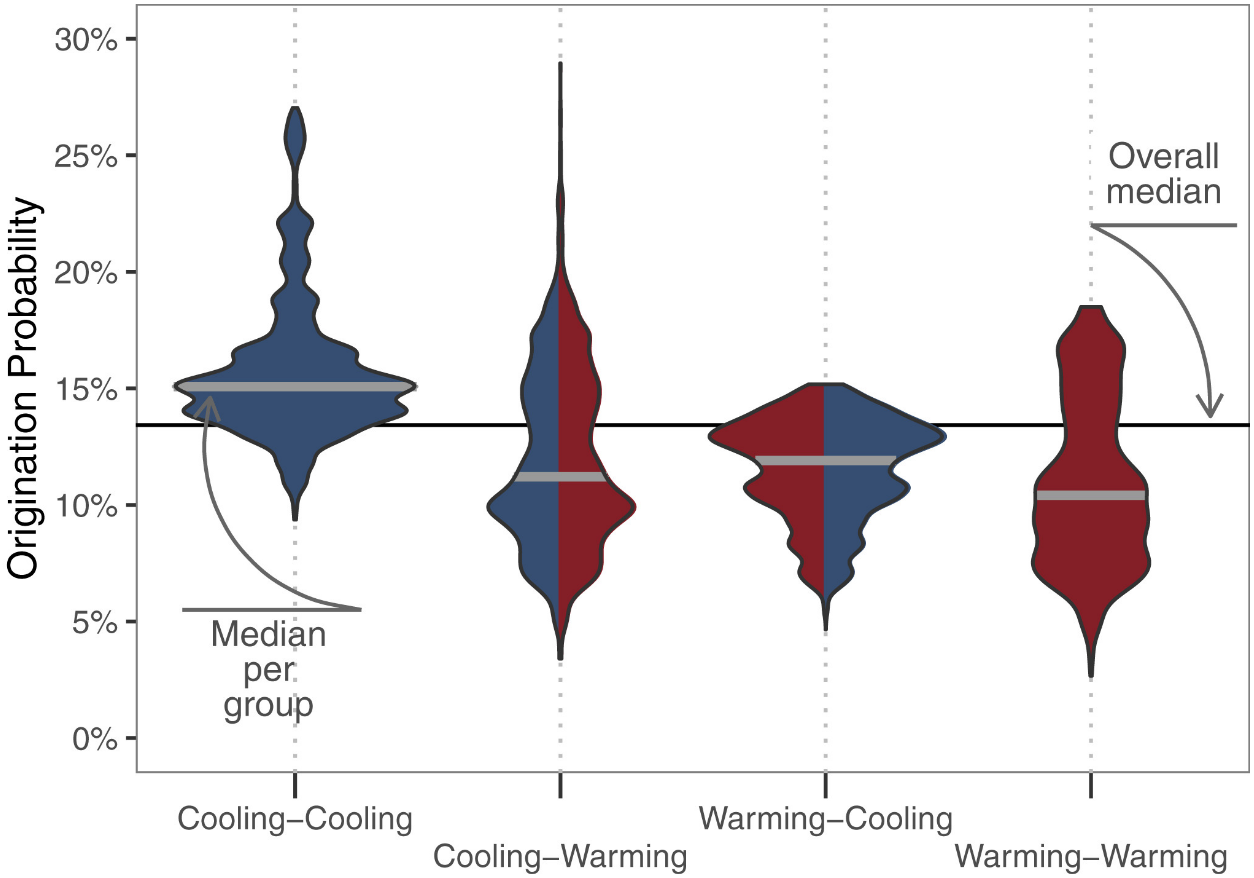

Figure 1: Origination probability. Total response distributions to paleoclimate interactions as predicted by GLMMs. Thick gray lines show the median origination probability per paleoclimate interaction, and the black line depicts the median probability for all interactions combined.

Effect size

The effect of cooling–cooling paleoclimate interactions on origination probability is large (Fig. 2 and SI Appendix, Table S2). The absolute difference between the mean origination probability of cooling–cooling compared to all other paleoclimate interactions was 3.7 [95% CI (3.7, 3.8)]. This difference represents a 27.8% percentage increase compared to all other interactions [95% CI

(27.4%, 28.3%)]. We used the Cohen’s d statistic to compute the effect size as a standardized measure. The Cohen’s d for cooling–cooling was greater than 1, indicating a large effect size. All results for the absolute difference, the percentage change, and the effect size are based on generalized mixed effect models and stay consistent when analyzed in a Bayesian regression framework (Fig. 2).

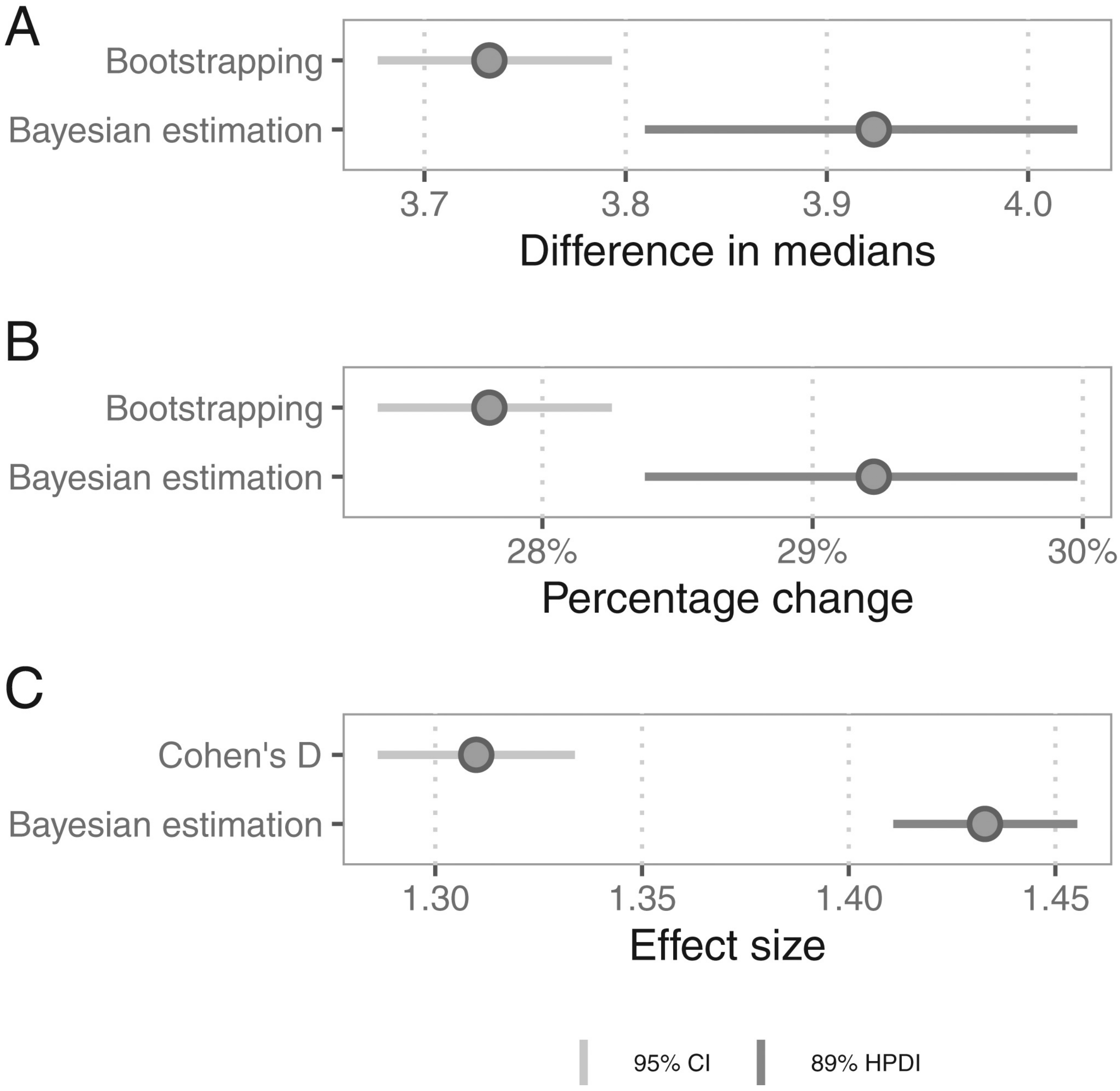

Figure 2: Effect size. (A) Difference in medians between origination probability after cooling–cooling compared to all other paleoclimate interactions. (B) Overall increase of origination probability after cooling–cooling paleoclimate interactions compared to baseline probability. (C) Cohen’s d effect size of the observed change in probability after cooling–cooling paleoclimate interactions. Points show median estimates. Light gray lines delineate 95% CIs

based on nonparametric bootstrapping. Dark gray lines depict 89% highest posterior density intervals (HPDIs) based on Bayesian regression.

<u>Group differences</u>

We additionally tested whether cooling–cooling paleoclimate interactions raised the origination probability of all studied marine groups and whether the signal remains robust through time (Fig. 3 and SI Appendix, Table S3). This was the case for all major phyla with sufficient data and throughout all 80 geologic stages, as all log-odds values including 95% CIs were above zero. Among all groups, Arthropoda, Brachiopoda, and Bryozoa showed an above average response to cooling–cooling paleoclimate interactions. Through time, the Paleozoic Era showed the highest origination probabilities, which then decrease through time, with the lowest values present in the Cenozoic Era. This decrease over time is mainly driven by changing abundances of taxa (SI Appendix, Fig. S13). Note that we excluded the Cambrian from the analysis due to insufficient data (see Materials and Methods). Genera from onshore settings showed a greater response to cooling–cooling paleoclimate interactions of 8.5% [95% credible interval (7.1%, 9.8%)] compared to genera from offshore settings (SI Appendix, Fig. S1). Our large effect size of cooling–cooling interactions on origination probability remained consistent throughout all studied groups and throughout the whole Phanerozoic.

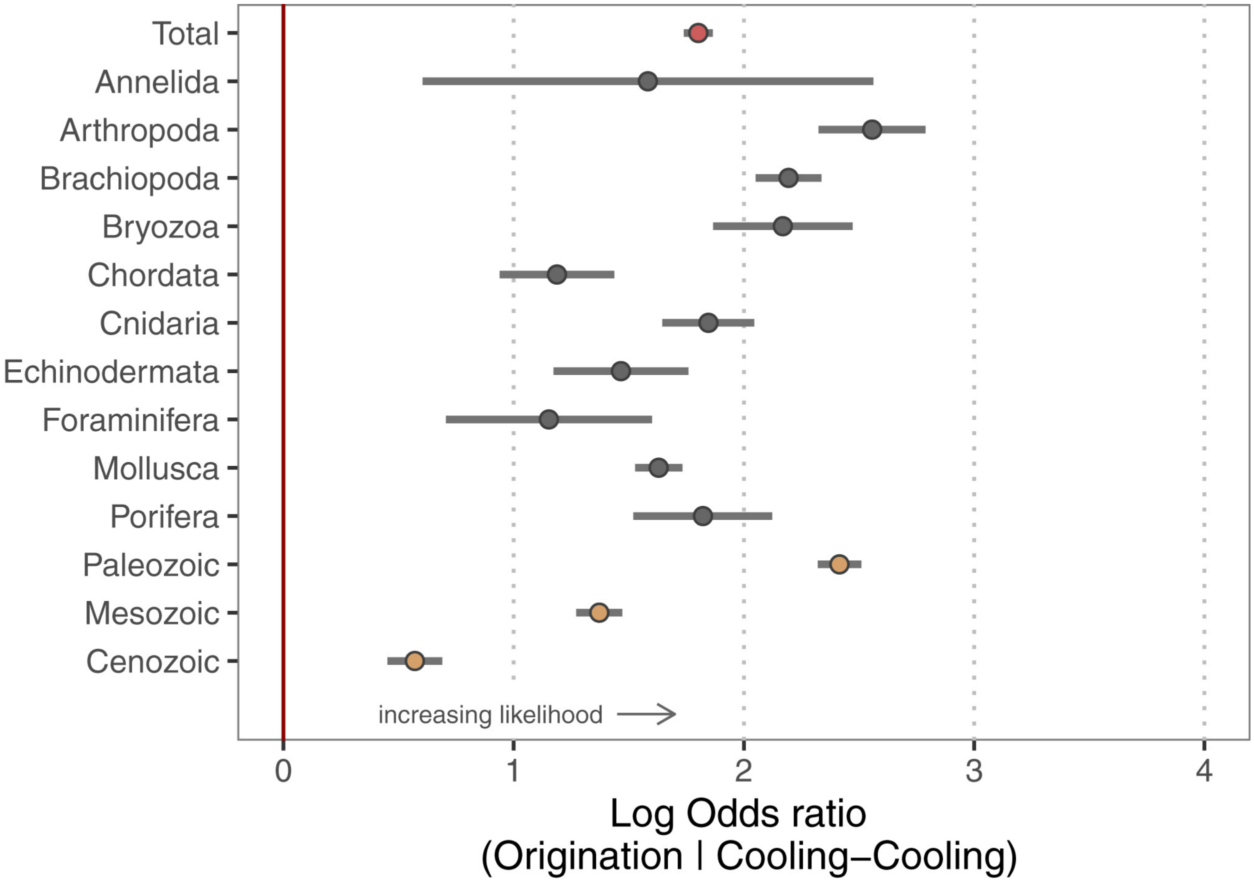

Figure 3: Group differences. Origination likelihood for all major phyla and across time after cooling–cooling compared to all other paleoclimate interactions. The red point shows the overall

response, gray points per phyla, and brown points response per era. Gray lines show 95% CIs. The phyla Hemichordata and Nematoda, as well as the Cambrian, were removed from the analysis due to insufficient data. The red line delineates a log-odds ratio of zero. Values above this line indicate a higher probability to originate after cooling–cooling compared to all other paleoclimate interactions.

Continental fragmentation

Approximating potential causal paths through which paleoclimate interactions can act on origination rates, we further tested the effect of continental fragmentation on origination within our modeling framework. We found that a short-term increase in continental fragmentation following on a long-term increase coincides with a substantial spike in origination rates (Fig. 4). The origination probability after such a continental fragmentation interaction was 22% [95% CI (21.1%, 23%)] greater than the average origination rate.

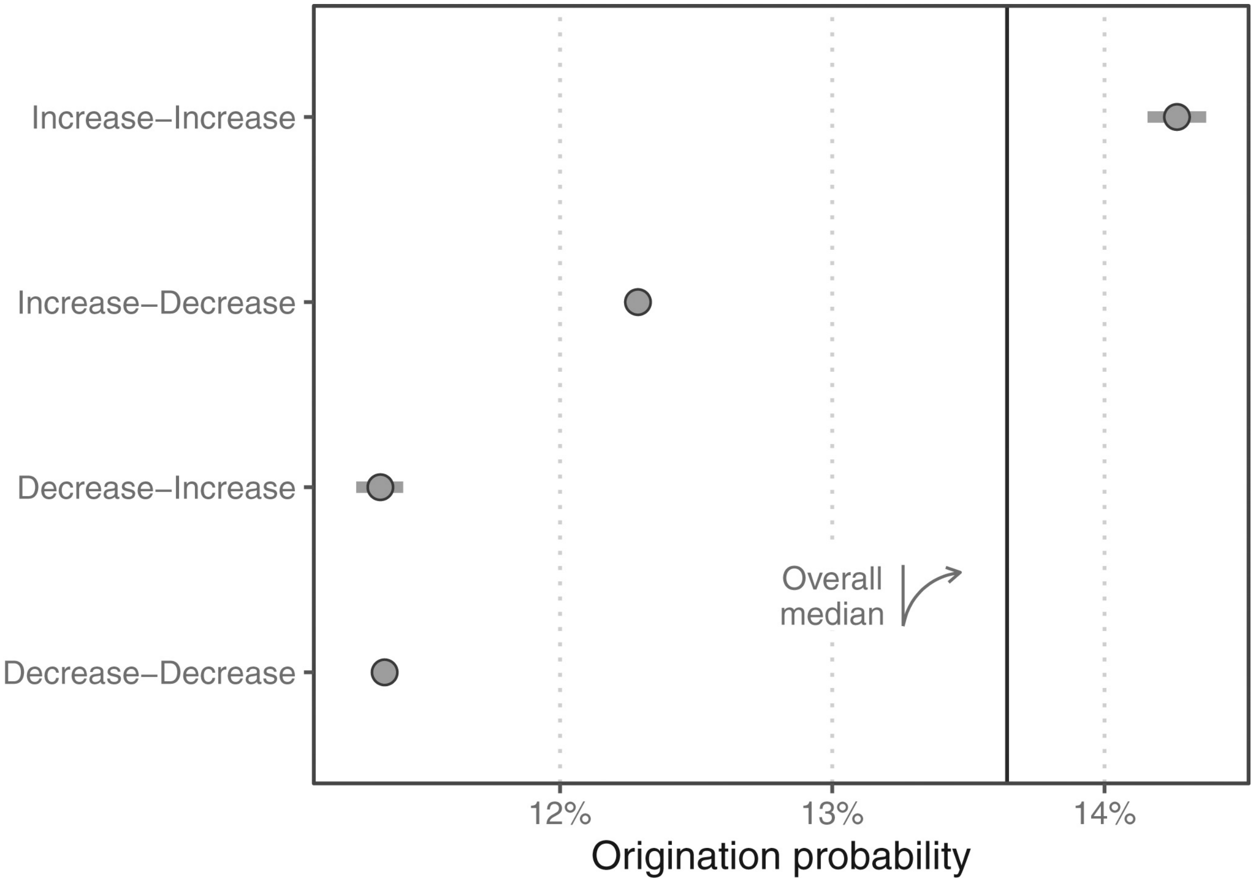

Figure 4: Continental fragmentation. Median origination response per continental fragmentation interaction as predicted by GLMMs based on a continental fragmentation index. The black line depicts the median origination probability for all marine genera, and gray lines delineate 95% CIs.

DISCUSSION

The interplay of short-term climate cooling adding to a long-term average global cooling coincided with a profound increase of origination probability. We found this effect to be consistent through time and across all studied groups. Previous studies on the relationship between temperature and origination came to ambiguous conclusions, ranging from a negative relationship (Mayhew et al., 2008) to no relationship (Alroy et al., 2000; Prothero, 1999) to a positive one (Mayhew et al., 2012). Our results show that the relationship between origination rates and temperature is dependent on baseline conditions, which were not previously considered. The large effect size and the conditional dependency of paleoclimate interactions may have obscured any apparent relationship between temperature and origination in previous analysis. Explicitly accounting for dynamic interactions will hence provide a more robust foundation to assess the relationship between Phanerozoic marine diversity and climate. This has been recently demonstrated for modern terrestrial and marine assemblages, for which biodiversity responses to recent climate change were conditional on the baseline climate (Antão et al., 2020).

Our results are remarkable, as we expected to detect a weakened origination signal after cooling–cooling paleoclimate interactions due to the “common cause” hypothesis (Peters, 2005). Sampling biases caused by low sea levels partly arise from the removal of originating taxa from the fossil record or a shift of their detection to a later origination datum, leading to an artificially reduced origination probability. These extrinsic biases of fossil data cannot be addressed by sampling standardization (Peters, 2006). The large effect size of cooling–cooling paleoclimate interactions might hence even be an underestimation of the true magnitude. However, we only tested the effect of temperature on origination rates and did not include other environmental parameters (e.g., sea level, nutrient input), which could be more direct drivers of origination rates than temperature (Cárdenas & Harries, 2010). Nevertheless, current research shows that temperature remains a significant predictor of origination rates after accounting for additional environmental parameters (Mayhew et al., 2012). Furthermore, temperature can act as a top-down effect, driving the change in other environmental parameters such as sea level and shelf area weathering. Directly correlating temperature to origination rates instead of fitting additional mediatory variables might hence give a more precise estimate of the relationship between climate and origination dynamics.

Other abiotic factors affecting origination probability are not related to temperature. Continental fragmentation can increase the number of geographic barriers, restricting animal movement and thus enhancing allopatric speciation rates (Kiessling, 2010; Valentine & Moores, 1970; Zaffos et al., 2017). Our results show that the effect of fragmentation on origination rates is particularly large when an increase in continental fragmentation adds to a previous long-term increase. A drop in eustatic sea level is an additional driver for habitat fragmentation. Cooling–cooling paleoclimate interaction, resulting in a drop in eustatic sea level due to glaciation, leads to reduced continental shelf area and emerging barriers in this main habitat of the majority of the studied fossil groups. Changes in habitat fragmentation are correlated to the rate of ecological interactions (Schuler et al., 2017; Tilman, 1994; Valentine, 1968) and speciation rates (Alroy, 2008; Mayr & O’Hara, 1986). Both variables used in our analysis, paleoclimate and continental fragmentation, thus share a common causal mechanism to drive origination probabilities. Our results may therefore support the importance of allopatric speciation through vicariance in the deep-time fossil record (Eldredge, 1971; Mayr, 1963).

Habitat fragmentation may not only drive origination rates but also influence the effect of paleoclimate interactions on extinction. Cooling–cooling paleoclimate interactions have also been shown to drive temperature-related extinctions in the fossil record, with warming–warming interactions showing the same signal, albeit with lower effect size (Mathes et al., 2021). Vicariance might explain why the effect size for warming–warming interactions on extinction risk is reduced compared to cooling–cooling, even though the supposed underlying mechanism of niche conservatism does not differentiate between the two types of synergistic paleoclimate interactions (Hopkins et al., 2014; Stigall, 2014; Wiens & Graham, 2005). During warming–warming paleoclimate interaction, marine taxa could potentially escape an adverse environment through range shifts. During cooling–cooling, however, geographic barriers resulting from sea level drop might impede migration, resulting in the observed increased extinction risk (Mathes et al., 2021) and origination probability (this study) compared to warming–warming and all antagonistic paleoclimate interactions. Our findings agree with this proposed mechanism, as we found that paleoclimate interactions have a stronger impact on the origination rate of shallow-water taxa, for which a drop in sea level does result in more habitat fragmentation than for offshore taxa (SI Appendix).

Our study supports that evolutionary processes interact with climate by complex effects showing conditional dependencies. Explicitly integrating these interactions within a dynamic modeling framework leads to an improved discernment of origination patterns in the fossil record. Previous studies on the relationship of temperature and biodiversity in Earth's history came to ambiguous conclusions, a nonconformance likely to be fixed in the future by accounting for paleoclimate interactions (SI Appendix, Figs. S2 and S3). However, the mechanisms underlying the grand association between evolution and the observed effect are still unclear. The interpretation offered here, a combination of niche conservatism and ecological effects arising from sea level change resulting in vicariance and allopatric speciation, could be at least partially tested by comparing responses of terrestrial and marine fossil groups to paleoclimate interactions. If sea level change plays a key role, terrestrial groups should show a distinctively different response to cooling–cooling compared to marine groups. Given the large effect of paleoclimate interactions on both extinction and origination, as well as the consistency of this effect through time and studied groups, determining the underlying causes of paleoclimate interactions will improve our mechanistic comprehension of evolutionary dynamics in Earth's history (Jablonski, 2008).

MATERIAL AND METHODS

Fossil data

All analyses were conducted at the genus level. We accessed data from the Paleobiology Database (PaleoDB, paleobiodb.org) on 21 April 2021, including all occurrences from the Ediacaran to the Holocene. We filtered the data to only comprise marine animal taxa and heterotrophic protists, i.e., the same taxonomic groups listed in Sepkoski's (Sepkoski, 2002) compendium, following common processing recommendations (Kocsis et al., 2019). Previous studies on the relationship between temperature and biodiversity were mainly based on Sepkoski's compendium, rendering these data optimal for comparison purposes of our model structures. We binned the data to one of 80 geological stages (Ogg et al., 2016), ranging from the Ordovician to the Pleistocene. Ordovician stages were resolved using biozone and formation entries due to potential stratigraphic errors (Kocsis et al., 2019). Further data cleaning included removal of uncertain taxonomical ranks, duplicates in bins, single-collection and single-reference taxa, and missing higher-level taxonomy. Taxa confined to a single stage (singletons) were excluded, as they tend to produce undesirable distortions of the fossil record (Foote, 2000). Collections from unlithified sediments were omitted to reduce sampling bias . We then applied shareholder quorum subsampling (SQS) for sampling standardization (Foote, 2000), using the divDyn R package (Kocsis et al., 2019). SQS is based on frequency distribution coverage of taxa, drawing collections until estimated coverage reaches a fixed target (i.e., until a shareholder quorum is attained). For this, we used a shareholder quorum of 0.8. SQS was applied excluding dominant taxa from all calculations involving frequencies and with a separate treatment of the largest collection in each time slice. We then used the first-appearance datum of a genus as its time of origination. The origination signal for each genus was then expressed with a 1 for the time of origination and a 0 for each time interval the genus was found in the fossil record after the time of origination. The final dataset contained 12 major marine fossil phyla with sufficient data to include in the subsequent analysis (SI Appendix, Fig. S4 and Table S4).

Climate proxy data

To reconstruct temperature change over time, we used the tropical whole-surface water (mixed layers <300 m deep) oxygen isotope data set from a compilation of marine carbonate isotopes (38). This temperature proxy is based on $\delta^{18}O$ values of well-preserved calcareous shells. To get from raw $\delta^{18}O$ values to temperature estimates, we applied the recommended data processing steps of Veizer and Prokoph (Veizer & Prokoph, 2015). We first adjusted for the long-term trend in oxygen isotopic composition of seawater and averaged records from tropical and subtropical records. We then assigned the temperature data to geological stages to provide global mean temperature for each of the 80 stages used in our analysis. We additionally tested whether our choice in $\delta^{18}O$ source and processing method biased our inference by repeating our whole analysis with $\delta^{18}O$ isotope values from a different compilation and a different conversion of isotope values to temperature (SI Appendix).

Generalized linear mixed effect models

All analyses were carried out in R (R Core Team, 2021). We used the lme4 package (Bates et al., 2015) to perform the regression analysis and the tidyverse package compendium (41) for

data processing and visualization. We quantified the effect of temperature change interacting with past temperature trends on origination probability using generalized linear mixed effect models (GLMMs) with a binomial family error (Bolker et al., 2009). We used the origination signal from the fossil data as a response variable and a single interaction term including the long-term temperature trend and the short-term temperature change as a predictor variable:
GLM (Origination ~ Trend : Change +(1|Genus), Family = Binomial).

Using the genus level as a random effect, we accounted for the multiple occurrences of the same genus within the time-series fossil data. Additionally including stages as a second random effect did not increase model performance (SI Appendix, Table S8 and Fig. S5).
The short-term temperature change was calculated as the change in temperature for each geologic stage compared to the previous stage. Long-term temperature trends were calculated using ordinary least squares following the processing steps of Mathes et al. (2021). For each stage included in the analysis, we calculated 10 stages starting one stage prior to the focal stage, each covering a successively growing time of temperature history. We then used a dynamic model framework to select the best performing long-term trend (SI Appendix, Table S5). This implies calculating 10 GLMMs for each trend while keeping the short-term change fixed. From these 10 GLMMs, we then selected the best performing model using Akaike's information criterion (AIC). Instead of calculating one model for all short-term changes, we distinguished short-term warming from short-term cooling. This enabled us to quantify the differences in origination probability per paleoclimate interaction (cooling–cooling, warming–cooling, cooling–warming, and warming–warming, for which the first word denotes the long-term temperature trend and the second word the short-term temperature change). We used AIC for comparison of model performance. For likelihood approximation, we applied adaptive Gauss-Hermite quadrature (Pinheiro & Chao, 2006), which reduces bias and is more robust than other approximation methods (Bolker et al., 2009). We used 25 quadrature points per scalar integral, which is the maximum number of nodes in the quadrature formula of the lme4 package.

Origination probability

We separated the predicted origination response of each type of paleoclimate interaction from our GLMMs using the predict() function on the actual fossil data. Any resulting distributions for the origination probability hence reflect climate conditions experienced by the focal fossil group. We calculated the average origination probability as the mean of both model intercepts (i.e., of the model for short-term warming and for short-term cooling).

Effect size

We applied nonparametric bootstrapping (Mooney, 1996) (SI Appendix, Fig. S6) and Bayesian estimation (Kruschke, 2013) to the predicted origination response of our GLMMs to calculate the difference in means between origination probability after cooling–cooling compared to all other paleoclimate interactions. While doing so, we accounted for the nonparametric nature of the data (SI Appendix, Fig. S7). Bootstrapping was conducted via the infer package (Bray et al., 2021) based on 2000 repetitions. For Bayesian estimation, we used a Markov chain Monte Carlo method with four chains, 1000 iterations, and 500 warm-up iterations via the brms package (Bürkner, 2017). We used a weakly informed prior for the group mean based on realistic values for origination rates. We further constrained this prior to values between 0 and 100, representing the absolute minimum and maximum values for origination rates expressed in percentage points. The prior for the response variable was sampled from the Student's t distribution, rendering the model more robust against outliers. We further modeled the sigma coefficient for each paleoclimate interaction individually, allowing groupwise comparisons. The prior for these group variances was sampled from the Cauchy distribution. All model estimates successfully converged using these priors and model parameters. The overall increase of origination probability after cooling–cooling paleoclimate interactions was calculated by dividing the estimated difference of means by the baseline probability of origination. Furthermore, we calculated the Cohen's d effect size based on the raw output of our GLMMs as well as posterior distributions after Bayesian estimation using the formula:

$$\frac{(\mu_1 - \mu_2)}{\sqrt{(\sigma_1^2 + \sigma_1^2)\,/\,2}}$$

We then calculated 95% Wald CIs for the applied nonparametric bootstrapping results and 89% highest posterior density intervals for the Bayesian estimation (McElreath, 2020). Cohen's d is reported to present the magnitude of the reported effects in a standardized, scale-independent metric and is aimed to facilitate the incorporation of our results in a meta-analytical framework.

Group differences

Based on the results from our GLMMs, we calculated the log-odds ratio for each major fossil group and for each Phanerozoic Era spanning all studied stages. A second approach was to group geologic stages together to get to a finer temporal resolution than the Phanerozoic Eras (SI Appendix, Table S3). Grouping of the stages was necessary to obtain a sufficient number of observations to calculate the log-odds ratio and was based on the number of stages included, resulting in evenly spaced intervals. The oldest interval ranged from the Tremadocian to Lochkovian, the second from the Pragian to the Artinskian, the third from the Kungurian to the Pliensbachian, the fourth from the Toarcian to the Turonian, and the youngest period from the Coniacian to the Pleistocene. We did not calculate group differences for phyla for which data were insufficient to get a log-odds ratio estimate. To compare changes between shallow and deep-water taxa, we used the environmental information included in the fossil occurrence dataset. We separately predicted the origination response for onshore and offshore taxa using our GLMMs. We then calculated the difference in means between origination probability after cooling–cooling compared to all other paleoclimate interactions for each group using Bayesian estimation. The comparison between onshore and offshore taxa was then conducted using samples from the posterior of the Bayesian estimation model (SI Appendix, Fig. S1).

Continental fragmentation

To estimate whether habitat space and vicariance might be the mechanisms through which paleoclimate interactions act on origination probability, we included continental fragmentation as an explanatory variable in our model framework. We used a continental fragmentation index (Zaffos et al., 2017) (SI Appendix, Fig. S8) accessed via the accompanying GitHub repository (https://github.com/UW-Macrostrat/PNAS_201702297) (Zaffos et al., 2017). Data processing was similar to processing of temperature data, including the calculation of short-term changes and long-term trends in continental fragmentation. We then compared the origination probability for marine genera for each possible interaction of short-term and long-term continental fragmentation (increase-increase, increase-decrease, decrease-increase, and decrease-decrease) using the same analysis as for paleoclimate.

Robustness testing

We further conducted additional tests on both raw data and our models to test for explicit biases in our analytical framework. These robustness tests and their results are described in detail in the accompanying supporting information file and include a model comparison between traditional model estimates and paleoclimate interactions, cross-correlation tests for temperature data and the continental fragmentation index, tests for the inclusion of an additional random effect in the GLMMs, tests for the dependence of inference on $\delta^{18}O$ isotope data for paleo-temperature estimation, and posterior predictive checks as well as convergence diagnostics for the Bayesian estimation.

Data availability

Raw and processed data and code data have been deposited in GitHub (https://github.com/Ischi94/palint-origin) and Figshare (https://figshare.com/s/a789b5bdd52035d59dfd).

Acknowledgments

This work was supported by the Deutsche Forschungsgemeinschaft (KI 806/16-1 and STE 2360/2-1) and is embedded in the Research Unit TERSANE (FOR 2332: Temperature-related stressors as a unifying principle in ancient extinctions). M.J.S. acknowledges support by European Research Council Grant No. 741413 Humans on Planet Earth.

References

Alroy, J. (2008). Dynamics of origination and extinction in the marine fossil record. *Proceedings of the National Academy of Sciences*, *105*(Supplement 1), 11536–11542. https://doi.org/10.1073/pnas.0802597105

Alroy, J., Koch, P. L., & Zachos, J. C. (2000). Global Climate Change and North American Mammalian Evolution. *Paleobiology*, *26*(4,), 259–288.

Antão, L. H., Bates, A. E., Blowes, S. A., Waldock, C., Supp, S. R., Magurran, A. E., Dornelas, M., & Schipper, A. M. (2020). Temperature-related biodiversity change across temperate marine and terrestrial systems. *Nature Ecology & Evolution*, *4*(7), 927–933. https://doi.org/10.1038/s41559-020-1185-7

Bates, D., Mächler, M., Bolker, B., & Walker, S. (2015). Fitting linear mixed-effects models using lme4. *Journal of Statistical Software*, 1–48. https://doi.org/10.18637/jss.v067.i01

Bolker, B. M., Brooks, M. E., Clark, C. J., Geange, S. W., Poulsen, J. R., Stevens, M. H. H., & White, J.-S. S. (2009). Generalized linear mixed models: A practical guide for ecology and evolution. *Trends in Ecology & Evolution*, *24*(3), 127–135.

Bray, A., Ismay, C., Chasnovski, E., Baumer, B., & Cetinkaya-Rundel, M. (2021). *infer: Tidy Statistical Inference* (0.5.4) [R]. https://CRAN.R-project.org/package=infer

Bürkner, P.-C. (2017). brms: An R package for Bayesian multilevel models using Stan. *Journal* *of Statistical Software*, *80*(1), 1–28.

Button, D. J. (2017). Mass extinctions drove increased global faunal cosmopolitanism on the supercontinent Pangaea. *NATURE COMMUNICATIONS*, 8. https://doi.org/10.1038/s41467-017-00827-7

Cárdenas, A. L., & Harries, P. J. (2010). Effect of nutrient availability on marine origination rates throughout the Phanerozoic eon. *Nature Geoscience*, *3*(6), 430–434. https://doi.org/10.1038/ngeo869

Eldredge, N. (1971). The Allopatric Model and Phylogeny in Paleozoic Invertebrates. *Evolution*, *25*(1), 156. https://doi.org/10.2307/2406508

Foote, M. (2000). Origination and extinction components of taxonomic diversity: General problems. *Paleobiology*, *26*(sp4), 74–102.

Gilman, S. E., Urban, M. C., Tewksbury, J., Gilchrist, G. W., & Holt, R. D. (2010). A framework for community interactions under climate change. *Trends in Ecology & Evolution*, *25*(6), 325–331. https://doi.org/10.1016/j.tree.2010.03.002

Hopkins, M. J., Simpson, C., & Kiessling, W. (2014). Differential niche dynamics among major marine invertebrate clades. *Ecology Letters*, *17*(3), 314–323. https://doi.org/10.1111/ele.12232

Jablonski, D. (2008). Extinction and the spatial dynamics of biodiversity. *Proceedings of the National Academy of Sciences*, *105*(Supplement 1), 11528–11535. https://doi.org/10.1073/pnas.0801919105

Kiessling, W. (2010). Promoting marine origination. *Nature Geoscience*, *3*(6), 388–389. https://doi.org/10.1038/ngeo874

Kocsis, À. T., Reddin, C. J., Alroy, J., & Kiessling, W. (2019). The R package divDyn for quantifying diversity dynamics using fossil sampling data. *Methods in Ecology and Evolution*, *10*(5), 735–743.

Kruschke, J. K. (2013). Bayesian estimation supersedes the t test. *Journal of Experimental Psychology: General*, *142*(2), 573.

Lister, A. M. (2004). The impact of Quaternary Ice Ages on mammalian evolution. *Philosophical Transactions of the Royal Society B: Biological Sciences*, *359*(1442), 221–241.

Maldonado-Coelho, M. (2012). Climatic oscillations shape the phylogeographical structure of Atlantic Forest fireeye antbirds (Aves: Thamnophilidae). *Biological Journal of the Linnean Society*, 25.

Mathes, G. H., van Dijk, J., Kiessling, W., & Steinbauer, M. J. (2021). Extinction risk controlled by interaction of long-term and short-term climate change. *Nature Ecology & Evolution*, *5*(3), 304–310. https://doi.org/10.1038/s41559-020-01377-w

Mayhew, P. J., Bell, M. A., Benton, T. G., & McGowan, A. J. (2012). Biodiversity tracks temperature over time. *Proceedings of the National Academy of Sciences*, *109*(38), 15141–15145. https://doi.org/10.1073/pnas.1200844109

Mayhew, P. J., Jenkins, G. B., & Benton, T. G. (2008). A long-term association between global temperature and biodiversity, origination and extinction in the fossil record. *Proceedings of the Royal Society B: Biological Sciences*, *275*(1630), 47–53. https://doi.org/10.1098/rspb.2007.1302

Mayr, E. (1963). Animal species and evolution. *Animal Species and Evolution.*

Mayr, E., & O'Hara, R. J. (1986). The biogeographic evidence supporting the Pleistocene forest refuge hypothesis. *Evolution*, *40*(1), 55–67. https://doi.org/10.1111/j.1558-5646.1986.tb05717.x

McElreath, R. (2020). *Statistical Rethinking, 2nd Edition*. https://learning.oreilly.com/library/view/-/9780429639142/?ar

Mooney, C. Z. (1996). Bootstrap statistical inference: Examples and evaluations for political science. *American Journal of Political Science*, 570–602.

Ogg, J. G., Ogg, G. M., & Gradstein, F. M. (2016). *A concise geologic time scale: 2016*. Elsevier.

Peters, S. E. (2005). Geologic constraints on the macroevolutionary history of marine animals. *Proceedings of the National Academy of Sciences*, *102*(35), 12326–12331. https://doi.org/10.1073/pnas.0502616102

Peters, S. E. (2006). Genus extinction, origination, and the durations of sedimentary hiatuses. *Paleobiology*, *32*(3), 387–407. https://doi.org/10.1666/05081.1

Pinheiro, J. C., & Chao, E. C. (2006). Efficient Laplacian and adaptive Gaussian quadrature algorithms for multilevel generalized linear mixed models. *Journal of Computational and Graphical Statistics*, *15*(1), 58–81.

Postigo-Mijarra, J. M., Morla, C., Barrón, E., Morales-Molino, C., & García, S. (2010). Patterns of extinction and persistence of Arctotertiary flora in Iberia during the Quaternary. *Review of Palaeobotany and Palynology*, 12.

Prothero, D. R. (1999). Does climatic change drive mammalian evolution? *GSA Today*, *9*(9), 1.

R Core Team. (2021). *R: A Language and Environment for Statistical Computing* (4.1.2) [R]. R Foundation for Statistical Computing. https://www.R-project.org/

Raup, D. M. (1979). Size of the Permo-Triassic Bottleneck and Its Evolutionary Implications. *Science*, *206*(4415), 217–218. https://doi.org/10.1126/science.206.4415.217

Schuler, M. S., Chase, J. M., & Knight, T. M. (2017). Habitat patch size alters the importance of dispersal for species diversity in an experimental freshwater community. *Ecology and Evolution*, *7*(15), 5774–5783. https://doi.org/10.1002/ece3.2858

Sepkoski, J. J. (2002). A compendium of fossil marine animal genera. *Bulletins of American Paleontology*, *363*, 1–560.

Stigall, A. L. (2014). When and how do species achieve niche stability over long time scales? *Ecography*, *37*(11), 1123–1132. https://doi.org/10.1111/ecog.00719

Svenning, J.-C., Eiserhardt, W. L., Normand, S., Ordonez, A., & Sandel, B. (2015). The influence of paleoclimate on present-day patterns in biodiversity and ecosystems. *Annual Review of Ecology, Evolution, and Systematics*, *46*(1), 551–572. https://doi.org/10.1146/annurev-ecolsys-112414-054314

Templeton, A. R. (2008). The reality and importance of founder speciation in evolution. *BioEssays*, *30*(5), 470–479. https://doi.org/10.1002/bies.20745

Tilman, D. (1994). Competition and Biodiversity in Spatially Structured Habitats. *Ecology*, *75*(1), 2–16. https://doi.org/10.2307/1939377

Valentine, J. W. (1968). Climatic Regulation of Species Diversification and Extinction. *Geological Society of America Bulletin*, *79*(2), 273. https://doi.org/10.1130/0016-7606(1968)79[273:CROSDA]2.0.CO;2

Valentine, J. W., & Moores, E. M. (1970). Plate-tectonic Regulation of Faunal Diversity and Sea Level: A Model. *Nature*, *228*(5272), 657–659. https://doi.org/10.1038/228657a0

Veizer, J., & Prokoph, A. (2015). Temperatures and oxygen isotopic composition of Phanerozoic oceans. *Earth-Science Reviews*, *146*, 92–104.

Wahl, L. M., Gerrish, P. J., & Saika-Voivod, I. (2002). Evaluating the Impact of Population Bottlenecks in Experimental Evolution. *Genetics Society of America*, *162*, 12.

Wiens, J. J., & Graham, C. H. (2005). Niche conservatism: Integrating evolution, ecology, and conservation biology. *Annual Review of Ecology, Evolution, and Systematics*, *36*(1), 519–539. https://doi.org/10.1146/annurev.ecolsys.36.102803.095431

Zaffos, A., Finnegan, S., & Peters, S. E. (2017). Plate tectonic regulation of global marine animal diversity. *Proceedings of the National Academy of Sciences*, *114*(22), 5653–5658. https://doi.org/10.1073/pnas.1702297114

Supplementary information

Model comparison

Previous studies used different estimates of temperature to deduce an association between origination and temperature (Cárdenas & Harries, 2010; Krug et al., 2009; Mayhew et al., 2008, 2012). Generally, simple models correlate static temperature estimates at each interval to biodiversity in the same interval. More complex models include temporal lags of temperature, allowing for a suspended response of biota to temperature change (Cárdenas & Harries, 2010; Mayhew et al., 2008). Most recent models are based on both estimates but additionally allow for interactions of static estimates and temporal lags (Mayhew et al., 2012). To test whether paleoclimate interactions perform better than these traditional model estimates, we calculated a GLMM for each model structure from simple to complex (static temperature, temporal lags, interactions). We then compared the performance of each model to a model allowing for paleoclimate interactions. The paleoclimate interaction models were based on the same model structure, but explicitly allowed for interactions of long-term temperature trends and short-term climate changes within a dynamic modeling framework. Comparison of model performance was based on AIC values with results being consistent with Bayesian information criterion (Table S6). We found that models including dynamic paleoclimate interactions performed better than their traditional counterparts in all 6 cases (Fig. S2). Models covering short-term cooling improved on average by 586 AIC values, and models covering short-term warming by 218 AIC values (Fig. S3). Our model comparison hence indicates that models including paleoclimate interactions are more parsimonious than their counterparts, despite their increased complexity. The large effect size and the cascading nature of paleoclimate interactions might have obscured or even inverted the apparent relationship between temperature and origination in traditional models, as it has been shown for other interactions in the fossil record (Ritterbush & Foote, 2017; Stigall, 2013). This might particularly be the case for cooling periods in Earth's system, as the model comparison shows that models with paleoclimate interactions have a sufficiently improved predictive accuracy for the response to cooling as compared to traditional models. The difference between model types is not as pronounced when dealing with warming periods, which we account to the lower effect size of paleoclimate interactions on both short-term and long-term warming (Fig. 1). Explicitly accounting for dynamic interactions within a flexible modeling framework as presented in our analysis might provide a more robust foundation to assess the relationship between Phanerozoic marine diversity and climate.

Cross-correlation

Testing a potential mechanism through which paleoclimate interactions can act on origination rates, we found that continental fragmentation shows a similar impact on origination rates as paleoclimate interaction (Fig. 4). We then account this similarity to a shared causal path through which both parameters, paleo-temperature and continental fragmentation, affect origination rates. However, the effect similarity might not only arise by a shared causal path but can be potentially biased by a high cross-correlation between both parameters. Especially a high correlation in time intervals with pronounced cooling might distort our interpretation, as both parameters showed an increase in origination rates subsequent to these (Fig. 1 and 4). Accordingly, we tested for crosscorrelation between our paleo-temperature estimates and the continental fragmentation index. As our analytical framework included a long-term trend going back up to ten stages, we additionally checked the cross-correlation ten stages prior and after the focal bin. We used Pearson's product moment correlation coefficient to estimate the correlation and the Fisher z-transformation to get confidence intervals (Fisher, 1921). We first detrended both time series, temperature and the continental fragmentation index, using first differences and additionally tested for auto-correlation in the residuals of the cross-correlation test by applying the Durbin-Watson test (Farebrother, 1980). We found no indication for a high cross-correlation, neither within the whole data set nor in the subset only including time intervals with cooler temperature than the average. Additionally dividing the data into the three chronological Eras (Paleozoic, Mesozoic, Cenozoic) yielded no significant crosscorrelation as well (Fig. S9, Table S7). Our analytical framework is hence not biased by a high correlation between parameters used to estimate effect sizes and can be applied for biologically meaningful inferences about dynamics in Earth's system.

Additional random effect

Fossil genera are repeatedly sampled throughout time in occurrence data. To account for these multiple occurrences, we used the genus-level as a random effect in our regression framework. However, it might be reasonable to add geological stages as a second random effect to account for auto-correlation within the time series data. We hence tested for the inclusion of this second random effect term in our analysis by comparing a model with both random effects to a model with genus-level variation and a second constant random effect by means of AIC ((Galwey, 2007). We found no support for the inclusion of geological stages as a second random effect in our models as AIC values showed that models with a constant random effect instead of stages performed better (Table S8). Additionally, re-running our whole analysis with models where stages were added as a second random effect showed no deviation from the original results, neither in the direction of the effect nor in magnitude (Fig. S5). We hence decided to restrict our models to one random effect (genus-level) as inference was robust to choice of random effects, and as we found no support for the inclusion of stages as a second term. Restricting the models to one random effect additionally yielded the possibility to use Gauss-Hermite quadrature for likelihood approximation (Pinheiro & Chao, 2006). Gauss-Hermite quadrature is less prone to biases and more precise compared to Laplace approximation (Bolker et al., 2009), which is used for any models with more than one random effect in the R package used for our model fitting (Bates et al., 2015).

Bayesian estimation

We applied two statistical approaches to calculate the effect (difference in means) from the predicted origination response of our GLMMs: Non-parametric bootstrapping and Bayesian estimation. Returning complete distributions of credible values for the effect and additionally for group means and their standard deviations (and the difference of group-wise standard deviations), Bayesian estimation provides richer information about samples compared to bootstrapping and other frequentist approaches (Kruschke, 2013). This increase in information comes with additional complexity and requires additional tests to secure a valid estimation of the effect size (McElreath, 2020). Visually inspecting the samples for each parameter from the Hamiltonian MCMC used to conduct our Bayesian estimation shows fast and good convergence of the sampling procedure. Similarly, rank histograms of the sampling procedure show good convergence and mixing of chains. The ratios of the effective sample size to total sample size from the joint posterior indicate low auto-correlation in parameters and a good model fit to the data. Rhat values, a common convergence diagnostic calculated by comparing the between- and within-chain estimates, show a good convergence and efficiency of the model fit for all parameters as well. A posterior predictive check of the Bayesian estimation comparing the observed outcome variable to simulated data sets from the posterior predictive distribution shows a good fit to the actual data distribution (Fig. S10). All diagnostics for the Bayesian estimation hence show that the reported effect and accompanying parameter estimates are robust and reliable.

Temperature data

To get an estimate of the global mean temperature for each geologic stage, we used the $\delta^{18}O$

values of well-preserved calcareous shells which are often considered as the best available temperature proxy for the fossil record (Song et al., 2019) (Fig. S11). Conversion of $\delta^{18}O$ values into temperature requires to account for the composition of seawater $\delta^{18}O$ in deep time. The exact composition is unknown and can only be estimated. We followed the argumentation of Veizer and Prokoph (2015), inferring a secular increase in seawater $\delta^{18}O$ values as a result of changes in how oxygen reservoirs are exchanged with the vastly larger oxygen reservoir in crust and mantle silicates. We adjusted for the secular trend in oxygen isotopic composition of seawater with the equation: $\delta^{18}O^{pw}$ (‰) = t^2 + 0.0046‰ t, where *pw* denotes Phanerozoic seawater in standard mean ocean water and t age in million years ago. We further averaged tropical and subtropical records. We subsequently binned temperature data on the basis of isotope values to geological stages to provide global mean temperature for each of the 80 stages used in our analysis (Fig. S8). We emphasize however that there are still many uncertainties about reconstructing paleo-temperature from $\delta^{18}O$ values and that the conversion we used for our analysis is commonly accepted and widely used but remains subject of considerable debate (Song et al., 2019; Veizer & Prokoph, 2015). To check whether our choice in $\delta^{18}O$ source and processing method biased our inference, we repeated our whole analysis with $\delta^{18}O$ isotope values from a different compilation. We downloaded the pre-processed data file from the supplementary material of Song et al. (2019) containing sea surface temperature estimates for the whole Phanerozoic. The underlying data base of isotope data from which the paleo-temperature was estimated contains both phosphatic and calcareous fossils. In stark contrast to Veizer and Prokoph (2015), an invariant oxygen isotope composition of seawater was assumed to convert the $\delta^{18}O$ isotope values to paleo-temperature estimates. The data was therefore suitable for our robustness test. Re-running our whole analysis with the data from Song et al. resulted in an overall smaller but still robust and substantial effect size (Table S9). Both the direction and the magnitude of the effect remained the same. We were hence able to detect the large effect of paleoclimate interaction on origination rates regardless of the underlying estimation for paleo-temperature, rendering this effect robust against underlying assumptions of temperature data processing.

Origination likelihood through time

The origination likelihood after cooling-cooling compared to all other paleoclimate interactions shows a decreasing trend through time (Fig. 3), with more variation over shorter timescales (Table S3). This trend might potentially show a decreasing importance of paleoclimate interactions through time on geologic scales, with a strong effect on the origination likelihood in the Paleozoic and less but still significant impact in more recent stages. An explanation for this might be that taxa generally showing an attenuated response to cooling-cooling are becoming more abundant in the Mesozoic and Cenozoic compared to taxa that are more responsive to cooling-cooling (Fig. S12). However, various unmeasured factors can potentially influence this trend as well, such as the extent of epicontinental seas or relative sea level changes. To quantify the importance of these unmeasured factors, we conducted an additional analysis estimating the proportion of variance in the origination likelihood that can be explained by the relative abundance of climate sensitive taxa through time alone. For this, we counted the occurrence of each phylum within five evenly spaced intervals spanning the Phanerozoic (see methods section). We then multiplied the log-odds ratio of each focal phylum with the number of occurrences per interval, and took the mean across all phyla for each interval. To allow a comparison between intervals, we then normalized the mean by dividing through the total number of occurrences within the interval. The resulting estimate ranged between zero and one and encapsulated the variation in the origination likelihood solely explained by the changing abundance of taxa through time. We then compared this estimate to the observed log-odds ratios per interval. If the estimated log-odds ratios would align with the observed values (i.e. showing a perfect correlation), then the overall decreasing trend would be solely driven by the changes in abundance of taxa through time. Any deviation from this alignment would indicate the impact of other, unobserved factors. Our results show an overall good alignment with some variability (Fig. S13). We then took the absolute difference between the estimated log-odds ratios and a perfect alignment (i.e., the variation that is not explained by the changes in abundance of taxa through time) and correlated them with the observed log-odds ratios. We found that these absolute differences were generally low during intervals with high observed log-odds ratios, and high during intervals with low ratios (Fig. S13). This might indicate that unobserved factors have a stronger impact when the overall effect of cooling-cooling on the origination likelihood is less pronounced. The decreasing trend through time, however, is mainly driven by the changing abundance of taxa as we found a good alignment of our estimated and observed log-odds ratios.

Dynamics of origination and extinction

Cooling-cooling paleoclimate interactions have also been shown to drive temperature related extinctions in the fossil record (Mathes et al., 2021). A high correlation between extinction rates and the origination signal used in our analysis would impede to causally disentangle whether paleoclimate interaction impacts origination, extinction, or both. If, for example, paleoclimate interactions increase the extinction rate but do not impact origination rates, a regression analysis would falsely show an effect on both origination and extinction if they are highly correlated. We therefore tested for cross-correlation between a variety of metrics for extinction rates and the origination signal used in our analysis, by calculating the Pearson's product moment correlation coefficient to estimate the correlation and the Fisher z-transformation to get confidence intervals (Fisher, 1921). The extinction metrics were calculated using the divDyn package (Kocsis et al., 2019) from the same data used to calculate the origination signal. Our results showed no substantial cross-correlation, neither with raw values nor after detrending the time series by first differences (Fig. S14). However, extinction rates could still affect the reported effect of paleoclimate interaction on origination rates, as extinction rates in the fossil record are known to be correlated with origination rates approximately 10 million years later (Alroy, 2008; Kirchner & Weil, 2000). High extinction rates in one bin could therefore affect the origination rate in the subsequent bin. Origination rates would hence follow the extinction signal, which itself is partly caused by paleoclimate interaction (Zaffos et al., 2017). Accordingly, we tested for a positive cross-correlation in our data between the extinction signal at one time bin and the origination signal at the following time bin. We found no indication for a positive cross-correlation, neither in the raw lagged data nor after detrending with first differences (Fig. S15). This indicates that the effect we report here reveals biologically meaningful patterns and is not substantially biased by the delayed recovery of biota from extinction.

Supplementary figures

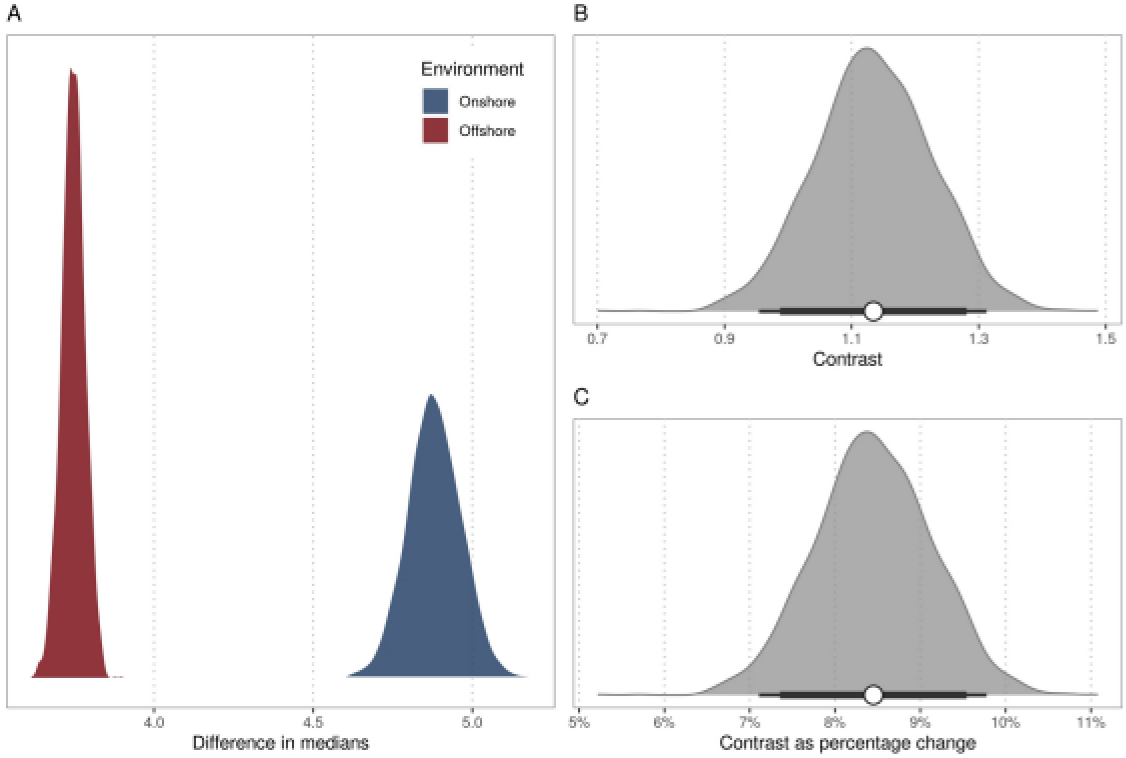

Fig. S1. Density plots of the origination response to cooling-cooling paleoclimate interaction per environment in which the fossil data was found (onshore versus offshore). A) Difference in medians between origination probability after cooling-cooling compared to all other paleoclimate interactions. B) Difference between the origination responses per environment as visualized in A). C) Difference between the origination responses per environment compared to baseline probability. Density is estimated from 2000 posterior samples of the Bayesian estimation. White points show the median values of the posterior. Thick black lines depict the 89% credible intervals, and the thinner black lines the 95% credible intervals.

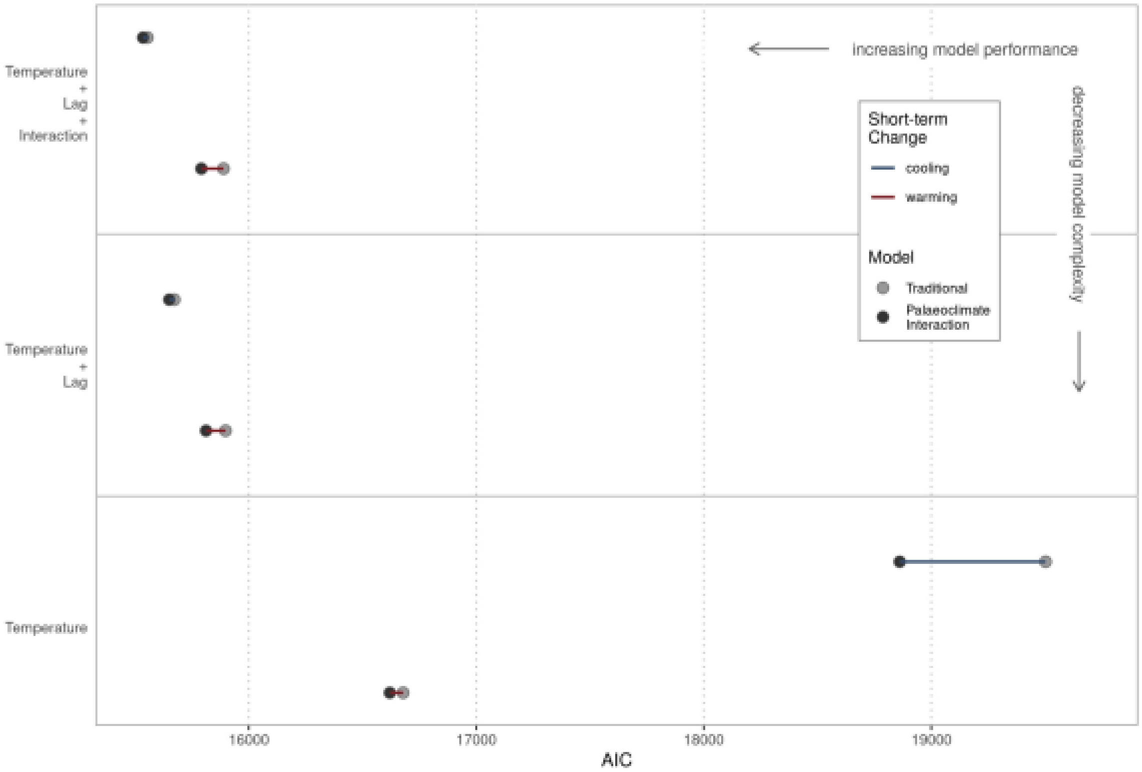

Fig. S2. Comparison of model performance for traditional models covering first- and second-order relationships of origination and temperature versus models allowing for paleoclimate interactions. Models allowing for paleoclimate interactions are based on the same model structure, but explicitly allow for interactions of long-term temperature trends and short-term climate changes within a dynamic modeling framework.

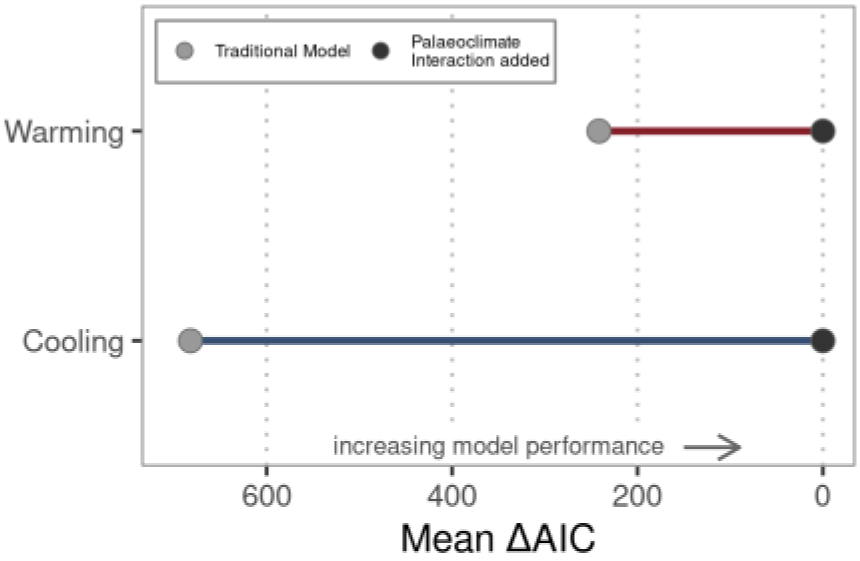

Fig. S3. Comparison of model performance for traditional models covering first- and second-order relationships of origination and temperature versus models allowing for paleoclimate interactions. The latter are based on the same model structure, but explicitly allow for interactions of long-term temperature trends and short-term climate changes within a dynamic modeling framework.

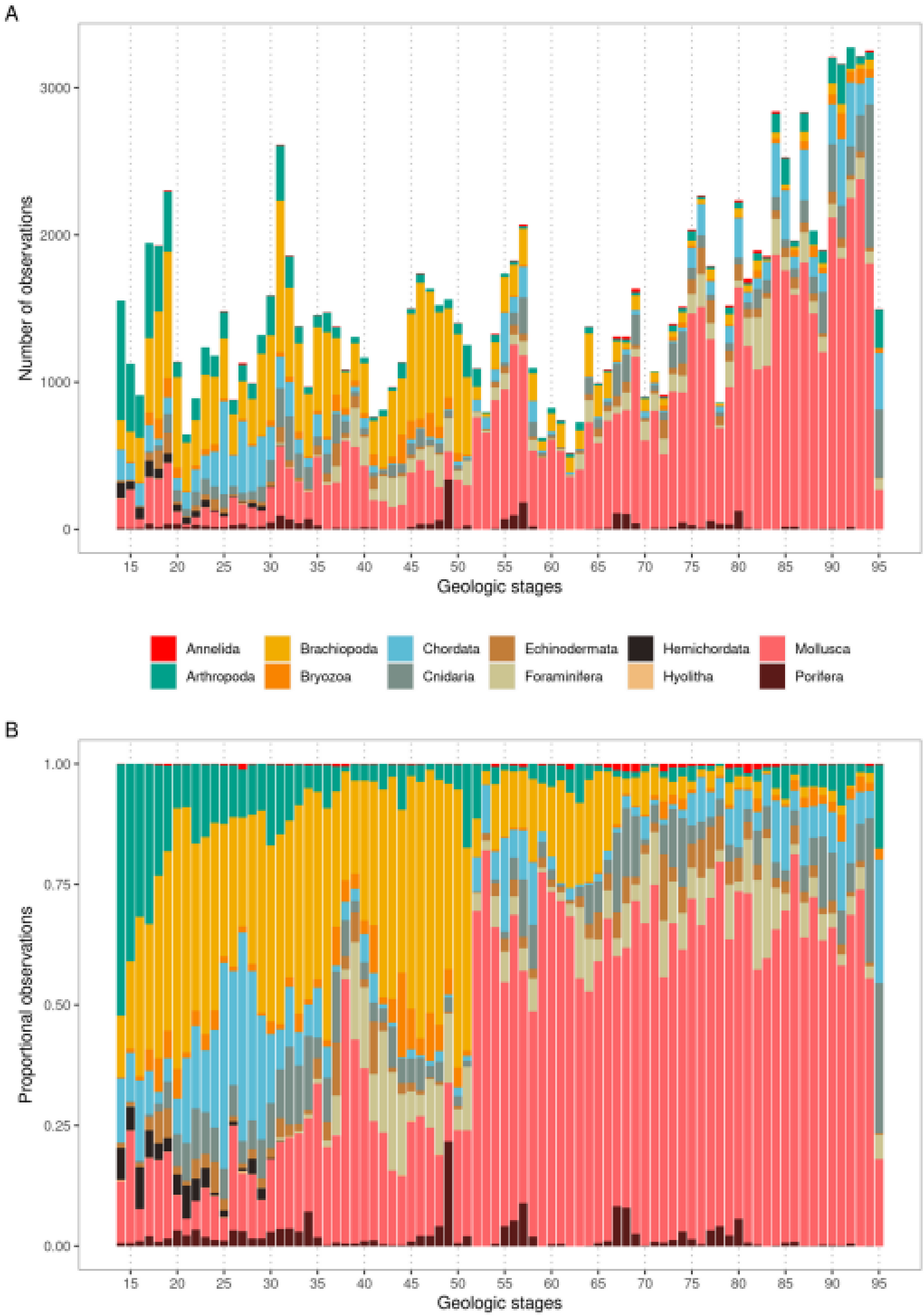

Fig. S4. A) Total number of observations per phyla and stage. B) Percentage of total number of observations per phyla and stage. Stage 14 (Tremadocian, 485 to 477 Ma) is the oldest, and stage 95 (Holocene, 0.01 to 0 Ma) the youngest interval.

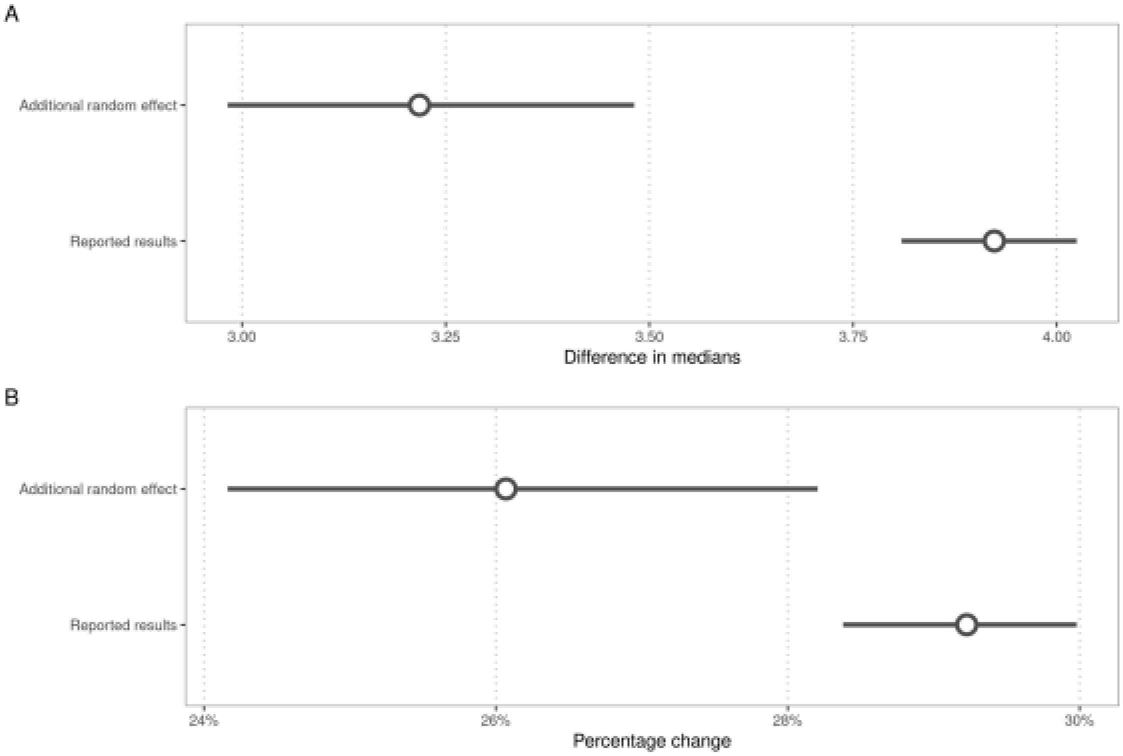

Fig. S5. Comparison of reported results to values based on re-running the whole analysis with models where stages were added as a second random effect. A) The raw difference in medians between origination probability after cooling-cooling compared to all other paleoclimate interactions. B) Overall increase of origination probability after cooling-cooling paleoclimate interactions compared to baseline probability. Results for the additional random effect are calculated using a similar Bayesian estimation model as for the reported results. Grey lines show 89% credible intervals based on the highest posterior density interval. Points show median estimates.

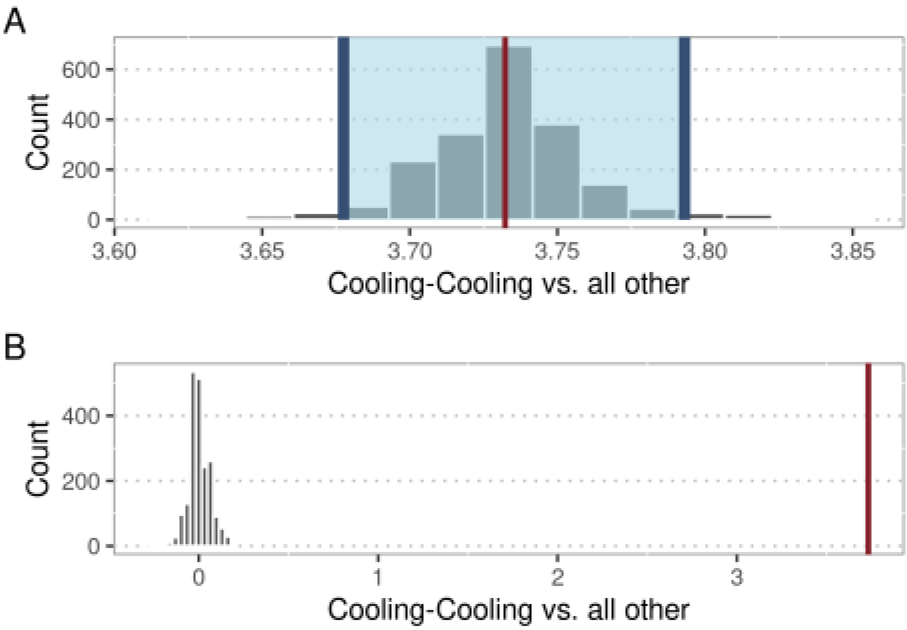

Fig. S6. Difference in means of origination responses after cooling-cooling compared to all other paleoclimate interactions, based on bootstrap resampling. A) Bootstrapped distribution of differences in medians. Red line shows observed difference and shaded area shows the 95% confidence interval. B) Simulation-based null distribution of difference in means compared to the observed difference (red line).

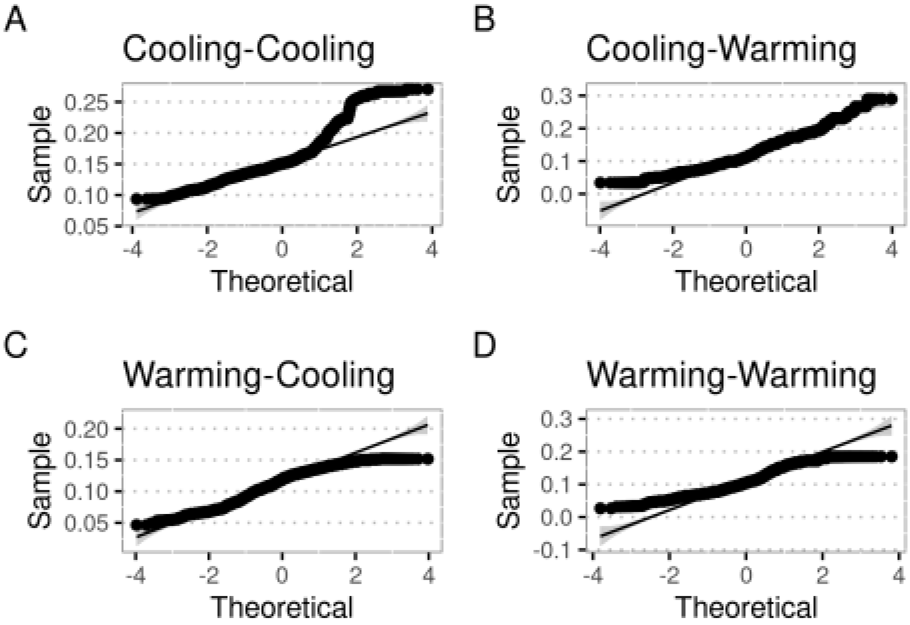

Fig. S7. Quantile-quantile plots for predicted responses of marine fossil groups after paleoclimate interactions. As these plots indicate deviations from normality, further estimates (difference in medians, percentage change, effect change) were calculated using non-parametric methods.

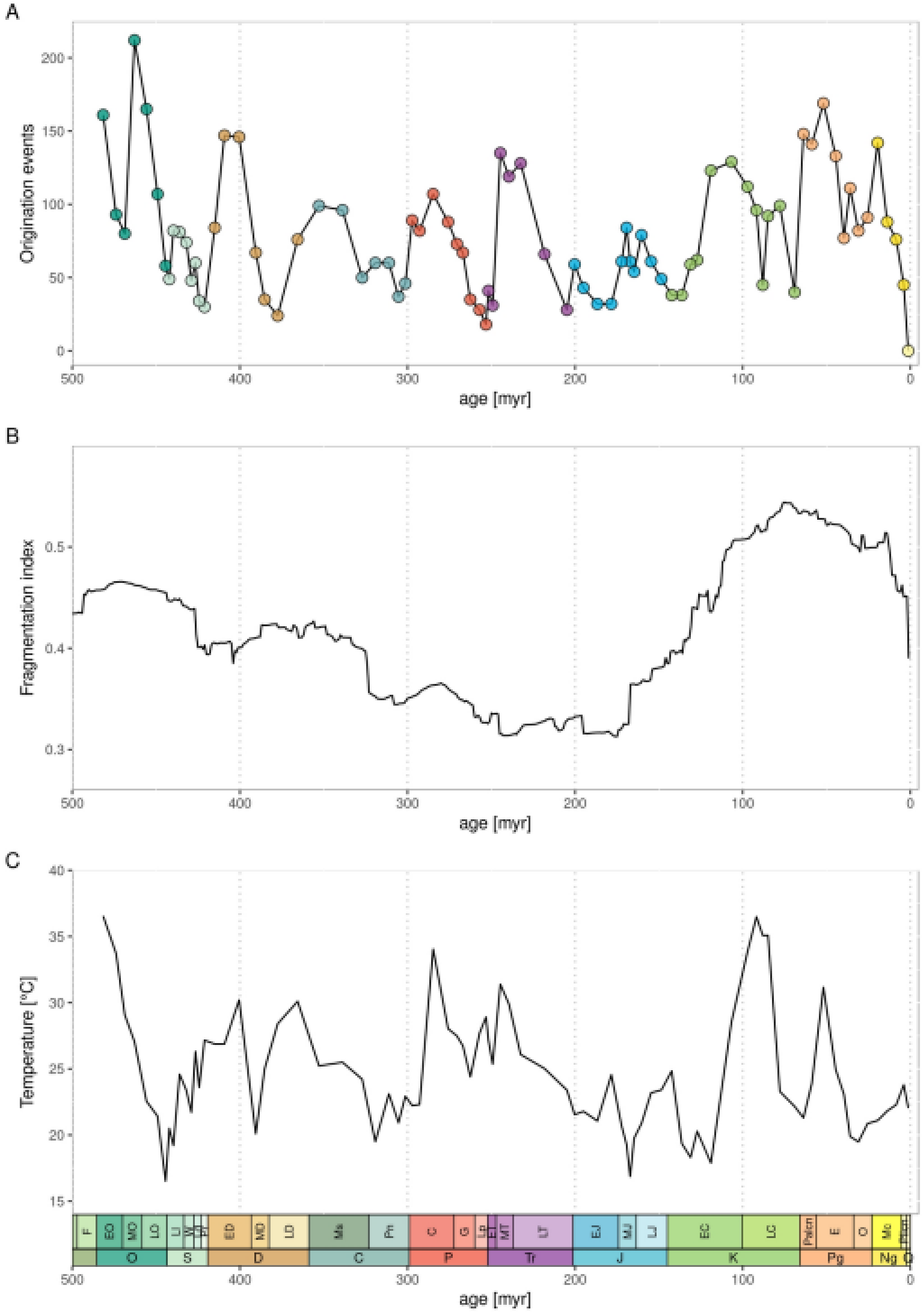

Fig. S8. Data used throughout the analytical framework. A) Origination events per stage used as the response variable in the GLMMs. Points are highlighted in the same color as the geologic period they belong to. B) The continental fragmentation index through the Phanerozoic (21). C) Mean by-stage global temperatures through the Phanerozoic as deduced from oxygen isotopes (17), used as the predictor variable in the GLMMs.

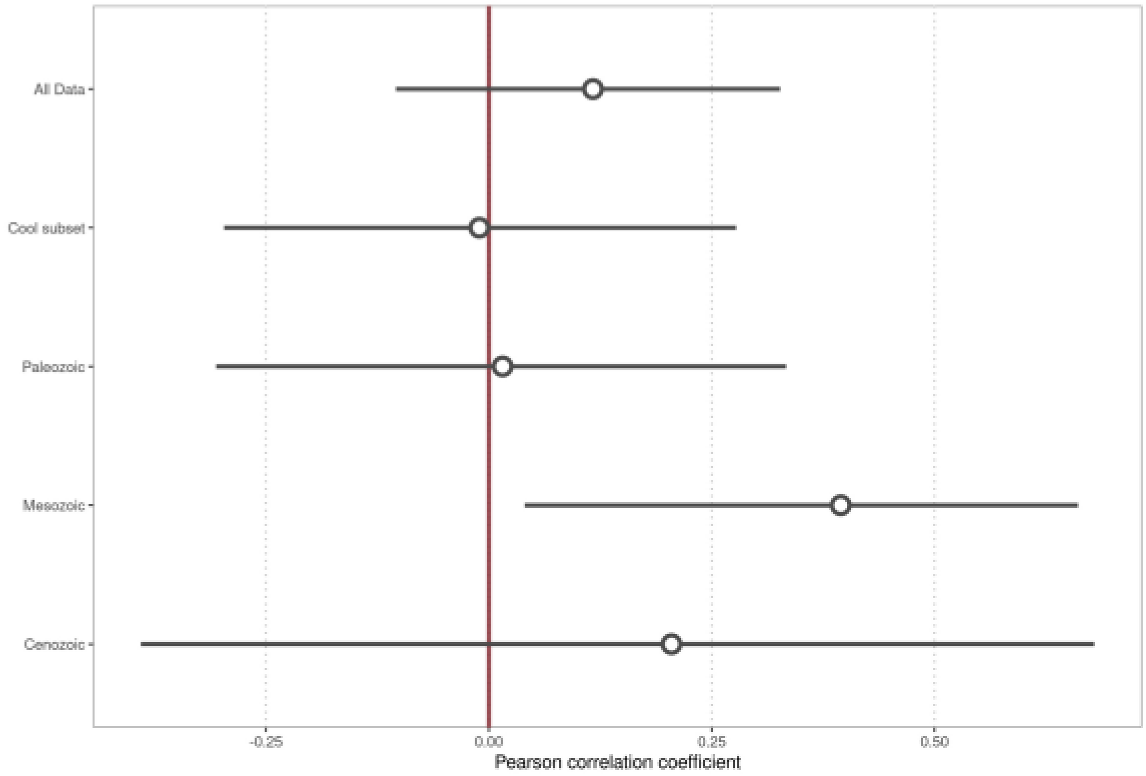

Fig. S9. Cross-correlation between paleo-temperature and the continental fragmentation index. We calculated the Pearson's product moment correlation coefficient and 95% confidence intervals for the correlation between the detrended time-series using first differences. The data was further divided in a subset where temperature is cooler than the mean temperature and into the three chronological Eras (Paleozoic, Mesozoic, Cenozoic).

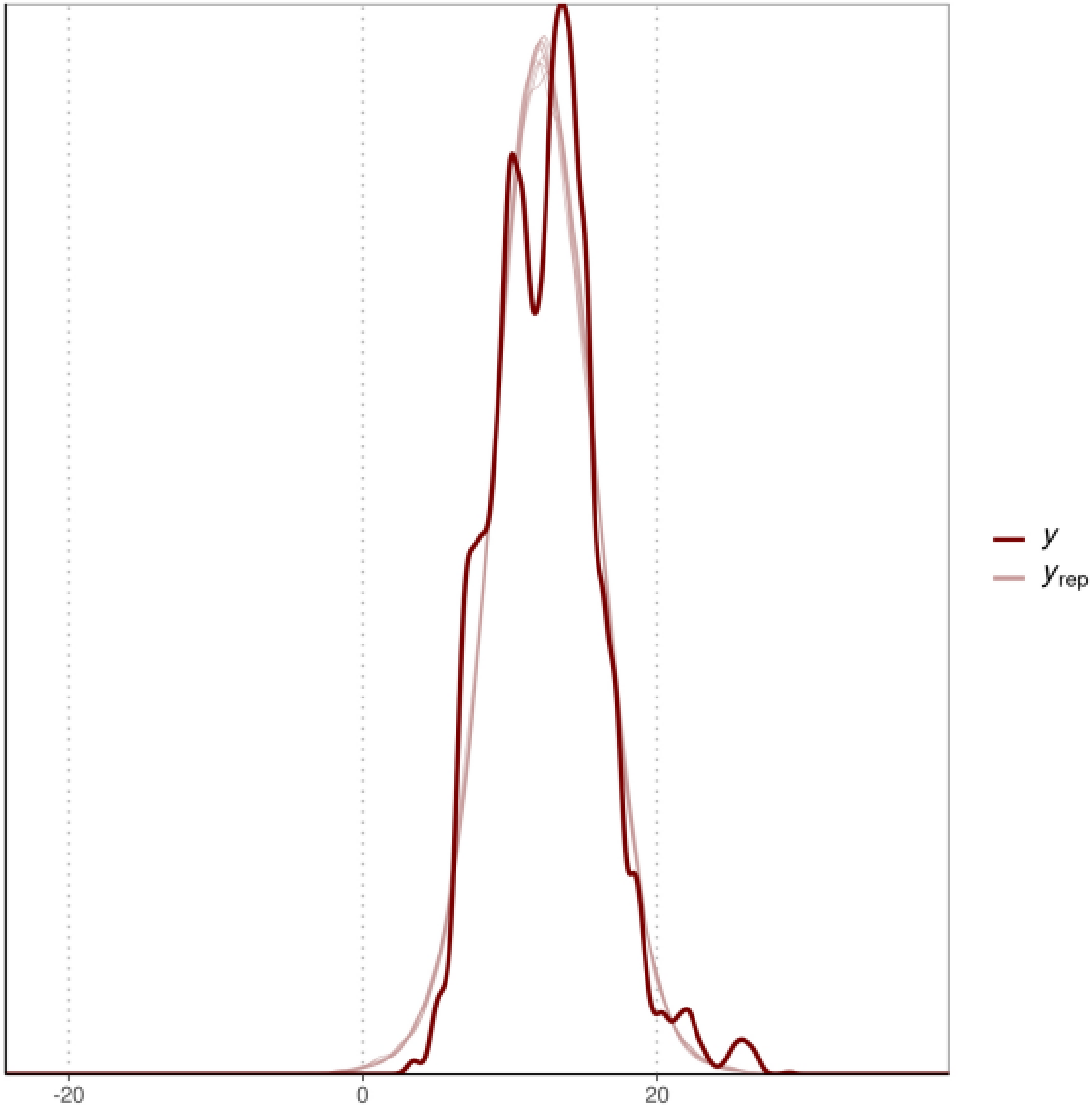

Fig. S10. Posterior predictive check for the Bayesian estimation model. The thick, darker red line shows the distribution of the observed data (y) and the lighter red lines show 10 simulations from the posterior distribution (yrep). The good fit of the model to the observed data indicates that the reported effect and accompanying parameter estimates are robust and reliable.

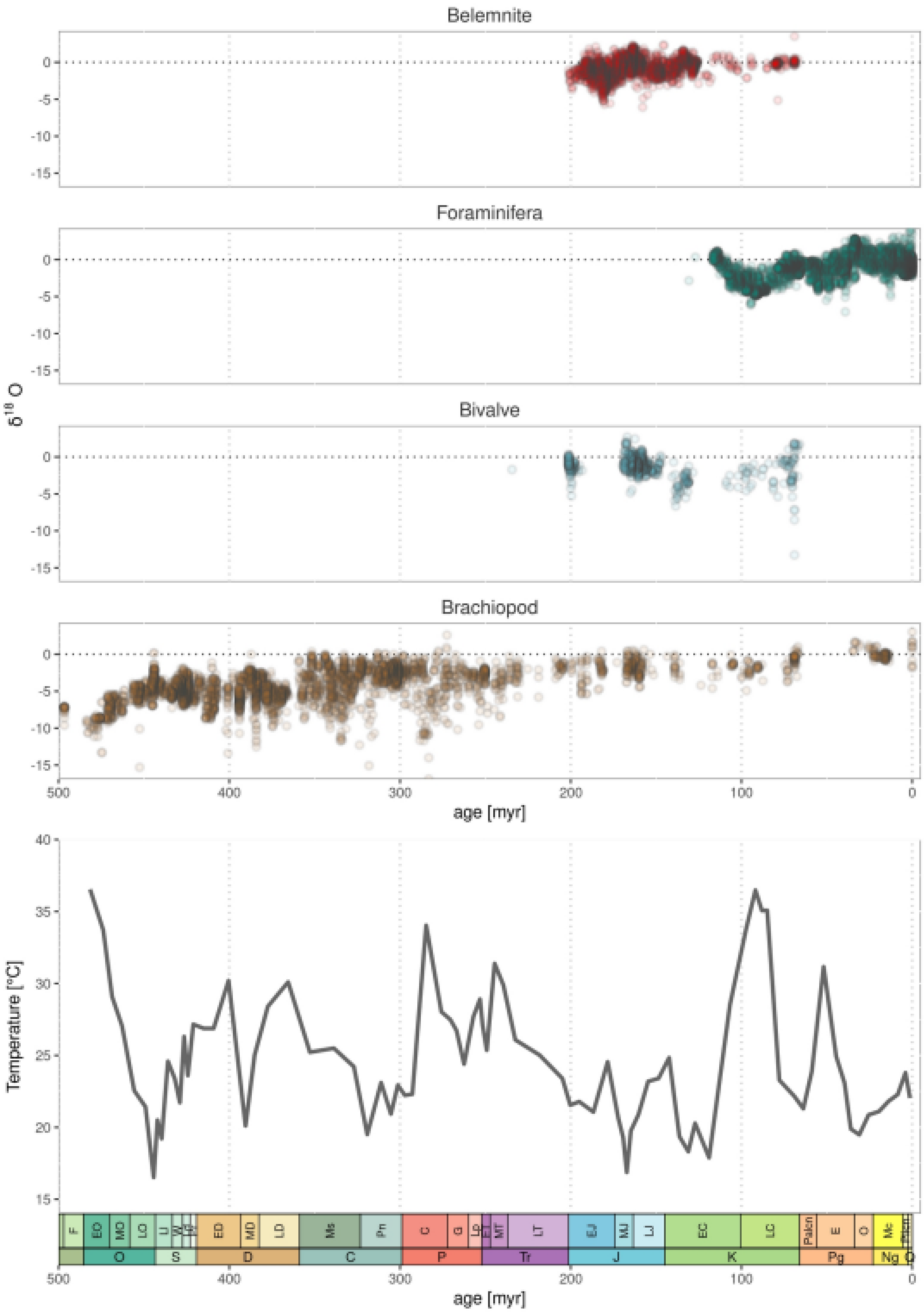

Fig. S11. Raw δ18O compilation of well-preserved calcareous shells throughout the Phanerozoic and conversion of δ18O values into paleo-temperature.

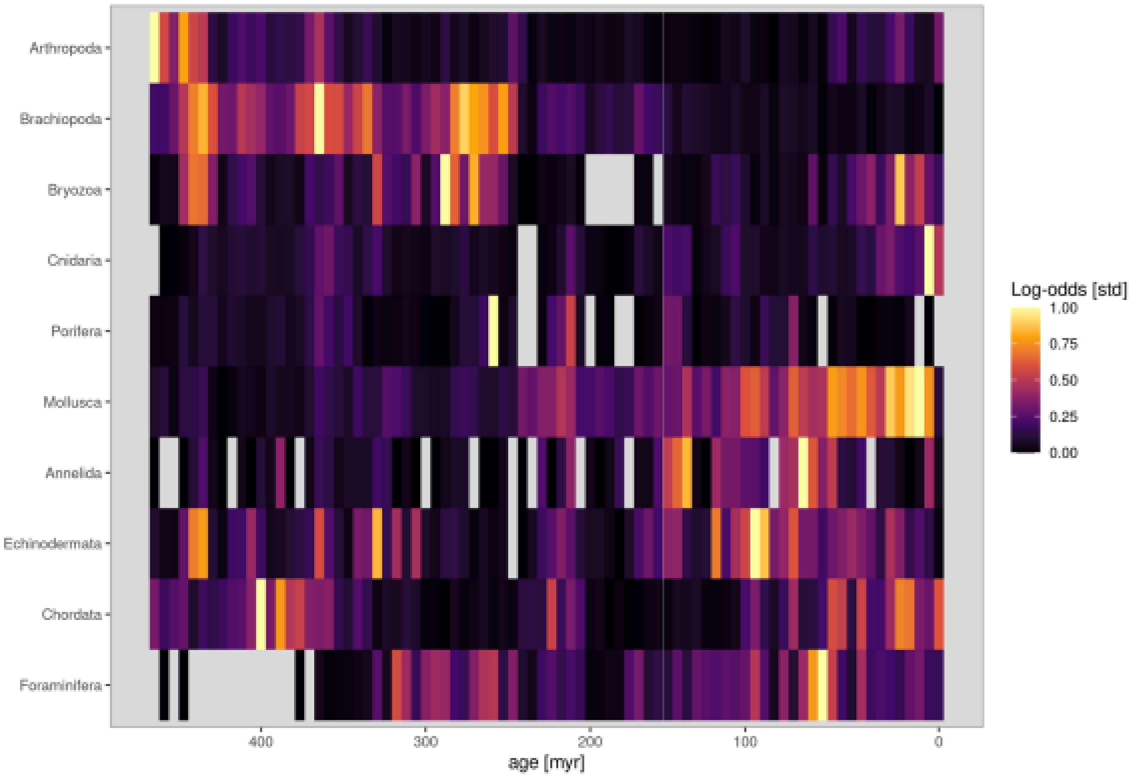

Fig. S12. Changes in the origination likelihood for all major phyla and across time after cooling-cooling compared to all other paleoclimate interactions. The origination likelihood is expressed as standardized log-odds ratios, where we multiplied the average origination likelihood of each phylum with the number of occurrences for each stage. The standardized log-odds hence additionally show when a phylum was most abundant. Phyla are arranged based on their average origination likelihood, with Arthropoda showing the highest and Foraminifera the lowest average origination likelihood (compare Fig. 3).

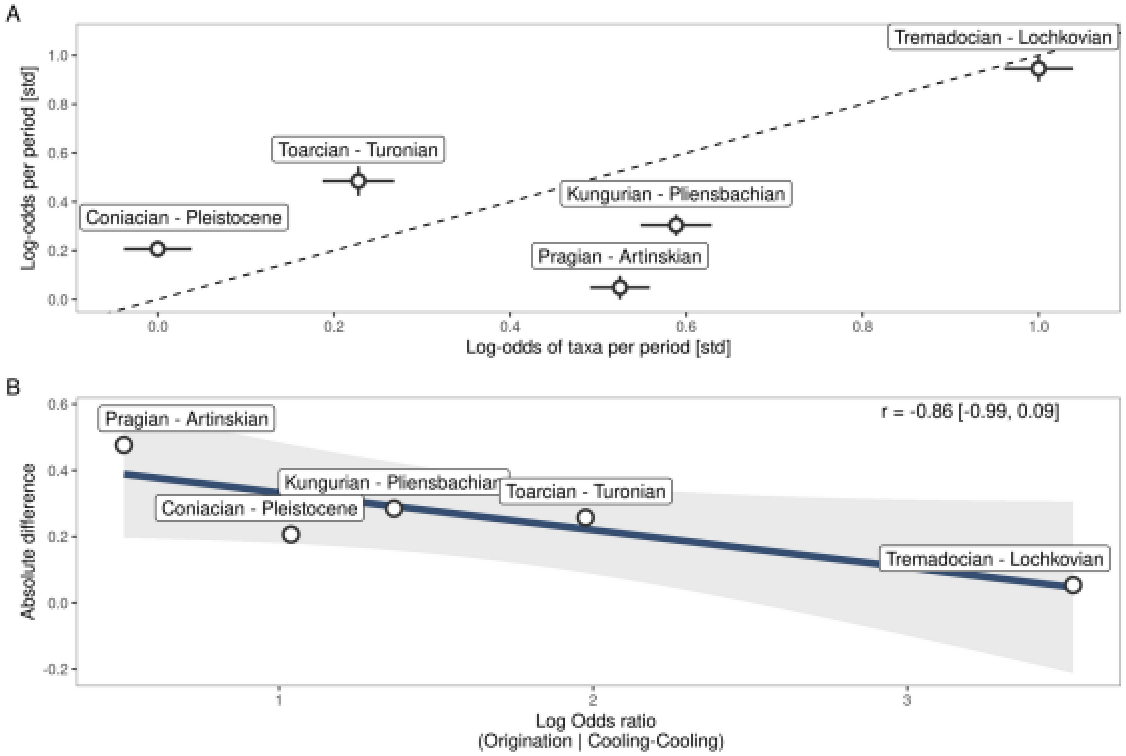

Fig. S13. Results of the analysis estimating the proportion of variance in the origination likelihood that can be explained by the abundance of taxa through time. A) Normalized log-odds ratios showing values if all variation would be explained by abundance of taxa through time alone, plotted against the actual normalized log-odds ratios on the x-axis. The dotted line delineates a perfect agreement between these parameters. Black lines show 95% confidence intervals. B) The difference between the actual values in A) and a perfect agreement (the dotted line) regressed against the observed log-odds ratio for each period. The annotation shows the overall Pearson r correlation coefficient with 95% confidence intervals. The blue line shows the overall trend based on linear regression, and the gray area the 95% confidence interval around this trend. Labels depict the period for which log-odds ratios were calculated (see methods section).

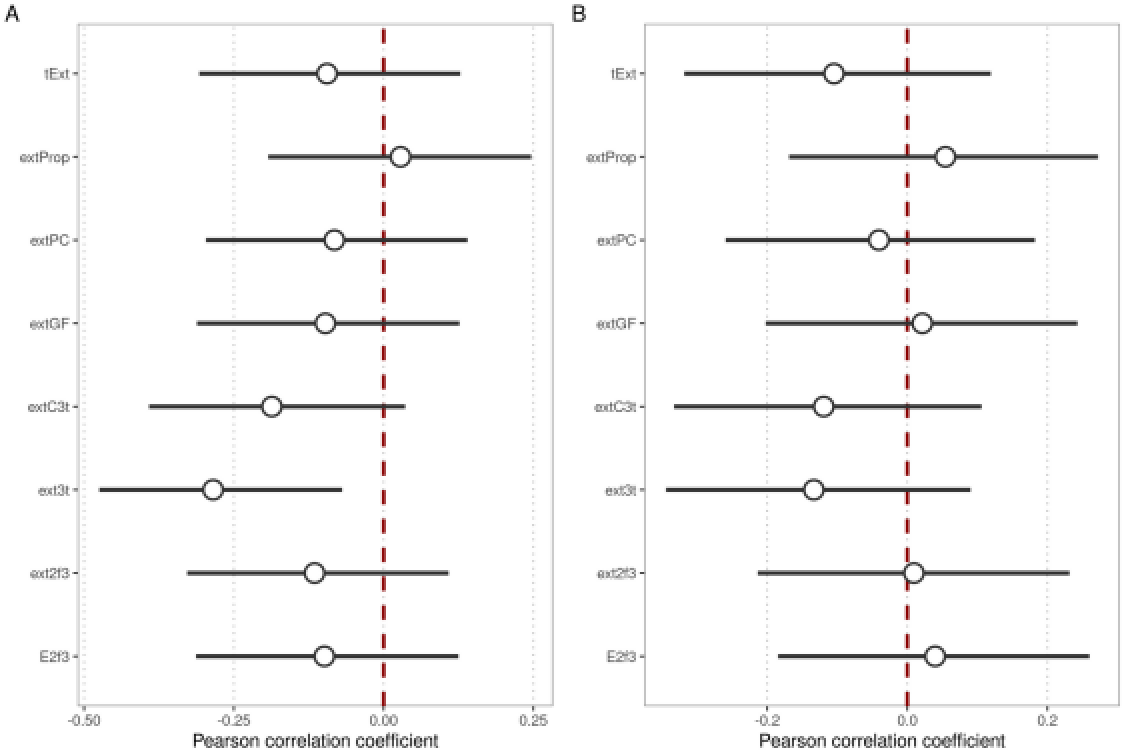

Fig. S14. The Pearson's product moment correlation coefficient for the correlation between the origination signal used in our analysis and various metrics for extinction, including 95% confidence intervals. A) Direct correlations between raw data. B) Correlation between detrended data using first differences. Metrics where calculated using the divDyn R package (18). tExt stands for the number of taxa getting extinct, extProp for the proportional extinctions including single-interval taxa, extPC for the per capita extinction rate, extGF for the gap-filler extinction rate, extC3t for the corrected three-timer extinction rate, ext3t for the three-timer extinction rate, ext2f3 for the secondfor-third extinction rate, and E2f3 for the second-for-third extinction proportion.

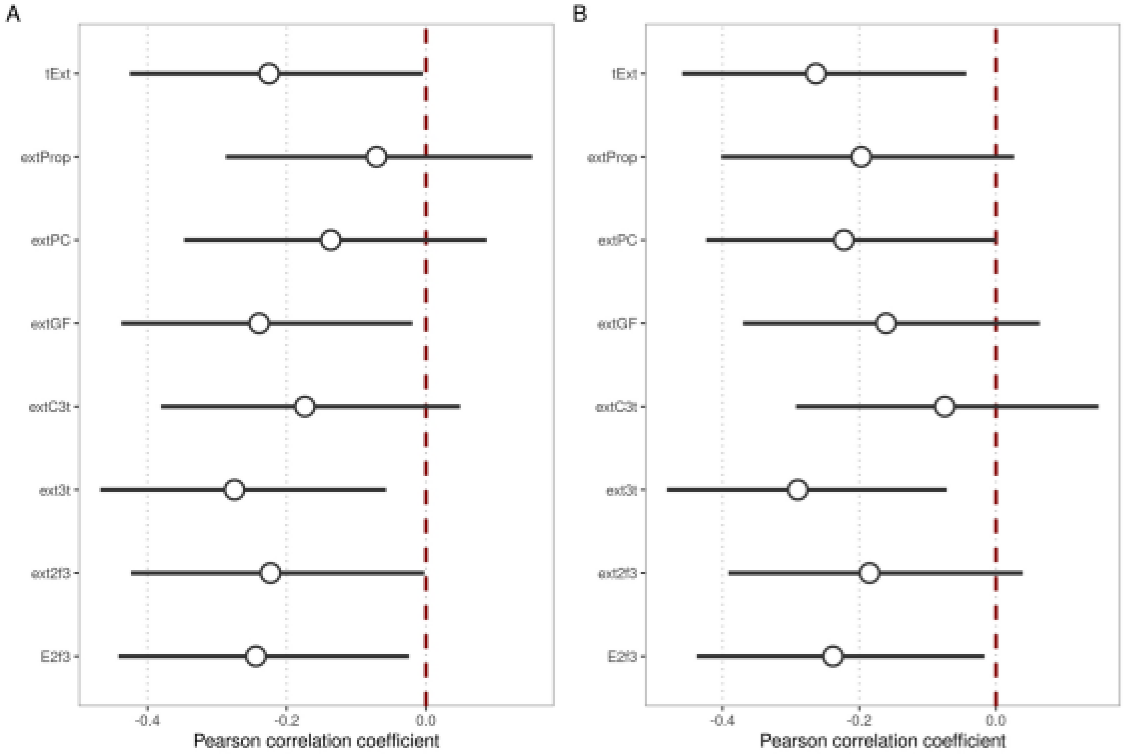

Fig. S15. The Pearson's product moment correlation coefficient for the correlation between various metrics for extinction at one time bin and the origination signal used in our analysis at the following time bin, including 95% confidence intervals. A) Direct correlations between raw data. B) Correlation between detrended data using first differences. Metrics where calculated using the divDyn R package (18). tExt stands for the number of taxa getting extinct, extProp for the proportional extinctions including single-interval taxa, extPC for the per capita extinction rate, extGF for the gap-filler extinction rate, extC3t for the corrected three-timer extinction rate, ext3t for the threetimer extinction rate, ext2f3 for the second-for-third extinction rate, and E2f3 for the second-for-third extinction proportion.

Supplementary tables

Table S1. Distribution of origination probability after each paleoclimate interaction for all studied fossil groups based on predictions of final GLMMs.

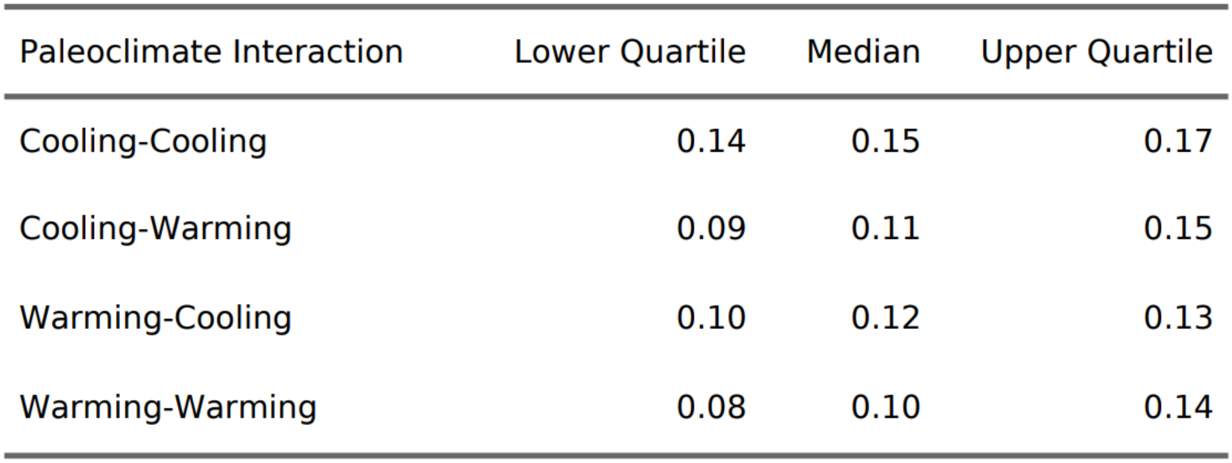

Paleoclimate Interaction	Lower Quartile	Median	Upper Quartile
Cooling-Cooling	0.14	0.15	0.17
Cooling-Warming	0.09	0.11	0.15
Warming-Cooling	0.10	0.12	0.13
Warming-Warming	0.08	0.10	0.14

Table S2. Effect size estimates for the difference in medians of origination probability, overall increase of origination probability and Cohen's d effect size including lower and upper bounds for 95% confidence intervals (Bootstrapping, Cohen's D) and 89% highest posterior density estimates (Bayesian Estimate).

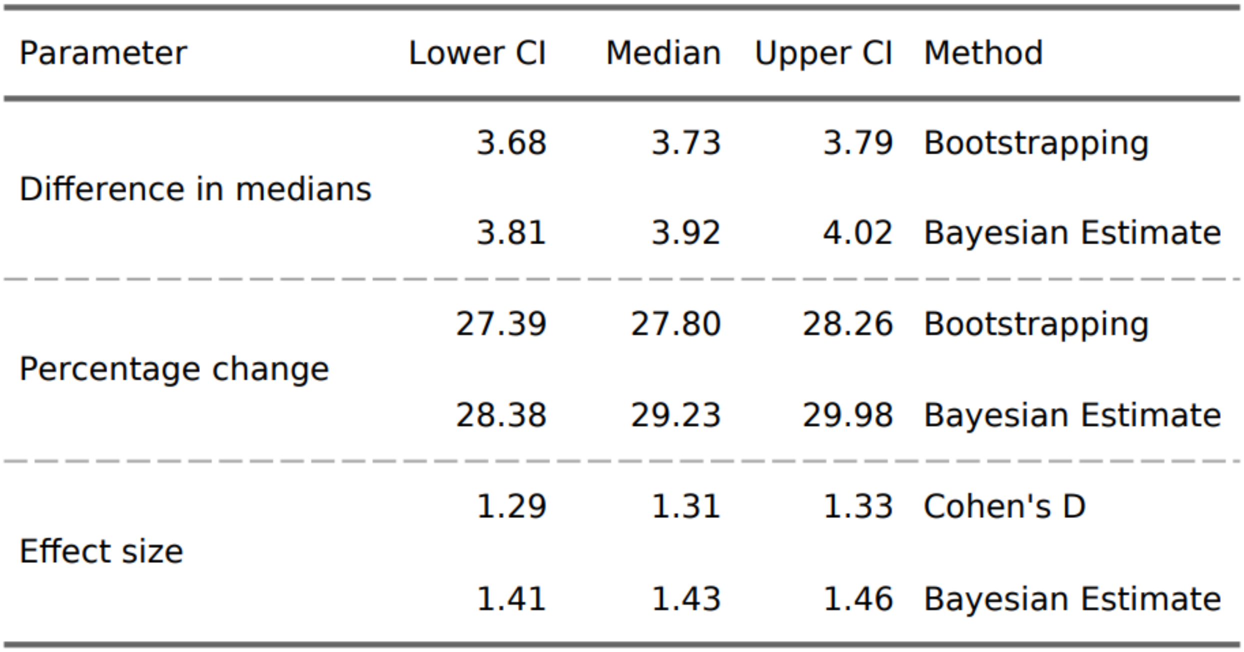

Parameter	Lower CI	Median	Upper CI	Method
Difference in medians	3.68	3.73	3.79	Bootstrapping
	3.81	3.92	4.02	Bayesian Estimate
Percentage change	27.39	27.80	28.26	Bootstrapping
	28.38	29.23	29.98	Bayesian Estimate
Effect size	1.29	1.31	1.33	Cohen's D
	1.41	1.43	1.46	Bayesian Estimate

Table S3. Origination probability for all major phyla and throughout time after cooling-cooling compared to all other paleoclimate interactions calculated as log odds ratio, including 95% confidence intervals. The Tremadocian is the oldest stage included in the analysis, and the Pleistocene the youngest. The phyla Hemichordata and Nematoda were removed from the analysis due to insufficient data.

Group	Lower CI	Log Odds ratio	Upper CI
Total	1.74	1.80	1.86
Annelida	0.60	1.58	2.56
Arthropoda	2.32	2.56	2.79
Brachiopoda	2.05	2.19	2.34
Bryozoa	1.87	2.17	2.47
Chordata	0.94	1.19	1.44
Cnidaria	1.65	1.85	2.04
Echinodermata	1.17	1.47	1.76
Foraminifera	0.71	1.15	1.60
Mollusca	1.53	1.63	1.73
Porifera	1.52	1.82	2.12
Tremadocian-Lochkovian	3.35	3.53	3.71
Pragian-Artinskian	0.34	0.51	0.67
Kungurian-Pliensbachian	1.22	1.37	1.51
Toarcian-Turonian	1.77	1.98	2.18
Coniacian-Pleistocene	0.92	1.04	1.15

Table S4. Number of classes, order, families, and genera within every major phylum after data cleaning and sampling-standardization.

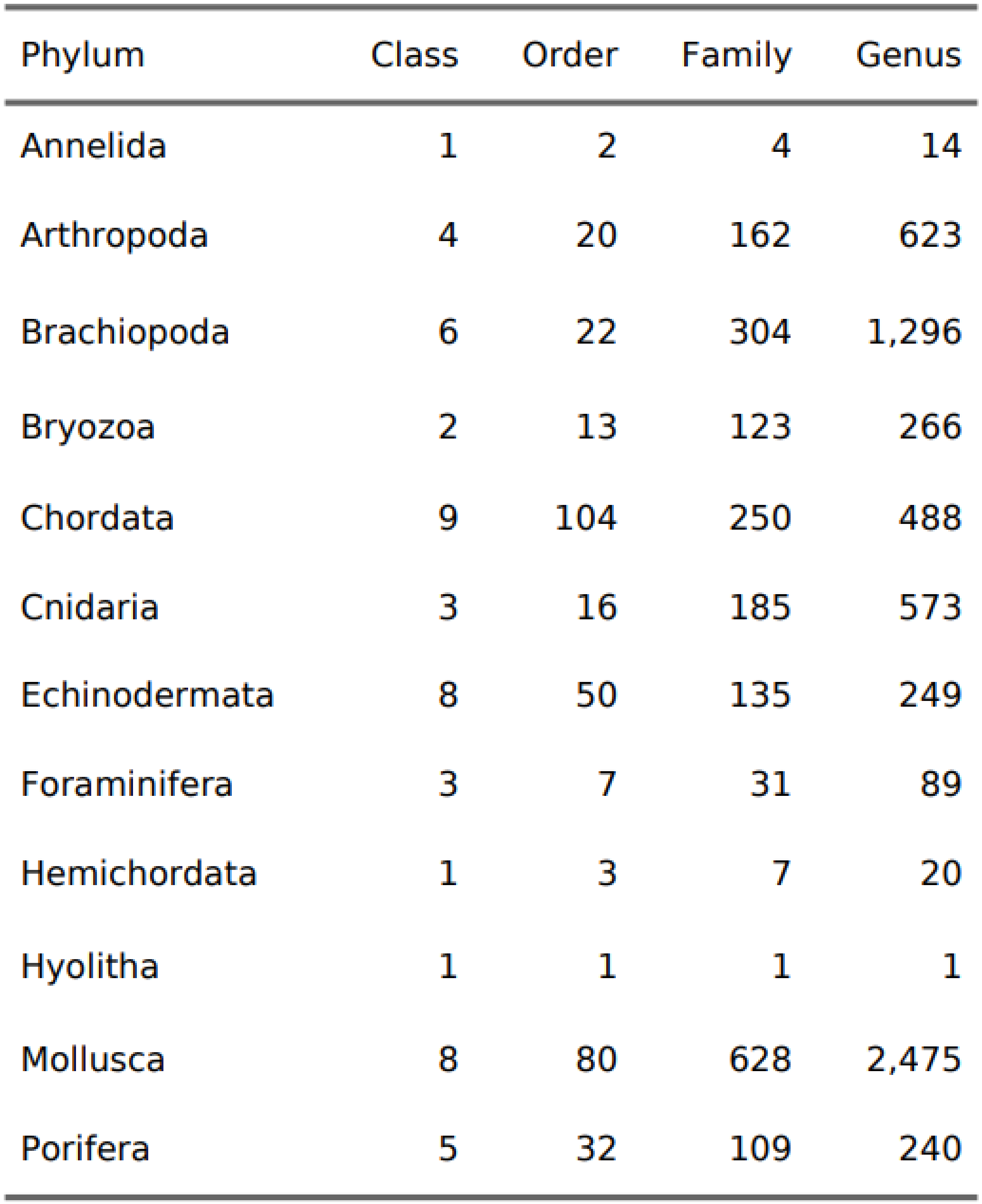

Phylum	Class	Order	Family	Genus
Annelida	1	2	4	14
Arthropoda	4	20	162	623
Brachiopoda	6	22	304	1,296
Bryozoa	2	13	123	266
Chordata	9	104	250	488
Cnidaria	3	16	185	573
Echinodermata	8	50	135	249
Foraminifera	3	7	31	89
Hemichordata	1	3	7	20
Hyolitha	1	1	1	1
Mollusca	8	80	628	2,475
Porifera	5	32	109	240

Table S5. Selection of the final model using a dynamic model framework. 10 GLMMs for each long-term trend per time bin were calculated while keeping the short-term change fixed. The final model for both short-term warming and cooling was then selected using the AIC of each model. Asterisk indicate the significance based on Gauss-Hermite quadrature, where one asterisk means p ≤ 0.05, two asterisk p ≤ 0.01, and three asterisk p ≤ 0.001.

Type	Model	Intercept	Interaction
Warming	trend.st1	-1.9 +- 0.02 ***	0.01 +- 0.05
	trend.st2	-1.91 +- 0.02 ***	-0.26 +- 0.06 ***
	trend.st3	-1.92 +- 0.02 ***	-0.38 +- 0.1 ***
	trend.st4	-1.91 +- 0.03 ***	-0.26 +- 0.11 *
	trend.st5	-1.92 +- 0.03 ***	-0.47 +- 0.1 ***
	trend.st6	-1.94 +- 0.03 ***	-0.64 +- 0.1 ***
	trend.st7	-1.94 +- 0.03 ***	-0.68 +- 0.11 ***
	trend.st8	-1.94 +- 0.03 ***	-0.7 +- 0.11 ***
	trend.st9	-1.91 +- 0.03 ***	-0.27 +- 0.13 *
	trend.st10	-1.9 +- 0.02 ***	-0.01 +- 0.13
Cooling	trend.st1	-1.82 +- 0.02 ***	0.19 +- 0.04 ***
	trend.st2	-1.83 +- 0.02 ***	0.27 +- 0.06 ***
	trend.st3	-1.82 +- 0.02 ***	0.86 +- 0.1 ***
	trend.st4	-1.79 +- 0.02 ***	1.44 +- 0.1 ***
	trend.st5	-1.81 +- 0.02 ***	1.34 +- 0.11 ***
	trend.st6	-1.83 +- 0.02 ***	1.32 +- 0.1 ***
	trend.st7	-1.85 +- 0.02 ***	1.25 +- 0.11 ***
	trend.st8	-1.87 +- 0.02 ***	1.22 +- 0.12 ***
	trend.st9	-1.88 +- 0.02 ***	1.26 +- 0.13 ***
	trend.st10	-1.88 +- 0.02 ***	1.31 +- 0.13 ***

Table S6. Comparison of model performance for traditional models covering first- and second order relationships of origination and climate versus models allowing for paleoclimate interactions. The latter are based on the same model structure, but explicitly allow for interactions of long-term temperature trends and short-term climate changes within a dynamic modeling framework (+ Pal. Int). Each model was tested for overdispersion including significance (indicated by stars, based on adaptive Gauss-Hermite quadrature approximation). Model comparison was based on Akaike's information criterion (AIC) and is consistent with Bayesian information criterion (BIC).

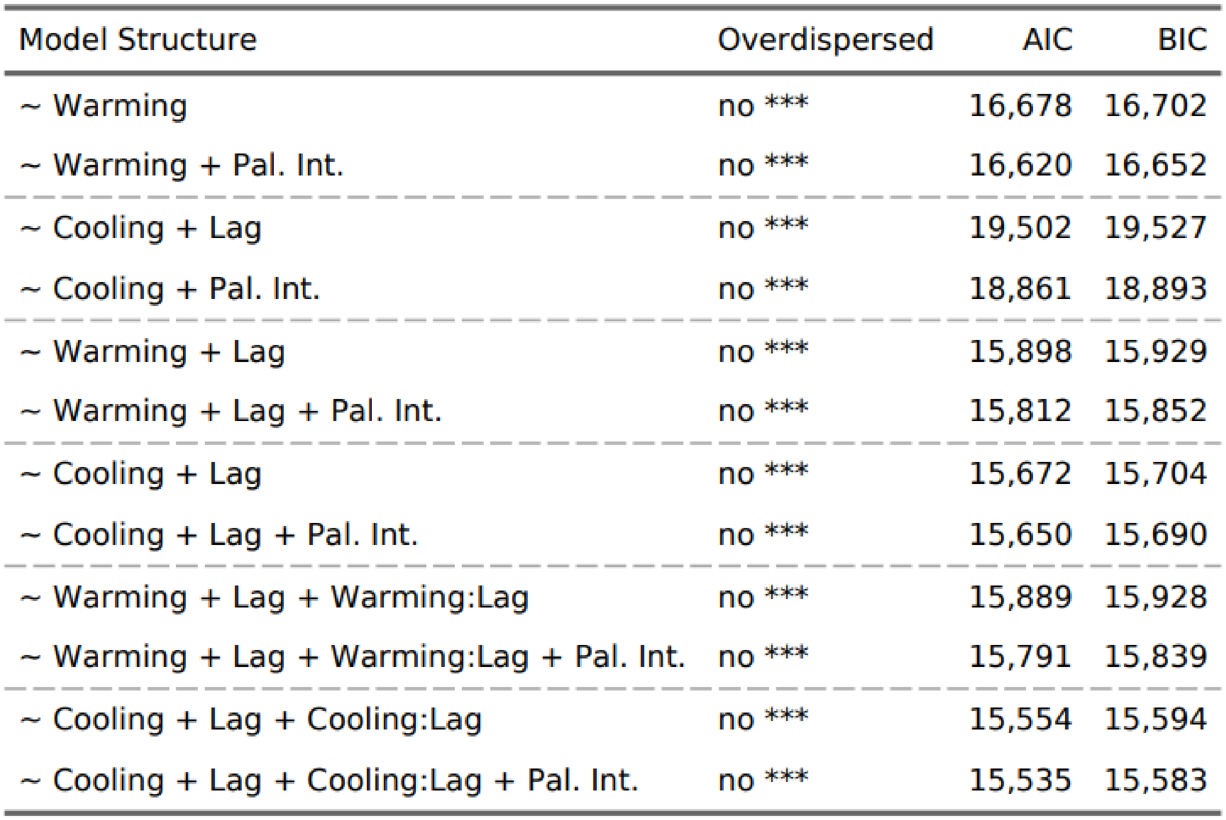

Model Structure	Overdispersed	AIC	BIC
~ Warming	no ***	16,678	16,702
~ Warming + Pal. Int.	no ***	16,620	16,652
~ Cooling + Lag	no ***	19,502	19,527
~ Cooling + Pal. Int.	no ***	18,861	18,893
~ Warming + Lag	no ***	15,898	15,929
~ Warming + Lag + Pal. Int.	no ***	15,812	15,852
~ Cooling + Lag	no ***	15,672	15,704
~ Cooling + Lag + Pal. Int.	no ***	15,650	15,690
~ Warming + Lag + Warming:Lag	no ***	15,889	15,928
~ Warming + Lag + Warming:Lag + Pal. Int.	no ***	15,791	15,839
~ Cooling + Lag + Cooling:Lag	no ***	15,554	15,594
~ Cooling + Lag + Cooling:Lag + Pal. Int.	no ***	15,535	15,583

Table S7. The Pearson's product moment correlation coefficient for the correlation between paleo-temperature and the continental fragmentation index (R) and the coefficient of determination (R-squared), including 95% confidence intervals for R (Lower and Upper CI). The data was further divided in a subset where temperature is cooler than the mean temperature and into the three chronological Eras (Paleozoic, Mesozoic, Cenozoic). We additionally tested for auto-correlation of disturbances using the Durbin-Watson test and report p-values (DW p-value).

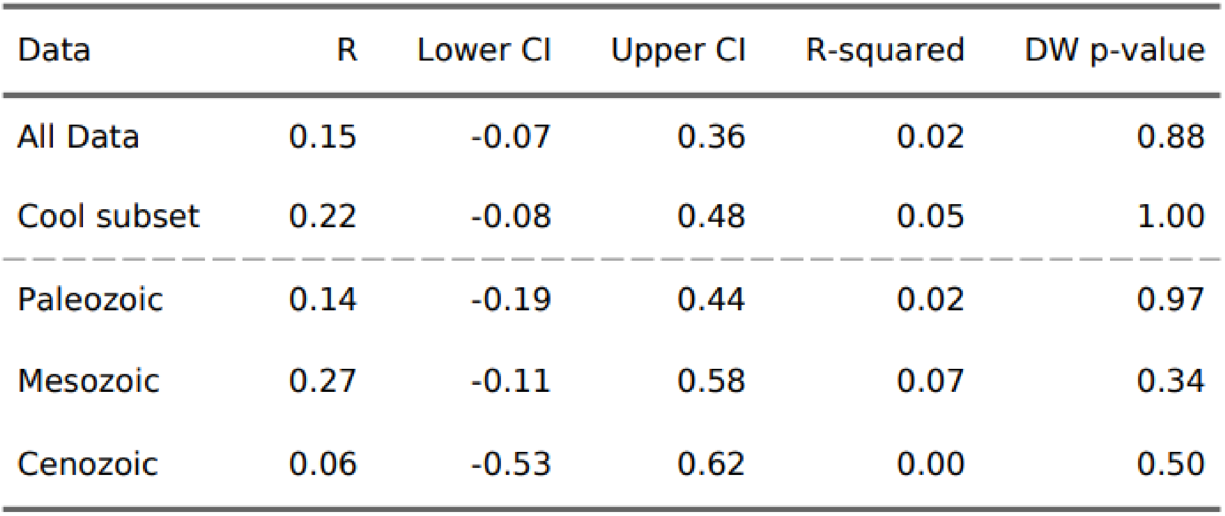

Data	R	Lower CI	Upper CI	R-squared	DW p-value
All Data	0.15	-0.07	0.36	0.02	0.88
Cool subset	0.22	-0.08	0.48	0.05	1.00
Paleozoic	0.14	-0.19	0.44	0.02	0.97
Mesozoic	0.27	-0.11	0.58	0.07	0.34
Cenozoic	0.06	-0.53	0.62	0.00	0.50

Table S8. Results for the test for inclusion of a second random effect on geologic stages within the regression framework. For both models covering short-term warming (Type = Warming) and short-term cooling (Type = Cooling), we calculated an additional model with a second random effect on stages (Added effect), as well as a null model with a constant second effect. Models where then compared by means of AIC and BIC values and the log-likelihood of each model.

Type	Model	AIC	BIC	logLik
Warming	Added effect	16,691	16,723	-8,342
	Null model	16,251	16,283	-8,122
Cooling	Added effect	18,932	18,965	-9,462
	Null model	18,192	18,224	-9,092

Table S9. Effect estimates for different data sources for the paleo-temperature data. The reported results are based on $\delta^{18}O$ processed as recommended by Veizer and Prokoph 2015. Repeating the whole analysis and estimating the effect (the difference in medians and the percentage change) including 89% credible intervals (CI) from highest posterior density intervals results in similar estimates.

Effect	Estimate	Lower CI	Upper CI	Isotope data
Difference in medians	1.64	1.53	1.71	Song et al. 2019
Percentage Change	12.30	11.53	12.88	
Difference in medians	3.92	3.81	4.02	Veizer & Prokoph 2015
Percentage Change	29.23	28.38	29.98	

Data and code availability

All data and code necessary to run analyses and produce final results are deposited in a public GitHub repository (https://github.com/lschi94/palint-origin), including instructions on how to reproduce results and all figures. The unprocessed data file containing fossil occurrences is freely available via Figshare.com (https://figshare.com/articles/dataset/Raw_fossil_data/14528925) or can be directly download from the Paleobiology Database (https://paleobiodb.org/data1.2/occs/list.csv?show=full).

SI references

Alroy, J. (2008). Dynamics of origination and extinction in the marine fossil record. *Proceedings of the National Academy of Sciences*, *105*(Supplement 1), 11536–11542. https://doi.org/10.1073/pnas.0802597105

Bates, D., Mächler, M., Bolker, B., & Walker, S. (2015). Fitting linear mixed-effects models using lme4. *Journal of Statistical Software*, 1–48. https://doi.org/10.18637/jss.v067.i01

Bolker, B. M., Brooks, M. E., Clark, C. J., Geange, S. W., Poulsen, J. R., Stevens, M. H. H., & White, J.-S. S. (2009). Generalized linear mixed models: A practical guide for ecology and evolution. *Trends in Ecology & Evolution*, *24*(3), 127–135.

Cárdenas, A. L., & Harries, P. J. (2010). Effect of nutrient availability on marine origination rates throughout the Phanerozoic eon. *Nature Geoscience*, *3*(6), 430–434. https://doi.org/10.1038/ngeo869

Farebrother, R. W. (1980). Pan's procedure for the tail probabilities of the Durbin-Watson statistic. *Journal of the Royal Statistical Society. Series C (Applied Statistics)*, *29*(2), 224–227.

Fisher, R. A. (1921). On the 'probable error' of a coefficient of correlation deduced from a small sample. *Metron*, *1*, 1–32.

Galwey, N. W. (2007). *Introduction to Mixed Modelling: Beyond Regression and Analysis of Variance.* John Wiley & Sons. http://www.123library.org/book_details/?id=20361

Kirchner, J. W., & Weil, A. (2000). Delayed biological recovery from extinctions throughout the fossil record. *Nature*, *404*(6774), 177–180. https://doi.org/10.1038/35004564

Kocsis, À. T., Reddin, C. J., Alroy, J., & Kiessling, W. (2019). The R package divDyn for quantifying diversity dynamics using fossil sampling data. *Methods in Ecology and Evolution*, *10*(5), 735–743.

Krug, A. Z., Jablonski, D., Valentine, J. W., & Roy, K. (2009). Generation of Earth's First-Order Biodiversity Pattern. *Astrobiology*, *9*(1), 113–124. https://doi.org/10.1089/ast.2008.0253

Kruschke, J. K. (2013). Bayesian estimation supersedes the t test. *Journal of Experimental Psychology: General*, *142*(2), 573.

Mathes, G. H., van Dijk, J., Kiessling, W., & Steinbauer, M. J. (2021). Extinction risk controlled by interaction of long-term and short-term climate change. *Nature Ecology & Evolution*, *5*(3), 304–310. https://doi.org/10.1038/s41559-020-01377-w

Mayhew, P. J., Bell, M. A., Benton, T. G., & McGowan, A. J. (2012). Biodiversity tracks temperature over time. *Proceedings of the National Academy of Sciences*, *109*(38), 15141–15145. https://doi.org/10.1073/pnas.1200844109

Mayhew, P. J., Jenkins, G. B., & Benton, T. G. (2008). A long-term association between global temperature and biodiversity, origination and extinction in the fossil record. *Proceedings of the Royal Society B: Biological Sciences*, *275*(1630), 47–53. https://doi.org/10.1098/rspb.2007.1302

McElreath, R. (2020). *Statistical Rethinking, 2nd Edition*. https://learning.oreilly.com/library/view/-/9780429639142/?ar

Pinheiro, J. C., & Chao, E. C. (2006). Efficient Laplacian and adaptive Gaussian quadrature algorithms for multilevel generalized linear mixed models. *Journal of Computational and*

Graphical Statistics, *15*(1), 58–81.

Ritterbush, K. A., & Foote, M. (2017). Association between geographic range and initial survival of Mesozoic marine animal genera: Circumventing the confounding effects of temporal and taxonomic heterogeneity. *Paleobiology*, *43*(2), 209–223. https://doi.org/10.1017/pab.2016.25

Song, H., Wignall, P. B., Song, H., Dai, X., & Chu, D. (2019). Seawater temperature and dissolved oxygen over the past 500 million years. *Journal of Earth Science*, *30*(2), 236–243.

Stigall, A. L. (2013). Analysing links between biogeography, niche stability and speciation: The impact of complex feedbacks on macroevolutionary patterns: Biotic and environmental impacts on speciation. *Palaeontology*, *56*(6), 1225–1238. https://doi.org/10.1111/pala.12003

Veizer, J., & Prokoph, A. (2015). Temperatures and oxygen isotopic composition of Phanerozoic oceans. *Earth-Science Reviews*, *146*, 92–104.

Zaffos, A., Finnegan, S., & Peters, S. E. (2017). Plate tectonic regulation of global marine animal diversity. *Proceedings of the National Academy of Sciences*, *114*(22), 5653–5658. https://doi.org/10.1073/pnas.1702297114

Manuscript 4

Nowhere to run: Lagged responses of tropical and polar planktonic foraminifera over 700,000 years of climate change,

Global Ecology and Biogeography, in submission

Gregor H. Mathes[1,2*], Carl J. Reddin[1,3], Wolfgang Kiessling[1], Gwen S. Antell[4], Erin E. Saupe[4], Manuel J. Steinbauer[2,5]

[1] Department of Geography and Geosciences, GeoZentrum Nordbayern, Friedrich-Alexander University Erlangen-Nürnberg (FAU), Erlangen, Germany.
[2] Bayreuth Center of Ecology and Environmental Research (BayCEER), University of Bayreuth, Bayreuth, Germany.
[3] Museum für Naturkunde, Leibniz Institute for Evolution and Biodiversity Science, Berlin, Germany.
[4] Department of Earth Sciences, University of Oxford, Oxford, United Kingdom.
[5] Department of Biological Sciences, University of Bergen, Bergen, Norway.
* Corresponding author: gregor.mathes@uni-bayreuth.de

ABSTRACT

Marine ecosystems are increasingly affected by anthropogenic climate change. It is unknown whether marine assemblages are able to shift their distributions fast enough to track suitable climate. We investigate the capacity of planktonic assemblages to keep pace with temperature changes using a 700,000 years fossil record of globally ubiquitous marine zooplankton (2,657 planktonic foraminifera assemblages composed of 38 species). By integrating across spatiotemporal scales, we provide powerful insights into faunal responses to a wide variety of climate change. Comparisons with paleoclimate reconstructions show that planktonic foraminifera assemblages generally tracked modest changes in temperature. However, disproportionately large climatic lags, in terms of range shifts required to match thermal optima, are accumulated by high latitude assemblages responding to climate warming and low latitude assemblages responding to climate cooling. High magnitudes of temperature changes led to large and often irreversible assemblage changes, pointing towards the presence of critical tipping points within these marine assemblages. The inability to move ranges fast enough to track shifts in suitable climates when climatic changes were high led to average range lags up to 554 km. How well assemblages react to climate warming or cooling was also dependent on the long-term climatic context. Our observations show that the vulnerability of marine assemblages to climate change is potentially more extensive than previously anticipated.

Introduction

Anthropogenic climate warming is threatening marine ecosystems (Pörtner et al., 2022). One key response of marine assemblages exposed to a changing climate is by tracking climatic niches in space via distribution shifts (Chen et al., 2011; Pinsky et al., 2013; Poloczanska et al., 2013). However, the potential for marine organisms to cope with climate change via dispersal remains uncertain (García Molinos et al., 2016; Munday et al., 2013). While individual species of marine ectotherms are predicted to closely track their thermal limits (Sunday et al., 2012), assemblages are unlikely to migrate cohesively (Graham et al., 1996; Reddin et al., 2018; Walther et al., 2002), leading to a disequilibrium or lag that generates a mismatch between ambient temperatures and conditions preferred by assemblages (Devictor et al., 2012; Menéndez et al., 2006; Svenning & Sandel, 2013). This may make certain assemblages vulnerable to population loss and even extinction under particular climate change scenarios (Reddin et al., 2022; Stuart-Smith et al., 2015) but more information is needed on the consistency and generality of responses. Climatic lags are well studied in terrestrial ecosystems but less so in marine, whose species distributions should better track climatic variables (Sunday et al., 2011), as long-term studies of climate change in the oceans are rare (Rosenzweig et al., 2008).

The exceptional fossil record of planktonic foraminifera (Protista) renders them an ideal model system to investigate climatic lags in marine zooplankton. Planktonic foraminifera are a globally ubiquitous component of marine zooplankton. Their calcite shells (tests) are well-preserved in seafloor sediments, allowing for a view into the composition of marine assemblages in the past with an extraordinary temporal and spatial resolution. Their tests have been used to investigate climatic and ecological changes in both modern and fossil systems (Antell et al., 2021; Ezard et al., 2011; Jonkers et al., 2019; Morard et al., 2015). Modern planktonic foraminifera assemblages show changes in community structure as a response to anthropogenic climate warming, but whether these assemblages lag behind the rate of climatic change is unknown (Jonkers et al., 2019). As individual foraminifera species show high niche stability over time (Antell et al., 2021), changes in assemblage composition in response to climatic changes can only occur through reorganization via shifts in species distribution, changes in relative abundance, or local extinction (Jackson & Sax, 2010).

The effect of climate change on spatio-temporal patterns in assemblages on a global scale is poorly understood (García Molinos et al., 2016). Most studies are limited to individual species rather than investigating shifts in assemblages (Dornelas et al., 2014). The fossil record poses the chance to fill this critical knowledge gap of changes within assemblages with its unique capacity to record how organisms responded to a wide range of climatic changes. As unique combinations of climatic variables existed in the past (Williams & Jackson, 2007) and are predicted to emerge in the future (Williams et al., 2007), crucial information for biotic responses to climate conditions outside modern human experience can be obtained from the fossil record. However, most studies taking advantage of the fossil record cover scales of 106 to 107 years (Kocsis et al., 2018; Martin-Garin et al., 2012; Reddin et al., 2018), far above timescales of modern relevance, or are restricted to single historical time steps (Greenstein & Pandolfi, 2008; Kiessling et al., 2012). The time continuous fossil record of planktonic foraminifera assemblages thus provides an exceptional opportunity to study the effect of climate change on spatio-temporal patterns in assemblages on a temporal scale relevant for modern-day ecosystem functioning.

Here we investigate the capacity of planktonic foraminifera assemblages to keep pace with climatic changes over the past 700,000 years of glacial-interglacial cycles at a 8 thousand year (ka) resolution. We base our analysis on a global dataset of Quaternary planktonic foraminifera records, being widely distributed within all oceans, together with a coupled Atmosphere–Ocean Generalized Circulation Model (AOGCM). For each foraminiferal assemblage, we calculate the climatic lag as the difference between the temperature estimated at the location and the temperature bio-indicated by the assemblage structure (i.e., the optimal temperature for the local assemblage given the preferred temperature niche of individual species, Fig. 1). A large value of the climatic lag (both positive and negative) means that the assemblage is not in equilibrium with adjacent temperatures. We then implement linear mixed effect models to quantify the climatic lag as a function of temperature change both on a global basis and within latitudinal bands (at low, mid, and high latitudes). We further model the global climatic lag through time and investigate how climatic lags can arise from the cyclicity of the glacial-interglacial periods. We expect fossil planktonic foraminifera assemblages to closely track climate change given the scale of our study, emphasizing long-term species turnover in response to long-term climatic processes.

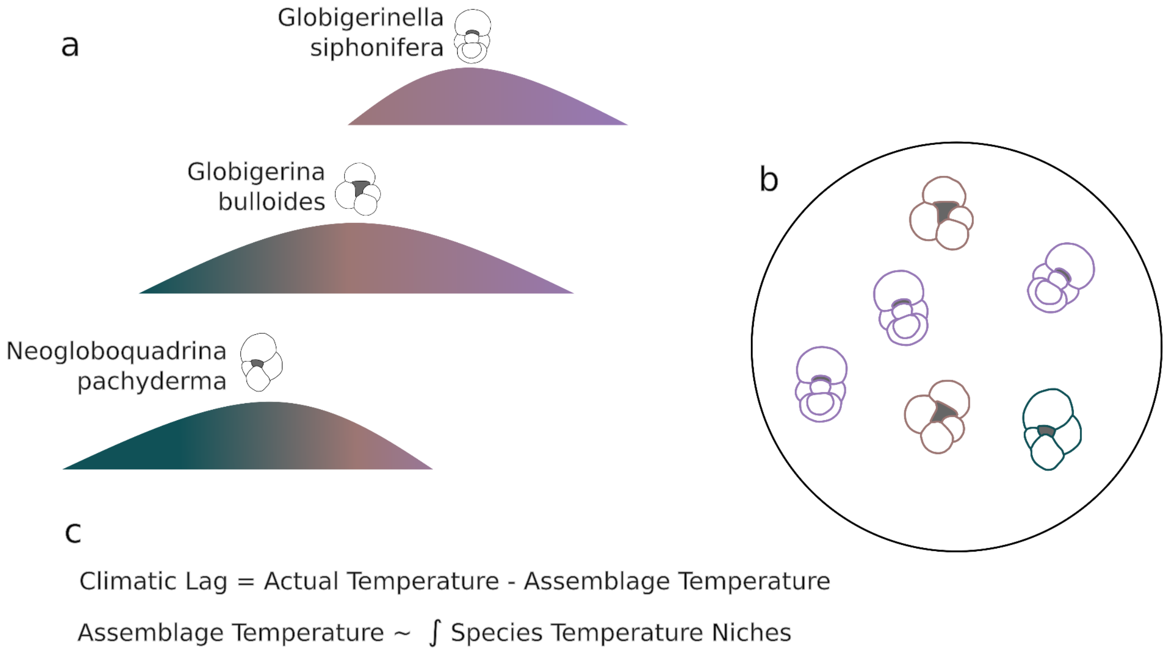

Figure 1: Calculation of the climatic lag of a planktonic foraminifera assemblage. (a) Individual planktonic foraminifera species occupy a specific temperature niche. By tracking the occurrences of fossil foraminifera species along the univariate axis of mean annual temperature, this temperature niche can be estimated for each species. (b) An assemblage of planktonic foraminifera consists of various species, each displaying a

characteristic temperature niche. The temperature an assemblage is preferring can be estimated by integrating the temperature niches of individual species via an ecological transfer function, which takes both species composition and relative abundance of species into account. We termed this preferred temperature of an assemblage the 'assemblage temperature'. (c) The climatic lag of the assemblage is then the difference between the actual temperature at the location of the assemblage and the assemblage temperature. The climatic lag therefore quantifies the mismatch between actual and preferred temperature of an assemblage.

MATERIAL AND METHODS

Fossil data

We compiled foraminiferal occurrences over the past 700 ka from various data sources and processed them following Antell et al. (2021). Sources include datasets from the PANGAEA Open Access library (www.pangaea.de), the Neptune database (Renaudie et al. 2020, nsb.mfn-berlin.de), and the ForCenS database (Siccha & Kucera, 2017). We harmonized the taxonomy based on currently valid nomenclature (Antell et al., 2021). Macro- and microperforate species were included, but benthic foraminifera were excluded. We excluded two species that originated within the last 700 ka and eight species that went extinct over that span to ensure all study species were extant throughout the entire study interval. All specimens were collected from sediment cores and core tops, with no live-collection samples, such as from plankton tows. Even the youngest sediment samples are estimated to be centuries or millennia in age (Jonkers et al., 2019). Thus, all specimens reflect preindustrial species distributions, predating anthropogenic global warming. Paleocoordinates were reconstructed by rotating modern coordinates according to a plate model, in accordance with Neptune methods (Matthews et al., 2016). We omitted records from sites at shallow depths (<100 m) where planktonic foraminifera cannot establish viable populations (Darling et al., 2007), under the assumption that any foraminifera at those sites drifted in from elsewhere. The exact minimum depth for reproduction is unknown and may vary with water conditions. We kept only those foraminifera occurrences with information about their relative abundance. The final dataset contained 38 species with 98,297 occurrences (Supplementary Data Table 1). These occurrence records were binned into 88 intervals of 8 ka resolution, from the recent subfossil record to 700 ka. The chosen bin length reflects the resolution of the coupled Atmosphere–Ocean Generalized Circulation Model outputs (4 ka), the time-averaging of fossil assemblages and imprecision in fossil ages [up to a few thousand years (Martin, 1999)], and the rate of climatic change (fluctuation from glacial minimum to interglacial maximum approximately every 50 ka). To minimize error in bin assignments due to age uncertainty, records were omitted if age estimates were derived from foraminiferal zones or had confidence intervals longer than 2 ka. Remaining records could be assigned confidently to a single time bin based on the mean age estimate. We use the term assemblage to refer to all species present within a sediment core at the same time bin-. The final dataset contained 2,657 assemblages (Supplementary Data Table 2).

Temperature data

Temperature is the single most important explanatory variable in regard to geographic distribution of foraminifera (Antell et al., 2021; Fenton et al., 2016; Yasuhara et al., 2020). The temperature in prehistoric oceans can be reconstructed using a coupled Atmosphere–Ocean Generalized Circulation Model (AOGCM). We obtained mean annual temperature estimates (MAT) from the UK Met Office Unified Model Hadley Centre Coupled Model, with the MOSES 2.1 land-surface model and top-down representation of interactive foliage and flora including a dynamic global vegetation model (Cox, 2001), following the precise configuration as stated in Antell et al. (2021). Fossil foraminifera occurrences were paired with AOGCM data from the midpoint of time bins (e.g., climate was modeled at 12 ka for occurrences 16 to 8-ka old). Foraminiferal species inhabit specific and consistent vertical ranges and do not participate in vertical diel migration as do some other plankton, although these protists do migrate to the mixed-layer depth to breed (Meilland et al., 2019). Therefore, we performed our analysis in the following two ways: using MAT at the sea surface or using MAT extracted from each focal species' depth range. We used the quantitative information on each species' modern depth range provided by Antell et al. (Antell et al., 2021) to assign taxa to one of the three following depth habitats: surface (40 m in the AOGCM), surface–subsurface (78 m), or subsurface (164 m).

Statistical analysis

Climatic lag:

All analyses were carried out in R v.4.1.2 (R Core Team, 2021). We used the tidyverse collection of R packages (Wickham et al., 2019) to transform and visualize data. We defined climatic lag as an accumulated delay in species' response to the change in temperatures, which we hypothesize as attributable to a species' inability to track climate change. Previous studies have used the term "climatic debt" for this metric (Bertrand et al., 2016; Devictor et al., 2012). However, the notation of 'debt' might imply that individuals within populations are stressed or threatened, which might not be the case with highly mobile planktonic organisms. We therefore use the term "climatic lag" for the accumulated delay throughout this study. To quantify the climatic lag, we first calculated the preferred temperature of each foraminiferal species by an ecological transfer function via the rioja R package (Juggins, 2020). As an ecological transfer function, we used weighted averaging partial least squares (WA-PLS) regression and calibration (Ter Braak et al., 1993). Performance of the WA-PLS transfer function was determined via leave-one-out cross-validation (Supplementary Data Fig. 1). WA-PLS requires the development of a calibration training set, which is then used to model the relationship between assemblages and temperature. We calibrated the WA-PLS function using a training set from time steps within the interquartile range of all temperature variation throughout the last 700 ka. This enabled us to estimate the relationship between each foraminiferal species and temperature at background times (i.e., during times of average climatic). We then used this relationship based on WA-PLS to calculate the assemblage temperature of each planktonic foraminifera assemblage in time (i.e., the preferred temperature as indicated by composition and relative abundance of individual species within an assemblage). The assemblage temperature is therefore informed by the sum of individual temperature niches of species within an assemblage. A temporal increase in the assemblage temperature directly reflects that the assemblage is increasingly composed of individuals belonging to species preferring higher temperature. In the next step, we calculated the climatic lag of each assemblage in time as the difference between the assemblage temperature (as calculated by WA-PLS) and the empirical seawater temperature (as estimated by the AOGCM). We then modeled the change in climatic lag as a function of temperature change. For this, we used linear mixed effect models [(lmm, (Bates et al., 2015)] with a random effect on temporal bins, in order to account for differential sampling effort within those bins. We calculated lmm's for the general global climatic lag as well as for latitudinal zones. We defined assemblages located between 0° and 30° absolute latitude as low latitude; between 30° and 60° as mid latitude; and above 60° as high latitude. To quantify uncertainty around the trend estimates based on the lmm, we used parametric bootstrapping. We additionally used these lmm's for the quantification of changes in climatic lag when the temperature increases by 1 to 3 degrees Celsius under a climate warming scenario.

Climatic lag through time:

We calculated the global climatic lag through time by summarizing the climatic lag of individual assemblages within each time bin, and calculated uncertainty around this average trend via bootstrapping. As planktonic foraminifera assemblages were unsampled in some time bins between 460 and 444 ka (Supplementary Data Fig. 2), the resulting global bin-to-bin climatic lag around this interval can be considered unreliable. Similarly, we calculated the mean global temperature by summarizing the mean annual seawater temperature estimates from the AOGCM of assemblages within each bin. We then correlated the global climatic lag through time with the mean global temperature to test how climatic lag is arising from temperature changes in time. We did this correlation for the global temperature at the focal time bin of each global climatic lag estimate and then added preceding temperature trends to the correlation model to test for legacy effects (Mathes et al., 2021; Svenning et al., 2015). These preceding temperature trends ranged back 8 ka (lag 1), 16 ka (lag 2), and 24 ka (lag 3). We additionally calculated a null model based on an intercept-only regression for means of comparison. For each model (null model, temperature at bin, temperature at bin and lag 1, temperature at bin and lag 2, temperature at bin and lag 3) we calculated the Akaike's Information Criterion [AIC, (Burnham, 1998)] to quantify model performance. We additionally quantified the uncertainty of each AIC value via leave-one-out cross validation. We then performed a model comparison by means of delta-AIC, which is calculated as the difference in AIC of each model to the model with the lowest AIC (i.e., with the best performance). By doing so, we were able to quantify the time range over which climate legacy effects had the strongest influence on global climatic lag while simultaneously showing the relative impact of global temperature (by comparison with the null model).

Climatic lag without relative abundance changes:

The climatic lag as calculated by means of WA-PLS is taking the relative abundance of individual species into account. To estimate the degree to which planktonic foraminifera assemblages respond to climatic changes by relative abundance changes of individual species, we additionally estimated climatic lag after omitting abundance changes of species. To do so, we calculated a species temperature index for each species as the average temperature of the species range based on occurrences. The assemblage temperature, the preferred temperature of an assemblage based on its species composition, is then calculated, for a given assemblage, as the average of all species' temperature indices. Climatic lag is then again calculated by the difference in assemblage temperature and the surface temperature estimate based on the AOGCM. This climatic lag estimate is hence only based on distribution shifts of individual species and is not taking relative abundance changes of species within assemblages into account. By comparing the trends of this occurrence based climatic lag to trends of the original climatic lag (based on relative abundance), it is possible to estimate the importance of abundance changes when assemblages respond to changes in temperature.

Surface-depth comparison:

We originally calculated the climatic lag for planktonic foraminifera assemblages based on the mean annual temperature estimate of the AOGCM at the surface. To test whether this biases our results, we additionally calculate climatic lag based on the temperature estimate at the preferred depth of each foraminifera species. We then compared resulting patterns and trends in the climatic lag between these two temperature estimate approaches. The differences between the two methods were small and resulting latitudinal patterns in climatic lag stayed the same (Supplementary Data Table 3). This is in line with previous studies of foraminifera ecology, where equivalent results were obtained based on data from the sea surface or at depth (Antell et al., 2021; Richter et al., 2019).

Range lag:

We calculated range lag as the difference between the required range velocity to track climatic changes and the realized velocity of assemblages, following Devictor et al. (Devictor et al., 2012). We first modeled the general trend in assemblage temperature from the equator to the poles for all observations across time via a linear regression model. We defined this as the spatial gradient in assemblage temperature, expressed in °C km-1. We then calculated the temporal trend of the assemblage temperature in response to climate change as °C 8 ka-1 via a lmm, accounting for differential sampling effort between bins using a random effect on temporal bins. Similar to climate velocity (Burrows et al., 2011), the ratio between the temporal trend in assemblage temperature and the spatial gradient in assemblage temperature then resulted in the velocity of assemblage temperature (°C km-1/°C 8 ka-1 = km 8 ka-1). Similarly, we calculated the temporal trend in temperature change (°C 8 ka-1) and divided it by the spatial gradient in temperature from the equator to the poles (°C km-1), to get the velocity of temperature change (km 8 ka-1). The difference between the spatiotemporal velocity of temperature and the velocity of assemblage temperature then resulted in the range lag, quantifying how much assemblages lag behind temperature changes in terms of range velocity. We calculated this range lag for all latitudinal zones (low, mid, high) responding to temperature warming or cooling.

RESULTS

Planktonic foraminifera assemblages generally track climatic changes over the past 700,000 years when those changes were minor but substantial climatic lags emerged under high climate change (Fig. 2, Supplementary Data Fig. 3). Assemblages responded to climatic changes by species turnover and/or abundance changes and were in equilibrium with adjacent climatic conditions when no climatic changes occurred through time (Fig. 2b). However, under a changing climate, assemblages were not able to closely track the new climatic conditions, resulting in a mismatch between the actual temperature at the site and the preferred temperature of the assemblage. This global climatic lag grew on average by 0.56°C (95% confidence interval (CI) [0.4, 0.7]) with every 1°C temperature change (Fig. 2b).

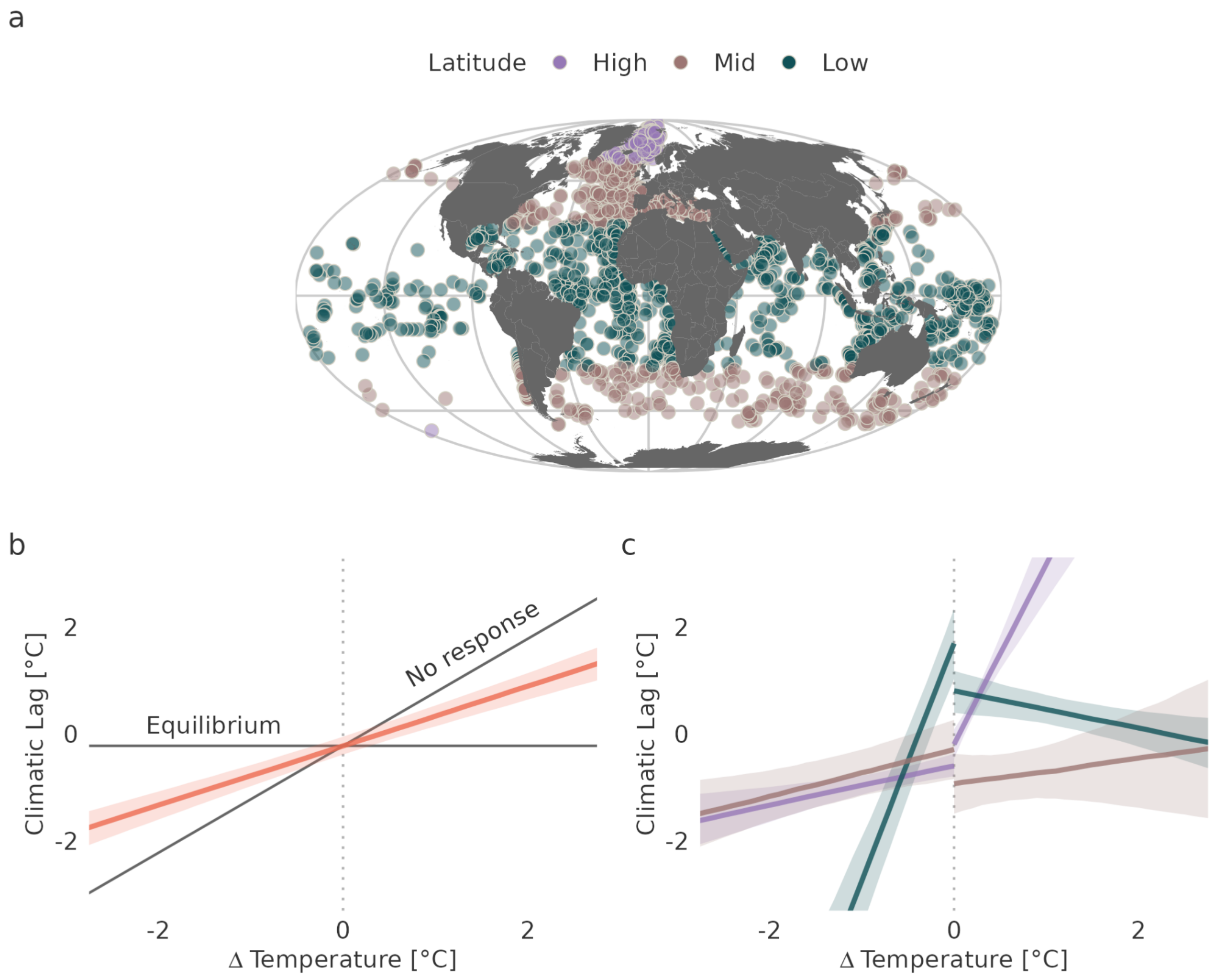

Figure 2: Trends in climatic lag. (a) Global distribution of foraminifera assemblages used in this work, coloured by latitudinal zones, 0-30, 30-60, 60-90 degrees absolute latitude. (b) The global climatic lag of all foraminifera assemblages as a function of temperature change. The horizontal equilibrium line shows complete temperature tracking when

assemblages respond ideally to a temperature change (e.g., 1°C warming leads to an assemblage showing preference for a 1°C warmer climate, resulting in zero climatic lag). The no response line shows no temperature tracking when assemblages are unable to respond to a temperature change (e.g., when assemblages show no community changes even if the temperature increases by 1°C, the resulting climatic lag is 1°C). (c) Latitudinal patterns of climatic lag as a function of temperature change. The coloured areas depict the 95% confidence interval of the focal regression slope.

Assemblages in high latitudes showed a similar response of moderate climatic lags under climate cooling but accumulated substantial climatic lags under a warming scenario (Fig. 2c). With every 1°C warming, the climatic lag in assemblages in high latitudes grew by 3.4°C (95% CI [2.0, 4.8]). Conversely, assemblages in low latitudes were least able to track climatic changes under a cooling scenario while being more in equilibrium with climate when the temperature increased. The mismatch between preferred and actual temperature in these low latitude assemblages grew by 4.4°C (95% CI [3.1, 5.8]) with every 1°C cooling. Surprisingly, low latitude assemblages showed a slightly decreasing climatic lag with increasing magnitude of warming (-0.4°C per 1°C warming, 95% CI [-0.7, 0]).

The range lag, the difference between the required range velocity to track climatic changes and the realized velocity, was substantially increased in high latitude assemblages after a period of warming (Fig. 3). While the absolute range lag for most assemblages was between 12 and 198 km per 8 ka, these high latitude assemblages experiencing warming accumulated a range lag of 553 km 8 ka-1 (95% CI [530, 575]). This indicates that planktonic assemblages were generally not in full equilibrium with climate, with the biggest mismatch arising in high latitudes after a warming period.

On a global scale, planktonic foraminifera assemblages were generally in equilibrium with climate throughout the past 700 ka (Fig. 4). The average global climatic lag fluctuated between -2°C and 2°C (Fig. 4a), with a period of significantly decreased values between 460 and 440 ka, which was artificially generated by a sampling hiatus in this period (Supplementary Data Fig. 2). How well assemblages react to climate warming or cooling was dependent on the long-term climatic context, with climatic changes over 16 ka having the strongest impact (Fig. 4 b and c). These 16 ka lasting climate legacies can explain up to 13.3% of variance of climatic lag (bootstrapped R-squared, 95% CI [13.1%, 13.4%]). This indicates that responses of assemblages to climatic changes were conditional on the preceding climate, such that climatic lag after a warming event was pronounced when the climate was generally warming over the preceding 16 ka and less so when the preceding 16 ka trend showed a climate cooling (Supplementary Data Fig. 4). Vice versa, climatic lag after a cooling period was increased after a 16 ka cooling trend but generally lower after a 16 ka warming trend.

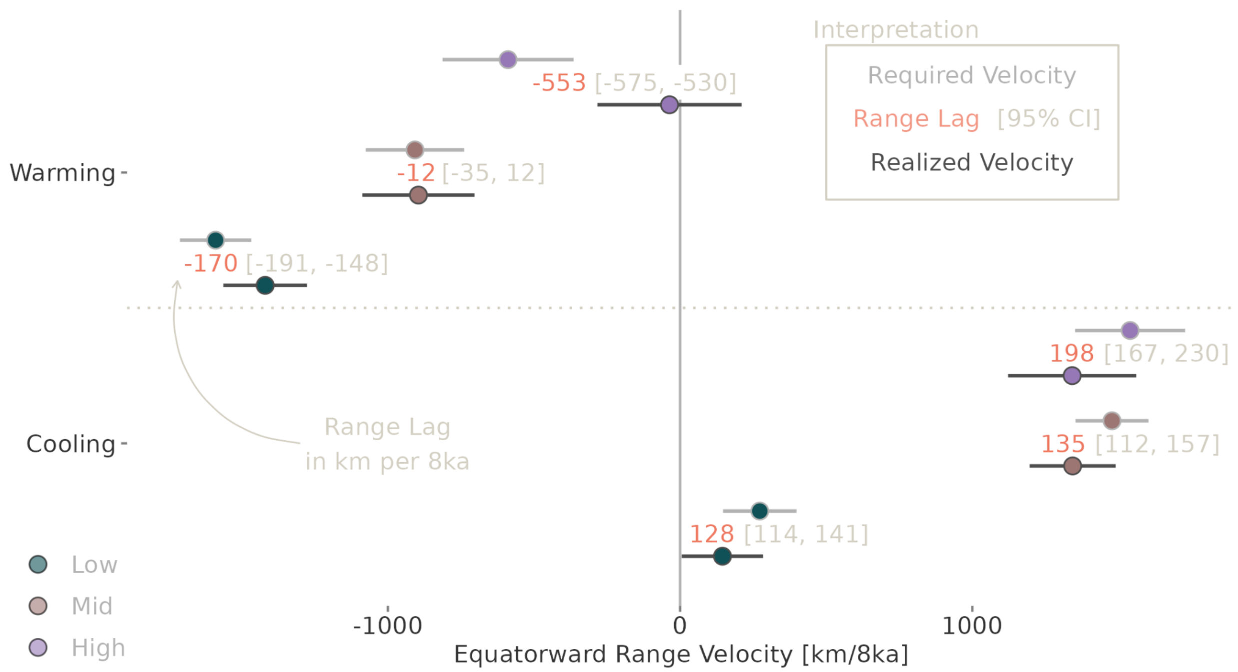

Figure 3: The range lag in km 8 ka-1, which is the difference between the required range velocity to track climatic changes and the realized velocity. The range lag here is summarized across either temperature cooling or temperature warming across the past 700 ka. The range lag is shown in orange and the range of the corresponding 95% confidence interval is in square brackets. A range lag of zero means assemblages are able to track climatic changes, with a higher range lag indicating higher disequilibrium dynamics. Coloured circles show mean estimates and lines show 95% confidence intervals for the realized velocity (the actual range velocity of assemblages as estimated from fossil data) in black, and the required velocity (the range velocity of assemblages needed to stay in equilibrium with climate) in gray. The point color indicates latitudinal zones.

We repeated all analyses after first using temperature at the sea surface with the temperatures derived at each species' preferred depth layer, whereby the magnitude and trends in climatic lag stayed the same (Supplementary Data Table 3). Similarly, calculating climatic lag on occurrences instead of relative abundance of individual foraminifera species revealed the same trends but resulted in higher magnitudes in climatic lag, for both the global climatic lag (Supplementary Data Fig. 5) and for latitudinal zones (Supplementary Data Fig. 6). This indicates that species within assemblages not only respond to climatic changes by shifting their distribution, but also by changing their abundance.

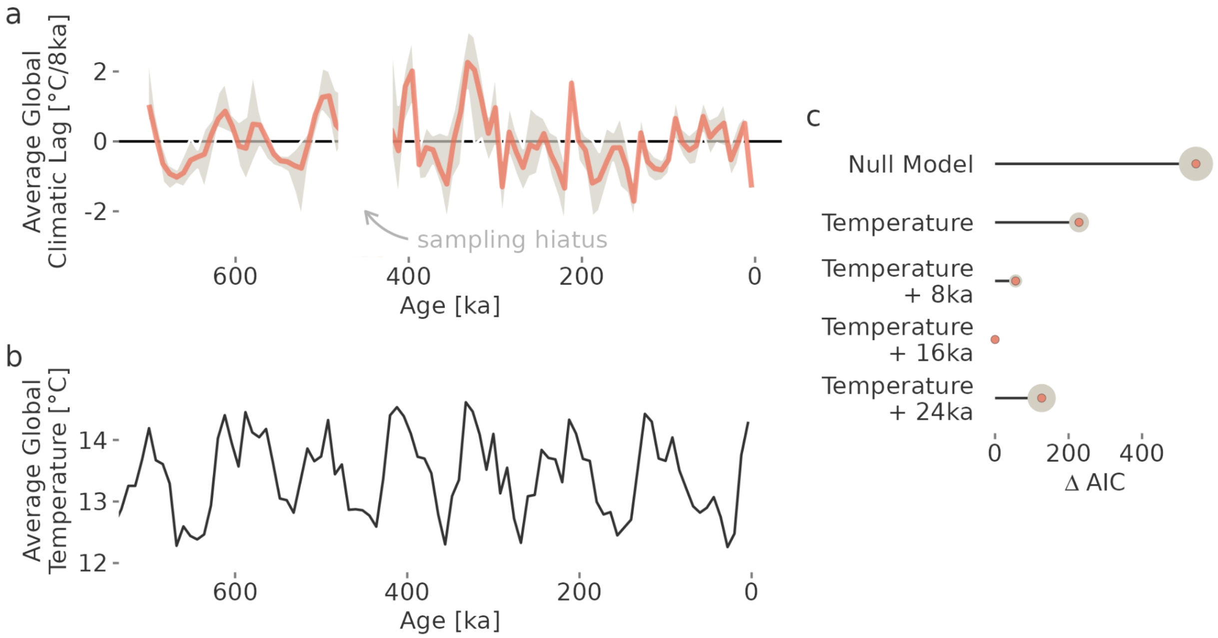

Figure 4: Global climatic lag across the past 700 ka and model comparison of its correlation with temperature changes. (a) Mean global climatic lag through time in orange along with the 95% confidence interval in gray. As planktonic foraminifera assemblages were unsampled in some time bins between 460 and 444 ka (Supplementary Data Fig. 2), the resulting global bin-to-bin climatic lag around this interval can be considered unreliable. (b) The mean global temperature through time as estimated by a coupled Atmosphere–Ocean Generalized Circulation Model. (c) Model performance for the correlation of the global temperature at the focal time bin and the global climatic lag (temperature), and preceding temperature trends (see Methods) to test for legacy effects. The null model was based on an intercept-only regression. Model comparison was based on AIC values, whereby the best performing model displays a delta-AIC of zero. Orange points show the mean estimate for the delta-AIC and the gray circles display the standard deviation around the mean estimate.

DISCUSSION

Our results show, over a global area and for 38 species, the ability of planktonic foraminifera assemblages to keep pace with climate change over the past 700 ka by both species distribution shifts and changes in relative abundances. However, this ability to track climate was not spatially consistent. Assemblages in high latitudes during warming and assemblages in low latitudes during cooling showed a high accumulation of lags in their biotic response to climate change, which we term climatic lag. This climatic lag may be surprising given the 8 ka resolution of our study, where we expected to see a higher ability of assemblages to track climate change over this ecologically long timescale (Hutchins & Fu, 2017), as marine species may be better able to track climate velocities (Lenoir et al., 2020; Pinsky et al., 2013; Sunday et al., 2012).

However, having ‘nowhere to run to’ may explain the extraordinarily high accumulation of lags of polar species during warming and tropical species during cooling.

Assemblages in particular latitudinal bands showing unexpectedly high climatic lags can be explained by the geometry of the globe in combination with a latitudinal diversity gradient and ecological priority effects. For example, high latitude assemblages are thought to show high rates of turnover under climate warming (Antão et al., 2022; Koltz et al., 2018) but our results indicate that for the past this supposedly high turnover was not sufficient to stay in equilibrium with climate (Fig. 2 and 3). Under climate warming, high latitude assemblages experience the greatest proportional loss of available habitat space (Reddin et al., 2022; Stanley, 1987). Whereas low latitude assemblages under climate warming can benefit from the higher species pool in the tropics as well as the novel equatorial climate suitable for range expansions, potentially resulting in the observed decrease in climatic lag. This explanation of high latitude assemblages accumulating large climatic debt under climate warming with low latitude assemblages not showing the same trend is in line with existing literature (Reddin et al., 2018, 2022; Storch et al., 2014; Walters et al., 2012). Under climate cooling, warm-adapted species in low latitudes are impeded from closely tracking preferred climates as the suitable habitat is no longer available (Stanley, 1987), potentially leading to the observed high climatic lags of tropical assemblages under cooling. The combination of geographic constraints at the equator and the poles with available diversity could similarly explain the pattern in range lags (Fig. 3). The particularly high range lag for high latitude assemblages during a climate warming, however, might also result from the generally higher rates of warming during deglaciation as opposed to the rates of ice sheet growth during glacial cycles (Lisiecki & Raymo, 2007).

Tipping points might be another potential explanation for the disproportionate response of low latitude assemblages to climatic cooling (1°C of cooling resulted in assemblages showing a preference for a 4.4°C cooler climate, on average) and high latitude assemblages responding to a warming scenario (1°C of warming resulted in assemblages showing a preference for a 3.4°C warmer climate, on average). If the degree of warming is exceeding a threshold, cool-adapted species at high latitudes are restricted to a smaller habitat area toward the poles where they might outnumber other species, leading to the observed pattern. Similarly, low latitude assemblages might be propelled into a new state of dominating warm-adapted species if the degree of cooling is high enough, as the remaining warm-adapted species are restricted to a smaller habitat area. The existence of tipping points within planktonic foraminifera assemblages might have far ranging implications for marine ecosystems under anthropogenic climate change (Pecl et al., 2017), if other marine plankton groups are showing the same response.

Climatic lag in general is a direct measure of the disequilibrium of assemblages with climate change (Bertrand et al., 2016; Garcia et al., 2014), which is arising from a combination of biotic and abiotic processes (Essl et al., 2015; Svenning & Sandel, 2013). However, long lasting legacies may be present in contemporary assemblages (Mathes et al., 2021; Svenning et al., 2015), impeding the identification of these processes. We found indication for such legacies in our analysis, with effects of past temperatures ranging back as far as 16 ka explaining up to 13% of variance in global climatic lag. The response of planktonic foraminifera assemblages to climate warming might therefore be conditional on the preceding climate, as it has been found for other marine groups as well (Burrows et al. 2019; Antão et al. 2020; Mathes et al. 2021a).

This dependency on the preceding climate might have implications for future climate change, with a longer-lasting climate warming potentially leading to ecological cascades within assemblages (Beaugrand 2015). Without considering how historical factors shape modern-day dynamics, current assessments of biodiversity as well as predictions under future climate change might hence be erroneous.

The mismatch of high latitudinal assemblages to a warming climate is particularly alarming as polar regions are projected to experience rapid and significant changes under anthropogenic climate change (Pörtner et al., 2022). If holoplankton assemblages in high latitudes are not able to adapt to these changes, as indicated by our data for foraminifera (Fig. 2 and 3 and Supplementary Data Fig. 7), substantial and long-lasting effects on ecosystem functioning are likely to emerge from local extirpations, novel species interactions and cascading effects (Bertrand et al., 2016; Svenning et al., 2015; Walther et al., 2002). Within assemblages in mid and low latitudes, anthropogenic climate warming may lead to species emerging as winners or losers resulting from asynchronous responses of individual species within assemblages and habitat contractions through poleward migration (Reddin et al., 2022). This can either reduce or impose constraints on species fitness, abundance and distributions (Antão et al., 2022), leading to community change. While severe climatic lags are likely for high latitudinal planktonic assemblages in the future, shifts in species distributions with widespread implications can hence be expected for all planktonic assemblages.

CONCLUSIONS

Here we showed how planktonic foraminifera assemblages, which are primary components of marine food webs and biogeochemical cycles, have responded to environmental change over past millennia in order to identify what makes certain assemblages more vulnerable to recent and future climate change. While planktonic foraminifera assemblages were on average in equilibrium with climate, substantial climatic lags emerged in high and low latitudes under specific temperature change scenarios. Understanding the underlying processes of these climatic lags, which occur when assemblages are no longer in equilibrium with climate, is crucial for predicting responses of assemblages under anthropogenic climate change, informing conservation planning, as well as understanding likely changes in ecosystem functioning (Svenning & Sandel, 2013).

References

Antão, L. H., Weigel, B., Strona, G., Hällfors, M., Kaarlejärvi, E., Dallas, T., Opedal, Ø. H., Heliölä, J., Henttonen, H., Huitu, O., Korpimäki, E., Kuussaari, M., Lehikoinen, A., Leinonen, R., Lindén, A., Merilä, P., Pietiäinen, H., Pöyry, J., Salemaa, M., … Laine, A.-L. (2022). Climate change reshuffles northern species within their niches. Nature Climate Change, 12(6), 587–592. https://doi.org/10.1038/s41558-022-01381-x

Antell, G. S., Fenton, I. S., Valdes, P. J., & Saupe, E. E. (2021). Thermal niches of planktonic foraminifera are static throughout glacial–interglacial climate change. Proceedings of the National Academy of Sciences, 118(18), e2017105118. https://doi.org/10.1073/pnas.2017105118

Bates, D., Mächler, M., Bolker, B., & Walker, S. (2015). Fitting linear mixed-effects models using lme4. Journal of Statistical Software, 1–48. https://doi.org/10.18637/jss.v067.i01

Bertrand, R., Riofrío-Dillon, G., Lenoir, J., Drapier, J., de Ruffray, P., Gégout, J.-C., & Loreau, M. (2016). Ecological constraints increase the climatic debt in forests. Nature Communications, 7(1), 12643. https://doi.org/10.1038/ncomms12643

Burnham, K. P. (1998). Model selection and multimodel inference. A Practical Information-Theoretic Approach.

Burrows, M. T., Schoeman, D. S., Buckley, L. B., Moore, P., Poloczanska, E. S., Brander, K. M., Brown, C., Bruno, J. F., Duarte, C. M., & Halpern, B. S. (2011). The pace of shifting climate in marine and terrestrial ecosystems. Science, 334(6056), 652–655.

Chen, I.-C., Hill, J. K., Ohlemüller, R., Roy, D. B., & Thomas, C. D. (2011). Rapid range shifts of species associated with high levels of climate warming. Science, 333(6045), 1024–1026.

Cox, P. M. (2001). Description of the" TRIFFID" dynamic global vegetation model.

Darling, K. F., Kucera, M., & Wade, C. M. (2007). Global molecular phylogeography reveals persistent Arctic circumpolar isolation in a marine planktonic protist. Proceedings of the National Academy of Sciences, 104(12), 5002–5007.

Devictor, V., Van Swaay, C., Brereton, T., Brotons, L., Chamberlain, D., Heliölä, J., Herrando, S., Julliard, R., Kuussaari, M., & Lindström, Å. (2012). Differences in the climatic debts of birds and butterflies at a continental scale. Nature Climate Change, 2(2), 121–124.

Dornelas, M., Gotelli, N. J., McGill, B., Shimadzu, H., Moyes, F., Sievers, C., & Magurran, A. E. (2014). Assemblage Time Series Reveal Biodiversity Change but Not Systematic Loss. Science, 344(6181), 296–299. https://doi.org/10.1126/science.1248484

Essl, F., Dullinger, S., Rabitsch, W., Hulme, P. E., Pyšek, P., Wilson, J. R., & Richardson, D. M. (2015). Delayed biodiversity change: No time to waste. Trends in Ecology & Evolution, 30(7), 375–378.

Ezard, T. H., Aze, T., Pearson, P. N., & Purvis, A. (2011). Interplay between changing climate and species' ecology drives macroevolutionary dynamics. Science, 332(6027), 349–351.

Fenton, I. S., Pearson, P. N., Dunkley Jones, T., & Purvis, A. (2016). Environmental predictors of diversity in recent planktonic foraminifera as recorded in marine sediments. PloS One, 11(11), e0165522.

Garcia, R. A., Cabeza, M., Rahbek, C., & Araújo, M. B. (2014). Multiple dimensions of climate change and their implications for biodiversity. Science, 344(6183), 1247579.

García Molinos, J., Halpern, B. S., Schoeman, D. S., Brown, C. J., Kiessling, W., Moore, P. J., Pandolfi, J. M., Poloczanska, E. S., Richardson, A. J., & Burrows, M. T. (2016). Climate velocity and the future global redistribution of marine biodiversity. Nature Climate Change, 6(1), 83–88. https://doi.org/10.1038/nclimate2769

Graham, R. W., Lundelius Jr, E. L., Graham, M. A., Schroeder, E. K., Toomey III, R. S., Anderson, E., Barnosky, A. D., Burns, J. A., Churcher, C. S., & Grayson, D. K. (1996). Spatial response of mammals to late Quaternary environmental fluctuations. Science, 272(5268), 1601–1606.

Greenstein, B. J., & Pandolfi, J. M. (2008). Escaping the heat: Range shifts of reef coral taxa in coastal Western Australia. Global Change Biology, 14(3), 513–528.

Hutchins, D. A., & Fu, F. (2017). Microorganisms and ocean global change. Nature Microbiology, 2(6), 1–11.

Jackson, S. T., & Sax, D. F. (2010). Balancing biodiversity in a changing environment: Extinction debt, immigration credit and species turnover. Trends in Ecology & Evolution, 25(3), 153–160.

Jonkers, L., Hillebrand, H., & Kucera, M. (2019). Global change drives modern plankton communities away from the pre-industrial state. Nature, 570(7761), 372–375. https://doi.org/10.1038/s41586-019-1230-3

Juggins, S. (2020). rioja: Analysis of Quaternary Science Data. https://cran.r-project.org/package=rioja

Kiessling, W., Simpson, C., Beck, B., Mewis, H., & Pandolfi, J. M. (2012). Equatorial decline of reef corals during the last Pleistocene interglacial. Proceedings of the National Academy of Sciences, 109(52), 21378–21383.

Kocsis, Á. T., Reddin, C. J., & Kiessling, W. (2018). The stability of coastal benthic biogeography over the last 10 million years: XXXX. Global Ecology and Biogeography, 27(9), 1106–1120. https://doi.org/10.1111/geb.12771

Koltz, A. M., Schmidt, N. M., & Høye, T. T. (2018). Differential arthropod responses to warming are altering the structure of Arctic communities. Royal Society Open Science, 5(4), 171503.

Lenoir, J., Bertrand, R., Comte, L., Bourgeaud, L., Hattab, T., Murienne, J., & Grenouillet, G. (2020). Species better track climate warming in the oceans than on land. Nature Ecology & Evolution, 4(8), 1044–1059.

Lisiecki, L. E., & Raymo, M. E. (2007). Plio–Pleistocene climate evolution: Trends and transitions in glacial cycle dynamics. Quaternary Science Reviews, 26(1–2), 56–69. https://doi.org/10.1016/j.quascirev.2006.09.005

Martin, R. E. (1999). Taphonomy and temporal resolution of foraminiferal assemblages. Modern Foraminifera, 281–298.

Martin-Garin, B., Lathuilière, B., & Geister, J. (2012). The shifting biogeography of reef corals during the Oxfordian (Late Jurassic). A climatic control? Palaeogeography, Palaeoclimatology, Palaeoecology, 365, 136–153.

Mathes, G. H., van Dijk, J., Kiessling, W., & Steinbauer, M. J. (2021). Extinction risk controlled by interaction of long-term and short-term climate change. Nature Ecology & Evolution, 5(3), 304–310. https://doi.org/10.1038/s41559-020-01377-w

Matthews, K. J., Maloney, K. T., Zahirovic, S., Williams, S. E., Seton, M., & Mueller, R. D. (2016). Global plate boundary evolution and kinematics since the late Paleozoic. Global and Planetary Change, 146, 226–250.

Meilland, J., Siccha, M., Weinkauf, M. F., Jonkers, L., Morard, R., Baranowski, U., Baumeister, A., Bertlich, J., Brummer, G.-J., & Debray, P. (2019). Highly replicated sampling reveals no diurnal vertical migration but stable species-specific vertical habitats in planktonic foraminifera. Journal of Plankton Research, 41(2), 127–141.

Menéndez, R., Megías, A. G., Hill, J. K., Braschler, B., Willis, S. G., Collingham, Y., Fox, R., Roy, D. B., & Thomas, C. D. (2006). Species richness changes lag behind climate change. Proceedings of the Royal Society B: Biological Sciences, 273(1593), 1465–1470. https://doi.org/10.1098/rspb.2006.3484

Morard, R., Darling, K. F., Mahé, F., Audic, S., Ujiié, Y., Weiner, A. K., André, A., Seears, H. A., Wade, C. M., & Quillévéré, F. (2015). PFR2: A curated database of planktonic foraminifera 18S ribosomal DNA as a resource for studies of plankton ecology, biogeography and evolution. Molecular Ecology Resources, 15(6), 1472–1485.

Munday, P. L., Warner, R. R., Monro, K., Pandolfi, J. M., & Marshall, D. J. (2013). Predicting evolutionary responses to climate change in the sea. Ecology Letters, 16(12), 1488–1500.

Pecl, G. T., Araújo, M. B., Bell, J. D., Blanchard, J., Bonebrake, T. C., Chen, I.-C., Clark, T. D., Colwell, R. K., Danielsen, F., & Evengård, B. (2017). Biodiversity redistribution under climate change: Impacts on ecosystems and human well-being. Science, 355(6332), eaai9214.

Pinsky, M. L., Worm, B., Fogarty, M. J., Sarmiento, J. L., & Levin, S. A. (2013). Marine taxa track local climate velocities. Science, 341(6151), 1239–1242.

Poloczanska, E. S., Brown, C. J., Sydeman, W. J., Kiessling, W., Schoeman, D. S., Moore, P. J., Brander, K., Bruno, J. F., Buckley, L. B., & Burrows, M. T. (2013). Global imprint of climate change on marine life. Nature Climate Change, 3(10), 919–925.

Pörtner, H. O., Roberts, D. C., Adams, H., Adler, C., Aldunce, P., Ali, E., Begum, R. A., Betts, R., Kerr, R. B., & Biesbroek, R. (2022). Climate change 2022: Impacts, adaptation and vulnerability.

R Core Team. (2021). R: A Language and Environment for Statistical Computing (4.1.2) [R]. R Foundation for Statistical Computing. https://www.R-project.org/

Reddin, C. J., Aberhan, M., Raja, N. B., & Kocsis, Á. T. (2022). Global warming generates predictable extinctions of warm- and cold-water marine benthic invertebrates via thermal habitat loss. Global Change Biology, gcb.16333. https://doi.org/10.1111/gcb.16333

Reddin, C. J., Kocsis, Á. T., & Kiessling, W. (2018). Marine invertebrate migrations trace climate change over 450 million years. Global Ecology and Biogeography, 27(6), 704–713. https://doi.org/10.1111/geb.12732

Renaudie, J., Lazarus, D. B., & Diver, P. (2020). NSB (Neptune Sandbox Berlin): An expanded and improved database of marine planktonic microfossil data and deep-sea stratigraphy. Palaeontol. Electron, 23, a11.

Richter, D. J., Watteaux, R., Vannier, T., Leconte, J., Frémont, P., Reygondeau, G., Maillet, N., Henry, N., Benoit, G., Silva, O. D., Delmont, T. O., Fernàndez-Guerra, A., Suweis, S., Narci, R., Berney, C., Eveillard, D., Gavory, F., Guidi, L., Labadie, K., … Jaillon, O. (2019). Genomic evidence for global ocean plankton biogeography shaped by large-scale current systems [Preprint]. Ecology. https://doi.org/10.1101/867739

Rosenzweig, C., Karoly, D., Vicarelli, M., Neofotis, P., Wu, Q., Casassa, G., Menzel, A., Root, T. L., Estrella, N., Seguin, B., Tryjanowski, P., Liu, C., Rawlins, S., & Imeson, A. (2008). Attributing physical and biological impacts to anthropogenic climate change. Nature, 453(7193), 353–357. https://doi.org/10.1038/nature06937

Siccha, M., & Kucera, M. (2017). ForCenS, a curated database of planktonic foraminifera census counts in marine surface sediment samples. Scientific Data, 4(1), 170109. https://doi.org/10.1038/sdata.2017.109

Stanley, S. B. (1987). Extinction. Scientific American Library.

Storch, D., Menzel, L., Frickenhaus, S., & Pörtner, H.-O. (2014). Climate sensitivity across marine domains of life: Limits to evolutionary adaptation shape species interactions. Global Change Biology, 20(10), 3059–3067.

Stuart-Smith, R. D., Edgar, G. J., Barrett, N. S., Kininmonth, S. J., & Bates, A. E. (2015). Thermal biases and vulnerability to warming in the world's marine fauna. Nature, 528(7580), 88–92.

Sunday, J. M., Bates, A. E., & Dulvy, N. K. (2011). Global analysis of thermal tolerance and latitude in ectotherms. Proceedings of the Royal Society B: Biological Sciences, 278(1713), 1823–1830.

Sunday, J. M., Bates, A. E., & Dulvy, N. K. (2012). Thermal tolerance and the global redistribution of animals. Nature Climate Change, 2(9), 686–690. https://doi.org/10.1038/nclimate1539

Svenning, J.-C., Eiserhardt, W. L., Normand, S., Ordonez, A., & Sandel, B. (2015). The influence of paleoclimate on present-day patterns in biodiversity and ecosystems. Annual Review of Ecology, Evolution, and Systematics, 46(1), 551–572. https://doi.org/10.1146/annurev-ecolsys-112414-054314

Svenning, J.-C., & Sandel, B. (2013). Disequilibrium vegetation dynamics under future climate change. American Journal of Botany, 100(7), 1266–1286.

Ter Braak, C. J. F., Juggins, S., Birks, H. J. B., & Van der Voet, H. (1993). Weighted averaging partial least squares regression (WA-PLS): Definition and comparison with other methods for species-environment calibration. In Multivariate environmental statistics (Issue 6, pp. 525–560). Elsevier.

Walters, R. J., Blanckenhorn, W. U., & Berger, D. (2012). Forecasting extinction risk of ectotherms under climate warming: An evolutionary perspective. Functional Ecology, 26(6), 1324–1338.

Walther, G.-R., Post, E., Convey, P., Menzel, A., Parmesan, C., Beebee, T. J., Fromentin, J.-M., Hoegh-Guldberg, O., & Bairlein, F. (2002). Ecological responses to recent climate change. Nature, 416(6879), 389–395.

Wickham, H., Averick, M., Bryan, J., Chang, W., McGowan, L. D., François, R., Grolemund, G., Hayes, A., Henry, L., & Hester, J. (2019). Welcome to the Tidyverse. Journal of Open Source Software, 4(43), 1686.

Williams, J. W., & Jackson, S. T. (2007). Novel climates, no-analog communities, and ecological surprises. Frontiers in Ecology and the Environment, 5(9), 475–482.

Williams, J. W., Jackson, S. T., & Kutzbach, J. E. (2007). Projected distributions of novel and disappearing climates by 2100 AD. Proceedings of the National Academy of Sciences, 104(14), 5738–5742. https://doi.org/10.1073/pnas.0606292104

Yasuhara, M., Wei, C.-L., Kucera, M., Costello, M. J., Tittensor, D. P., Kiessling, W., Bonebrake, T. C., Tabor, C. R., Feng, R., & Baselga, A. (2020). Past and future decline of tropical pelagic biodiversity. Proceedings of the National Academy of Sciences, 117(23), 12891–12896.

Supplementary data

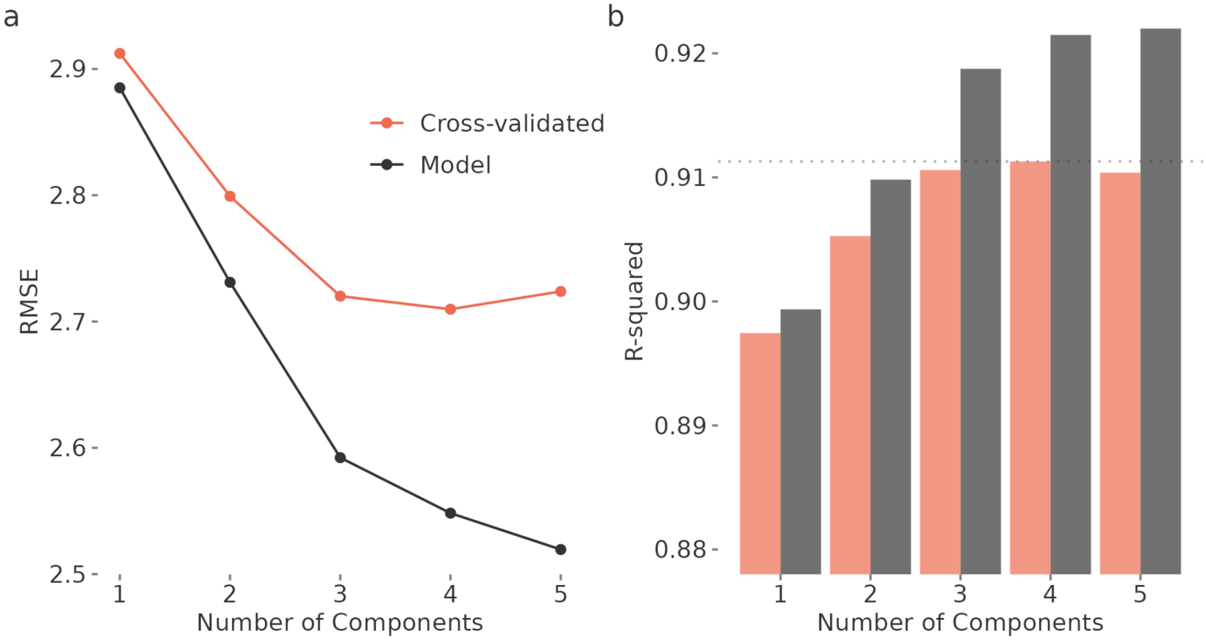

Supplementary Data Fig. 1: Weighted averaging partial least squares (WA-PLS) regression was used to estimate the relationship between assemblage composition of planktonic foraminifera and ambient temperature. (a) The performance of the model was assessed on the training subset (black line and points) and by leave-one-out cross-validation (orange line and points) via the root mean square error (RMSE). The appropriate number of components to use in the subsequent analysis was chosen by minimizing the cross-validated RMSE, which resulted in 4 components. (b) The R^2 *value for the WA-PLS regression based on cross-validation (orange) and test subset (black) as a function of the number of components.*

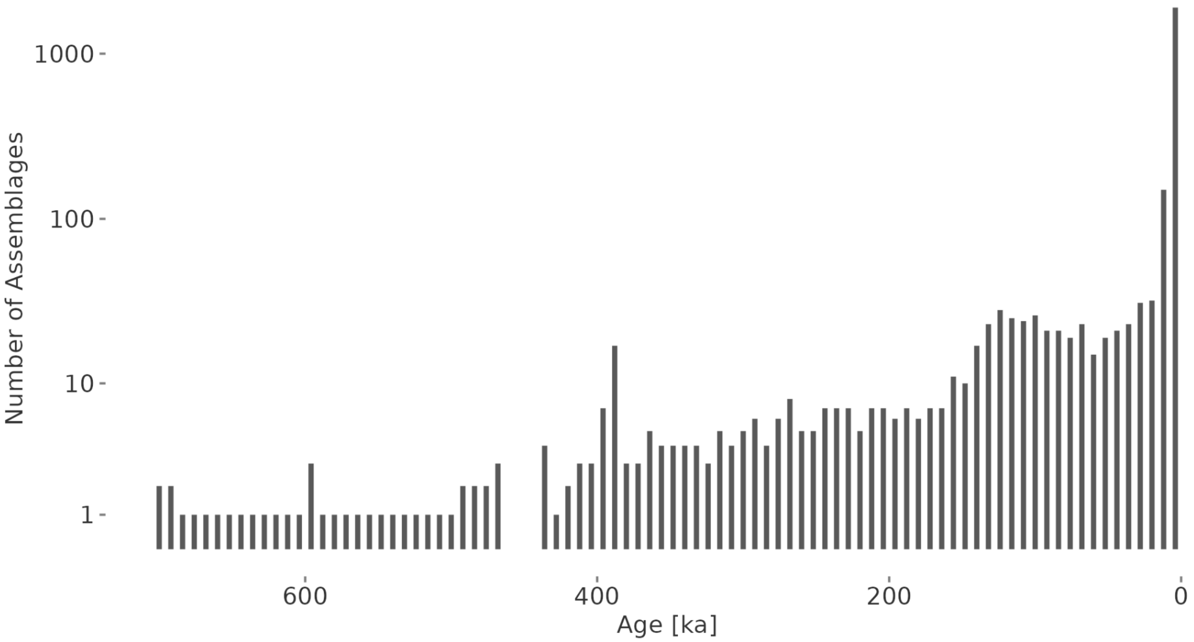

Supplementary Data Fig. 2: The number of planktonic foraminifera assemblages through time. As planktonic foraminifera assemblages were unsampled in some time bins between 460 and 444 ka, the resulting global bin-to-bin climatic lag around this interval can be considered unreliable. Note that the number of assemblages is plotted on a logarithmic scale.

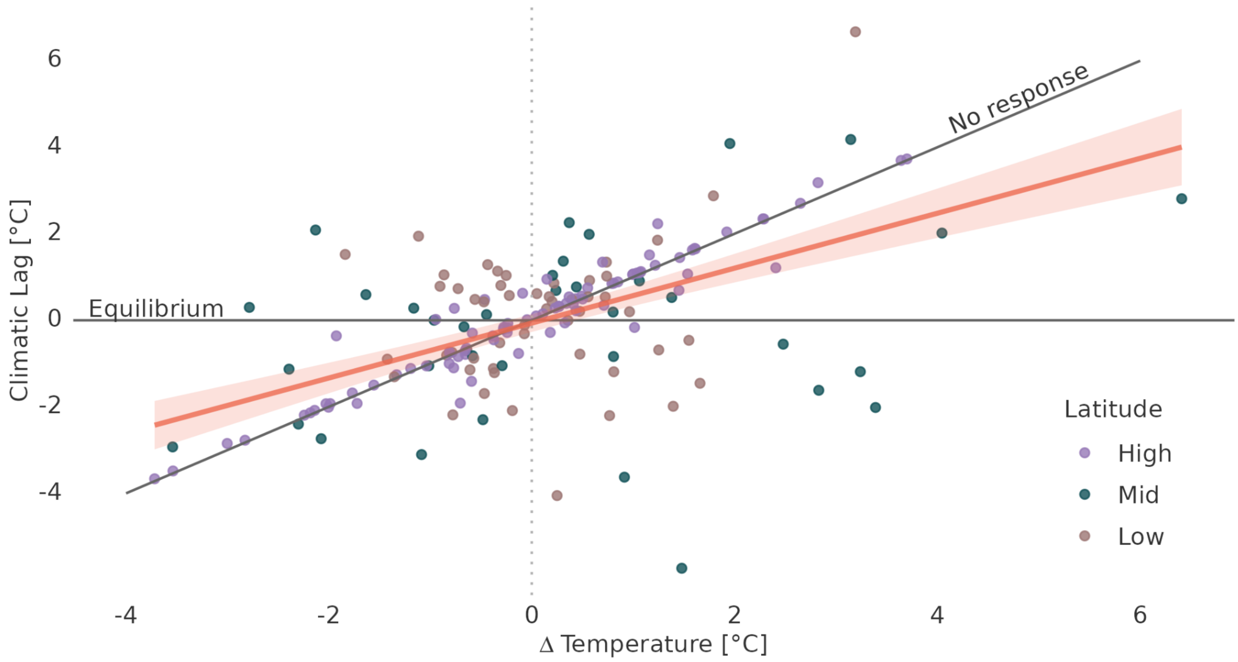

Supplementary Data Fig. 3: The global climatic lag of all foraminifera assemblages as a function of temperature change, without adjusting for differential sampling effort within bins. The horizontal equilibrium line shows complete temperature tracking when assemblages respond ideally to a temperature change (e.g., 1°C warming leads to an assemblage showing preference for a 1°C warmer climate, resulting in zero climatic lag). The no response line shows no temperature tracking when assemblages are unable to respond to a temperature change (e.g., when assemblages show no community changes even if the temperature increases by 1°C, the resulting climatic lag is 1°C).

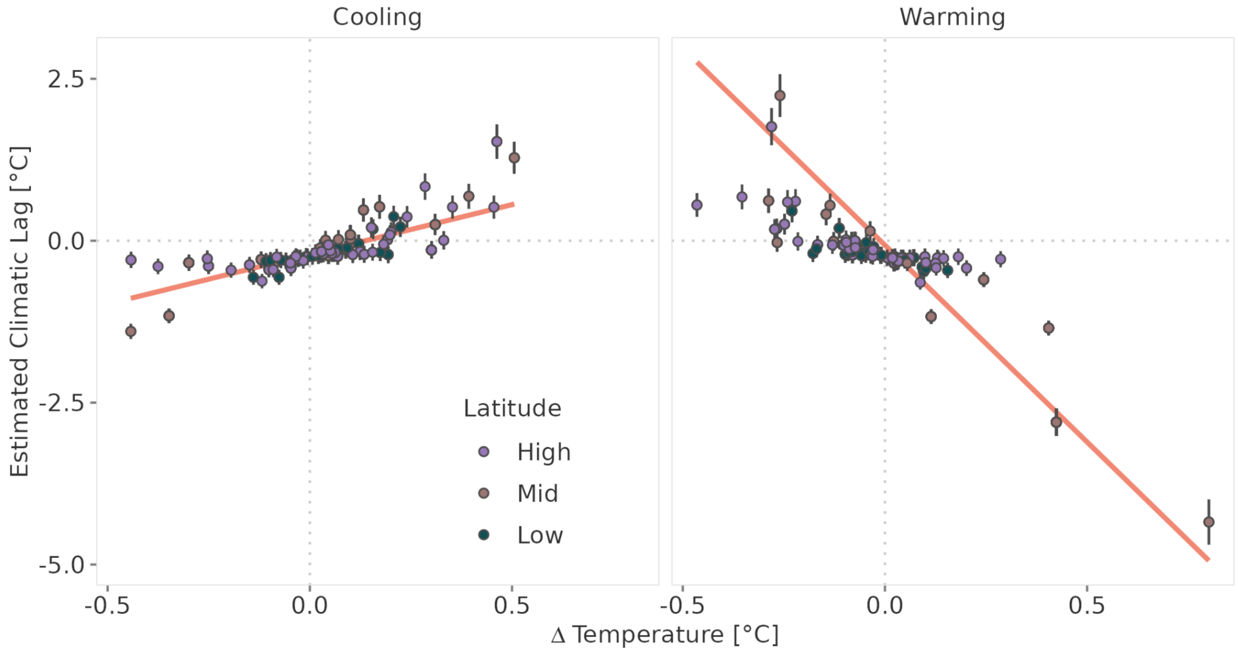

Supplementary Data Fig. 4: Legacy effects of past temperature on the response of planktonic foraminifera assemblages to climate change. The climatic lag as estimated by linear mixed effect models was conditional on whether the preceding 16 ka temperature trend showed a cooling or warming. Coloured points are showing the mean estimate for the climatic lag and lines the 95% confidence interval per latitudinal zone. The orange line is showing the average trend.

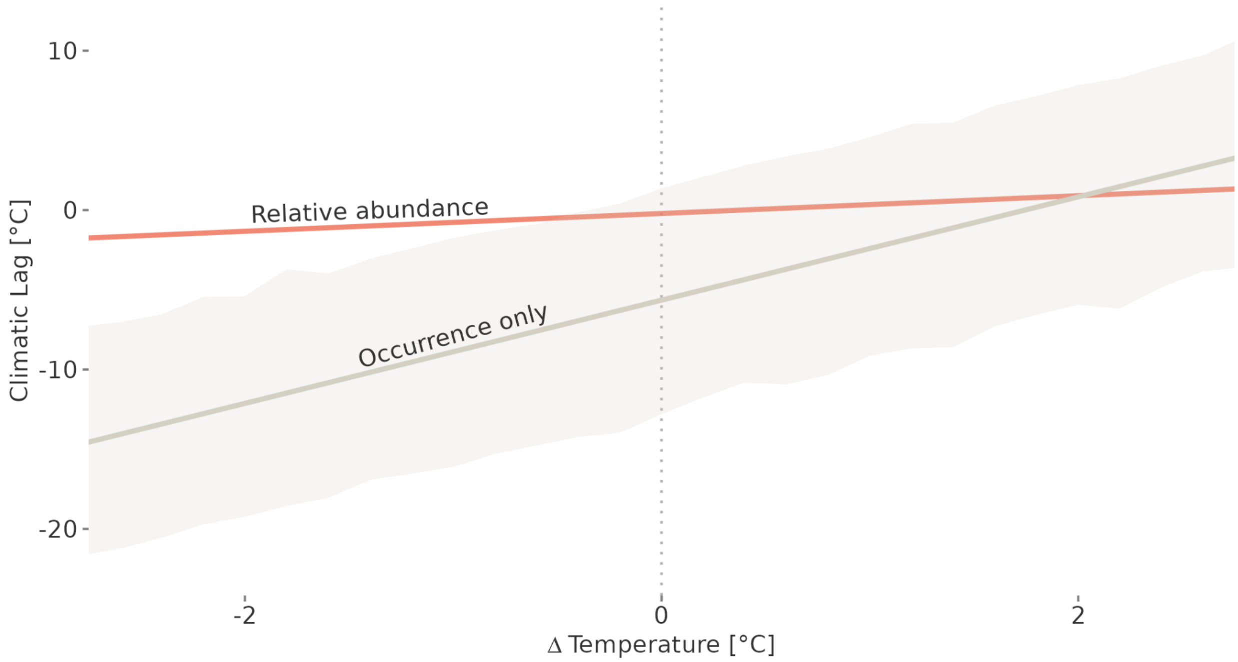

Supplementary Data Fig. 5: The global climatic lag of all foraminifera assemblages as a function of temperature change, based on the preferred temperatures of assemblages estimated by including the relative abundance of individual species (orange line), or by occurrences only (gray line). The gray area depicts the 95% confidence interval of the regression slope. *The global climatic lag of all foraminifera assemblages as a function of temperature change, based on the preferred temperatures of assemblages estimated by including the relative abundance of individual species (orange line), or by occurrences only (gray line). The gray area depicts the 95% confidence interval of the regression slope.*

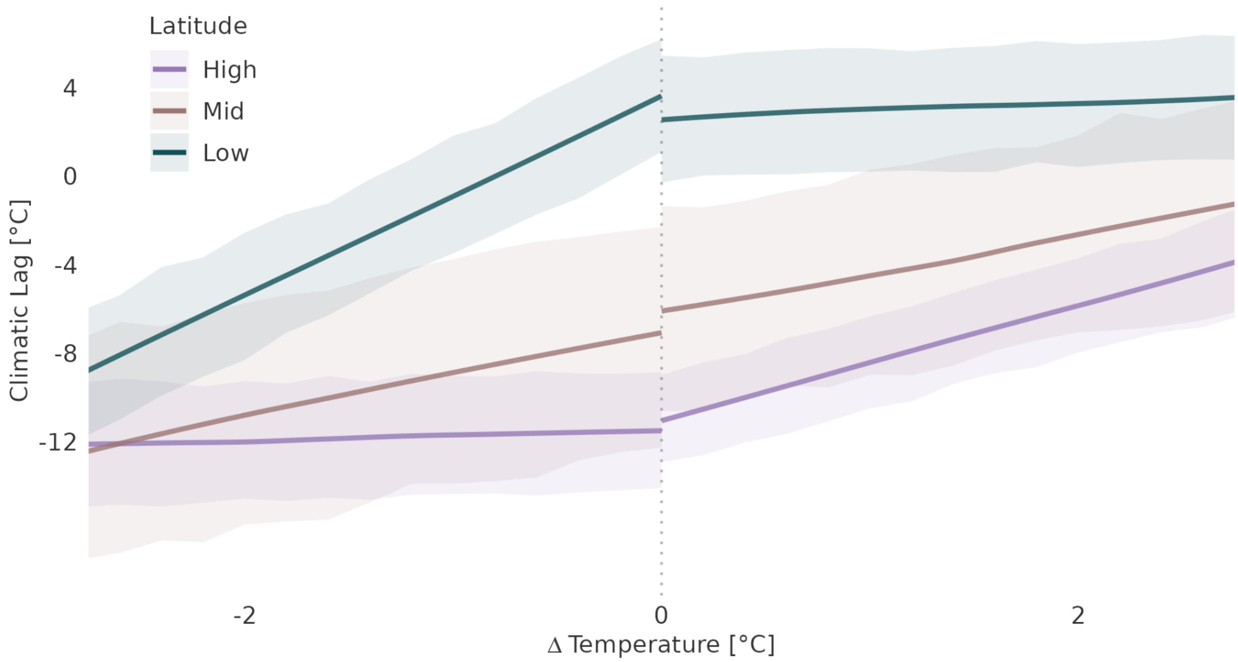

Supplementary Data Fig. 6: The climatic lag of foraminifera assemblages per latitudinal zone as a function of temperature change, based on the preferred temperatures of assemblages estimated by occurrences only. The coloured areas depict the 95% confidence interval of the focal regression slope.

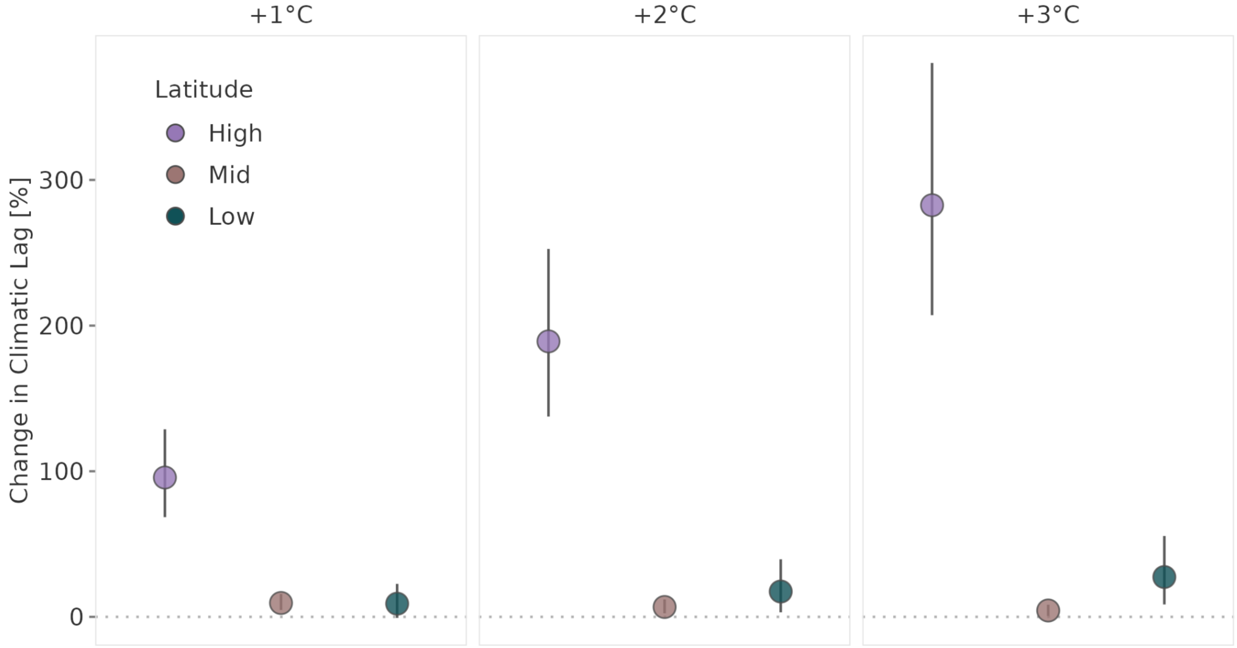

Supplementary Data Fig. 7: The estimated percentage change in climatic lag based on linear mixed effect models when ambient temperatures increase by 1°C, 2°C, or 3°C. Coloured points show the mean estimate for the percentage change per latitudinal zone and lines indicate the focal 95% confidence interval.

Supplementary Data Table 1: Number of occurrences per species for the cleaned dataset for the whole time period (total) and latitudinal zones, 0-30, 30-60, 60-90 degrees absolute latitude. The dataset contains 38 species with 98,297 total occurrences.

Species	**Total**	**High**	**Mid**	**Low**
Beella digitata	3,336	11	1,028	2,297
Beella megastoma	35	35		
Beella praedigitata	28		16	12
Globigerina bulloides	6,358	468	2,536	3,354
Globigerina falconensis	4,384	75	1,727	2,582
Globigerina umbilicata	32		32	
Globigerinella adamsi	193			193
Globigerinella calida	4,276	3	1,242	3,031
Globigerinella siphonifera	5,274	14	1,569	3,691
Globigerinoides conglobatus	3,186		660	2,526
Globigerinoides ruber	5,564	23	1,808	3,733
Globoconella inflata	4,442	254	2,373	1,815
Globoquadrina conglomerata	986	6	42	938
Globorotalia flexuosa	19			19
Globorotalia tumida	2,891	9	194	2,688
Globorotalia ungulata	28			28
Globorotaloides hexagonus	1,016		105	911
Globoturborotalita rubescens	3,150	2	797	2,351
Globoturborotalita tenella	3,485	3	852	2,630

Hirsutella hirsuta	2,465	31	1,356	1,078
Hirsutella scitula	4,000	90	1,682	2,228
Hirsutella theyeri	373			373
Menardella menardii	3,747		480	3,267
Neogloboquadrina dutertrei	5,141	110	1,468	3,563
Neogloboquadrina pachyderma	3,854	765	1,984	1,105
Orbulina suturalis	40		40	
Orbulina universa	5,029	72	1,867	3,090
Pulleniatina obliquiloculata	3,607		476	3,131
Sphaeroidinella dehiscens	1,641		111	1,530
Trilobatus sacculifer	4,768	2	1,063	3,703
Trilobatus trilobus	3,595	2	794	2,799
Truncorotalia crassaformis	2,767	8	758	2,001
Truncorotalia crassula	65		65	
Truncorotalia tosaensis	15		4	11
Truncorotalia truncatulinoides	3,998	13	2,012	1,973
Turborotalita cristata	48		48	
Turborotalita humilis	865	10	490	365
Turborotalita quinqueloba	3,596	694	1,900	1,002

Supplementary Data Table 2: Number of assemblages sampled in the northern hemisphere (Global North) and the southern hemisphere (Global South), for each latitudinal zone, 0-30, 30-60, 60-90 degrees absolute latitude.

Latitudinal Zone	Global North	Global South
High	423	1
Mid	607	326
Low	782	528

Supplementary Data Table 3: The mean estimate for the change in climatic debt if temperature increases by 1°C (red background) or decreases by 1°C (blue background), for each latitudinal zone, 0-30, 30-60, 60-90 degrees absolute latitude. The estimate is based on linear mixed effect models and was calculated either based on the surface temperature (Surface) or the temperature derived at each species' preferred depth layer (Preferred Depth). Values in square brackets indicate the 95% confidence interval.

Latitudinal Zone	**Surface**	**Preferred Depth**
High	3.42 [2.02, 4.81]	3.42 [2.08, 4.75]
	0.36 [0.05, 0.67]	0.36 [0.06, 0.66]
Mid	0.25 [-0.62, 1.11]	0.25 [-0.64, 1.13]
	0.43 [0, 0.87]	0.43 [0.01, 0.86]
Low	-0.36 [-0.72, 0.01]	-0.36 [-0.75, 0.03]
	4.44 [3.08, 5.8]	4.44 [3.09, 5.79]

Manuscript 5

The joint world of macroecology and terrestrial palaeoecology

Global Ecology and Biogeography, in review

Suzette G.A. Flantua[1*], Ondřej Mottl[1], Vivian A. Felde[1], Thomas Giesecke[2], Henry Hooghiemstra[3], Severin D.H. Irl[4,5], Jonathan Lenoir[6], Gregor H. Mathes[7,8], Crystal N.H. McMichael[4], Alistair Seddon[1], Manuel Steinbauer[8,9], Carolina Tovar[10], Ole Reidar Vetaas[11], H. John B. Birks[1,12], John-Arvid Grytnes[1]

[1] Department of Biological Sciences, University of Bergen and Bjerknes Centre for Climate Research, Bergen, Norway.
[2] Department of Physical Geography, Utrecht University, Utrecht, The Netherlands.
[3] Institute for Biodiversity and Ecosystem Dynamics, Department of Ecosystem and Landscape Dynamics, University of Amsterdam, Amsterdam, The Netherlands.
[4] Biogeography and Biodiversity Lab, Institute of Physical Geography, Goethe-University Frankfurt, Frankfurt am Main, Germany.
[5] BayCEER, Bayreuth Centre of Ecology and Environmental Research, University of Bayreuth, Bayreuth, Germany.
[6] UMR CNRS 7058, Ecologie et dynamique des systèmes anthropisés (EDYSAN), Amiens, France.
[7] Department of Geography and Geosciences, GeoZentrum Nordbayern, Friedrich-Alexander University Erlangen-Nürnberg, Erlangen, Germany.
[8] Bayreuth Center of Ecology and Environmental Research, University of Bayreuth, Bayreuth, Germany.
[9] Department of Biological Sciences, University of Bergen, Bergen, Norway.
[10] Royal Botanic Gardens, Kew, Surrey, UK.
[11] Department of Geography, University of Bergen, Bergen, Norway.
[12] Environmental Change Research Centre, University College London, London, UK.
* Corresponding author: s.g.a.flantua@gmail.com

ABSTRACT

Background: We discuss opportunities for transdisciplinary research between terrestrial macroecology and palaeoecology, and highlight key research topics that benefit from an interdisciplinary integration in terms of a common understanding of robust data practices and the successful interchange of methodologies and approaches

Research challenges and opportunities: We highlight the pitfalls related to the increasing availability of palaeoecological data should the two disciplines continue to work separately with discipline-centred methods (i.e. 'multidisciplinary isolation'). We briefly address differences in perspectives on niche space, adaptation, and fossil pollen assemblages, among others, while also arguing that macroecology and palaeoecology have more in common than is often perceived. Many opportunities are at hand that can strengthen both disciplines and we specify research topics in need of a strong integration

Outlook: We advocate for the need for cross-discipline-friendly guidelines that explain the foundational data knowledge by users from any discipline and which will guide the user to best practices with specific recommendations for filtering procedures of palaeoecological data. We also highlight the high potential in methodological interchange between macroecology and palaeoecology ('methodological recycling') in quantitative analysis where macroecology can contribute with its solid experience of handling large datasets and innovative advances in numerical ecology of large, complex datasets heterogeneous across space and time. Sharing palaeoecological perspectives and supporting correct use of open-access palaeoecological databases can provide the needed integration with macroecology to achieve a holistic understanding of global-change ecology on multiple spatial and temporal scales.

INTRODUCTION

The importance of long-term data for understanding ecological patterns

With biodiversity loss being one of the major challenges of our society and the rising concern that an increasing wave of extinctions may be imminent (McCauley et al., 2015), enhancing our understanding of natural processes and biotic responses to global change is crucial. The potential to predict the impact of future stressors strongly depends on our understanding of general mechanisms and interactions (Brook & Alroy, 2017; Flessa & Jackson, 2005a; Kerr et al., 2007; Stigall, 2013). Macroecology plays an essential role in understanding the threats that global changes pose to biodiversity. Still, Brown emphasised already in 1989 the importance of long-term history and historical ecology when studying macroecological patterns in the present and future (Brown, 1989). Through fossil pollen sequences, and the determination of larger plant fossils, palaeoecology has provided detailed information on the vegetation history of thousands of localities worldwide. It has enhanced our understanding of local-to-regional variation in climate, human impact, and other environmental drivers over time. Integrating research ideas, data and analytical approaches from macroecology and palaeoecology will enhance our ability to quantify and model natural processes and develop new research questions much needed in global-change ecology.

Here, we reflect on opportunities for global-change ecology by enhancing 'transdisciplinary research' between macroecology and palaeoecology, and highlight key macroecological questions that benefit from integrating time series of the past (Fig. 1). Such research is much a joint effort using shared conceptual frameworks drawing together on disciplinary-specific theories, concepts, and approaches to address common problems and research topics (Aagaard-Hansen, 2007). We first discuss the obstacles hindering a more widespread use of fossil pollen data – and highlight the potential and pitfalls related to the increasing availability of palaeo-data when used in a more isolated 'multidisciplinary manner' (Researchers work in parallel or sequentially from a disciplinary-specific base to address common problems but in a separate manner; adjusted from Aagaard-Hansen (2007); Fig. 2A). We discuss the prospects for combining the two disciplines into 'interdisciplinary research' (Researchers work jointly but still from disciplinary-specific bases to address common problems; Aagaard-Hansen, 2007), with a focus on the Quaternary using fossil plant remains. The latter reflects the authors' greater familiarity with the terrestrial fossil pollen record.

We also highlight specific topics of common interest to macroecology and palaeoecology where we see that macroecological patterns could benefit from incorporating a palaeoecological perspective. We acknowledge that our selected topics are limited compared to the exciting research we foresee. Notwithstanding, we hope that the reader will appreciate the highlighted topics, including niche space, no-analogue assemblages and climates, speciation, and extinction.

The temporal dimensions of ecological fields

The field of 'Ecology' (coined in 1866 by Ernst Haeckel: Egerton, 2013) has branched out into multiple disciplines that study the relationships between organisms, ecosystems, and the physical environment at all scales of space and time (Odum & Barrett, 2004). Temporal scale is a key axis to subdivide a number of ecological disciplines from palaeontology and palaeobiology through palaeoecology and historical ecology to modern ecology (Fig. 1).

A major division in palaeoecology (Fig. 1) is between Quaternary-time palaeoecology (i.e. last 2.58 million years (Ma)) and deep-time palaeoecology (Jackson, 2001). A clear difference between 'historical', 'long-term', and 'deep-time' ecology is currently lacking, and their varying usage in the literature exemplifies how these concepts are discipline dependent (Giesecke et al. 2018: Rull 2012). Some have suggested 'long-term ecology' to refer to observational ecological datasets at the scale of a decade to a century (up to 180 yr in some exceptions; Lindenmayer et al., 2012; Magurran et al., 2010) while others suggest palaeoecology to be 'true long-term ecology' (Rull 2012) though the latter can also cover decadal research. Macroecology is cross-temporal research field (Fig. 1) within ecology with a long history (e.g. Alexander von Humboldt used macroecological approaches; Schrodt et al., 2019), but it was not until 1989 that the field of macroecology was first described as a separate and standalone discipline (Brown & Maurer, 1989; Brown, 1995).

An increasing number of recent papers have called for the integration between the 'newly arisen and maturing' macroecology and well-established palaeoecology. From the side of macroecology, excellent overviews have been provided (Beck et al., 2012; Lyons and Smith, 2010; McGill, 2019; Kerr & Dobrowski, 2013), for instance the combination of macroecology with deep-time (faunal) palaeoecology (Fritz et al., 2013) and with marine palaeoecology (Yasuhara et al., 2017). Especially in the field of nature conservation, palaeoecologists have long called for the addition of long-term or pre-historical (observed beyond modern science) perspectives (Box 1; e.g. Birks, 1996, 2012, 2019a; Delcourt & Delcourt, 1998; Flessa & Jackson, 2005; Rull 2012, 2014; Vegas-Vilarrúbia et al., 2011; Willis & Birks, 2005). Perhaps this integration is more imminent than previously envisioned as palaeoecology has a strong macroecological character in terms of the taxonomic and temporal scale dealing with ecological patterns over periods ranging from decades to millions of years. In addition, the number of palaeoecological studies that cover large spatial scales has increased thanks to the substantial and expanding amount of open-access data (Williams et al. 2018). With the definition used for 'macroecology' (Box 1) –

large in at least one of the scale (taxonomic, temporal, or spatial), with a strong emphasis on statistical descriptions of ecological attributes and geographical patterns – we argue that palaeoecological research is essentially moving to be macroecological palaeoecology.

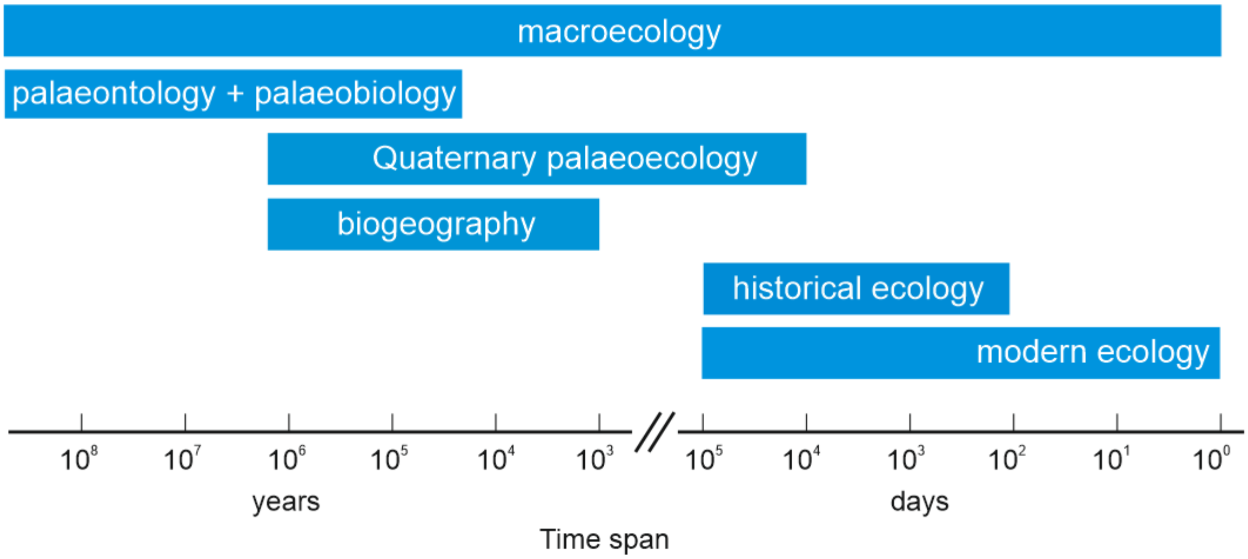

Figure 1 | Different ecology disciplines and their temporal time scales on which data are gathered and assessed. (Adapted from Rull, 2020).

THE ERA OF PALEO-DATA AVAILABILITY

Many broad-scale ecological patterns can now be assessed using an unprecedented quantity of palaeoecological data, covering the three dimensions of space, time, and taxonomy at the same time (Table 1). For example, the open-access database of Neotoma has a global coverage consisting of more than 5000 Quaternary pollen-stratigraphic datasets (Williams et al., 2018) providing an open source archive for a range of proxy data for any interdisciplinary user. In fact, palaeoecology has a long history of making data freely accessible (Table 1; Brewer et al., 2012; Goring et al., 2015) and easy sourcing of the database is now facilitated by web APIs and accompanying R packages (neotoma and neotoma2). However, critical challenges and pitfalls arise regarding the use of palaeodata when disciplines continue to work in parallel and separately (multidisciplinary research, see Fig. 2A) without knowing about typical pitfalls (cf. the ‘knowns’) within a given discipline.

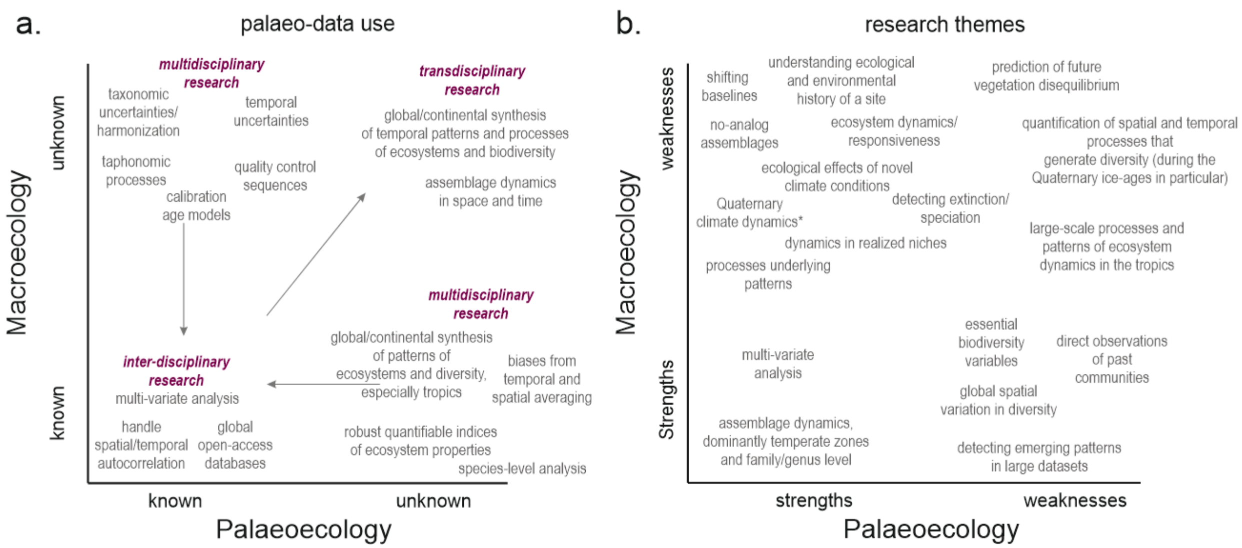

*Figure 2 | A holistic view of the opportunities and challenges in global-change ecology in a trans-disciplinary macro-palaeo world. a) In the use of palaeo-data and the analyses of large palaeoecological dataset compilations, there are known and unknown matters for both the fields of macroecology and palaeoecology. With the development of cross-discipline-friendly guidelines and open-science research in terms of methods and coding, the integration of macroecology and palaeoecology can move from doing 'multidisciplinary research' to 'interdisciplinary research', and more excitingly towards collaborating closely in 'transdisciplinary research' in global-change ecology. b) Achievable research themes are equally dependent on the degree of integration between the two fields in which it is pivotal to understand the strengths (knowns) and challenges (unknowns) of each field, and where opportunities are at hand to jointly address and circumvent these challenges to explore exciting new research grounds. Definitions: Multidisciplinary research: Researchers work in parallel or sequentially from a disciplinary-specific base to address common problems but in a separate manner (adjusted from Aagaard-Hansen, 2007). Interdisciplinary research: Researchers work jointly but still from disciplinary-specific bases to address common problems (Aagaard-Hansen, 2007). Transdisciplinary research: Researchers work jointly using a shared conceptual framework drawing together disciplinary-specific theories, concepts, and approaches to address common problems and research topics (adjusted from Aagaard-Hansen, 2007). Multidisciplinary isolation: The situation in which researchers from different disciplines use the same data and perhaps also target similar research questions but nevertheless work in isolation. This setting substantially increases the risk of being unaware of crucial background knowledge needed for proper data handling and analysis, which consequently jeopardises the robustness of the outcomes of analyses on these data. *Quaternary climate dynamics: refers here to "snapshot" research (Flantua et al. 2020) for hypothesis formulation and research themes highly focused on the present (interglacial period) while disregarding the dynamic past of the Quaternary in which >80% were glacial and cool interstadial conditions. The "extreme" snapshot at LGM is a poor representation for the rest of the Quaternary (Flantua et al. 2020)*

The use of palaeoecological data by users from other disciplines is hampered by its specialised terminology and multidimensional complexity at coarser temporal and taxonomic resolution compared to modern ecological data (Fig. 2; Birks, 2012; Blois, 2012; Rull, 2014). Handling such uncertainties is challenging but should not impede the wider use of palaeoecological data. A protocol or guide for the use of such data is however missing to date and this hampers integration with macroecology by inadequate use of the data (Wuest et al., 2020). The strongest and fastest integration between disciplines will be achieved from open-source software and data accompanied by 'cross-discipline-friendly guidelines', i.e. guidelines made specifically for users of any scientific background focused on clarifying concepts but also to guide the user to best practices with data specific recommendations. Any data user needs to know the specific 'knowns' in palaeoecology that are 'unknowns' outside the field (Fig. 2A) that will inevitably and critically affect analyses and conclusions if not accounted for (Blois, 2012; Brewer et al., 2012; Pardoe et al. 2021). Examples include: (i) dealing with taxonomic and temporal uncertainties in the palaeoecological record; (ii) the relevance of taphonomic processes related to depositional environments; and (iii) knowledge about criteria to identify the quality of the sampled sequences. In an attempt to fulfil such needs for fossil pollen sequences to be used for continental and global analyses, [For review: Authors anonymous] et al. (GEB, in review) present a stepwise guide to process and standardise data from public and private sources including a protocol for best practices and sets of inferences (related to the above mentioned issues) for appropriate data analyses. For other valuable palaeoecological proxies, such as diatoms and phytoliths, such guides are still missing but soon in high demand as more open-access databases become available (e.g. Benito et al. 2022).

Table 1: Past and present databases containing Quaternary fossil pollen data at historical to deep-time scales.

Database	**Time period**	**Region**	**Existence**	**Key papers**
ACER	Last glacial cycle (73-15 ka)	global	Part of publication, now in PANGAEA	Sánchez Goñi et al. 2017
African Pollen Database	1 Ma to present	Africa	Started in 1996 and developed independently.	Vincens et al. 2007; Ivory et al. 2020; Runge et al., 2021
Alpine Pollen Database	1 Ma to present	Eurasian	Developed in parallel to the EPD with open access sequences moved to the EPD, since 2019 constituent database of Neotoma	van der Knaap et al.. 2005.

Canadian Pollen Database	1 Ma to present		Started in the 1980s, many datasets became part of the North American Pollen Database and subsequently Neotoma	
Chinese Pollen Database	1 Ma to present		Private initiative, some sequences in Neotoma	Herzschuh et al., 2019
Cooperative Holocene Mapping Project (COHMAP)	Holocene		Started in the 70s and 80s and became the seed of the North American Pollen Database	COHMAP Members 1988, Wright et al. 1993
Deep-time Palynology Database	30 Ma – 10 Ma	Global, mostly South America	New constituent database inn Neotoma to host deep-time datasets	
East Asian fossil Pollen Database	1 Ma to present	East Asia	Private initiative	Cao et al. 2013 RPP; Cao et al. 2022
EMBSeCBIO pollen database	Holocene?	Eastern Mediterranean-Black Sea-Caspian-Corridor	Private initiative, https://researchdata.reading.ac.uk/309/	Marinova et al. 2017
European Pollen Database (EPD)	1 Ma to present		Started in 1989, since 2016 constituent database of Neotoma with data available through Neotoma since 2022	Fyfe et al. 2009, Giesecke et al. 2014
Global Pollen Database (GPD)			Developed out of a combination of pollen databases and became	Grimm et al. 2013

			the seed data for the development of Neotoma 2006	
Iberian Peninsula database	Holocene		Private initiative, https://researchdata.reading.ac.uk/369/	Harrison et al. 2022
Indo-Pacific Database	1 Ma to present		Initially part of the BIOME6000 project, currently in CABAH database and partly in Neotoma	
Japanese Pollen Database	1 Ma to present		Initially private initiative, now constituent database in Neotoma	Takahara et al. 2000
Latin American Pollen Database	1 Ma to present	Mexico, Central and South America	Started in 1994, did not develop its own storage facilities, but became part of the GPD and now a constituent database of Neotoma	Flantua et al. 2015
Neotoma		Global	Established in 2006, received the GPD and constituent databases over the course of the 2010s.	Williams et al., 2018 https://www.neotomadb.org/
North American Pollen Database	1 Ma to present		Started in 1990, part of the GPD and thus Neotoma	
Paleobiology database	10 Ma to 100 kyr		Started in 1998 in the Phanerozoic Marine Paleofaunal Database initiative (1998-2000) and further expanded with additional funding in the following years	https://paleobiodb.org; http://www.pbdb.org/
PANGAEA	1 Ma to present	Global	Partial overlap with Neotoma	Diepenbroek, 2018
Pollen Database for the Russian Far East (PDSRFE)			Started in 1995, then part of the GPD, and now in Neotoma. Will be supervised by EPD in the future.	Bartlein & Webb, 2021

Siberia (Northern Asian) fossil pollen database	Last 40 kyr		Available at https://doi.pangaea.de/10.1594/PANGAEA.898616	Cao et al. 2020.

A potential knowledge gap, leading to misunderstandings, in the use of palaeoecological data from a macroecological perspective is the interpretation of the observed palaeoecological community (Fig. 2B). Fossil assemblages are indirect observations of the actual past plant community, where biases exist in the representation of taxa from temporal and spatial averaging (Bush, 1995 ; Cleal et al. 2021; Pardoe et al. 2021). For example, the source area of an observed pollen assemblage can be quite large (e.g. medium-sized lakes of 100–200 km^2 with a substantial basin size from where pollen are captured), and it is therefore necessary to find ways to handle false absences (i.e. some pollen taxa are not well preserved, or plants produce very little pollen) and false presences (i.e. well-preserved taxa, well distributed and can come from far distances which does not imply their presence at the study site). As a result, observations based on fossil data cannot be directly compared with modern ecological studies (e.g. Bush 1995; Giesecke et al. 2017). Recent reviews by Cleal et al. (2021) and Pardoe et al. (2021), however, provide valuable overviews of the strengths and weaknesses of existing measures of taxonomic diversity from palaeo-data. A key and still open question in global-change ecology pushed by transdisciplinary research is how to develop measures for diversity that can link both the past and present observations (e.g. essential biodiversity variables derived from palaeoecological data), and better predict the future changes?

METHODOLOGICAL APPROACHES AND NUMERICAL ANALYSIS

Macroecology and palaeoecology share many numerical methods developed in community ecology to handle species composition data, e.g. to quantify similarity and/or dissimilarity of different species/taxa assemblages or to present various summaries of sample properties such as the number of taxa and their relative abundances (diversity estimation). Both disciplines have adopted multivariate methods such as ordinations and classification approaches (Fig. 2A, known-knowns), although multivariate analysis circumventing the temporal and taxonomic uncertainties in palaeoecological data is still a major challenge (Birks, 2019a; Cleal et al. 2021; Huntley, 1996; Pardoe et al. 2021; Rull, 2014). Multivariate methods are essential to compare assemblages of taxa in different vegetation and biomes, and along environmental gradients (e.g. climate, elevation, latitude, etc) to detect patterns and trends that can be explained ecologically. Also, just as spatial autocorrelation is a key factor to consider in macroecological studies (e.g. Legendre & Legendre, 2012, Kissling & Carl et al. 2007; Dormann et al. 2007) likewise the stratigraphical order needs to be considered in palaeoecological studies (e.g. Gordon & Birks, 1972; Fig. 2A).

Palaeoecological inferences are based on our mechanistic understanding of natural processes deduced from modern and macroecological studies, and present-day distributions are used to understand and reconstruct the past (hindcasting from present-day calibration). A popular example is the ‘biomisation technique’ in which fossil pollen or macrofossil data are assigned to plant functional types and biomes based on knowledge of the present, which are then used to reconstruct biomes in the past (Prentice et al., 1996; see schematic figure 2 in Marchant et al., 2001). In palaeoecology, this has been very common due to difficulties in obtaining direct environmental data (e.g. temperature) to model past biome distributions. Such approaches have even been adapted for macroecological research. For instance, weighted-average partial least squares regression (WA-PLS) is an approach that was initially developed to reconstruct environmental conditions from fossil pollen assemblages (Birks, 1994; Birks et al., 1990; ter Braak & Juggins, 1993; ter Braak et al., 1993), and has now been adapted and implemented for modern-day datasets covering decades (e.g. Bertrand et al. 2011, Bhatta et al. 2018). On the other hand, macroecological approaches could be applied to palaeoecological data to reconstruct climatic conditions, such as the use of the community temperature index to assess thermophilisation rates. Indeed, many macroecological studies have replaced the WA-PLS approach with a Species Temperature Index approach (STI, popularised by studies such as Devictor et al. 2012) to compute community weighted mean values based on species optima estimated from an independent data set. This exemplifies how, between macroecology and palaeoecology, there is a great potential for assimilating, adjusting, and combining approaches for advanced transdisciplinary analysis (Fig. 2A), and thus for tackling long-identified, urgent research questions that have been hindered until now by scale, data complexity, and a lack of a common language (Rapacciuolo & Blois, 2019. This methodological interchange between disciplines we call ‘methodological recycling’ which is the implementation, integration, and adaptation of methodologies from other disciplines to different sets of data than those they were initially developed for but similar in nature.

Building bridges between macroecology and palaeoecology for transdisciplinary research involves not only understanding and acknowledging the limitations of data but also finding ways to target exciting, achievable questions at hand. For instance, studying macroecological responses at the species level is essential for many questions related to how species and ecosystems respond to environmental change in different parts of the world (e.g. Antao et al. 2020; Lenoir et al. 2020; Vellend et al. 2012). However, macroecologists focusing on species-level research questions with palaeoecological data will likely be quickly disappointed by the taxonomic uncertainties surrounding such data. Although species-level analysis of range-shifts dynamics, for instance, has been performed in numerous palaeoecological studies (e.g. Giesecke et al. 2017), the number of species for which similar spatio-temporal analyses can be carried out is limited.

New research in functional palaeoecology (Brussel and Brewer, 2021) is now targeting the large databases of functional traits (the TRY plant trait database, Kattge et al. 2020; the Global Biodiversity Information Facility, https://www.gbif.org/; BiolFlor, Kühn et al. 2004). Initially assembled for macroecological purposes, studies to assess temporal changes in plant trait composition and functional responses are now rapidly increasing (e.g. Brussel & Brewer, 2021; Fyfe et al. 2010; Van der Sande 2019). Innovative approaches to tackle taxonomic differences and obtain meaningful assemblage-weighted values are needed (see Veeken et al. 2022 using Bayesian modelling), while considerable care should be taken in the interpretation of these pollen-derived proxies (Birks, 2020; Van der Sande 2019). However, undoubtedly, the exciting questions ahead in a transdisciplinary macro-palaeo world are those implemented at the assemblage level after taxonomic and temporal uncertainties are properly dealt with (Fig. 2A, [For review: Authors anonymous] (GEB, in review); Rapacciuolo & Blois, 2019; Veeken et al. 2022).

BRIDGING SCALES FOR TRANSDISCIPLINARY RESEARCH

Initially, macroecological research focused on describing emerging spatial patterns supported by correlative methods at broader spatial scales (Blackburn & Gaston, 2006), but then it expanded to sourcing increasingly larger datasets and using more advanced methods to assess patterns across space and time (Smith et al., 2008). However, the call to strengthen its mechanistic understanding of correlative processes behind the patterns has been echoed widely and for decades (Fig. 2B; Brown, 1999; Beck et al., 2012; Wuest et al., 2020). The main argument is that macroecology needs to strengthen its capacity to demonstrate cause and effect (Kerr et al., 2007), not only by correlative means but also by the integration of processes into hypotheses and models (Cabral et al., 2017; Wuest et al., 2020). One of the issues for macroecological research when inferring processes from contemporary data is that assemblages and observed metrics are always dependent on past conditions (e.g. range or migration lags, priority effects, critical thresholds, cascading effects, disequilibrium dynamics). The only way to integrate these past drivers is via palaeoecological knowledge and data, and develop solid approaches to assess temporal processes by means of time series (Detto et al. 2012; Sugihara et al. 2012).

Palaeoecology, on the other hand, has a strong process-based emphasis wherein temporal patterns are assessed by explicit consideration of the local, ecological processes that contributed to the observed changes (Birks, 2013b). Such thinking can enrich macroecological models looking into demographic, spatial, and biotic and abiotic drivers and processes by: (i) jointly formulating testable predictions and hypotheses; (ii) aiding in the selection of relevant variables and parameters in models; and (iii) helping the interpretation and/or validation of model outputs. Palaeoecology can, vice versa, benefit from the strong quantitative modelling approaches embedded in macroecology (see section V.) and the traditions of merging data over broad spatial scales to achieve a holistic understanding of global-change ecology (Fig. 2B).

Niche space and “adaptation”

How macroecologists and palaeoecologists understand niche space in relation to adaptation, speciation, and extinctions is of fundamental importance for the integration of these research fields. The environmental conditions of the niche space and corresponding range size of any species are bound by their geographical settings and these conditions vary geographically. Differences in temperature, precipitation, and partial pressure of CO_2 (pCO_2) partition the niche space between taxa at high and low latitudes and elevations, for instance. A climatic niche (macro- and micro-climate) of a genus or clade may be viewed as a genetically coded tolerance to, for instance, high temperature and low water-balance. Each species in the same clade (or genus) will therefore share to a considerable extent an adaptive trait with other species from the same clade (or genus) (Fig. 3 A,B). This is related to phylogenetic niche conservatism (Hawkins et al. 2005; Vetaas et al. 2018) where the underpinning assumption is that species within a phylogenetic clade inherit certain niche properties from sister species (Araujo et al., 2013; Hawkins et al., 2014).

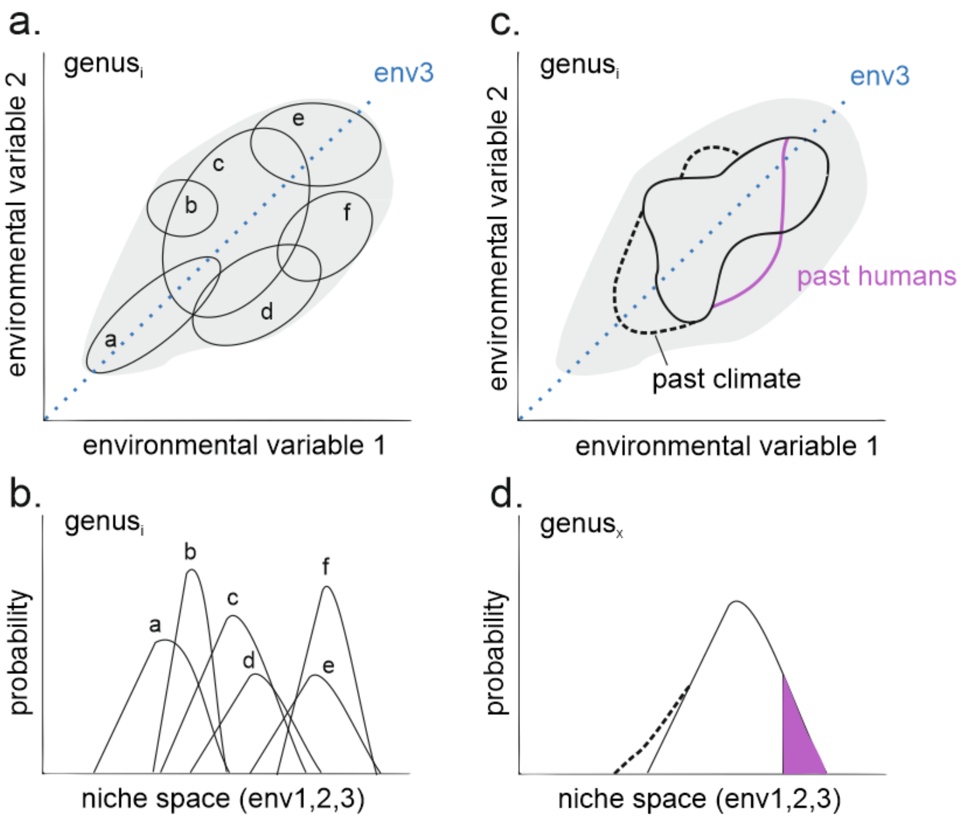

Figure 3 | Phylogenetic niche conservatism and influences by climate and humans. a) Different taxa (a-f) jointly make up the genus-level niche space with (b) overlapping and unique niche space. c) Genus-level niche space is likely to have been slightly different in the past under different climatic conditions (dashed) while humans (purple line) often cause (d) current niche space to appear smaller than potentially available.

Palaeoecological data can give valuable insights into the degree and magnitude of niche construction by humans related to the habitat reduction or destruction, translocations (introductions), and extinctions and extirpations, among others (Bolvin et al., 2016; Grace et al., 2019). Species' ranges could have been reduced over time due to human influence (Fig. 3 C,D), causing a mismatch between the present-day range and environmental conditions shaping the original range size and thus the original niche space occupied by species. This provides strong evidence that temporal snapshots of models based on the present alone are not necessarily able to predict reliably the range size dynamics and quantify the fundamental niche and adaptability of species (see Jackson & Overpeck, 1990).

Ecological niche models (ENMs) coupled with the high spatial and temporal resolution of large palaeoecological databases seems like a very promising way to identify how individual species and/or their ranges as well as different aspects of diversity changed through time (see for instance Darroch and Saupe, 2018; Macias-Fauria & Willis, 2013; Pardoe et al. 2021; Poli et al. 2022; Villalobos et al. 2015). However, the existence of truncated niches (fundamental niches that extend beyond the limit of current climatic conditions; Feeley & Silman, 2010), no-analogue assemblages, and human impact on niche space have significant consequences for ENMs or species distribution models (SDM) as used abundantly in macroecological, phylogeographical, and biogeographical studies (Nogués-Bravo, 2009). These factors undermine the usefulness of these models trained under contemporary conditions for palaeoclimate hindcasting or future predictions (Collevatti et al., 2013; Fitzpatrick et al., 2018; Ordonez & Williams, 2013; Reitalu et al. Roberts & Hamann, 2011; Santini et al. 2021). Ignoring such palaeoecological input for macroecological models, that is, ignoring that truncated niches may exist, inevitably leads to the overestimated prediction of substantial range-size contractions and extinctions during this century of climate change (Feeley & Silman, 2010; Sax et al., 2013; Veloz et al., 2012). Therefore, we support the use of multi-temporal models (Nogues-Bravo et al., 2006) that cover the complete distribution range of taxa through time (Barbet-Massin et al., 2010; Maiorano et al., 2013; Darroch et al., 2022), and we join the urgent call for critical consideration and calibration of ENM and SDM outputs of past and future distributions based on modern niche space alone. Though hurdles need to be passed to confidently use fossil pollen data in validating ENM and SDM (i.e. handle taxonomic and temporal uncertainties, effect of taphonomic and dispersal processes; Cleal et al. 2021), these records are the best available direct evidence we have of vegetation dynamics through time. Again, palaeocologists will need to provide the means and guidelines to handle such noise in palaeo-data to consequently be a valuable source of model validation in interdisciplinary research.

Related to niche space and adaptability, we identify a mixed-use of the terminology ‘adaptation’ within the different disciplinary discourses for which we clarify usage here (see also Cheplick (2020). Varying meanings of the same terms can pose a serious hurdle to advance inter- and transdisciplinary research (Aagaard-Hasen, 2007). There exists a loose usage of the word ‘adaptation’ in the ecological literature in such a way that under conditions of environmental change, it is commonly stated that plants ‘adapt’ their niche space and here phenotypic plasticity is commonly referred to as ‘adaptation’. However, palaeoecologists assume that plants are going to make use of the unfilled niche space or tolerance niche that is available (Fig. 3) supported by research offering insights into the temporal variation in realized niche space (e.g. Jackson & Williams, 2004; Veloz et al., 2012). Here phenotypic plasticity is considered a genetically inherited adaptability that requires little to no adaptation in an evolutionary sense. If we would accept that in an evolutionary sense plants can ‘adapt’ easily to new environmental conditions, the modern niche would fail to be a reliable reference for any model of deep-time reconstruction, and the foundations of disciplines such as palaeoecology, geology, palaeoceanography, and palaeolimnology would crumble. The concepts of realized vs fundamental niche is certainly a well-known concept in macroecology but palaeoecology has the advantage of being able to study the temporal variations in realized niches through time. Therefore, for consistency in terminology, we suggest avoiding the undefined use of ‘adaption’ but specifying either the evolutionary meaning defined by ‘adaptive evolution’ or ‘evolutionary adaptation’ or ‘phenotypic adaptation’ through phenotypic variation and without mutation (Ho & Zhang, 2018).

No-analogue assemblages and climate

For over nine decades, palaeoecology has been engaged in understanding climate tracking (i.e. range shifts and expansions) of plants in the light of climate variability (i.e. the glacial-interglacial fluctuations). With the increased availability of modern and fossil pollen datasets, research in the Northern Hemisphere moved forward in two parallel developments namely (i) the spatial mapping of taxa (e.g. Huntley & Birks, 1983; Thompson, 1988; Webb, 1988; von Post, 1924) and (ii) the numerical matching of fossil and modern pollen assemblages using multivariate distance metrics (‘analogue technique’; Birks & Gordon, 1985; Overpeck et al., 1985; Huntley, 1990).

With the help of increasing data availability and the development of the analogue technique, important insights have been derived into past assemblage dynamics (Jackson & Williams, 2004). First, late Quaternary map sequences for European and North American pollen taxa detect substantial differences in the timing, magnitude, and direction of taxa responses to climate change (Huntley & Birks, 1983; Williams et al., 2004; Birks, 2019a; Giesecke et al. 2017; Giesecke & Brewer, 2018; Brewer et al., 2017). Second, through the combined use of fossil pollen data with climate simulations, several studies provide evidence that many taxa in North America occupied distinct realised niches in the past – today only being a subset (Fig. 3) – in comparison to the present while other taxa have remained relatively stable (Jackson & Overpeck, 2000; Veloz et al., 2012; Maiorano et al., 2013; Ordonez, 2013). In addition, Williams & Webb (2001) show the existence of no-analogue climates (North America) that closely mirror no-analogue pollen assemblages in terms of timing, magnitude, and location. As novel (no-analogue to present) combinations of climatic variables existed in the past and are predicted to emerge in the future (Williams & Jackson, 2007), the correlation structure among these variables is also likely to change over this century as it has in the past (Jackson et al., 2009; Jackson & Williams, 2004). This could mean that WA-PLS approaches in palaeoecology and macroecology might be less reliable than alternative methods based on species-specific indicator values for community weighted means, but more research is needed to compare such approaches in different parts of the world.

The advent of accessible climate simulation models covering different periods over the last 21 ka (e.g. Osman et al., 2021) aided the question of whether past no-analogue assemblages were the consequence of range-shift dynamics that were out of pace with climate (i.e. still catching up with shifting climate) or whether they represented an equally foreign climate not experienced today. Therefore, the combined use of fossil pollen databases with palaeoclimate simulations pushes hypothesis testing on range-shift dynamics to a new level and provides a relatively recent overlapping field between macroecology and palaeoecology (see for instance Poli et al., 2022). The development of a multivariate analogue technique in palaeoecology has been complemented by the concept of ‘climate-change velocity’ (Loarie et al., 2009) as a measure to compare the velocity of biotic responses, reflected in range-size changes detected by fossil pollen data, to the spatial rate of climate change. Follow-up papers with a palaeoecological background now include a combined approach to late-glacial times in North America (Ordonez, 2013; Ordonez & Williams, 2013) and Europe (Svenning & Sandel, 2013). The approach captures the essence of future nature conservation by predicting the likely magnitude of vegetation disequilibrium with a no-analogue climate (Birks, 2019a; Fitzpatrick et al., 2017; Ohlemüller et al., 2006; Svenning & Sandel, 2013; Trisos et al. 2020 ; Willis & Birks, 2005).

Speciation

Although speciation cannot be inferred from pollen morphology – as it is famously known for its high morphological conservatism (Matamoro-Vidal et al., 2015; Reitalu et al., 2015) – palaeoecology can offer hints on events of speciation and evolutionary adaptation by the following:

i. First appearance of a new species: As a species becomes sufficiently abundant and prevalent to become fossilised, palaeoecological records can detect such ecological success and provide a potential benchmark for constraining phylogenetic trees (e.g. Sauquet et al., 2009; Thronhill et al., 2012) or the timing of the uplift of mountain ranges (e.g. Kirschner & Hoorn, 2020; Hoorn et al., 2017), for instance. Note, however, that the first appearance of a taxon can be the result of either range-size dynamics or evolutionary adaptation.

ii. Confirmed presence of taxon/genus in a different habitat space (e.g. biome or elevation): Examples of evolutionary adaptation at the genus level and from palaeoecological records are rare but illustrative. Especially long fossil pollen records that overlap with evolutionary and geological time scales provide such key insights (see global overview of long fossil pollen records by Hooghiemstra et al., 2022). An example is the neotropical Borreria, which was originally an element of lowland savannah. A long Andean pollen record covering most of the Pleistocene (2550 m asl; Funza09, Colombia) shows the appearance of Borreria at 2.02 Ma within an open-structured forest and later also within closed forest (1.58 Ma; Hooghiemstra, 1984; Torres et al., 2013). This long-term trend might be taken as ‘adaptation’ in the evolutionary sense and a case where phenotypic plasticity became ‘fixed’ into genetic adaptation (Price et al., 2003). Alternative hypotheses are that the genus has a very broad fundamental niche (as many Northern Hemisphere tree species appear to have) or that different species are involved at 2.02 and 1.58 Ma.

iii. Palaeoenvironmental conditioning of recent evolutionary radiations: Climatic variability is among the abiotic variables that drive increased rates of speciation (evolutionary radiations; Nürk et al., 2019). However, it is still widely debated if either environmental dynamics or stability explains the geographical distribution of biodiversity hotspots (e.g. Dynesius & Jansson, 2000; Fordham et al., 2019). Long, continuous fossil pollen records can provide insights into the degree of environmental variability or stability over Quaternary time scales. For instance, the reconstruction of range-size dynamics in alpine ecosystems based on such long records revealed a highly dynamics environment in tropical mountains that likely were the underlying forces through time to set the stage for hyperdiverse regions (alpine páramo flora in the Andes; Flantua et al., 2019).

Extinctions

Building species niches through time can help us understand under which circumstances extinction results from the disappearance of environmental characteristics matching a species' fundamental niche (environmental effect). Circumstances include (i) a too rapid shift in the spatial availability representation of the fundamental niche (dispersal or adaptation lags); (ii) a decline in the realised niche (biotic interactions by migration or evolution of enemies); (iii) a shift in the species characteristics (overspecialisation); (iv) failure in developing polyploids which is a mechanism to overcome damaged gene sets in high mountain taxa in particular where UV radiation is high (see for instance Kirchheimer et al. 2016).

Total extinction, that is, the loss of a species from Earth that was previously present, is inherently difficult to quantify as it requires both a sufficiently long time series and global occurrence records. As processes leading to total extinction under natural conditions can only be understood when macroecological and palaeoecological data are combined, our knowledge on extinctions as well as their frequency in Earth history is limited (Conde et al., 2019). For instance, there appears to be only two documented cases of total extinction of plants by natural causes in the Quaternary (Aracites interglacialis; Mamakowa & Velichkevich, 1993; Birks, 2019a; Picea critchfieldii; Jackson & Weng, 1999), with none so far in the tropics (Bush & Mosblech, 2012; Torres et al., 2013) though the latter could be related to the high species diversity not identified pollen at species level. Even though the coarse taxonomic resolution of palaeoecological data would miss a certain number of possible extinctions, numbers of documented extinctions in palaeoecology under substantial climate change periods are orders of magnitude lower from those predicted by macroecological models based on the present towards the future (Birks 2019a; Willis & MacDonald, 2011). With very few exceptions, global extinction should be preceded by a decline in abundance in many local sites ultimately culminating in the global disappearance of a taxon. Extinction risk can only emerge with a macroecological, global perspective, while understanding the causes underlying the extinction process is impossible without a palaeoecological time-series that captures the preceding population dynamics.

A challenging aspect of extinction processes is the inherent problem of detection. Extinctions are hard to quantify because they are mainly associated with rare species in the first place, or taxa that have become rare due to a geographically widespread ecological trend towards local population extinction. Therefore, a key challenge is to assess how we can extrapolate from dynamics observed in common species to the dynamics of rare species and thus undetected extinctions. This is a problem as regions that support large numbers of rare species (such as islands or mountains) are often small and temporally ephemeral. However, macroecology could provide mechanistic models to describe macroevolution including speciation and extinctions to bridge these issues (Maurer, 1999; Velasco & Pinto-Ledezma, 2018; Rangel et al. 2018). Complementary to that, palaeoecological data can indicate taxon senescence, which links extinction risk to a taxon's age and is in fundamental contrast to the Red Queen hypothesis that states that the probability of a taxon going extinct is independent of its age (Raia et al., 2016; Žliobaitė et al., 2017). The 'bad luck of bad genes' question is thus fundamental not only in linking macroecology and palaeoecology, but also in integrating the interaction between macro-and microevolution by combining time series of species' traits and distributions on macroecological scales.

CONCLUSIONS AND PERSPECTIVES FOR GLOBAL-CHANGE ECOLOGY

Here, we discuss the advantages of combining macroecology and palaeoecology in terms of global-change ecology, and the sharing of data and approaches while discussing the strengths and challenges ahead in doing so. We elaborate on key topics in both disciplines, such as the niche concept and the meaning of adaptation, no-analogue climates and assemblages, speciation, and extinctions. We summarise both disciplines and evaluate their position with regard to other fields of research, and evaluate key prospects for the integration of these disciplines and the transdisciplinary opportunities in a macro-palaeoecological integration.

With regard to macroecology, palaeoecology can contribute with cross-discipline-friendly guidelines and its strong understanding of the influence of deep-time events on present-day biodiversity and the mechanisms of ecological processes through time; features that have been called for to strengthen the field of macroecology. The palaeoecological community has offered ample opportunities to reach out to the broader ecology community in terms of research questions (e.g. Birks, 1996; 2012; 2019a; Seddon et al. 2014), and statistical techniques (e.g. Birks & Gordon, 1985; Birks, 2013a). In addition, there has been the rise of 'spin-off' fields such as conservation palaeobiology (Willis & Birks, 2005; Barnosky et al., 2017) in both terrestrial (Birks, 2012 and references therein; Dietl & Flessa, 2011) and marine ecosystems (e.g. O'Dea et al., 2017; Yasuhara et al., 2012).

Regarding palaeoecology, macroecology can contribute with its strong understanding of handling large datasets across broad spatial scales and innovative advances in numerical ecology and statistical analyses of large and complex data on species assemblages. Especially the versatile and now increasingly common use in macroecology of sophisticated methods for statistical inference such as Bayesian networks, Markov networks, generalised additive mixed models (GAMMs) and generalized linear mixed-effects models (GLMs and GLMMs) or hierarchical models could be trailblazing approaches for innovative research in palaeoecology. Macroecology is also moving forward with structural equation modelling (SEMs) approaches which are additional powerful tools to assess causes and effects in model predictions (Grace et al. 2010). In a transdisciplinary macro-palaeo world, modelling techniques like GLMMs, GLMs, GAMs and especially SEMs could become the recommended approaches to use, especially when extrapolating outside the range of calibration values and dealing with transdisciplinary research (Fan et al. 2016; Smith et al. 2014).

Palaeoecology and macroecology together can play a key role in advancing global-change research with the increase of open-access data globally (e.g. sPlotOpen, Bruelheide et al. 2019; Sabatini et al. 2021; Neotoma, Williams et al. 2018), but here we point to an important aspect that requires attention in any continental and global syntheses. Our understanding and assumptions of modern and Quaternary vegetation patterns are mostly based on Northern Hemispheric patterns, and there is little support at present that such findings can be extrapolated readily to the tropics (Huntley & Webb, 1988; Lenoir et al. 2020; Ritchie 1985; Rull, 2020). Southern Hemisphere regional or continental syntheses are hampered by the lack of open-access datasets to a similar extent as the Northern Hemisphere (but see Carrillo-Bastos et al., 2012; Flantua et al., 2007; Marchant et al., 2018; Rull & Montoya, 2014; Runge et al. 2021; Smith & Mayle, 2017). In addition, insights into climate-driven vegetation migration or turnover since glacial times are hindered by the current lack of tropical records that go back to the LGM (Flantua et al., 2015: Mottl & Flantua et al 2021). However, re-established data mobilisation efforts are now underway for different tropical regions (e.g. Lézine et al. 2021), so opportunities will soon arise to develop inter-hemispheric and cross-tropical hypotheses.

A key aspect to reduce the research gap between the Northern and Southern Hemisphere is the sharing of analytical tools and the publishing of methodology papers accompanied by detailed explanations of the data-processing steps and analytical procedures with software source code (e.g. R, Julia, Python; Rapacciuolo & Blois, 2019; Wolkovich et al., 2012). To lessen this gap, individual scientists should actively participate and contribute to practical ways to decrease barriers (Rapacciuolo & Blois, 2019) to truly support global research – perhaps those from the Global North even more so (Maas et al., 2021). Although 'palaeoecoinformatics' has been around for a few decades now (Brewer et al., 2012; Goring et al., 2015), the more open-access character in macroecological research of publishing codes for multivariate analyses can positively influence palaeoecological research. The recent movement to increase the visibility and development of research software in R (R-universe system and rOpenSci) could serve as valuable platforms to launch community-driven packages dedicated to providing standardised and reproducible processing of palaeoecological data (see for instance the frameworks and R-packages by Blarquez et al. 2014 and [For review: Authors anonymous] (GEB, in review) to process and standardize sedimentary charcoal and fossil pollen records, respectively).

We hope that the reader can now appreciate the significant added value of integrating macroecology into palaeoecology and vice versa, the vast opportunities in methodological recycling, and the valuable place that this integration takes in the overarching field of ecology. Will macroecology bridge the gap between modern ecology and palaeoecology that many have been advocating for? Will paleoecology contribute to the adequate use of palaeoecological data by cross-discipline-friendly guidelines and welcome the implementation of new approaches to data to tackle new fields in global-change ecology? Perhaps we are heralding an integration between macroecology and Quaternary palaeoecology that will be the starting point for ecologists in general to appreciate the vast opportunities lying ahead to integrate philosophies, data, and methods to answer critical questions in global-change ecology.

BOX 1

Macroecology | Macroecology operates at broad taxonomic, spatial, and/or temporal scales (Kerr et al., 2007; Smith et al., 2008; McGill, 2019). Macroecology navigates between biogeography, palaeoecology/palaeobiology, and macroevolution with its strong statistical approach and search for emergent patterns across space and time, incorporating data from all time scales (Fig. 1), from modern ecology (hours, days, decades, e.g. Fisher et al., 2010; Lembrechts et al. 2022 Glob Chang Bio) through historical ecology (centuries, millennia, e.g. Szabó 2014) to deep-time ecology (geological age; e.g. Butterfield, 2007). The concept of 'macroecology' was originally coined by Orians (1989), popularised by Brown and Maurer

(1989), and finally fully described in the synthetic book by Brown (1995). Initially, macroecology staged itself using correlative methods to describe spatial patterns, with little attention for the processes behind them. Through time, macroecology moved from being ‘geographical ecology’, with abundant use of maps showing concordance (Blackburn & Gaston, 2006), to statistical descriptions of ecological attributes and geographical patterns using stochastic simulations and mechanistic modelling (Villalobos & Rangel, 2014). Specifically, macroecology has benefitted from a few decades of increasing research to use stochastic simulation models and test biodiversity patterns across space and time (Smith et al., 2008). The position of macroecology relative to other more specific disciplines or subfields of ecology became further defined and redefined – and often questioned – through time, such as in comparison to biogeography (Blackburn & Gaston, 2002; Kent, 2005, 2007) and global change biology (Kerr et al., 2007). Advocates of macroecology never shied away from positioning this field amidst biogeography, palaeoecology, palaeobiology, palaeontology, macroevolution, global change biology, and community ecology, postulating that the top-down statistical approach of macroecology unified all (Maurer, 2000; Nee, 2002; Kent, 2005).

Palaeoecology of past vegetation | Botanical palaeoecology has provided detailed information on the vegetation history of thousands of localities worldwide and has enhanced our understanding of local variation in climate, human impact, and other environmental drivers. Over the last c. 100 years, numerous cores and profiles have been studied globally for their palaeoecological proxies, which include fossil pollen, plant macrofossils, diatoms, and phytoliths, among many others (see recent reviews by Birks & Berglund, 2018 and Daniau et al., 2019). Initially, palaeoecology was used for temporal correlation between different sediment cores (similar deposited layers at different localities) and for relative dating, but paleoecology’s use diversified and deepened after the 1950s when the focus was more on botanical and ecological reconstructions of past vegetation around the world (Birks, 2005, 2019a). With the increasing number of fossil pollen sequences, studies focusing on making spatial reconstructions of vegetation changes through space and time became more attractive. Pioneering work on regional scales took place in Europe (von Post 1924, Safer 1935, Firbas 1949) even before the development of radiocarbon dating. Initial compilation of independently dated pollen diagrams were conducted in North America (e.g. Davis, 1976; Bernabo & Webb, 1977) and Europe (e.g. Huntley & Birks, 1983; Birks, 1989), and later on in the tropics (e.g. Flantua et al., 2007; Jago & Boyd, 2003) and the arctic (e.g. Brubaker et al., 2005). With a root in deep-time geological sciences, and later incorporating vegetation and ecological sciences, Quaternary palaeoecology (Fig. 1) has strong affinities to a range of different disciplines (Birks, 2012, and references therein) also welcoming cross-disciplinary approaches (Mayle & Iriarte, 2014; Rull, 2010, 2014). It has long ties with historical ecology, archaeology, and more recent approaches have been eager to strengthen bridges with biogeography, vegetation modelling, conservation biology, and restoration ecology, among others (Birks & Berglund, 2018).

Author contributions

SGAF, HJBB, and JAG conceived the ideas for this paper and the Macroecology & Palaeoecology workshop (Bergen, Norway, April 2019) where all authors participated (except

GHM). SGAF led the writing with section contributions by CT, GHM, HH, HJBB, JAG, MJS, and OM. All authors contributed critically to the drafts and gave final approval for publication.

Acknowledgments

SGAF, OM, VF, AWRS, HJBB, JAG acknowledge ERC Advanced Grant (no. 741413, Humans on Planet Earth (HOPE)) for financially supporting the workshop and HOPE work during 2018-2022. SGAF additionally acknowledges support from Trond Mohn Stiftelse (TMS) and University of Bergen for the startup grant 'TMS2022STG03'. GHM and MJS acknowledge Deutsche Forschungsgemeinschaft (DFG) grant STE 2360/2-1 as part of the Research Unit TERSANE (FOR 2332). We thank Cathy Jenks for her help with the workshop and text edits for this paper, and Kuber Bhatta and Alistair Seddon (UiB) for their contributions during the workshop.

References

Aagaard-Hansen, J. (2007). The challenges of cross-disciplinary research. Social Epistemology, 21(4), 425–438. https://doi.org/10.1080/02691720701746540

Anderson, P. M., Ložkin, A. V., & Severo-Vostočnyj Naučnyj Centr (Eds.). (2002). Late quaternary vegetation and climate of Siberia and the Russian Far East: (palylogical and radiocarbon database). NESC FEB RAS.

Barbet-Massin, M., Thuiller, W., & Jiguet, F. (2010). How much do we overestimate future local extinction rates when restricting the range of occurrence data in climate suitability models? Ecography, 33(5), 523 878–886. https://doi.org/10.1111/j.1600-0587.2010.06181.x

Barnosky, A. D., Hadly, E. A., Gonzalez, P., Head, J., Polly, P. D., … Zhang, Z. (2017). Merging paleobiology with conservation biology to guide the future of terrestrial ecosystems. Science, 355(6325). https://doi.org/10.1126/science.aah4787

Beck, J., Ballesteros-Mejia, L., Buchmann, C. M., Dengler, J., Fritz, S. A., … Dormann, C. F. (2012). What's on the horizon for macroecology? Ecography, 35(8), 673–683. https://doi.org/10.1111/j.1600-0587.2012.07364.x

Benito, X., Feitl, M., Carrevedo, M. L., Vélez, M. I., Escobar, J., … Fritz, S. C. (2022). Tropical South America Diatom Database: a tool for studying the macroecology of microorganisms. Diatom Research, 1–13. https://doi.org/10.1080/0269249X.2022.2078429

Bhatta, K. P., Birks, H. J. B., Grytnes, J.-A., & Vetaas, O. R. (2019). Weighted average regression and environmental calibration as a tool for quantifying climate-driven changes in vegetation. Journal of Plant Ecology, 12(3), 460–473. https://doi.org/10.1093/jpe/rty039

Birks, H. J. B. (1996). Contributions of Quaternary palaeoecology to nature conservation. Journal of Vegetation Science, 7(1), 89–98. https://doi.org/10.2307/3236420

Birks, H. J. B. (2012). Ecological palaeoecology and conservation biology: controversies, challenges, and compromises. International Journal of Biodiversity Science, Ecosystem Services & Management, 8(4), 292–304. https://doi.org/10.1080/21513732.2012.701667

Birks, H. J. B. (2019). Contributions of Quaternary botany to modern ecology and biogeography. Plant Ecology & Diversity, 12(3–4), 189–385. https://doi.org/10.1080/17550874.2019.1646831

Birks, H. J. B. (2020). Reflections on the Use of Ecological Attributes and Traits in Quaternary Botany. Frontiers in Ecology and Evolution, 8. https://www.frontiersin.org/article/10.3389/fevo.2020.00166

Birks, H. J. B., & Berglund, B. E. (2018). One hundred years of Quaternary pollen analysis 1916–2016. Vegetation History and Archaeobotany, 27(2), 271–309. https://doi.org/10.1007/s00334-017-0630-

Birks, H. J. B., & Gordon, A. D. (1985). Numerical Methods in Quaternary Pollen Analysis. Academic Press.

Birks, H. J. B., Heiri, O., Seppä, H., & Bjune, A. E. (2011). Strengths and weaknesses of quantitative climate reconstructions based on Late-Quaternary biological proxies [Application/pdf]. The Open Ecology Journal, 3, 68–110. https://doi.org/10.7892/BORIS.10005

Blackburn, T. M., & Gaston, K. J. (2002). Macroecology is distinct from biogeography. Nature, 418(6899), 723–723. https://doi.org/10.1038/418723b

Blackburn, T. M., & Gaston, K. J. (2006). There's more to macroecology than meets the eye. Global Ecology and Biogeography, 15(6), 537–540. https://doi.org/10.1111/j.1466-8238.2006.00276.x

Blarquez, O., Vannière, B., Marlon, J. R., Daniau, A.-L., Power, M. J., … Bartlein, P. J. (2014). Paleofire: An R package to analyse sedimentary charcoal records from the Global Charcoal Database to reconstruct past biomass burning. Computers & Geosciences, 72, 255–261. https://doi.org/10.1016/j.cageo.2014.07.020

Blois, J. L. (2012). update: Stemming "ignorance creep" in paleoecology and biogeography. Frontiers of Biogeography, 4(3). http://escholarship.org/uc/item/00c905kp

Boivin, N. L., Zeder, M. A., Fuller, D. Q., Crowther, A., Larson, G., … Petraglia, M. D. (2016). Ecological consequences of human niche construction: Examining long-term anthropogenic shaping of global species distributions. Proceedings of the National Academy of Sciences of the United States of America, 113(23), 6388–6396. https://doi.org/10.1073/pnas.1525200113

Brewer, S., Jackson, S. T., & Williams, J. W. (2012). Paleoecoinformatics: applying geohistorical data to ecological questions. Trends in Ecology & Evolution, 27(2), 104–112. https://doi.org/10.1016/j.tree.2011.09.009

Brook, B. W., & Alroy, J. (2017). Pattern, process, inference and prediction in extinction biology. Biology Letters, 13(1), 20160828. https://doi.org/10.1098/rsbl.2016.0828

Brown, J. H. (1995). Macroecology. University of Chicago Press. https://press.uchicago.edu/ucp/books/book/chicago/M/bo3632297.html

Brown, J. H. (1999). Macroecology: Progress and Prospect. Oikos, 87(1), 3–14. JSTOR. https://doi.org/10.2307/3546991

Brown, J. H., & Maurer, B. A. (1989). Macroecology: The division of food and space among species on continents. Science, 243(4895), 1145–1150. https://doi.org/10.1126/science.243.4895.1145

Brussel, T., & Brewer, S. C. (2021). Functional paleoecology and the pollen-plant functional trait linkage. Frontiers in Ecology and Evolution, 8. https://www.frontiersin.org/article/10.3389/fevo.2020.564609

Bush, M. B. (1995). Neotropical plant reproductive strategies and fossil pollen representation. The American Naturalist, 145(4), 594–609.

Bush, M. B., & Mosblech, N. A. S. (2012). Quaternary Tropical Plant Extinction: A Paleoecological Perspective from the Neotropics. In L. Hannah (Ed.), Saving a Million Species: Extinction Risk from Climate Change (pp. 199–214). Island Press/Center for Resource Economics. https://doi.org/10.5822/978-1-61091-182-5_12

Cabral, J. S., Valente, L., & Hartig, F. (2017). Mechanistic simulation models in macroecology and biogeography: state-of-art and prospects. Ecography, 40(2), 267–280. https://doi.org/10.1111/ecog.02480

Cheplick, G. P. (2020). The semantics of evolutionary adaptation: clarification and evaluation. Journal of Biological Education, 0(0), 1–14. https://doi.org/10.1080/00219266.2020.1739116

Cleal, C., Pardoe, H. S., Berry, C. M., Cascales-Miñana, B., Davis, B. A. S., … Uhl, D. (2021). Palaeobotanical experiences of plant diversity in deep time. 1: How well can we identify past plant diversity in the fossil record? Palaeogeography, Palaeoclimatology, Palaeoecology, 576, 110481. https://doi.org/10.1016/j.palaeo.2021.110481

COHMAP Members. (1988). Climatic Changes of the Last 18,000 Years: Observations and Model Simulations. Science, 241(4869), 1043–1052. https://doi.org/10.1126/science.241.4869.1043

Daniau, A.-L., Desprat, S., Aleman, J. C., Bremond, L., Davis, B., … Urrego, D. H. (2019). Terrestrial plant microfossils in palaeoenvironmental studies, pollen, microcharcoal and phytolith. Towards a comprehensive understanding of vegetation, fire and climate changes over the past one million years. Revue de Micropaléontologie, 63, 1–35. https://doi.org/10.1016/j.revmic.2019.02.001

Darroch, S. A. F., Saupe, E. E., Casey, M. M., & Jorge, M. L. S. P. (2022). Integrating geographic ranges across temporal scales. Trends in Ecology & Evolution. https://doi.org/10.1016/j.tree.2022.05.005

Delcourt, P. A., & Delcourt, H. R. (1998). Paleoecological insights on conservation of biodiversity: A focus on species, ecosystems, and landscapes. Ecological Applications, 8(4), 921–934. https://doi.org/10.1890/1051-0761(1998)008[0921:PIOCOB]2.0.CO;2

Devictor, V., Julliard, R., Couvet, D., & Jiguet, F. (2008). Birds are tracking climate warming, but not fast enough. Proceedings of the Royal Society B: Biological Sciences, 275(1652), 2743–2748. https://doi.org/10.1098/rspb.2008.0878

Dietl, G. P., & Flessa, K. W. (2011). Conservation paleobiology: putting the dead to work. Trends in Ecology & Evolution, 26(1), 30–37. https://doi.org/10.1016/j.tree.2010.09.010

Dynesius, M., & Jansson, R. (2000). Evolutionary consequences of changes in species' geographical distributions driven by Milankovitch climate oscillations. Proceedings of the National Academy of Sciences, 97(16), 9115–9120. https://doi.org/10.1073/pnas.97.16.9115

Egerton, F. N. (2013). History of ecological sciences, Part 47: Ernst Haeckel's Ecology. The Bulletin of the Ecological Society of America, 94(3), 222–244. https://doi.org/10.1890/0012-9623-94.3.222

Feeley, K. J., & Silman, M. R. (2010). Biotic attrition from tropical forests correcting for truncated temperature niches. Global Change Biology, 16(6), 1830–1836. https://doi.org/10.1111/j.1365- 620 2486.2009.02085.x

Fitzpatrick, M. C., Blois, J. L., Williams, J. W., Nieto‐Lugilde, D., Maguire, K. C., & Lorenz, D. J. (2018). How will climate novelty influence ecological forecasts? Using the Quaternary to assess future reliability. Global Change Biology, 24(8), 3575–3586. https://doi.org/10.1111/gcb.14138

Flantua, S. G. A., Hooghiemstra, H., Grimm, E. C., Behling, H., Bush, M. B., … Van Boxel, J. H. (2015). Updated site compilation of the Latin American Pollen Database. Review of Palaeobotany and Palynology, 223, 104–115. https://doi.org/10.1016/j.revpalbo.2015.09.008

Flantua, S. G. A., O'Dea, A., Onstein, R. E., Giraldo, C., & Hooghiemstra, H. (2019). The flickering connectivity system of the north Andean páramos. Journal of Biogeography, 46(8), 1808–1825 https://doi.org/10.1111/jbi.13607

Flantua, S. G. A., Payne, D., Borregaard, M. K., Beierkuhnlein, C., Steinbauer, M. J., … Field, R. (2020). Snapshot isolation and isolation history challenge the analogy between mountains and islands used to understand endemism. Global Ecology and Biogeography, 29(10), 1651–1673. https://doi.org/10.1111/geb.13155

Fordham, D. A., Brown, S. C., Wigley, T. M. L., & Rahbek, C. (2019). Cradles of diversity are unlikely relics of regional climate stability. Current Biology, 29(10), R356–R357. https://doi.org/10.1016/j.cub.2019.04.001

Fyfe, R. M., de Beaulieu, J.-L., Binney, H., Bradshaw, R. H. W., Brewer, S., … Tonkov, S. (2009). The European Pollen Database: past efforts and current activities. Vegetation History and Archaeobotany, 18(5), 417–424. https://doi.org/10.1007/s00334-009-0215-9

Gajewski, K. (2008). The Global Pollen Database in biogeographical and palaeoclimatic studies. Progress in Physical Geography: Earth and Environment, 32(4), 379–402. https://doi.org/10.1177/0309133308096029

Gaudreau, D., & Webb III, T. (1985). Late-Quaternary pollen stratigraphy and isochrone maps for the Northeastern United States. In V. M. Bryant & R. G. Holloway (Eds.), Pollen records of Late645 Quaternary North American sediments (pp. 247–280). American Association of Stratigraph Palynologists.

Giesecke, T., Brewer, S., Finsinger, W., Leydet, M., & Bradshaw, R. H. W. (2017). Patterns and dynamics of European vegetation change over the last 15,000 years. Journal of Biogeography, 44(7), 1441– 1456. https://doi.org/10.1111/jbi.12974

Giesecke, T., Davis, B., Brewer, S., Finsinger, W., Wolters, S., … Bradshaw, R. H. W. (2014). Towards mapping the late Quaternary vegetation change of Europe. Vegetation History and Archaeobotany, 23(1), 75–86. https://doi.org/10.1007/s00334-012-0390-y

Giesecke, T., Kuneš, P., Reitalu, T., & Editors, S. F. (2018). Millennial to centennial vegetation change. Journal of Vegetation Science, 29(3), 357–359. https://doi.org/10.1111/jvs.12650

Gordon, A. D., & Birks, H. J. B. (1974). Numerical methods in Quaternary palaeoecology. New Phytologist, 73(1), 221–249. https://doi.org/10.1111/j.1469-8137.1974.tb04621.x

Grace, J. B., Anderson, T. M., Olff, H., & Scheiner, S. M. (2010). On the specification of structural equation models for ecological systems. Ecological Monographs, 80(1), 67–87. https://doi.org/10.1890/09-659 0464.1

Grimm, E. C., Bradshaw, R. H. W., Flantua, S. G. A., Giesecke, T., Lézine, A.-M., … Williams, J. W. (2013). Databases and their application. In The Encyclopedia of Quaternary Science (pp. 831–838). Elsevier.

Harrison, S. P., Villegas-Diaz, R., Cruz-Silva, E., Gallagher, D., Kesner, D., … Paillard, J. (2022). The Reading Palaeofire Database: an expanded global resource to document changes in fire regimes from sedimentary charcoal records. Earth System Science Data, 14(3), 1109–1124. https://doi.org/10.5194/essd-14-1109-2022

Ho, W.-C., & Zhang, J. (2018). Evolutionary adaptations to new environments generally reverse plastic phenotypic changes. Nature Communications, 9(1), 350. https://doi.org/10.1038/s41467-017-669 02724-5

Hooghiemstra, H., Pérez, G. S., Torres Torres, V., Berrío, J.-C., Lourens, L., & Flantua, S. G. A. (2022). 60 years of scientific deep drilling in Colombia: the north Andean guide to the Quaternary. Scientific Drilling, 30, 1–15. https://doi.org/10.5194/sd-30-1-2022

Hoorn, C., Bogotá-A, G. R., Romero-Baez, M., Lammertsma, E. I., Flantua, S. G. A., … Chemale Jr, F. (2017). The Amazon at sea: Onset and stages of the Amazon River from a marine record, with special reference to Neogene plant turnover in the drainage basin. Global and Planetary Change, 153, 51–65. https://doi.org/10.1016/j.gloplacha.2017.02.005

Huntley, B. (1996). Quaternary palaeoecology and ecology. Quaternary Science Reviews, 15(5), 591–606. https://doi.org/10.1016/0277-3791(96)00015-7

Jackson, S. T. (2001). Integrating ecological dynamics across timescales: Real-time, Q-time, and deep-time. Palaios, 16(1), 1–2. https://doi.org/10.1669/0883-1351(2001)016<0001:IEDATR>2.0.CO;2

Jackson, S. T., & Overpeck, J. T. (2000). Responses of plant populations and communities to environmental changes of the late Quaternary. Paleobiology, 26, 194–220.

Jackson, S. T., & Weng, C. (1999). Late Quaternary extinction of a tree species in eastern North America. Proceedings of the National Academy of Sciences of the United States of America, 96(24), 13847–685 13852.

Jackson, S. T., & Williams, J. W. (2004). Modern analogs in Quaternary paleoecology: Here today, gone yesterday, gone tomorrow? Annual Review of Earth and Planetary Sciences, 32(1), 495–537. https://doi.org/10.1146/annurev.earth.32.101802.120435

Kattge, J., Bönisch, G., Díaz, S., Lavorel, S., Prentice, I. C., … Wirth, C. (2020). TRY plant trait database – enhanced coverage and open access. Global Change Biology, 26(1), 119–188. https://doi.org/10.1111/gcb.14904

Kent, M. (2005). Biogeography and macroecology. Progress in Physical Geography: Earth and Environment, 29(2), 256–264. https://doi.org/10.1191/0309133305pp447pr

Kerr, J. T., & Dobrowski, S. Z. (2013). Predicting the impacts of global change on species, communities and ecosystems: it takes time. Global Ecology and Biogeography, 22(3), 261–263. https://doi.org/10.1111/geb.12036

Kerr, J. T., Kharouba, H. M., & Currie, D. J. (2007). The Macroecological contribution to global change solutions. Science, 316(5831), 1581–1584. https://doi.org/10.1126/science.1133267

Kissling, W. D., & Carl, G. (2008). Spatial autocorrelation and the selection of simultaneous autoregressive models. Global Ecology and Biogeography, 17(1), 59–71.

Legendre, P., & Legendre, L. (2012). Numerical Ecology (3rd ed., Vol. 24). Elsevier. https://www.elsevier.com/books/numerical-ecology/legendre/978-0-444-53868-0

Lembrechts, J. J., van den Hoogen, J., Aalto, J., Ashcroft, M. B., De Frenne, P., … Lenoir, J. (2022). Global maps of soil temperature. Global Change Biology, 28(9), 3110–3144. https://doi.org/10.1111/gcb.16060

Lenoir, J., Bertrand, R., Comte, L., Bourgeaud, L., Hattab, T., … Grenouillet, G. (2020). Species better track climate warming in the oceans than on land. Nature Ecology & Evolution, 4(8), 1044–1059. https://doi.org/10.1038/s41559-020-1198-2

Lézine, A.-M., Ivory, S., Gosling, W., & Scott, L. (2022). The African Pollen Database (APD) and tracing environmental change: State of the Art. In Quaternary Vegetation Dynamics – The African Pollen Database (pp. 5–12). CRC Press. https://doi.org/10.1201/9781003162766-2

Loarie, S. R., Duffy, P. B., Hamilton, H., Asner, G. P., Field, C. B., & Ackerly, D. D. (2009). The velocity of climate change. Nature, 462(7276), 1052–1055. https://doi.org/10.1038/nature08649

Maas, B., Pakeman, R. J., Godet, L., Smith, L., Devictor, V., & Primack, R. (2021). Women and Global South strikingly underrepresented among top-publishing ecologists. Conservation Letters, n/a(n/a), e12797. https://doi.org/10.1111/conl.12797

Macias-Fauria, M., & Willis, K. J. (2013). Landscape planning for the future: using fossil records to independently validate bioclimatic envelope models for economically valuable tree species in Europe. Global Ecology and Biogeography, 22(3), 318–333. https://doi.org/10.1111/j.1466- 8238.2012.00781.x

Magurran, A. E., Baillie, S. R., Buckland, S. T., Dick, J. McP., Elston, D. A., … Watt, A. D. (2010). Long722 term datasets in biodiversity research and monitoring: assessing change in ecological communities through time. Trends in Ecology & Evolution, 25(10), 574–582. https://doi.org/10.1016/j.tree.2010.06.016

Mamakowa, K., & Velichkevich, F. (1993). Aracites interglacialis Wielicz. - extinct plant found in the floras of the Mazovian [Alexandria, Likhvinian] Interglacial in Poland , Belarus, Russia and the Ukraine. Environmental Science, 33, 321–341.

Marchant, R., Almeida, L., Behling, H., Berrio, J. C., Bush, M., … Salgado-Labouriau, M. L. (2002). Distribution and ecology of parent taxa of pollen lodged within the Latin American Pollen Database. Review of Palaeobotany and Palynology, 121(1), 1–75. https://doi.org/10.1016/S0034- 6667(02)00082-9

Marchant, R., Behling, H., Berrio, J. C., Cleef, A., Duivenvoorden, J., … Van der Hammen, T. (2001). Mid733 to Late-Holocene pollen-based biome reconstructions for Colombia. Quaternary Science Reviews, 20(12), 1289–1308.

Maurer, B. A. (2000). Macroecology and consilience. Global Ecology & Biogeography, 9, 275–280. Mayle, F. E., & Iriarte, J. (2014). Integrated palaeoecology and archaeology – a powerful approach for understanding pre-Columbian Amazonia. Journal of Archaeological Science, 51, 54–64. https://doi.org/10.1016/j.jas.2012.08.038

McCauley, D. J., Pinsky, M. L., Palumbi, S. R., Estes, J. A., Joyce, F. H., & Warner, R. R. (2015). Marine defaunation: Animal loss in the global ocean. Science, 347(6219), 1255641. https://doi.org/10.1126/science.1255641

McGill, B. J. (2019). The what, how and why of doing macroecology. Global Ecology and Biogeography, 28(1), 6–17. https://doi.org/10.1111/geb.12855

McGill, B. J., Dornelas, M., Gotelli, N. J., & Magurran, A. E. (2015). Fifteen forms of biodiversity trend in the Anthropocene. Trends in Ecology & Evolution, 30(2), 104–113. https://doi.org/10.1016/j.tree.2014.11.006

Mottl, O., Flantua, S. G. A., Bhatta, K. P., Felde, V. A., Giesecke, T., … Williams, J. W. (2021). Global acceleration in rates of vegetation change over the past 18,000 years. Science, 372(6544), 860–864. https://doi.org/10.1126/science.abg1685

Nogués‐Bravo, D. (2009). Predicting the past distribution of species climatic niches. Global Ecology and Biogeography, 18(5), 521–531. https://doi.org/10.1111/j.1466-8238.2009.00476.x

Nürk, N. M., Linder, H. P., Onstein, R. E., Larcombe, M. J., Hughes, C. E., … Pirie, M. D. (2020). Diversification in evolutionary arenas—Assessment and synthesis. Ecology and Evolution, 10(12), 6163–6182. https://doi.org/10.1002/ece3.6313

Odum, E. P., & Barrett, G. W. (2004). Fundamentals of Ecology (5th ed.). Thomson Brooks/Cole.

Ohlemüller, R., Gritti, E. S., Sykes, M. T., & Thomas, C. D. (2006). Towards European climate risk surfaces: the extent and distribution of analogous and non-analogous climates 1931–2100. Global Ecology and Biogeography, 15(4), 395–405. https://doi.org/10.1111/j.1466-822X.2006.00245.x

Ordonez, A., & Williams, J. W. (2013). Climatic and biotic velocities for woody taxa distributions over the last 16 000 years in eastern North America. Ecology Letters, 16(6), 773–781. https://doi.org/10.1111/ele.12110

Orians, G. H. (1980). Micro and macro in ecological theory. BioScience, 30(2), 79–79. https://doi.org/10.2307/1307908

Osman, M. B., Tierney, J. E., Zhu, J., Tardif, R., Hakim, G. J., … Poulsen, C. J. (2021). Globally resolved surface temperatures since the Last Glacial Maximum. Nature, 599(7884), 239–244. https://doi.org/10.1038/s41586-021-03984-4

Overpeck, J. T., Webb, T., & Prentice, I. C. (1985). Quantitative interpretation of fossil pollen spectra: Dissimilarity coefficients and the method of modern analogs. Quaternary Research, 23(1), 87–108. https://doi.org/10.1016/0033-5894(85)90074-2

Pardoe, H. S., Cleal, C. J., Berry, C. M., Cascales-Miñana, B., Davis, B. A. S., … Uhl, D. (2021). Palaeobotanical experiences of plant diversity in deep time. 2: How to measure and analyse past plant biodiversity. Palaeogeography, Palaeoclimatology, Palaeoecology, 580, 110618. https://doi.org/10.1016/j.palaeo.2021.110618

Poli, P., Guiller, A., & Lenoir, J. (2022). Coupling fossil records and traditional discrimination metrics to test how genetic information improves species distribution models of the European beech Fagus sylvatica. European Journal of Forest Research, 141(2), 253–265. https://doi.org/10.1007/s10342- 021-01437-1

Prentice, C., Guiot, J., Huntley, B., Jolly, D., & Cheddadi, R. (1996). Reconstructing biomes from palaeoecological data: a general method and its application to European pollen data at 0 and 6 ka. Climate Dynamics, 12(3), 185–194. https://doi.org/10.1007/BF00211617

Price, T. D., Qvarnström, A., & Irwin, D. E. (2003). The role of phenotypic plasticity in driving genetic evolution. Proceedings of the Royal Society B: Biological Sciences, 270(1523), 1433–1440. https://doi.org/10.1098/rspb.2003.2372

Rapacciuolo, G., & Blois, J. L. (2019). Understanding ecological change across large spatial, temporal and taxonomic scales: integrating data and methods in light of theory. Ecography, 42(7), 1247–1266. https://doi.org/10.1111/ecog.04616

Rull, V. (2010). Ecology and palaeoecology: Two approaches, one objective. The Open Ecology Journal, 3(2), 1–5. https://doi.org/10.2174/1874213001003020001

Rull, V. (2012a). Palaeobiodiversity and taxonomic resolution: linking past trends with present patterns. Journal of Biogeography, 39(6), 1005–1006. https://doi.org/10.1111/j.1365-2699.2012.02735.x

Rull, V. (2012b). Community ecology: diversity and dynamics over time. Community Ecology, 13(1), 102–2 116. https://doi.org/10.1556/ComEc.13.2012.1.13

Rull, V. (2014). Time continuum and true long-term ecology: from theory to practice. Frontiers in Ecology and Evolution, 2. https://doi.org/10.3389/fevo.2014.00075

Rull, V. (2020). Quaternary ecology, evolution, and biogeography (1st ed.). Elsevier. Santini, L., Benítez‐López, A., Maiorano, L., Čengić, M., & Huijbregts, M. A. J. (2021). Assessing the reliability of species distribution projections in climate change research. Diversity and Distributions, n/a(n/a). https://doi.org/10.1111/ddi.13252

Sax, D. F., Early, R., & Bellemare, J. (2013). Niche syndromes, species extinction risks, and management under climate change. Trends in Ecology & Evolution, 28(9), 517–523. https://doi.org/10.1016/j.tree.2013.05.010

Schrodt, F., Santos, M. J., Bailey, J. J., & Field, R. (2019). Challenges and opportunities for biogeography— What can we still learn from von Humboldt? Journal of Biogeography, 0(0). https://doi.org/10.1111/jbi.13616

Smith, F. A., Lyons, S. K., Morgan Ernest, S. K., & Brown, J. H. (2008). Macroecology: more than the division of food and space among species on continents. Progress in Physical Geography: Earth and Environment, 32(2), 115–138. https://doi.org/10.1177/0309133308094425

Svenning, J.-C., & Sandel, B. (2013). Disequilibrium vegetation dynamics under future climate change. American Journal of Botany, 100(7), 1266–1286. https://doi.org/10.3732/ajb.1200469

Szabó, P. (2015). Historical ecology: past, present and future. Biological Reviews of the Cambridge Philosophical Society, 90(4), 997–1014. https://doi.org/10.1111/brv.12141

Szafer, W. (1935). The significance of isopollen lines for the investigation of the geographical distribution of trees in the postglacial period. Polska Akad. Umiej.

Takahara, H., Sugita, S., Harrison, S. P., Miyoshi, N., Morita, Y., & Uchiyama, T. (2000). Pollen-based reconstructions of Japanese biomes at 0,6000 and 18,000 14C yr BP. Journal of Biogeography, 27(3), 665–683.

ter Braak, C. J. F., Juggins, S., Birks, H. J. B., & Van der Voet, H. (1993). Weighted Averaging Partial Least Squares regression (WA-PLS): definition and comparison with other methods for species819 environment calibration. In G. P. Patil & C. R. Rao (Eds.), Multivariate Environmental Statistics (pp. 525–560). Elsevier Science Publishers. https://citeseerx.ist.psu.edu/viewdoc/download?doi=10.1.1.74.6015&rep=rep1&type=pdf

Thornhill, A. H., Popple, L. W., Carter, R. J., Ho, S. Y. W., & Crisp, M. D. (2012). Are pollen fossils useful for calibrating relaxed molecular clock dating of phylogenies? A comparative study using Myrtaceae. Molecular Phylogenetics and Evolution, 63(1), 15–27. https://doi.org/10.1016/j.ympev.2011.12.003

Torres, V., Hooghiemstra, H., Lourens, L., & Tzedakis, P. C. (2013). Astronomical tuning of long pollen records reveals the dynamic history of montane biomes and lake levels in the tropical high Andes during the Quaternary. Quaternary Science Reviews, 63, 59–72. https://doi.org/10.1016/j.quascirev.2012.11.004

van der Knaap, W. O., van Leeuwen, J. F. N., Finsinger, W., Gobet, E., Pini, R., … Ammann, B. (2005). Migration and population expansion of Abies, Fagus, Picea, and Quercus since 15000 years in and across the Alps, based on pollen-percentage threshold values. Quaternary Science Reviews, 24(5), 645–680. https://doi.org/10.1016/j.quascirev.2004.06.013

van der Sande, M. T., Gosling, W., Correa-Metrio, A., Prado-Junior, J., Poorter, L., … Bush, M. B. (2019). A 7000-year history of changing plant trait composition in an Amazonian landscape; the role of humans and climate. Ecology Letters, 22(6), 925–935. https://doi.org/10.1111/ele.13251

Veeken, A., Santos, M. J., McGowan, S., Davies, A. L., & Schrodt, F. (2022). Pollen-based reconstruction reveals the impact of the onset of agriculture on plant functional trait composition. Ecology Letters, n/a(n/a). https://doi.org/10.1111/ele.14063

Vellend, M., Baeten, L., Myers-Smith, I. H., Elmendorf, S. C., Beausejour, R., … Wipf, S. (2013). Global meta-analysis reveals no net change in local-scale plant biodiversity over time. Proceedings of the National Academy of Sciences, 110(48), 19456–19459. https://doi.org/10.1073/pnas.1312779110

Veloz, S. D., Williams, J. W., Blois, J. L., He, F., Otto-Bliesner, B., & Liu, Z. (2012). No-analog climates and shifting realized niches during the late quaternary: implications for 21st-century predictions by species distribution models. Global Change Biology, 18(5), 1698–1713 https://doi.org/10.1111/j.1365-2486.2011.02635.x

Vetaas, O. R., Grytnes, J.-A., Bhatta, K. P., & Hawkins, B. A. (2018). An intercontinental comparison of niche conservatism along a temperature gradient. Journal of Biogeography, 45(5), 1104–1113. https://doi.org/10.1111/jbi.13185

Villalobos, F., & Rangel, T. F. (2014). Geographic patterns of biodiversity. In M. Benítez, O. Miramontes, & A. Valiente-Banuet (Eds.), Frontiers in Ecology, Evolution and Complexity (pp. 1–11). CopIt ArXives.

von Post, L. (1924). Ur de sydsvenska skogarnas regionala historia under post-arktisk tid. Geologiska Föreningens i Stockholm Förhandlingar, 46, 83–128.

Wiens, J. J. (2004). Speciation and ecology revisited: Phylogenetic niche conservatism and the origin of species. Evolution, 58(1), 193–197. https://doi.org/10.1111/j.0014-3820.2004.tb01586.x

Williams, J. W., Grimm, E. C., Blois, J. L., Charles, D. F., Davis, E. B., … Takahara, H. (2018). The Neotoma Paleoecology Database, a multiproxy, international, community-curated data resource. Quaternary Research, 89(1), 156–177. https://doi.org/10.1017/qua.2017.105

Williams, J. W., Jackson, S. T., & Kutzbach, J. E. (2007). Projected distributions of novel and disappearing climates by 2100 AD. Proceedings of the National Academy of Sciences, 104(14), 5738–5742. https://doi.org/10.1073/pnas.0606292104

Williams, J. W., Shuman, B. N., & Webb, T. (2001). Dissimilarity analyses of Late-Quarternary vegetation and climate in eastern North America. Ecology, 82(12), 3346–3362. https://doi.org/10.1890/0012- 9658(2001)082[3346:DAOLQV]2.0.CO;2

Williams, J. W., Shuman, B. N., Webb, T., Bartlein, P. J., & Leduc, P. L. (2004). Late-Quaternary vegetation dynamics in North America: Scaling from taxa to biomes. Ecological Monographs, 74(2), 309–334. https://doi.org/10.1890/02-4045

Willis, K. J., & Birks, H. J. B. (2006). What Is natural? The need for a long-term perspective in biodiversity conservation. Science, 314(5803), 1261–1265. https://doi.org/10.1126/science.1122667

Willis, K. J., & MacDonald, G. M. (2011). Long-term ecological records and their relevance to climate change predictions for a warmer world. Annual Review of Ecology, Evolution, and Systematics, 42(1), 267–287. https://doi.org/10.1146/annurev-ecolsys-102209-144704

Wolkovich, E. M., Regetz, J., & O'Connor, M. I. (2012). Advances in global change research require open science by individual researchers. Global Change Biology, 18(7), 2102–2110. https://doi.org/10.1111/j.1365-2486.2012.02693.x

Wüest, R. O., Zimmermann, N. E., Zurell, D., Alexander, J. M., Fritz, S. A., … Karger, D. N. (2020). Macroecology in the age of Big Data – Where to go from here? Journal of Biogeography, 47(1), 1– 12. https://doi.org/10.1111/jbi.13633

Yasuhara, M., Tittensor, D. P., Hillebrand, H., & Worm, B. (2017). Combining marine macroecology and palaeoecology in understanding biodiversity: microfossils as a model: Marine macroecology882 palaeoecology integration. Biological Reviews, 92(1), 199–215. https://doi.org/10.1111/brv.12223

Žliobaitė, I., Fortelius, M., & Stenseth, N. C. (2017). Reconciling taxon senescence with the Red Queen's hypothesis. Nature, 552(7683), 92–95. https://doi.org/10.1038/nature24656

Manuscript 6

Climate legacies accelerated global rates of change in plant assemblages over the last 21000 years

Nature Communications, in review

Gregor H. Mathes[1,2*], Wolfgang Kiessling[2], Ondřej Mottl[3], Suzette G.A. Flantua[3], H. John B. Birks[3,4], John-Arvid Grytnes[5], Manuel J. Steinbauer[1,5]

[1] BayCEER, Bayreuth Centre of Ecology and Environmental Research, University of Bayreuth, Bayreuth, Germany.
[2] Department of Geography and Geosciences, GeoZentrum Nordbayern, Friedrich-Alexander University Erlangen-Nürnberg, Erlangen, Germany.
[3] Department of Biological Sciences, University of Bergen, and Bjerknes Centre for Climate Research, Bergen, Norway.
[4] Environmental Change Research Centre, University College London, London, UK.
[5] Department of Biological Sciences, University of Bergen, Bergen, Norway.
* Corresponding author: gregor.mathes@uni-bayreuth.de

ABSTRACT

Past climate is an important factor for current biodiversity and ecosystem processes, but the temporal scales of climate legacies in global plant assemblages are currently unknown. Here we show that global vegetation dynamics over ecological timescales (centuries to millennia) are affected by the interaction of long-term and short-term climate change. We assess the responses of terrestrial plant assemblages to the compound effect of climate legacies and interactions over the past 21,000 years. Based on a global compilation of 1,748 fossil pollen sequences, we evaluate within a Bayesian framework how rates of palynological change, a proxy for vegetation change, were driven by the interaction between long-term temperature trends and short-term temperature changes. We find that vegetation changes were substantially greater when short-term temperature changes added to long-term trends in the same direction. Plant assemblages experiencing such synergistic climate interactions over periods of 100 to 1,000 years were on average 15% more likely to show high turnover than under non-synergistic conditions. We further show that tropical climate zones are particularly more prone to this effect of climate interactions than cold and dry areas. Using climate estimates during the last 1,000 years together with climate estimates under various shared socioeconomic pathways until 2100, we predict an increase in global rates of vegetation change between 78% and 125% compared to a pre-human baseline. Our results illustrate that the response of ecosystems to climate change is strongly dependent on the preceding climate state, that is the current and future ecosystem responses carry a strong climate legacy. Ecological studies might substantially underestimate the impact of the current climate warming when climate history is not taken into consideration.

INTRODUCTION

Assessing how terrestrial communities will respond to climate change is a primary challenge in maintaining biological diversity and the various functions terrestrial ecosystems provide (Jump & Peñuelas, 2005; Urban, 2015; Warren et al., 2013). Both short-term (decades to centuries) and long-term (centuries to millennia) climatic history are known to be major drivers of biodiversity dynamics (Antão et al., 2020; Broderick et al., 2022; Delgado-Baquerizo et al., 2018; Hawkes et al., 2020; Monger et al., 2015; Ogle et al., 2015; Strickland et al., 2015; Svenning et al., 2015). The legacy effect of the dynamic interaction of short-term and long-term climate history, though, has not yet been quantified for modern global ecosystems (Benito et al., 2020). Complex ecosystem feedbacks arising from climate legacies and interactions might render current assessments of biodiversity changes under future climate scenarios to be erroneous if feedbacks are not explicitly taken into consideration (Benito et al., 2020; Ogle et al., 2015).

Species tend to retain ancestral ecological traits through time (Wiens et al., 2010; Wiens & Graham, 2005), resulting in a characteristic adaptation to climatic conditions. Climate change can lead to a mismatch between the preferred niche space of taxa and new climatic conditions (Wiens et al., 2010), especially when the preference for a particular climatic niche is strong (Fig. 1). Climatic change might be less deleterious for species when added to a long-term temperature trend in the opposite direction (e.g., a short-term cooling following a prolonged warming trend). On the contrary, a short-term change following a prolonged trend in the same direction may drive species increasingly out of their climate envelope. Communities under such synergistic changes would thus need to show high rates of turnover to stay in equilibrium with climate. We hypothesise therefore that a period of climate warming may have diverging impacts depending on the previous climatic trajectory (Fig. 1a). Accordingly, we expect plant assemblages to show higher rates of change under synergistic climate interaction (Fig. 1b). This effect might be further exacerbated by the potentially increased occurrence of compound climate extremes (i.e., the interaction of multiple major hazards) after synergistic temperature changes (AghaKouchak et al., 2020; Zscheischler et al., 2018).

Here we assess the relationship between rates of vegetation change (estimated from pollen data) and the interaction of short-term temperature change (spanning 100 years) with the preceding longer-term temperature trend (spanning 100 to 1,000 years) over the past 21,000 years. We base our analysis on 1,465 fossil pollen sequences from the Neotoma Paleoecology Database (Williams et al., 2018) covering all continents except Antarctica (Extended Data Fig. 1, Extended Data Table 1), with continentally harmonised taxonomies and updated age-depth models and their uncertainties (Extended Data Fig. 2). We test the expectation of temperature change to have a higher impact on ecosystem dynamics when added to previous trends in the same direction (synergistic interactions), by calculating rates of assemblage change for both synergistic (cooling-cooling, warming-warming) and antagonistic (cooling-warming, warming-cooling) climate interactions. We then implement generalised linear hierarchical models to quantify the rate of change as a function of short-term temperature change interacting with long-term temperature trends. Any difference between the impacts of synergistic and antagonistic interactions on turnover could have important implications for plant assemblages under future climate change. We use the insights gained to forecast future rates of vegetation change under various IPCC scenarios. We employ a Bayesian framework to propagate uncertainty from one analytical step to the next and a dynamic multi-model approach to cover a range of interval lengths (100–1,000 years) for climatic trends. With the latter multi-model approach, we test whether there is a temporal decay effect of climate legacy on plant assemblages and over which temporal scales these legacies are detectable and strongest. With our results we target crucial information for improving forecasts of ecological responses to future environmental change.

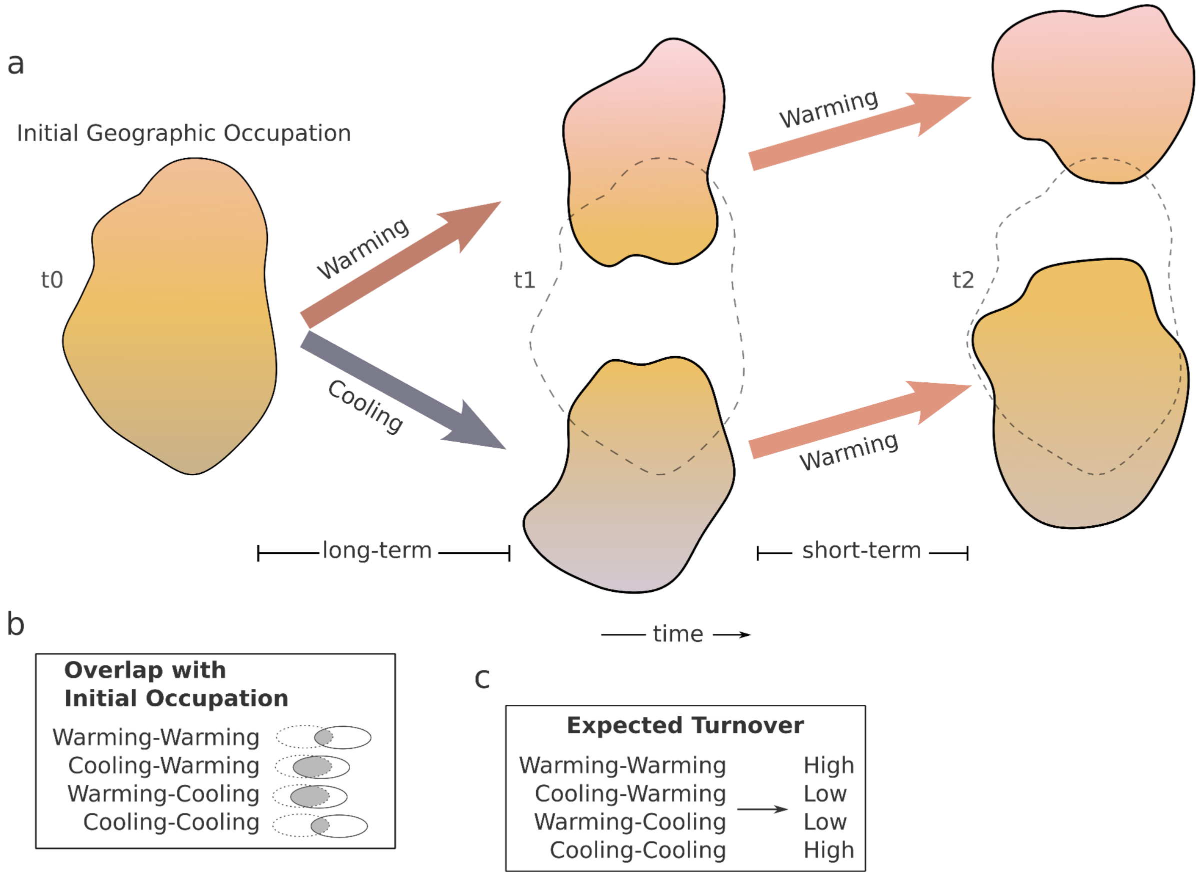

Figure 1: The response of plant assemblages to a climatic change might differ depending on the preceding long-term climatic changes. (a) As individual species show a specific adaptation to climate (initial geographic occupation, t0), both a climate cooling and warming (red and blue arrows) might result in a mismatch between species requirements and actual climatic conditions (at t1), causing species to migrate. If a short-term warming adds to a previous warming, species might respond by tracking their preferred climatic conditions through abundance changes and/or range shifts in distribution, with consequently high rates of change on the pollen sequence level (at t2). If the same short-term warming adds to a previous cooling period, some species might be able to return to the centre of their initial occupation, resulting in lower abundance changes and range shifts and consequently lower rates of change. (b) The expected overlap of the occupied space at t2 with the initial geographic occupation at t0. (c) Arising from this hypothesised mechanism that species show less overlap with their initial geographic occupation

if a short-term climate change adds to a previous long-term trend in the same direction, we expect higher rates of vegetation change after synergistic climate interactions (warming-warming, cooling-cooling).

RESULTS

Rate of palynological change (RoC) during the last 21 ka

The global rate of change (RoC) has varied through time but increased towards modern times (Extended Data Fig. 3). RoC has steadily increased from the end of the last glacial maximum to approximately 12 thousand calibrated years BP (ka). RoC then remained stable between 9 and 1.6 ka, preceded by a slight drop in RoC between 12 and 9 ka. Beginning at around 1.6 ka, RoC increased remarkably and reached its maximum in modern times.

Estimated RoC after each climate interaction

Synergistic climate interaction substantially drives high vegetation dynamics expressed by increased rates of assemblage changes (Fig. 2a). The association is non-linear, with higher RoC occurring after more intense short-term warming and cooling (Extended Data Fig. 4 and 5). Antagonistic climate interaction, to the contrary, results in lower global RoC across all long-term trends. To quantify the difference in legacy effects of synergistic and antagonistic interactions on vegetation change, we grouped model predictions into a low and high turnover category. Rates above the median RoC per continent are characterised as “high turnover” and rates below the continental average as “low turnover”. We then compared the number of high versus low turnover events per climate interaction (i.e., the turnover ratio). Synergistic interactions increase the probability for a high turnover by 14.7% [95% CI (3.4%, 25.2%)] compared to antagonistic interactions (Fig. 2a). The turnover ratio is 1.34 [95% CI (1.07, 1.67)] for synergistic interactions (Fig. 2b). This indicates that both short-term warming adding to a long-term warming trend and short-term cooling adding to a long-term cooling trend substantially increase the risk of plant assemblages shifting into a high turnover state. All calculated risk metrics (turnover ratio, change in risk, and absolute risk) are mostly outside the region of practical equivalence (a range of parameter values with practically no effect, Extended Data Fig. 6, Extended Data Table 2), suggesting that we are revealing ecologically meaningful patterns.

Spatial differences in the turnover ratio

We show a high spatial variability in climate legacies both in terms of magnitude and direction of turnover (Fig. 3a). Plant assemblages in Europe, Africa, Latin America, and Oceania display high turnover ratios after a warming-warming or cooling-cooling interaction. North America in particular shows a relatively low risk of going into a phase of high turnover after cooling-cooling interactions. After synergistic climate interactions in either direction, tropical climate classes are up to 28 times more likely to shift into a state of high turnover (Fig. 3b), with highest turnover detected in tropical rainforests. Climate classes characterised by a temperate climate are similarly high-risk areas with a substantially increased turnover ratio, but here ratios after cooling-cooling interactions are generally higher than after warming-warming. In contrast, climate classes with a cold and dry climate show a tendency towards lower turnover ratios after synergistic climate interaction. The majority of climate classes, however, tend to shift into a phase of high plant assemblage turnover after synergistic climate interactions, while antagonistic interactions do not result in such a substantial increase. The turnover ratio is highest at the equator and generally decreases towards the poles (Extended Data Fig. 7a) reflecting a strong latitudinal gradient of vegetation responses to climate legacies. Similarly, sequences at the high latitudes generally experience more temperature variability (i.e., standard deviation in the short-term change) and vice versa (Extended Data Fig. 7b), indicating that assemblages adapted to a narrower niche are more susceptible to climate legacies and interactions.

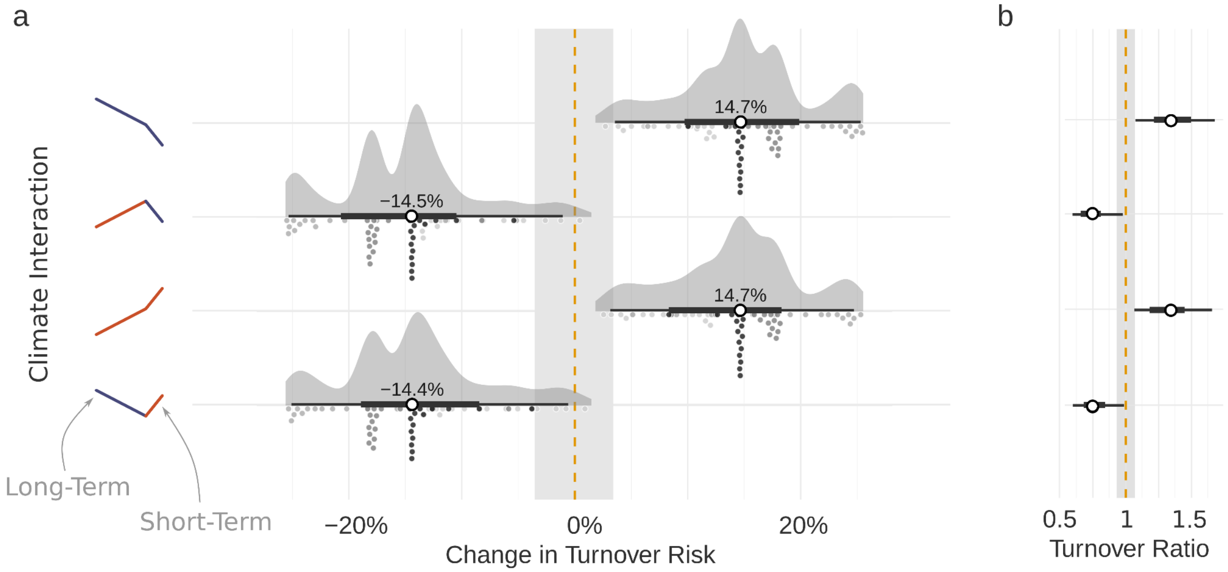

Figure 2: Estimated global turnover metrics after each climate interaction. The type of climate interaction (cooling-cooling, warming-cooling, warming-warming, cooling-warming) is indicated by the coloured lines, where the first line represents the long-term temperature trend and the second line the short-term climate change. Red lines indicate warming, and blue lines cooling. (a) Estimated change in turnover risk per climate interaction. White points and the label show the median estimate for the change in turnover risk. Coloured points show the model-wise estimates covering long-term trends from 100 to 1,000 years. (b) Estimated turnover ratios (the ratio of high to low turnover events) per climate interaction. White points show the median estimate for turnover ratio. In both (a) and (b), the thick black line depicts the 55% credible interval, and the thin black line the 95% credible interval. The shaded grey area indicates the region of practical equivalence (ROPE), which covers a range of values generated from null models

Length of long-term trends

Vegetation dynamics carry the ecological memory of past temperature trends at all temporal scales ranging from 100 to 1,000 years with the strongest legacy effect from a 100 yr back. All long-term trends show an increase in RoC after synergistic climate interactions (Extended Data Fig. 4 and 5). A model comparison based on leave-one-out cross-validation shows that a 100 year long-term trend has the highest model performance but with all models showing a similarly high performance (Extended Data Fig. 8). This indicates that the legacy effect of climate on ecological processes driving vegetation dynamics is present on time scales between 100 to 1,000 years. All models performed significantly better than null models (Extended Data Fig. 8a).

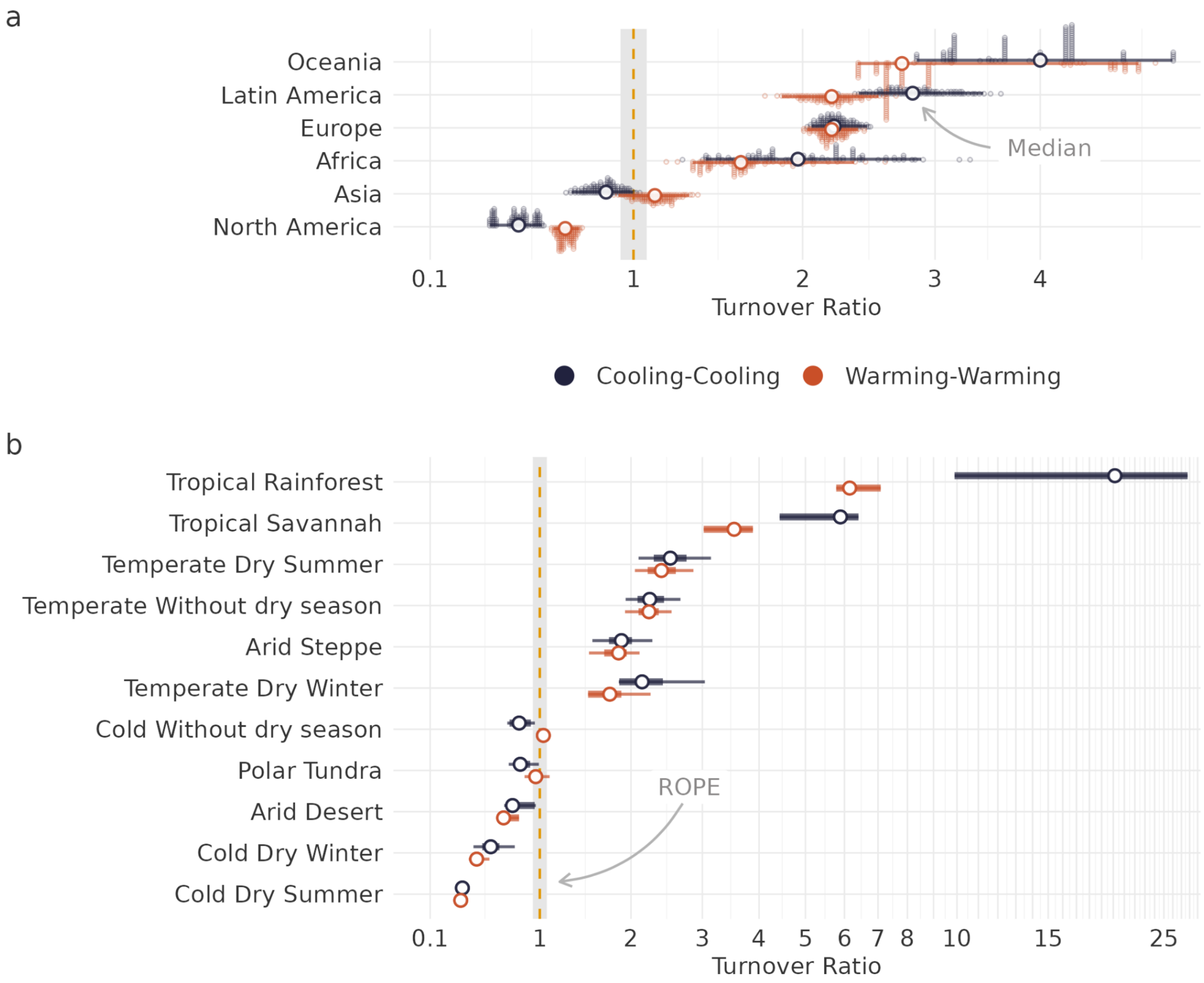

Figure 3: Estimated turnover ratios (the ratio of high to low turnover events per climate interaction) after synergistic climate interactions (warming-warming and cooling-cooling climate interaction) for each continent and climate class. Note that the turnover ratio is plotted on a log-transformed scale. (a) The turnover ratio per continent. (b) The turnover ratio per climate class. Outlined points show the median estimate for turnover ratio. The thicker line depicts the 55% credible interval, and the thinner line the 95% credible interval. Cooling-cooling interactions are shown in blue, and warming-warming interactions are shown in red. The shaded grey area indicates the region of practical equivalence (ROPE), which covers a range of values generated from null models.

Increase in RoC under shared socioeconomic pathways

The global RoC in terrestrial plant assemblages might increase by up to 117% [95% CI (106%, 125%)] until 2100, relative to the past 21 ka. We used our models trained on RoC over the last 21 ka to predict future rates of change across shared socioeconomic pathways(Riahi et al., 2017) (SSPs, Fig. 4). We then calculated the increase in RoC due to a warming-warming climate interaction relative to the average rate over the last 21 ka. In the near term (2021–2040), all SSPs result in an increase of RoC by approximately 92% [95% CI (85%, 99%)]. Out of 100 predictions under SSP5 (Fossil-fuelled Development) for the long-term period (2081–2100), all result in a RoC at least twice as high compared to rates during the last 21 ka, reaching a maximum at an increase of 134%. The average increase in RoC in the long term for SSP1 (Sustainability) is 41% lower than the RoC for SSP5.

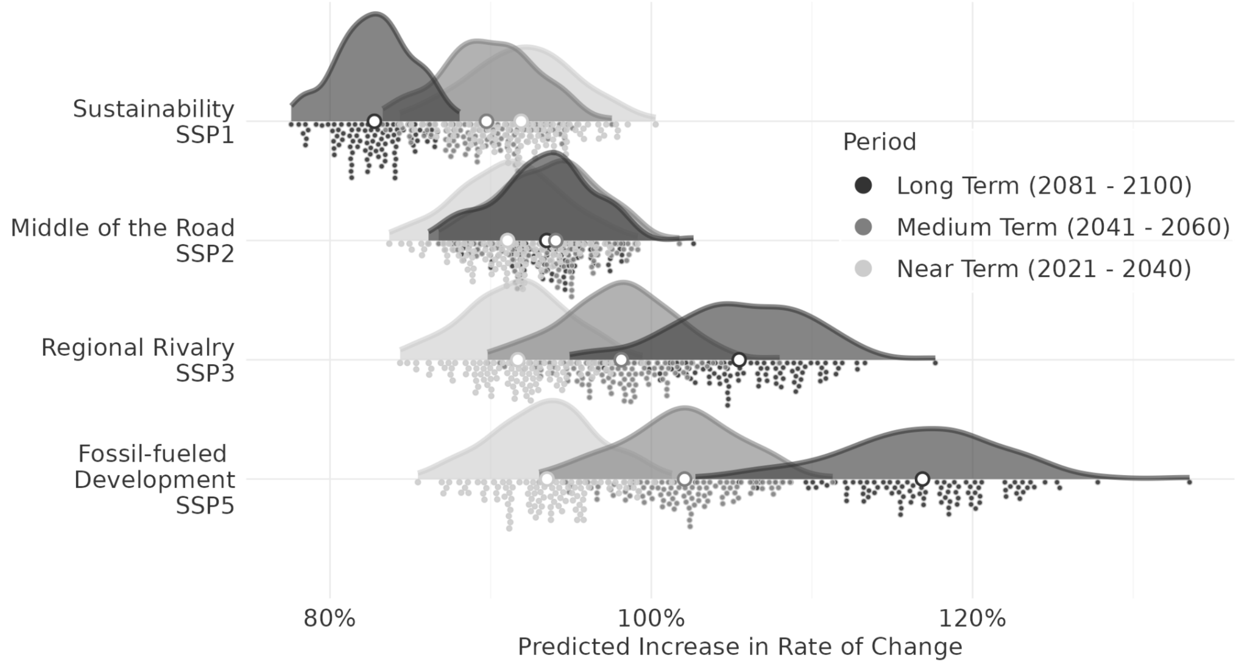

Figure 4: Predicted increase of rates of vegetation change after warming-warming climate interaction under shared socioeconomic pathways (SSPs) compared to rates during the last 21 ka. Shaded lines and densities illustrate the distribution of predicted values for each SSP(Riahi et al., 2017) for a long-term, medium-term, and near-term period. Outlined points show the median increase in turnover ratio per period.

DISCUSSION

Ecological memory driven by climate legacy is detectable and quantifiable in vegetation dynamics through time. Importantly, ecosystem responses differ globally depending on timing, duration, magnitude and interaction. Short-term temperature change adding to a long-term trend in the same direction coincides with a substantially increased risk for plant assemblages to shift into a phase of high turnover, potentially resulting in the emergence of novel communities (Staples et al., 2022) and long-lasting consequences on ecosystem functioning (Svenning et al., 2015). This dependency on the preceding temperature is found across multiple scales, with long-term trends ranging 100 to 1000 years back in time. Particularly tropical climate classes are highly sensitive to these climate legacies and synergistic climate interactions, being on average six times more likely to shift into a state of high turnover. As the current climate change exceeds the temperature of the previous millennia (Arias et al., 2021), considering synergistic climate interactions is of great importance.

Our results are in line with previous findings from the fossil record spanning millions of years, where the relationship between evolutionary change and climate change is dependent on the preceding temperature (Mathes, Kiessling, et al., 2021; Mathes, van Dijk, et al., 2021). For ecological timescales (centuries to millennia), numerous reports of climate legacies show that past climate is an important driver for both key ecosystem processes (Benito et al., 2020; Broderick et al., 2022; Delgado-Baquerizo et al., 2018; Hawkes et al., 2020; Monger et al., 2015; Ogle et al., 2015; Strickland et al., 2015) and biodiversity (Antão et al., 2020; Svenning et al., 2015). Climate legacies in current ecosystems arise from the interaction between modern and preceding climate, and are therefore a specific form of climate interaction. To understand modern-day biodiversity dynamics responding to current and future climate conditions, climate interactions are of vital importance. In particular, any changes in either the direction or magnitude, of either the short-term or the long-term climatic trend, result in varying consequences to the plant assemblage. If climate interactions and other palaeoclimatic legacies are not specifically incorporated, assessments of biodiversity dynamics under future climate change are likely to be erroneous. For example, species distribution models assume equilibrium between species' ranges and the environment (De Marco et al., 2008; Spencer, 2020) but such ranges are likely to be subject to time lags shaped by preceding climatic changes (Svenning et al., 2011, 2015). In addition, numerous studies train climate-vegetation models aimed at quantifying climatic lags considering climate during the last century (Bertrand et al., 2011; Ding et al., 2020; Kelly & Goulden, 2008; Wu et al., 2015), thus fitting assemblages to climatic conditions that are perhaps the least influential in driving rates of vegetation change (Extended Data Fig. 8). To overcome these issues and to move towards a mechanistic understanding of fundamental evolutionary and ecological processes, it is essential to integrate fossil and contemporary data (Fritz et al., 2013) and to continue the collection of datasets spanning multiple timescales (Brewer et al., 2012). We therefore argue moving towards a more holistic approach by integrating all available information about past climate and its feedbacks (i.e., climate legacies and interactions) when studying ecological systems.

Climate legacies and interactions influence the applicability of models using so-called climate analogues, i.e. locations that share statistically similar climates (Koven, 2013; Williams et al., 2007), either across time (i.e., with past or future climates) or across space (i.e., between locations). These analogues have been used to estimate, for example, the impact of future climate change on crop yields (Pugh et al., 2016) or on economic growth in urban areas (Hallegatte et al., 2007). If analogue locations, however, have a different climatic history (i.e., type and magnitude of climate interaction), locations with apparent analogue climates would show a deviating response to climate change, rendering the analogue approach unreliable. The difference in vegetation responses among locations with contemporary similar climate can be substantial as indicated by our results, where we show that the same climate change can either increase or decrease assemblage turnover, depending on the preceding climate state. Therefore, it is pivotal for any model predicting vegetation dynamics based on the climate analogue approach to incorporate the climatic history.

Tropical climate classes appear to be the places where synergistic climate interactions have the strongest impact on plant assemblages (Fig. 3). Hypothetically, tropical assemblages may be more sensitive to climatic change, as they evolved in areas with low temporal temperature variation (Deutsch et al., 2008; Janzen, 1967; Sheldon et al., 2018). This adaptation to a narrow climatic niche could explain the observed pattern, as species might reach their niche edges faster after synergistic climate interactions. This explanation of species with a narrower niche exhibiting a higher susceptibility to climate interactions is in line with our findings of a decreasing turnover ratio towards the poles (Extended Data Fig. 7a) and a lower temperature variability at sequences near the equator (Extended Data Fig. 7b). Alternatively, the exceptionally high susceptibility of tropical assemblages to synergistic climate interactions can be related to high internal forest dynamics. Transitions between different forest states as a result of shifting dominance of taxa have been shown in tropical forests (de Boer et al., 2013; Mayle et al., 2004), displaying high turnover during hundreds of years. This suggests that at an assemblage level, tropical systems are expected to show naturally high responsiveness to climate change, possibly by alternative ecosystem states. Regardless of whether the high rates of change in tropical assemblages found here are driven by spatial range-shift dynamics (niche tracking) or changes in plant assemblages (shifting dominance of taxa), tools capable of predicting whether these high rates of change are indicative of the system approaching a critical threshold are needed (Brock & Carpenter, 2010; Dakos et al., 2008; Scheffer et al., 2009).

With a prolonged warming trend under anthropogenic climate change, both the frequency and magnitude of synergistic climate interactions (warming-warming) will increase. According to our model estimates, global rates of vegetation change will increase substantially in the near, medium, and long term, even for the most optimistic shared socioeconomic pathway (Fig. 4). We emphasise, however, that the turnover metric used in this analysis is based on plant assemblages that might have been time-averaged. The projected increase in vegetation change under future climate change might therefore be subject to biases. Likewise, we do not include the impact of human activities on rates of vegetation change in our analysis, as we primarily aim to analyse the effects of climate interactions. The compound effect of anthropogenic perturbations and climate interactions might result in a cascading dynamic (Lawrence et al., 2020), potentially increasing rates of vegetation change even beyond our predictions. With the current acceleration of rates for both human activities (Steffen et al., 2015) and climate warming (Smith et al., 2015), we therefore expect global rates of vegetation change to increase to levels unobserved throughout the last 21 ka. Combining the effect of climate interactions with information about human pressure on the Earth System should be the focus of future research. An integrative approach could be a key step to understanding the complex feedbacks among humans, climate, and ecosystems (Fritz et al., 2013; Mottl, Flantua, et al., 2021).

In conclusion, our study highlights that current terrestrial ecosystems cannot be studied in an isolated manner from their past climatic context and that a climatic legacy from as far as 1000 years ago influences plant assemblages of today. We show that the response of plant assemblages is strongly dependent on the preceding climate, in particular that a short-term climate change adding to a long-term trend in the same direction substantially increases rates of vegetation change. We provide evidence that the time period considered to understand current vegetation dynamics reflected in changes in plant assemblages reaches hundreds of years back in time and spans multiple scales. The explicit integration of these climate legacies and interactions may lead to a higher accuracy for assessments predicting biodiversity change under an accelerating trend of climate warming. As warming-warming climate interactions are expected to increase in frequency and magnitude in the future, terrestrial plant assemblages are likely to shift into rates of change unprecedented throughout the previous 21 ka.

MATERIALS AND METHODS

Pollen data

All analyses were carried out in R (R Core Team, 2021) using R v.4.1.2. We used the tidyverse collection of R packages (Wickham et al., 2019) to transform and visualise data. We obtained fossil pollen data from the Neotoma Paleoecology Database using the neotoma R package (Goring et al., 2015) on 2nd May 2022. We followed the methodological approach of Mottl et al. (2021) to filter and prepare the pollen data for the calculation of rates of palynological change. To develop age-depth models, we selected control-point types (see the included types in Reimer et al. (2020)), and calibrated the radiocarbon dates using the IntCal20, SHCal20, or mixed calibration curves (Hogg et al., 2020; Reimer et al., 2020). Calibration curves were assigned based on the geographical location of the records and the recommended boundaries (Hogg et al., 2020). For each sequence with at least five chronological control points, we constructed an age-depth model using the bchron R package (Haslett & Parnell, 2008) to generate 1000 possible age estimates for all sample depths at the original sampling resolution of the original fossil pollen sequences. We used these 1000 draws to build posterior estimates of age uncertainty. We calculated the median age estimate for each sample depth to obtain the default age used in these analyses. All ages are expressed in calibrated years before radiocarbon present (cal yr BP, where 0 yr BP = 1950 CE) or as kiloannum BP (ka), also in calibrated years before radiocarbon present.

We performed our analyses using the following delimitation of continents: North America, Latin America, Europe, Africa, Asia, and Oceania. The boundary between North America and Latin America is placed at the border between the US and Mexico, while the boundary between Europe and Asia is placed at the border between Russia and adjacent countries in Eastern Europe, including Finland, Belarus, Ukraine, Bulgaria, and Greece. Taxa lists for North America, Latin America, Europe, Oceania, and Asia were harmonised to the taxonomically highest-precision pollen morphotypes identifiable by most palynologists. The European harmonisation was adjusted from Giesecke et al. (2019) (Level = MHVar2, http://www.europeanpollendatabase.net/data/downloads/image/EPD_P_VARS_high3.csv). Taxonomic harmonisations for other regions were developed as part of the HOPE project (North America, Latin America, Asia, Oceania) and will be made available on Figshare upon acceptance of the manuscript. Data from African sequences are used at the original site-level taxonomic resolution.

In order to obtain the highest quality of pollen data we conducted the following filtration processes:

A. Fossil pollen grain counts: for each fossil pollen sequence, we only include terrestrial taxa of selected ecological groups (see Mottl et al. (2021)). We have excluded all samples that contain less than 25 pollen grain counts, and only include sequences if at least 50% of all samples contain at least 150 pollen grains.
B. Depositional environments: we only include sequences of certain depositional environments (see Mottl et al. (2021)).
C. Age limitation: we only include sequences which span between 1ka and 6ka (or 1ka and 8ka for Europe and North America). The length of each sequence is determined by the 95% quantile of the age estimation of each level. We exclude all samples whose 95% quantile is older than 21ka. In addition, we exclude all samples for which the age has been extrapolated for more than 3000 years.
D. We exclude all sequences with fewer than five samples

For each pollen sequence, we additionally identified the Köppen-Geiger climate classification following Beck et al. (2018). The number of sequences per climate class used in this work are listed in Extended Data Table 1.

Rate of change (RoC) analysis

We estimated the magnitude of palynological compositional change per 100 years as rate of change (RoC) via the R-Ratepol package (Mottl et al., 2020; Mottl, Flantua, et al., 2021; Mottl, Grytnes, et al., 2021). We smoothed the pollen data using Shepard's 5-term filter (Davis, 2002; Mottl, Grytnes, et al., 2021). To reduce bias originating from uneven temporal sampling resolution in the original pollen sequences, we used the moving window approach implemented in the R-Ratepol package with a bin width of 500 years and a time increment of 100 years (i.e., five window shifts). We also used the chi-squared metric as a dissimilarity index to reduce the sensitivity of our analysis to the uncertainty associated with rare pollen taxa (Mottl, Grytnes, et al., 2021). Uncertainties in pollen sampling as well as from age-depth models were propagated in the calculation of RoC by iteratively sampling pollen grains and age sequences. We repeated this iteration 1,000 times and subsequently used the median value of all RoC iterations as the final RoC score (Extended Data Fig. 2 a-c).

Temperature data

We estimated the mean annual air temperature for each sample depth in a pollen sequence using the CHELSA-TraCE21k downscaling algorithm and data(Karger et al., 2021) (Extended Data Fig. 2 d-e). We first extracted the entire temperature time series from the algorithm for one pollen sequence, spanning the last 21,000 years in 100-year time steps. We then fitted a natural spline on this time series and selected the temperature at the age of each RoC estimate. We repeated the process with the age value of each RoC estimate subtracted by 100 years, estimating the temperature 100 years before the actual observation in the pollen sequence. We then calculated the 100 year short-term temperature change by subtracting the temperature at the actual observation with the temperature 100 years ago. To get the 100 year long-term temperature trend, we subtracted the temperature at age-100 years with the temperature at age-200 years. Similarly, we calculated the 250 year long-term temperature trend by subtracting the temperature at age-100 years with the temperature at age-350 years. We then divided the result by 2.5 to get the trend standardised to 100 years. We repeated this process for the 500 year and 1,000 year long-term temperature trend. Each long-term trend hence reached from the starting point of the focal interval to the beginning of the short-term change (Extended Data Fig. 2e), and captured the temperature change per 100 years over this interval.

Generalised linear hierarchical models

We quantified the effect of temperature change interacting with past temperature trends on the RoC using Bayesian generalised linear hierarchical models (GLHMs). We fitted these models via the Stan probabilistic programming language (Carpenter et al., 2017) and the brms R package (Bürkner, 2017). For each model, we used a Markov Chain Monte Carlo algorithm with four chains and 5,000 samples for each chain. Model convergence and fit to the data was checked thoroughly via convergence diagnostics and the expected log predictive density of a model (Extended Data Fig. 9, Extended Data Fig. 10, Extended Data Table 3). We fitted an individual model for each long-term trend ranging from 100 to 1,000 years. The general equation of each model is:

Rate of Change ~ Δ*Tchange:*Δ*Ttrend +(*Δ*Tchange:*Δ*Ttrend | Continent / Ecozone / ID)*

We thereby allow the effect of the short-term temperature change (ΔTchange) interacting with the long-term temperature trend (ΔTtrend) on the RoC to vary within each pollen sequence (ID), which are nested within climate classes (Ecozone), which are nested within continents (Continent). This corresponds to a GLHM with a nested random intercept and a nested random slope term (Bolker et al., 2009). Model errors are assumed to follow a beta family distribution with a logit-link. Priors were chosen via prior predictive checks by constraining samples from the prior distribution to a feasible outcome space (McElreath, 2020).

Model comparison

We compared the model performance of each long-term trend varying from a length of 100 to a length of 1,000 years via the theoretical expected log pointwise predictive density (ELPD) estimated using cross-validation (Extended Data Fig. 8). For cross-validation, we used efficient approximate leave-one-out cross-validation (LOO) via the loo R package (Vehtari et al., 2017). We fitted multiple models with differing long-term trend length (ranging from 100 to 1,000 years) to test (1) whether the effect of climate interactions on RoC changes with temporal scale or whether the inference stays robust independent of the long-term trend length; and (2) to identify and quantify the period over which the climate legacy has the strongest influence on vegetation dynamics in terms of rates of palynological change. We additionally fitted null models for the model comparison, where the rate of change was either assumed to be constant (fixed intercept) or variable over continents (random effect on continent).

Climate interaction

To interpret model estimates, we created a grid of equally spaced short-term changes from -2°C to 2°C with equally spaced long-term trends similarly ranging from -2°C to 2°C. This range captures the vast majority of temperature changes and trends observed in the actual data. We then sampled from the posterior predictive distribution of each GLHM over this grid via the tidybayes R package (Kay, 2022). We then summarised all estimated RoC for long-term trends below 0°C and short-term changes below 0°C as a cooling-cooling climate interaction; all RoC for long-term trends above 0°C and short-term changes below 0°C as a warming-cooling climate interaction; all RoC for long-term trends below 0°C and short-term changes above 0°C as a cooling-warming climate interaction; and all RoC for long-term trends above 0°C and short-term changes above 0°C as a warming-warming climate interaction.

This procedure ensures capturing a range of potential long-term trends and short-term changes while having the same amount of observations per climate interaction.

Risk metrics

We used the estimated RoC from our GLHMs to quantify risk metrics for the plant assemblages (Extended Data Table 2). We grouped individual rates of change into a low and high turnover category, where rates above the average (median) RoC across all models are characterised as "high turnover", and rates below the overall average as "low turnover". We then divided the amount of high by the amount of low turnover events per climate interaction. We termed this metric turnover ratio, which corresponds to a classical relative risk metric. This turnover ratio enabled us to quantify the risk of shifting into a phase of high turnover after synergistic climate interaction, compared to antagonistic climate interaction. We additionally calculated the absolute risk per climate interaction of assemblages to shift into a phase of high turnover by dividing the number of high turnover events by the total number of events (Extended Data Fig. 6a), showing the actual difference in risk after synergistic or antagonistic climate change. We then calculated the risk increase after synergistic climate interaction by subtracting the absolute risk of antagonistic interaction from the absolute risk of synergistic interaction (Extended Data Fig. 6b). The risk increase illustrates the estimated difference in the probability of shifting into a phase of high turnover after synergistic climate interaction compared to antagonistic climate interaction.

Region of practical equivalence

To test whether estimated risk metrics (turnover ratio/ relative risk, absolute risk, risk increase) are a result of random chance alone, we calculated a region of practical equivalence (Kruschke, 2018) (ROPE, Extended Data Fig. 11). The ROPE indicates a range of parameter values that are practically equivalent to the null values, which in this case corresponds to an equal risk after synergistic and antagonistic climate interactions. Estimated values falling outside this range indicate a risk difference between antagonistic and synergistic climate interactions that could not be generated by chance alone. We calculated the ROPE by iteratively simulating RoC generated from a beta distribution similar to the distribution of RoC in the actual data. We then randomly assigned those simulated rates to either synergistic or antagonistic climate interactions. From these distributions, we then calculated risk metrics for each type of climate interactions and summarised them via 95% credible intervals

Shared socioeconomic pathways

We used our GLHMs trained on the rate of palynological change over the last 21 ka to predict future rates across shared socioeconomic pathways (Riahi et al., 2017) (SSPs). We extracted the global mean atmosphere temperature estimate from the CMIP6 models ensemble (Eyring et al., 2016) for each SSP and each time period (near-term, medium-term, long-term) via the IPCC interactive atlas (Gutiérrez et al., 2021; Iturbide, Maialen et al., 2021). For this, we selected an annual season without any aggregation and saved the multidimensional output as NetCDF files. For each pollen sequence within our data, we then extracted the estimated temperature at the site for each SSP and period via the NetCDF files. We similarly estimated the temperature for the years 1950, 1850, 1700, 1450, and 1000 CE for each pollen sequence via the CHELSA-TraCE21k downscaling algorithm (Karger et al., 2021) and natural splines. Using these historical temperature estimates and the predicted temperature for each SSP, we then calculated the 100 year short-term changes and the 100, 250, 500, and 1000 year long-term trends similar to the long-term estimations approach described above. Using our GLHMs and the interaction between these short-term changes and long-term trends, we then predicted the rate of change under each SSP and for each period. In a final step, we calculated the relative change of these predictions to the average (median) rate of change of the past 21 ka, and averaged the result over all long-term trends.

Effect of temperature variability on turnover ratio

We estimated the relationship between turnover ratio and latitude as well as the relationship between turnover ratio and temperature variability to test whether species experiencing less climatic variability are more susceptible to climate interactions. As we are interested in the general trend of each relationship, we first standardised the pollen sequence-wise turnover ratio estimated from GLHMs and regressed it against the latitude of each sequence, as well as the standard deviation in short-term temperature change across the whole sequence (temperature variability) via a Bayesian regression with a Gaussian distribution.

Turnover ratio through time

To calculate the turnover ratio through time, we assigned the RoC values to bins with equal width (200 years) spanning the last 14 ka (data for ages between 21 and 14 ka were insufficient to calculate robust estimates for the turnover ratio). We then calculated the turnover ratio of the increase in turnover events after synergistic climate interaction compared to antagonistic climate interaction for each bin, averaging over long-term trends (Extended Data Fig. 12b). To check whether the choice in bin width might bias our estimates, we assigned RoC values to 50 bins containing an equal number of observations by letting the width of each bin vary (Extended Data Fig. 12a).

Robustness testing

In addition to the estimation of the region of practical equivalence (ROPE, Extended Data Fig. 11), we performed various robustness tests to check whether our estimates are statistically sound. We first tested the fit of each final GLHM to the actual pollen data via posterior predictive checks, comparing draws from the posterior predictive distribution with the distribution of rates of change from the actual data for each model. Overall, we found a good agreement between GLHMs and actual data (Extended Data Fig. 9 and Extended Data Fig. 10), indicating that the model fitting procedure was appropriate for the data at hand. The models themselves converged successfully, with conventional convergence and efficiency diagnostics for the used Markov Chain Monte Carlo algorithms showing a high performance (Extended Data Table 3).

As we quantified the RoC over a paleoecological short timespan (i.e., 100 years), the resulting estimates were comparably low and ranged between 0 and 0.3. To model this distribution of RoC values for inference, we decided to use a beta family distribution for the likelihood (see Generalised linear hierarchical models). However, RoC can theoretically reach values higher than 1 (Mottl et al., 2020; Mottl, Flantua, et al., 2021; Mottl, Grytnes, et al., 2021), which is not covered by the beta distribution. To test whether this might bias our results, we additionally fitted a GLHM with a gamma error distribution. This model was based on the 100 year long-term trend, which showed the best performance in the original models (Extended Data Fig. 8b). Metrics estimated from this gamma model were in the range of the original model, indicating that the inference presented here is robust to the choice of the underlying error distribution for the GLHMs. Turnover ratios after synergistic climate interaction were between 1.04 and 1.19, while antagonistic climate interactions resulted in values between 0.82 and 1.03. We similarly found that tropical climate classes were more sensitive to climate changes, with turnover ratios ranging up to 9.89 based on the gamma model. Predicted increase in RoC across shared socioeconomic pathways based on the gamma model was between 82.2% (SSP1, long-term) and 125% (SSP5, long-term), which is in line with our initial results based on models with a beta family error distribution.

We additionally tested whether the trend in turnover ratio per continent and climate class (Fig. 3) can be explained by the number of samples for each estimate. For this, we used a Bayesian measurement error model to estimate the relationship between turnover ratio and sample size. The model indicated that the turnover ratio slightly decreases with increasing sample size for both the continent-wide analysis and the climate class analysis (Extended Data Fig. 13a and c), but we found the relationship to be not consistent (i.e., the 95% credible interval includes zero for the slope estimate, Extended Data Fig. 13b and d). This indicates that our results are not confounded by a sampling bias through variational sampling on the continent or climate class level.

We further evaluated the power of our statistical procedure by simulating RoC for pollen sequences and estimating the difference in simulated RoC for antagonistic climate interactions compared to synergistic climate interactions, as a function of sample size (Extended Data Fig. 14). We performed these power calculations for a difference of 0 between RoC (assessing type I errors, Extended Data Fig. 14a) and a difference similar to the one we found in the actual data (assessing type II errors, Extended Data Fig. 14b). According to these simulations, our analytical framework has excellent power to avoid both false positives and false negatives. Because of the high statistical power of our procedure, the low dependency on variational sampling, the good fit of our GLHMs to the data, and the consensus in estimation of all models spanning different long-term lengths, we are confident that we are describing true ecological patterns.

References

AghaKouchak, A., Chiang, F., Huning, L. S., Love, C. A., Mallakpour, I., Mazdiyasni, O., Moftakhari, H., Papalexiou, S. M., Ragno, E., & Sadegh, M. (2020). Climate extremes and compound hazards in a warming world. Annual Review of Earth and Planetary Sciences, 48(1), 519–548. https://doi.org/10.1146/annurev-earth-071719-055228

Antão, L. H., Bates, A. E., Blowes, S. A., Waldock, C., Supp, S. R., Magurran, A. E., Dornelas, M., & Schipper, A. M. (2020). Temperature-related biodiversity change across temperate marine and terrestrial systems. Nature Ecology & Evolution, 4(7), 927–933. https://doi.org/10.1038/s41559-020-1185-7

Arias, P., Bellouin, N., Coppola, E., Jones, R., Krinner, G., Marotzke, J., Naik, V., Palmer, M., Plattner, G.-K., & Rogelj, J. (2021). Climate Change 2021: The Physical Science Basis. Contribution of Working Group14 I to the Sixth Assessment Report of the Intergovernmental Panel on Climate Change; Technical Summary.

Beck, H. E., Zimmermann, N. E., McVicar, T. R., Vergopolan, N., Berg, A., & Wood, E. F. (2018). Present and future Köppen-Geiger climate classification maps at 1-km resolution. Scientific Data, 5(1), 180214. https://doi.org/10.1038/sdata.2018.214

Benito, B. M., Gil‐Romera, G., & Birks, H. J. B. (2020). Ecological memory at millennial time‐scales: The importance of data constraints, species longevity and niche features. Ecography, 43(1), 1–10. https://doi.org/10.1111/ecog.04772

Bertrand, R., Lenoir, J., Piedallu, C., Riofrío-Dillon, G., de Ruffray, P., Vidal, C., Pierrat, J.-C., & Gégout, J.-C. (2011). Changes in plant community composition lag behind climate warming in lowland forests. Nature, 479(7374), 517–520. https://doi.org/10.1038/nature10548

Bolker, B. M., Brooks, M. E., Clark, C. J., Geange, S. W., Poulsen, J. R., Stevens, M. H. H., & White, J.-S. S. (2009). Generalized linear mixed models: A practical guide for ecology and evolution. Trends in Ecology & Evolution, 24(3), 127–135.

Brewer, S., Jackson, S. T., & Williams, J. W. (2012). Paleoecoinformatics: Applying geohistorical data to ecological questions. Trends in Ecology & Evolution, 27(2), 104–112. https://doi.org/10.1016/j.tree.2011.09.009

Brock, W. A., & Carpenter, S. R. (2010). Interacting regime shifts in ecosystems: Implication for early warnings. Ecological Monographs, 80(3), 353–367. https://doi.org/10.1890/09-1824.1

Broderick, C. M., Wilkins, K., Smith, M. D., & Blair, J. M. (2022). Climate legacies determine grassland responses to future rainfall regimes. Global Change Biology, gcb.16084. https://doi.org/10.1111/gcb.16084

Bürkner, P.-C. (2017). brms: An R package for Bayesian multilevel models using Stan. Journal of Statistical Software, 80(1), 1–28.

Carpenter, B., Gelman, A., Hoffman, M. D., Lee, D., Goodrich, B., Betancourt, M., Brubaker, M., Guo, J., Li, P., & Riddell, A. (2017). Stan: A probabilistic programming language. Journal of Statistical Software, 76(1), 1–32.

Dakos, V., Scheffer, M., van Nes, E. H., Brovkin, V., Petoukhov, V., & Held, H. (2008). Slowing down as an early warning signal for abrupt climate change. Proceedings of the National Academy of Sciences, 105(38), 14308–14312. https://doi.org/10.1073/pnas.0802430105

Davis, J. C. (2002). Statistics and data analysis in geology (3rd ed). J. Wiley.

de Boer, E. J., Hooghiemstra, H., Vincent Florens, F. B., Baider, C., Engels, S., Dakos, V., Blaauw, M., & Bennett, K. D. (2013). Rapid succession of plant associations on the small ocean island of Mauritius at the onset of the Holocene. Quaternary Science Reviews, 68, 114–125. https://doi.org/10.1016/j.quascirev.2013.02.005

De Marco, P., Diniz-Filho, J. A. F., & Bini, L. M. (2008). Spatial analysis improves species distribution modelling during range expansion. Biology Letters, 4(5), 577–580. https://doi.org/10.1098/rsbl.2008.0210

Delgado-Baquerizo, M., Eldridge, D. J., Travers, S. K., Val, J., Oliver, I., & Bissett, A. (2018). Effects of climate legacies on above- and belowground community assembly. Global Change Biology, 24(9), 4330–4339. https://doi.org/10.1111/gcb.14306

Deutsch, C. A., Tewksbury, J. J., Huey, R. B., Sheldon, K. S., Ghalambor, C. K., Haak, D. C., & Martin, P. R. (2008). Impacts of climate warming on terrestrial ectotherms across latitude. Proceedings of the National Academy of Sciences, 105(18), 6668–6672.

Ding, Y., Li, Z., & Peng, S. (2020). Global analysis of time-lag and -accumulation effects of climate on vegetation growth. International Journal of Applied Earth Observation and Geoinformation, 92, 102179. https://doi.org/10.1016/j.jag.2020.102179

Eyring, V., Bony, S., Meehl, G. A., Senior, C. A., Stevens, B., Stouffer, R. J., & Taylor, K. E. (2016). Overview of the Coupled Model Intercomparison Project Phase 6 (CMIP6) experimental design and organization. Geoscientific Model Development, 9(5), 1937–1958. https://doi.org/10.5194/gmd-9-1937-2016

Fritz, S. A., Schnitzler, J., Eronen, J. T., Hof, C., Böhning-Gaese, K., & Graham, C. H. (2013). Diversity in time and space: Wanted dead and alive. Trends in Ecology & Evolution, 28(9), 509–516. https://doi.org/10.1016/j.tree.2013.05.004

Giesecke, T., Wolters, S., van Leeuwen, J. F. N., van der Knaap, P. W. O., Leydet, M., & Brewer, S. (2019). Postglacial change of the floristic diversity gradient in Europe. Nature Communications, 10(1), 5422. https://doi.org/10.1038/s41467-019-13233-y

Goring, S., Dawson, A., Simpson, G. L., Ram, K., Graham, R. W., Grimm, E. C., & Williams, J. W. (2015). neotoma: A Programmatic Interface to the Neotoma Paleoecological Database. Open Quaternary, 1. https://doi.org/10.5334/oq.ab

Gutiérrez, J. M., Jones, R. G., Narisma, G. T., Alves, L. M., Amjad, M., Gorodetskaya, I. V., Grose, M., Klutse, N. A. B., Krakovska, S., & Li, J. (2021). Atlas. Climate Change.

Hallegatte, S., Hourcade, J.-C., & Ambrosi, P. (2007). Using climate analogues for assessing climate change economic impacts in urban areas. Climatic Change, 82(1–2), 47–60. https://doi.org/10.1007/s10584-006-9161-z

Haslett, J., & Parnell, A. (2008). A simple monotone process with application to radiocarbon-dated depth chronologies. Journal of the Royal Statistical Society: Series C (Applied Statistics), 57(4), 399–418. https://doi.org/10.1111/j.1467-9876.2008.00623.x

Hawkes, C. V., Shinada, M., & Kivlin, S. N. (2020). Historical climate legacies on soil respiration persist despite extreme changes in rainfall. Soil Biology and Biochemistry, 143, 107752. https://doi.org/10.1016/j.soilbio.2020.107752

Hogg, A. G., Heaton, T. J., Hua, Q., Palmer, J. G., Turney, C. S., Southon, J., Bayliss, A., Blackwell, P. G., Boswijk, G., Bronk Ramsey, C., Pearson, C., Petchey, F., Reimer, P., Reimer, R., & Wacker, L. (2020). SHCal20 southern hemisphere calibration, 0–55,000 Years cal BP. Radiocarbon, 62(4), 759–778. https://doi.org/10.1017/RDC.2020.59

Iturbide, Maialen, Fernández, Jesús, Gutiérrez, José Manuel, Bedia, Joaquín, Cimadevilla, Ezequiel, Díez-Sierra, Javier, Manzanas, Rodrigo, Casanueva, Ana, Baño-Medina, Jorge, Milovac, Josipa, Herrera, Sixto, Cofiño, Antonio S., San Martín, Daniel, García-Díez, Markel, Hauser, Mathias, Huard, David, & Yelekci, Özge. (2021). Repository supporting the implementation of FAIR principles in the IPCC-WGI Atlas (v2.0-final) [Computer software]. Zenodo. https://doi.org/10.5281/ZENODO.3691645

Janzen, D. H. (1967). Why mountain passes are higher in the tropics. The American Naturalist, 101(919), 233–249.

Jump, A. S., & Peñuelas, J. (2005). Running to stand still: Adaptation and the response of plants to rapid climate change. Ecology Letters, 8(9), 1010–1020. https://doi.org/10.1111/j.1461-0248.2005.00796.x

Karger, D. N., Nobis, M. P., Normand, S., Graham, C. H., & Zimmermann, N. E. (2021). CHELSA-TraCE21k v1.0. Downscaled transient temperature and precipitation data since the last glacial maximum [Preprint]. Climate Modelling/Modelling only/Holocene. https://doi.org/10.5194/cp-2021-30

Kay, M. (2022). tidybayes: Tidy Data and Geoms for Bayesian Models (v3.0.2) [Computer software]. Zenodo. https://doi.org/10.5281/ZENODO.1308151

Kelly, A. E., & Goulden, M. L. (2008). Rapid shifts in plant distribution with recent climate change. Proceedings of the National Academy of Sciences, 105(33), 11823–11826. https://doi.org/10.1073/pnas.0802891105

Koven, C. D. (2013). Boreal carbon loss due to poleward shift in low-carbon ecosystems. Nature Geoscience, 6(6), 452–456. https://doi.org/10.1038/ngeo1801

Kruschke, J. K. (2018). Rejecting or accepting parameter values in Bayesian estimation. Advances in Methods and Practices in Psychological Science, 1(2), 270–280.

Lawrence, J., Blackett, P., & Cradock-Henry, N. A. (2020). Cascading climate change impacts and implications. Climate Risk Management, 29, 100234. https://doi.org/10.1016/j.crm.2020.100234

Mathes, G. H., Kiessling, W., & Steinbauer, M. J. (2021). Deep-time climate legacies affect origination rates of marine genera. Proceedings of the National Academy of Sciences, 118(36), e2105769118. https://doi.org/10.1073/pnas.2105769118

Mathes, G. H., van Dijk, J., Kiessling, W., & Steinbauer, M. J. (2021). Extinction risk controlled by interaction of long-term and short-term climate change. Nature Ecology & Evolution, 5(3), 304–310. https://doi.org/10.1038/s41559-020-01377-w

Mayle, F. E., Beerling, D. J., Gosling, W. D., & Bush, M. B. (2004). Responses of Amazonian ecosystems to climatic and atmospheric carbon dioxide changes since the last glacial maximum. Philosophical Transactions of the Royal Society of London. Series B: Biological Sciences, 359(1443), 499–514. https://doi.org/10.1098/rstb.2003.1434

McElreath, R. (2020). Statistical Rethinking, 2nd Edition. https://learning.oreilly.com/library/view/-/9780429639142/?ar

Monger, C., Sala, O. E., Duniway, M. C., Goldfus, H., Meir, I. A., Poch, R. M., Throop, H. L., & Vivoni, E. R. (2015). Legacy effects in linked ecological–soil–geomorphic systems of drylands. Frontiers in Ecology and the Environment, 13(1), 13–19. https://doi.org/10.1890/140269

Mottl, O., Flantua, S. G. A., Bhatta, K. P., Felde, V. A., Giesecke, T., Goring, S., Grimm, E. C., Haberle, S., Hooghiemstra, H., Ivory, S., Kuneš, P., Wolters, S., Seddon, A. W. R., & Williams, J. W. (2021). Global acceleration in rates of vegetation change over the past 18,000 years. Science, 372(6544), 860–864. https://doi.org/10.1126/science.abg1685

Mottl, O., Grytnes, J.-A., Seddon, A. W. R., Steinbauer, M. J., Bhatta, K. P., Felde, V. A., Flantua, S. G. A., & Birks, H. J. B. (2020). R-Ratepol package. https://github.com/HOPE-UIB-BIO/R-Ratepol-package

Mottl, O., Grytnes, J.-A., Seddon, A. W. R., Steinbauer, M. J., Bhatta, K. P., Felde, V. A., Flantua, S. G. A., & Birks, H. J. B. (2021). Rate-of-change analysis in paleoecology revisited: A new approach. Review of Palaeobotany and Palynology, 293, 104483. https://doi.org/10.1016/j.revpalbo.2021.104483

Ogle, K., Barber, J. J., Barron‐Gafford, G. A., Bentley, L. P., Young, J. M., Huxman, T. E., Loik, M. E., & Tissue, D. T. (2015). Quantifying ecological memory in plant and ecosystem processes. Ecology Letters, 18(3), 221–235. https://doi.org/10.1111/ele.12399

Pugh, T. A. M., Müller, C., Elliott, J., Deryng, D., Folberth, C., Olin, S., Schmid, E., & Arneth, A. (2016). Climate analogues suggest limited potential for intensification of production on current croplands under climate change. Nature Communications, 7(1), 12608. https://doi.org/10.1038/ncomms12608

R Core Team. (2021). R: A Language and Environment for Statistical Computing (4.1.2) [R]. R Foundation for Statistical Computing. https://www.R-project.org/

Reimer, P. J., Austin, W. E. N., Bard, E., Bayliss, A., Blackwell, P. G., Bronk Ramsey, C., Butzin, M., Cheng, H., Edwards, R. L., Friedrich, M., Grootes, P. M., Guilderson, T. P., Hajdas, I., Heaton, T. J., Hogg, A. G., Hughen, K. A., Kromer, B., Manning, S. W., Muscheler, R., … Talamo, S. (2020). The IntCal20 northern hemisphere radiocarbon age calibration curve (0–55 cal kBP). Radiocarbon, 62(4), 725–757. https://doi.org/10.1017/RDC.2020.41

Riahi, K., van Vuuren, D. P., Kriegler, E., Edmonds, J., O'Neill, B. C., Fujimori, S., Bauer, N., Calvin, K., Dellink, R., Fricko, O., Lutz, W., Popp, A., Cuaresma, J. C., Kc, S., Leimbach, M., Jiang, L., Kram, T., Rao, S., Emmerling, J., … Tavoni, M. (2017). The Shared Socioeconomic Pathways and their energy, land use, and greenhouse gas emissions implications: An overview. Global Environmental Change, 42, 153–168. https://doi.org/10.1016/j.gloenvcha.2016.05.009

Scheffer, M., Bascompte, J., Brock, W. A., Brovkin, V., Carpenter, S. R., Dakos, V., Held, H., van Nes, E. H., Rietkerk, M., & Sugihara, G. (2009). Early-warning signals for critical transitions. Nature, 461(7260), 53–59. https://doi.org/10.1038/nature08227

Sheldon, K. S., Huey, R. B., Kaspari, M., & Sanders, N. J. (2018). Fifty years of mountain passes: A perspective on Dan Janzen's classic article. The American Naturalist, 191(5), 553–565.

Smith, S. J., Edmonds, J., Hartin, C. A., Mundra, A., & Calvin, K. (2015). Near-term acceleration in the rate of temperature change. Nature Climate Change, 5(4), 333–336. https://doi.org/10.1038/nclimate2552

Spencer, H. G. (2020). Beyond Equilibria: The Neglected Role of History in Ecology and Evolution. The Quarterly Review of Biology, 95(4), 311–321. https://doi.org/10.1086/711803

Staples, T. L., Kiessling, W., & Pandolfi, J. M. (2022). Emergence patterns of locally novel plant communities driven by past climate change and modern anthropogenic impacts. Ecology Letters.

Steffen, W., Broadgate, W., Deutsch, L., Gaffney, O., & Ludwig, C. (2015). The trajectory of the Anthropocene: The Great Acceleration. The Anthropocene Review, 2(1), 81–98. https://doi.org/10.1177/2053019614564785

Stephens, L., Fuller, D., Boivin, N., Rick, T., Gauthier, N., Kay, A., Marwick, B., Armstrong, C. G., Barton, C. M., Denham, T., Douglass, K., Driver, J., Janz, L., Roberts, P., Rogers, J. D., Thakar, H., Altaweel, M., Johnson, A. L., Sampietro Vattuone, M. M., … Ellis, E. (2019). Archaeological assessment reveals Earth’s early transformation through land use. Science, 365(6456), 897–902. https://doi.org/10.1126/science.aax1192

Strickland, M. S., Keiser, A. D., & Bradford, M. A. (2015). Climate history shapes contemporary leaf litter decomposition. Biogeochemistry, 122(2–3), 165–174. https://doi.org/10.1007/s10533-014-0065-0

Svenning, J.-C., Eiserhardt, W. L., Normand, S., Ordonez, A., & Sandel, B. (2015). The influence of paleoclimate on present-day patterns in biodiversity and ecosystems. Annual Review of Ecology, Evolution, and Systematics, 46(1), 551–572. https://doi.org/10.1146/annurev-ecolsys-112414-054314

Svenning, J.-C., Fløjgaard, C., Marske, K. A., Nógues-Bravo, D., & Normand, S. (2011). Applications of species distribution modeling to paleobiology. Quaternary Science Reviews, 30(21–22), 2930–2947.

Urban, M. C. (2015). Accelerating extinction risk from climate change. Science, 348(6234), 571–573. https://doi.org/10.1126/science.aaa4984

Vehtari, A., Gelman, A., & Gabry, J. (2017). Practical Bayesian model evaluation using leave-one-out cross-validation and WAIC. Statistics and Computing, 27(5), 1413–1432.

Warren, R., VanDerWal, J., Price, J., Welbergen, J. A., Atkinson, I., Ramirez-Villegas, J., Osborn, T. J., Jarvis, A., Shoo, L. P., Williams, S. E., & Lowe, J. (2013). Quantifying the benefit of early climate change mitigation in avoiding biodiversity loss. Nature Climate Change, 3(7), 678–682. https://doi.org/10.1038/nclimate1887

Wickham, H., Averick, M., Bryan, J., Chang, W., McGowan, L. D., François, R., Grolemund, G., Hayes, A., Henry, L., & Hester, J. (2019). Welcome to the Tidyverse. Journal of Open Source Software, 4(43), 1686.

Wiens, J. J., Ackerly, D. D., Allen, A. P., Anacker, B. L., Buckley, L. B., Cornell, H. V., Damschen, E. I., Jonathan Davies, T., Grytnes, J.-A., Harrison, S. P., Hawkins, B. A., Holt, R. D., McCain, C. M., & Stephens, P. R. (2010). Niche conservatism as an emerging principle in ecology and conservation biology: Niche conservatism, ecology, and conservation. Ecology Letters, 13(10), 1310–1324. https://doi.org/10.1111/j.1461-0248.2010.01515.x

Wiens, J. J., & Graham, C. H. (2005). Niche conservatism: Integrating evolution, ecology, and conservation biology. Annual Review of Ecology, Evolution, and Systematics, 36(1), 519–539. https://doi.org/10.1146/annurev.ecolsys.36.102803.095431

Williams, J. W., Grimm, E. C., Blois, J. L., Charles, D. F., Davis, E. B., Goring, S. J., Graham, R. W., Smith, A. J., Anderson, M., Arroyo-Cabrales, J., Ashworth, A. C., Betancourt, J. L., Bills, B. W., Booth, R. K., Buckland, P. I., Curry, B. B., Giesecke, T., Jackson, S. T., Latorre, C., … Takahara, H. (2018). The Neotoma Paleoecology Database, a multiproxy, international, community-curated data resource. Quaternary Research, 89(1), 156–177. https://doi.org/10.1017/qua.2017.105

Williams, J. W., Jackson, S. T., & Kutzbach, J. E. (2007). Projected distributions of novel and disappearing climates by 2100 AD. Proceedings of the National Academy of Sciences, 104(14), 5738–5742. https://doi.org/10.1073/pnas.0606292104

Wu, D., Zhao, X., Liang, S., Zhou, T., Huang, K., Tang, B., & Zhao, W. (2015). Time-lag effects of global vegetation responses to climate change. Global Change Biology, 21(9), 3520–3531. https://doi.org/10.1111/gcb.12945

Zscheischler, J., Westra, S., van den Hurk, B. J. J. M., Seneviratne, S. I., Ward, P. J., Pitman, A., AghaKouchak, A., Bresch, D. N., Leonard, M., Wahl, T., & Zhang, X. (2018). Future climate risk from compound events. Nature Climate Change, 8(6), 469–477. https://doi.org/10.1038/s41558-018-0156-3

Acknowledgements

This work was supported by the European Research Council (Grant No. 741413/ Humans on Planet Earth), the Deutsche Forschungsgemeinschaft (KI 806/16-1 and STE 2360/2-1/ FOR 2332: Temperature-related stressors as a unifying principle in ancient extinctions), and the Trond Mohn Stiftelse (TMS) and University of Bergen (Grant No. TMS2022STG03/ Past, Present and Future of Alpine Biomes Worldwide)

Data and code availability

All code files wil be made publicly available at https://github.com/HOPE-UIB-BIO/HOPE_Climate_legacies upon acceptance of the manuscript. All data and code are available for reviewers.

Competing interests

The authors declare no competing interests.

Extended Data

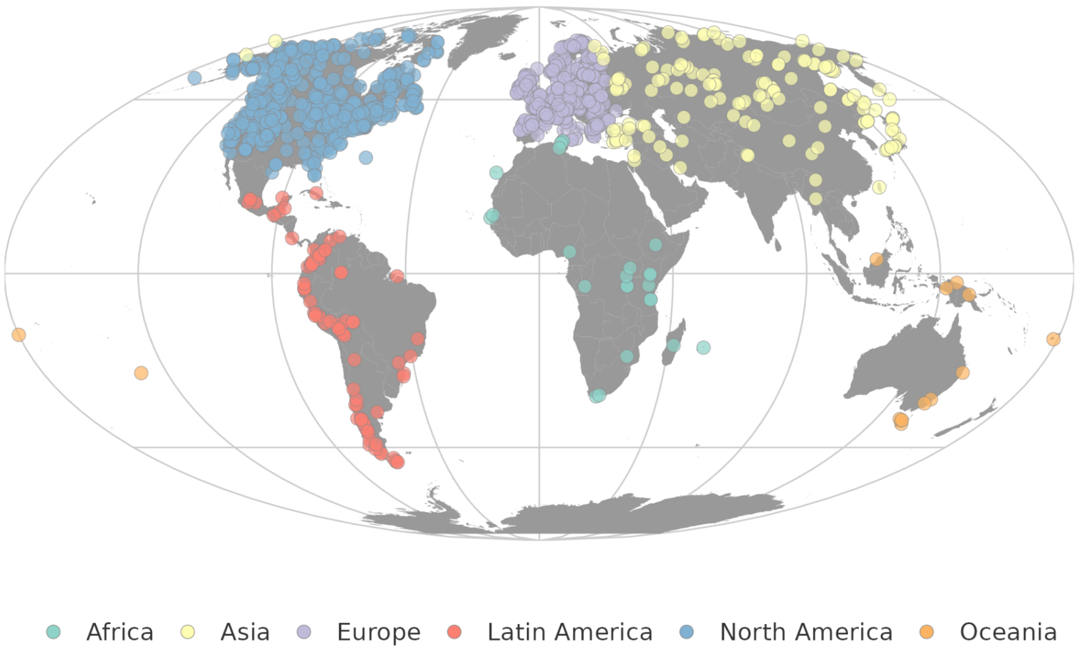

Extended Data Fig. 1: Spatial distribution of pollen sequences used in this work. Fossil pollen data were obtained from the Neotoma Paleoecology Database and filtered to reduce sampling biases (see Materials and Methods and Extended Data Table 1).

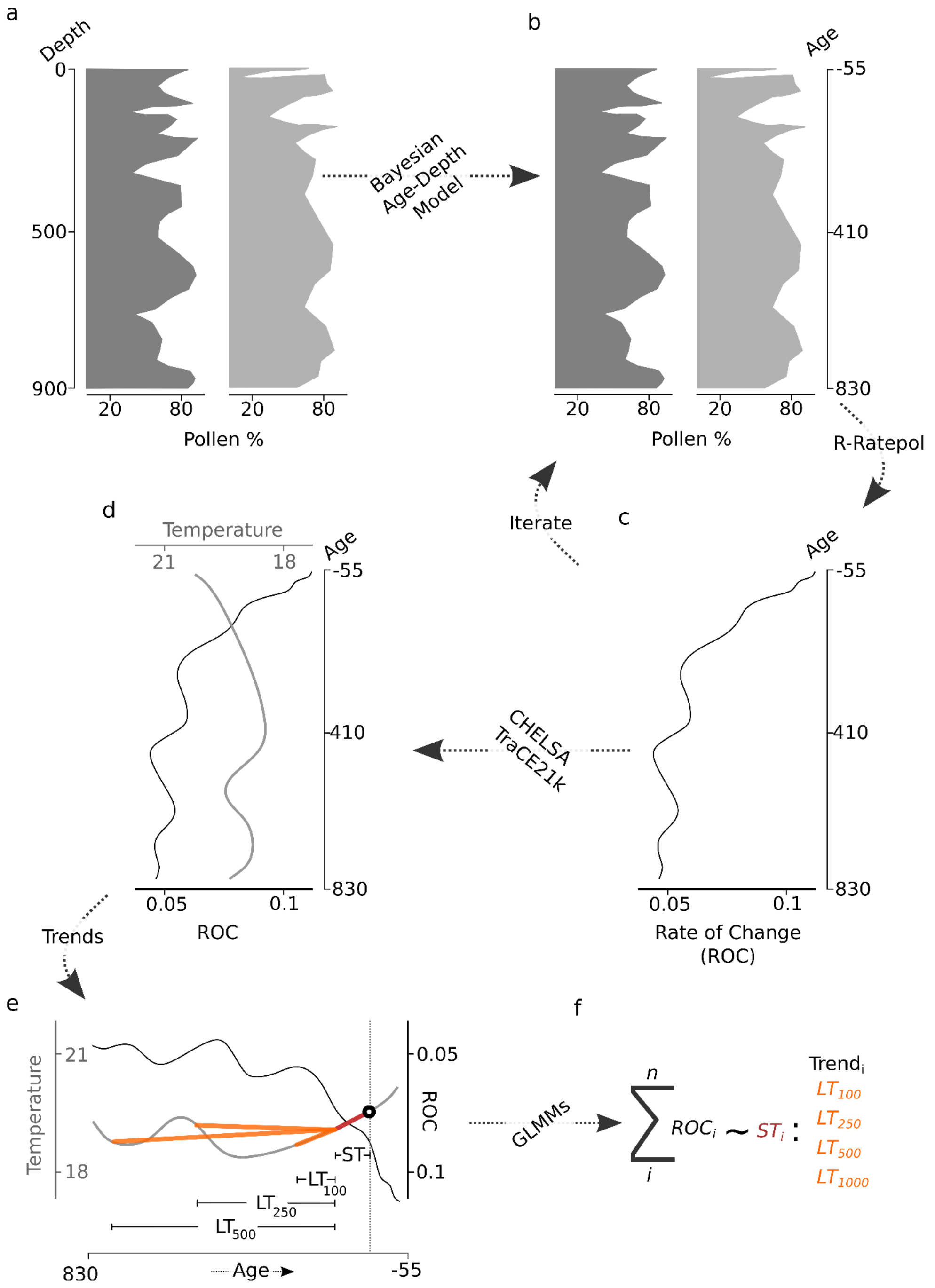

Extended Data Fig. 2: Methodological workflow (see Methods section as well). (a) Pollen sequences are harmonised taxonomically per continent (except for Africa). (b) For each sequence, we construct a Bayesian age-depth model to generate 1000 possible age estimates for all sample depths at the original sampling resolution. (c) We sample aged estimates for each sample depth in a pollen sequence and calculate the rate of change (RoC) score for each depth via the R-Ratepol package(Mottl et al., 2020). We repeat this whole procedure from the age estimate sampling to the rate calculation 1000 times and subsequently calculate the median

RoC as well as the standard deviation for each depth in a focal pollen sequence. (d) Mean annual air temperature for each sample depth in a pollen sequence is calculated via the CHELSA-TraCE21k downscaling algorithm using the median age estimate from the Bayesian age-depth model and the coordinates of the site. (e) We then calculate long-term trends for each sample depth (depicted by the black point) in the pollen sequence with varying lengths (depicted by the orange lines). Additionally, we calculate a short-term temperature change spanning 100 years (depicted by the red line). (f) In a time-continuous analysis, we then regress the RoC at the sample depth i of the pollen sequence against the interaction of the short-term change with the long-term trend of the focal sample depth. For this, we use generalised linear hierarchical models (GLHMs) with a beta error distribution and a log-link, accounting for the underlying data structure via random effects on the pollen sequence nested within a climate class nested within a continent.

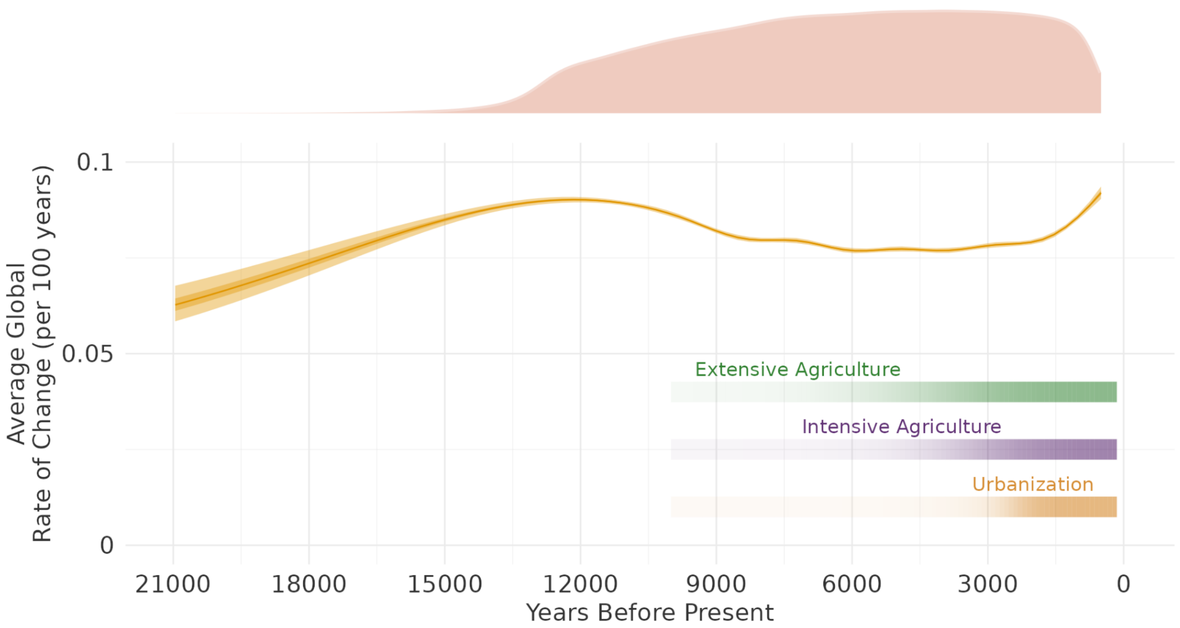

Extended Data Fig. 3: The calculated median global rate of vegetation change over time. The dark yellow line depicts the average trend and the yellow shading the 55% and 95% credible intervals. The distribution on the top shows the marginal distribution of observations over time. Coloured rectangles depict anthropogenic changes during the past 10,000 years estimated from archaeological expert elicitation(Stephens et al., 2019).

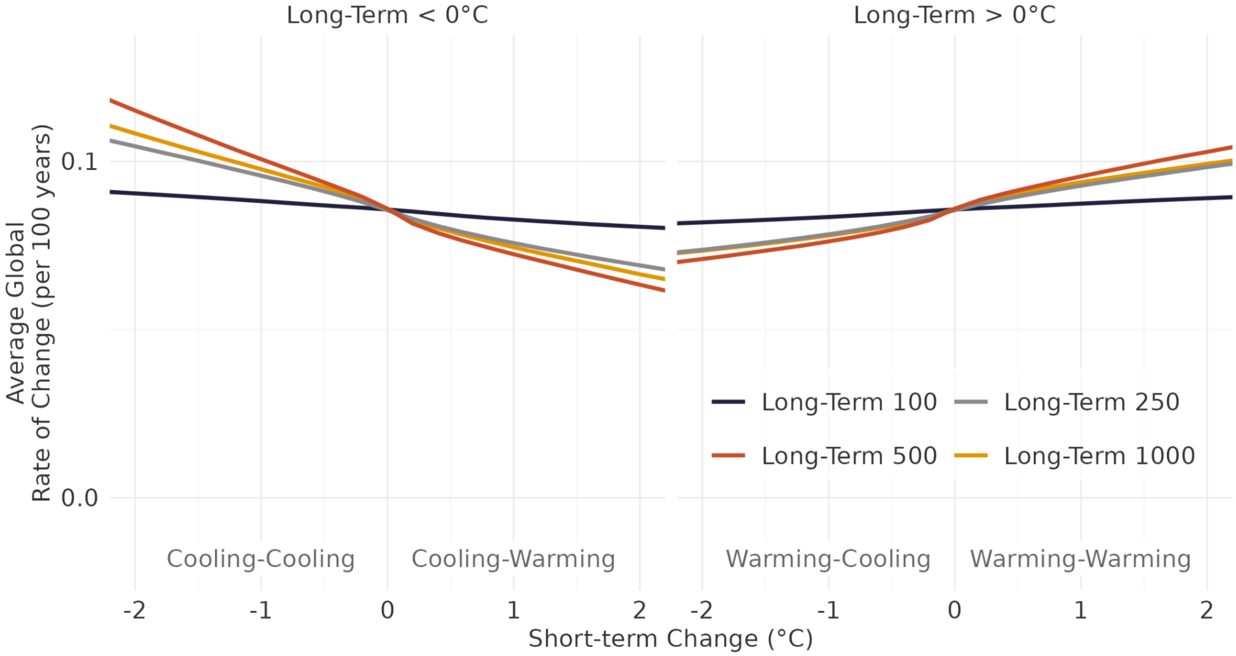

Extended Data Fig. 4: Estimated median trend lines for the global rate of change (RoC) score as a function of long-term temperature interacting with a short-term change. Model predictions for the RoC along a gradient of short-term temperature changes, for both long-term cooling (Long-Term < 0°C) and long-term warming (Long-Term > 0°C), based on a grid of equally spaced short-term changes from -2°C to 2°C with equally spaced long-term trends similarly ranging from -2°C to 2°C. Lines show median trends for models with varying length of long-term trends, ranging from 100 to 1000 years.

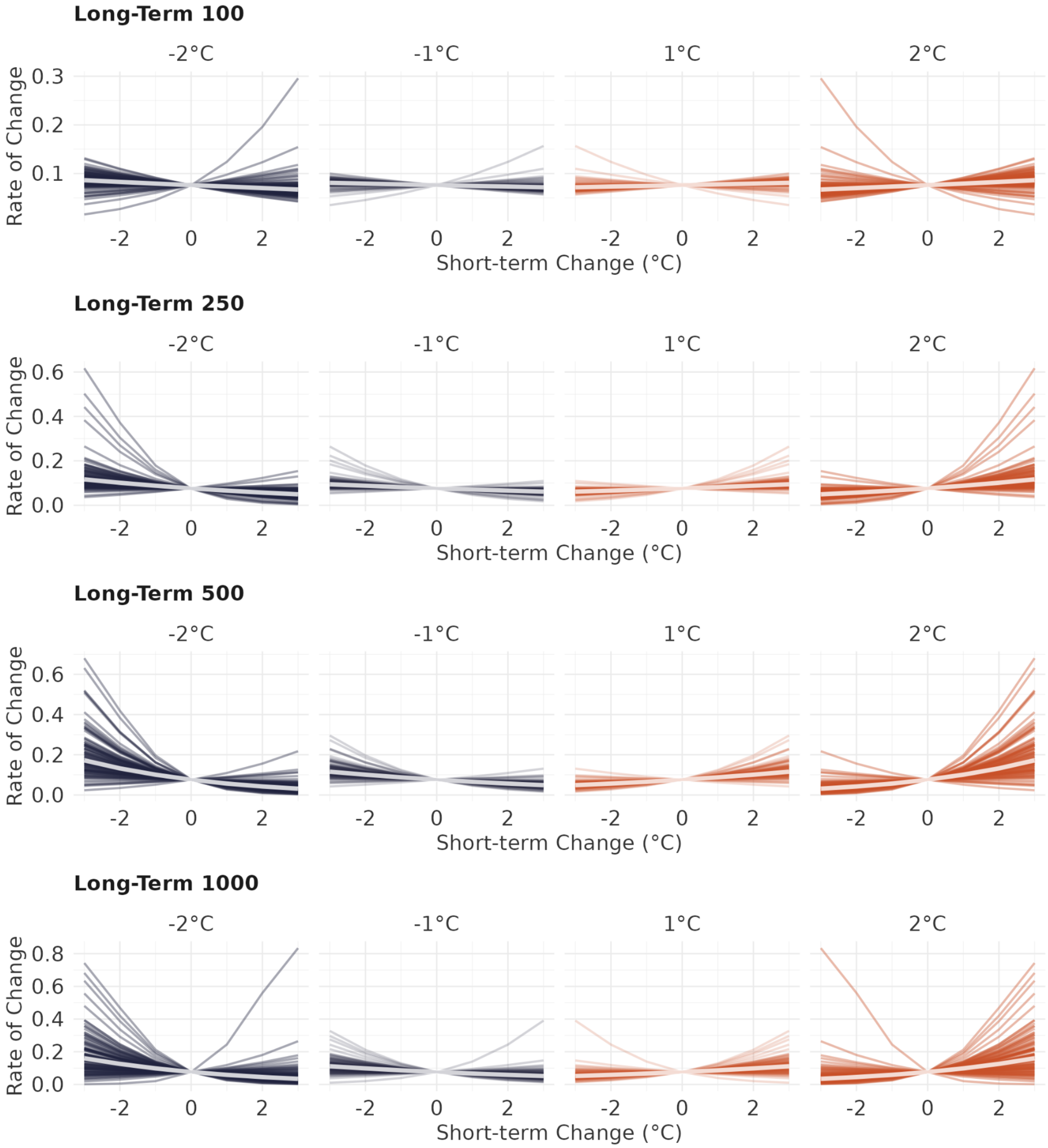

Extended Data Fig. 5: Individual model estimates for the global rate of change (RoC) over a grid of equally spaced short-term changes from -2°C to 2°C with equally spaced long-term trends similarly ranging from -2°C to 2°C. Coloured lines are 100 draws from the posterior for each model, and the thicker grey line shows the median trend averaged over all draws. Estimates are based on models with varying length of long-term trends, ranging from 100 to 1000 years.

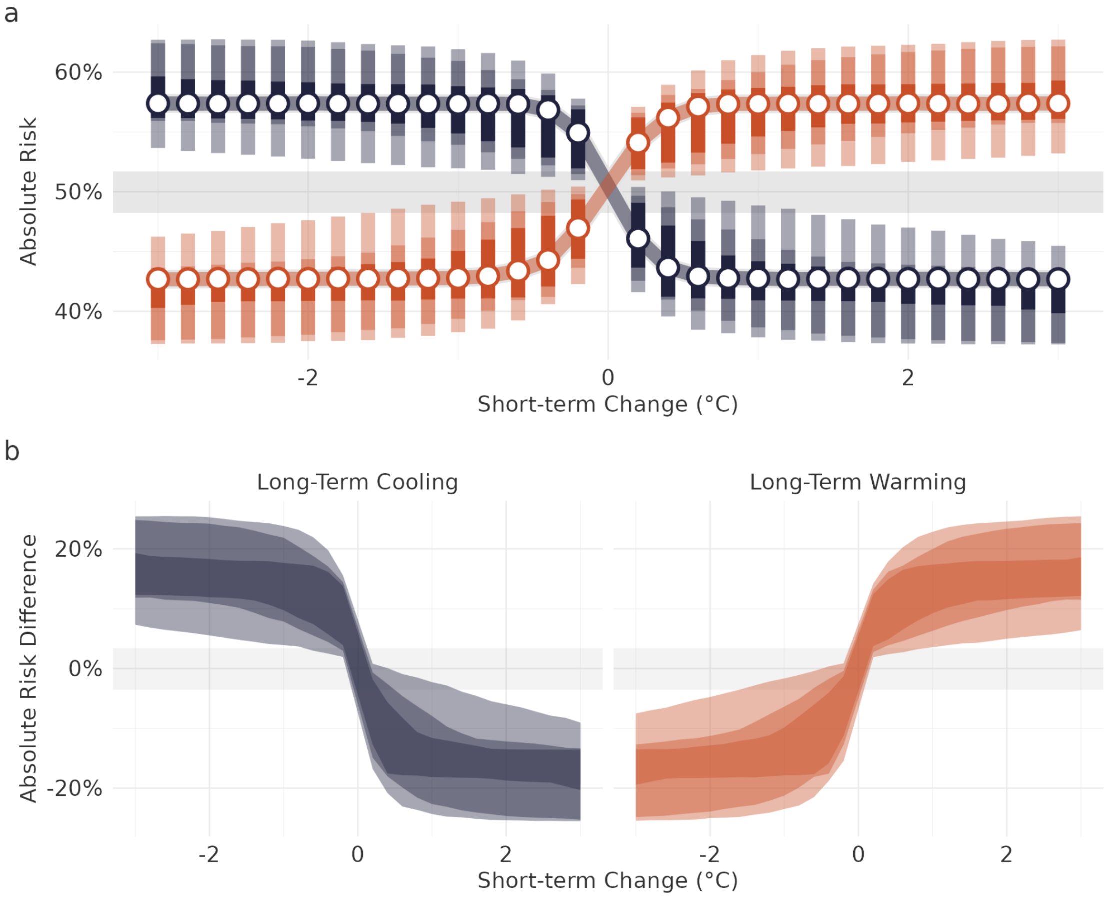

Extended Data Fig. 6: Absolute risk and difference in absolute risk for plant assemblages to shift into high turnover state for all climate interactions. (a) The absolute risk conditional on the long-term temperature trend and a grid of short-term temperature change. Long-term warming is illustrated in red, and long-term cooling in blue. The points show the average absolute risk to shift into high turnover, the dark shaded areas show the 55% credible intervals, and the lighter shaded areas the 95% credible intervals. (b) The difference in absolute risk between long-term cooling and long-term warming, conditional on short-term changes. During synergistic climate interactions (long-term cooling adding to a short-term cooling, and long-term warming adding to a short-term warming), the risk is substantially increased. On the contrary, the risk to shift into high turnover is low for antagonistic climate interactions (long-term cooling adding to a short-term warming, and long-term warming adding to a short-term cooling). Red shaded areas show the long-term warming, and blue areas the long-term cooling trend. Darker shaded areas depict the 55% credible interval, and lighter shaded areas the 95% credible interval. The grey area shows the region of practical equivalence.

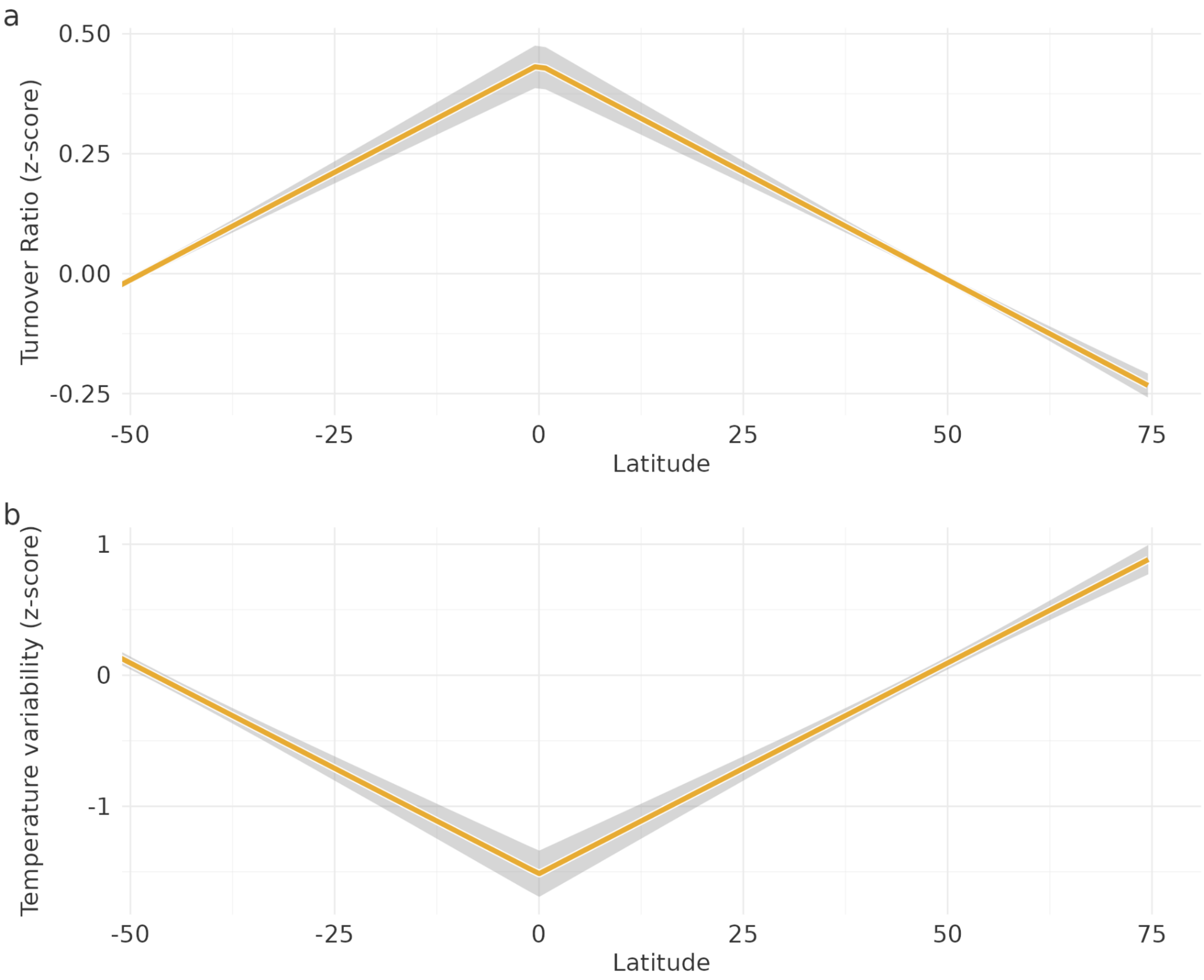

Extended Data Fig. 7: Estimated relationship between turnover ratio (ratio of high to low turnover events) and temperature variability to test whether species experiencing less temperature variability are more susceptible to climate interactions. (a) The relationship between standardised turnover ratio and latitude of each pollen sequence. (b) The relationship between the standard deviation in short-term temperature change across the whole sequence (temperature variability, standardised) and latitude. Coloured lines show the average trend and the grey area the 95% credible interval around this trend. Trends were estimated via a Bayesian regression with a gaussian distribution.

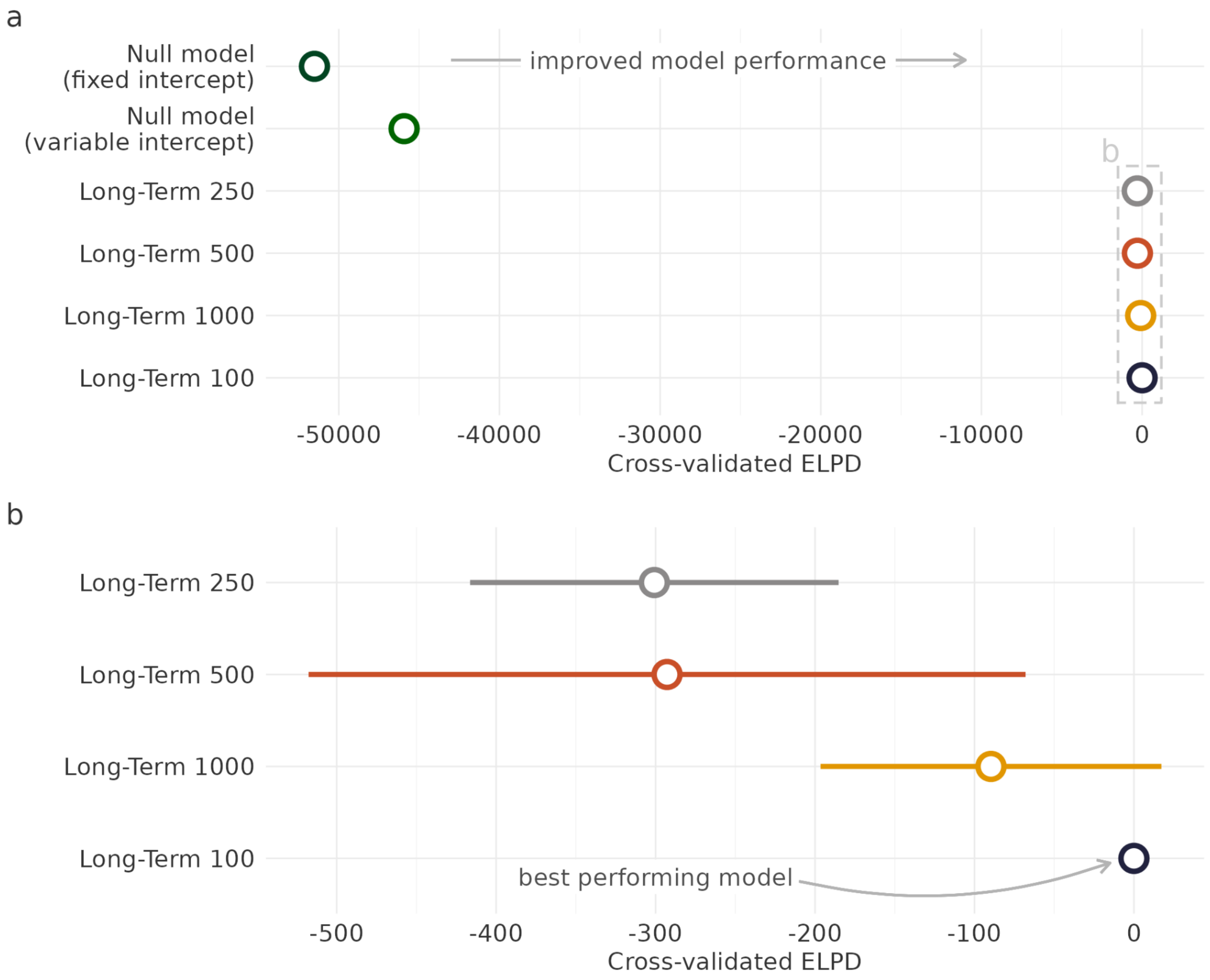

Extended Data Fig. 8: Model comparison for the models where the rate of change was regressed against the interaction of a short-term temperature change (spanning 100 years) with a long-term temperature trend. The comparison was conducted via the expected log predictive density (ELPD) of a model calculated via leave-one-out cross-validation. Each model was compared to the best performing model (which has a cross-validated ELPD of zero accordingly), with a higher divergence indicating a lower model performance.

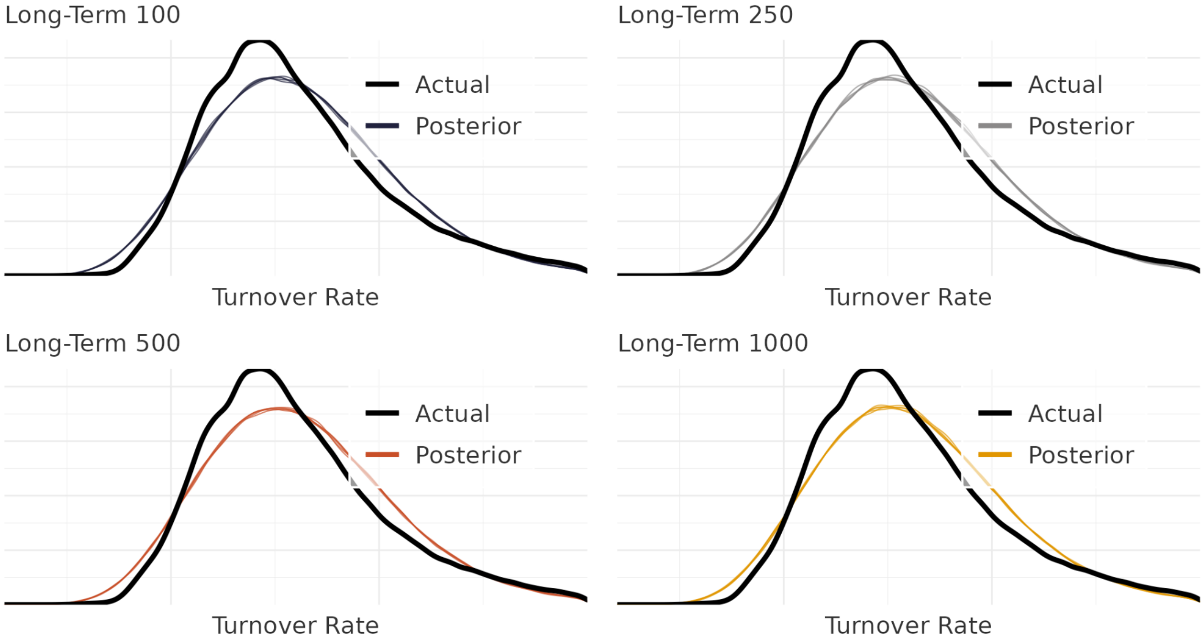

Extended Data Fig. 9: Graphical posterior predictive checks for all full models. The thick dark line depicts the distribution of the actual rate of vegetation change. The thinner coloured lines show 5 kernel density estimates generated from the posterior predictive distribution. The posterior predictive draws follow the actual rate of assemblage change distribution closely for all models, indicating a good fit to the data.

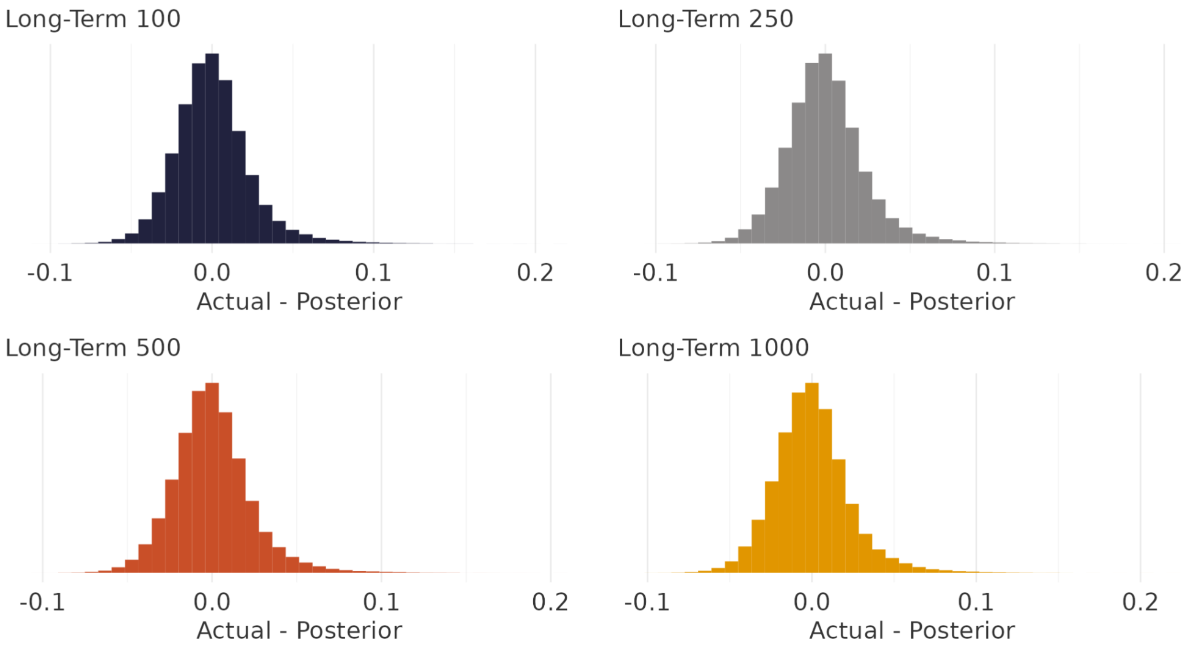

Extended Data Fig. 10: Graphical posterior predictive checks for all full models. The coloured histograms show the distribution for the contrast between the actual turnover rate and a draw from the posterior predictive distribution for all models. The histograms therefore depict the distribution of predictive errors. The errors are normally distributed for all models and generally low, indicating a good fit to the data.

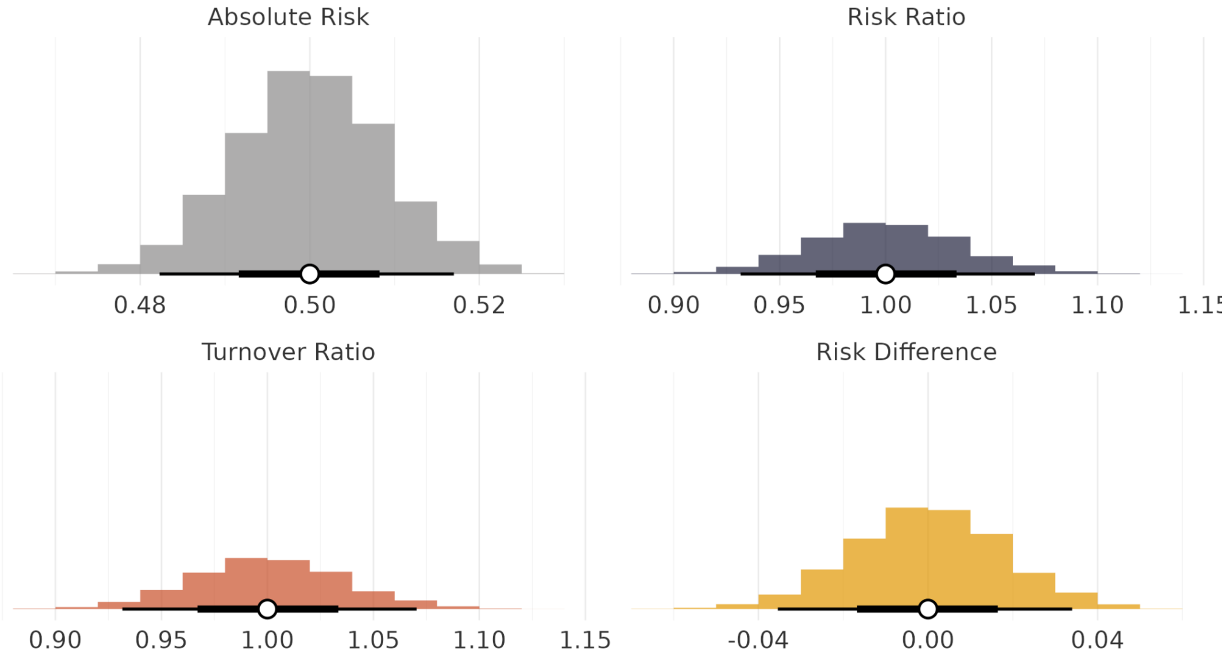

Extended Data Fig. 11: The region of practical equivalence (ROPE) for all risk metrics. The ROPE indicates a range of parameter values that are practically equivalent to the null values, which in this case corresponds to an equal risk after synergistic and antagonistic climate interactions. The coloured histograms show the distribution of simulated metric values. The points depict the median value for the focal ROPE of the metric, the thicker black line is the 55% credible interval, and the thinner black line is the 95% credible interval.

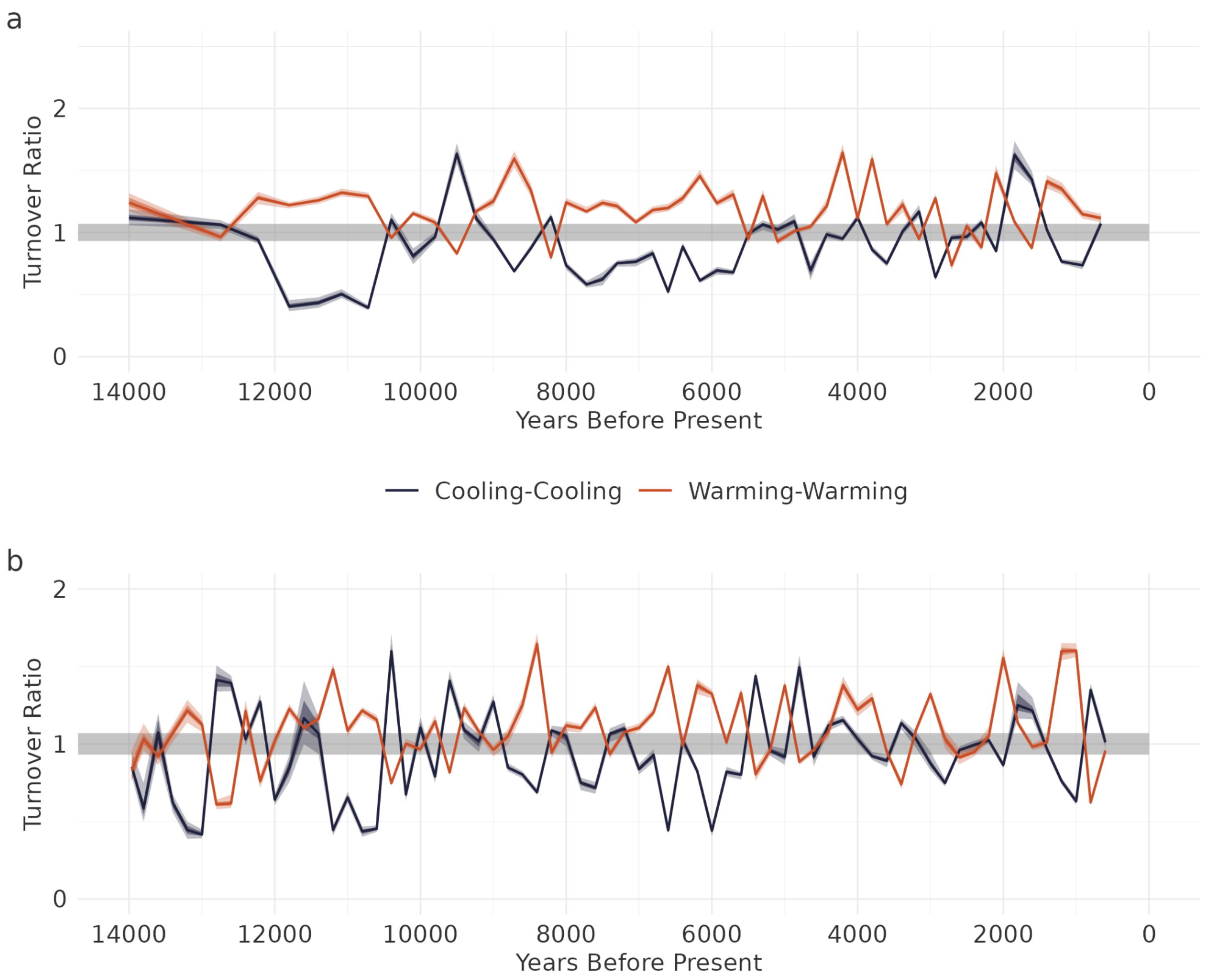

Extended Data Fig. 12: Temporal trend of the turnover ratio after synergistic climate interactions during the past 14,000 years (data for ages between 21 and 14 ka were insufficient to calculate robust estimates for the turnover ratio). The blue lines show the trend after cooling-cooling climate interactions, and the red lines after warming-warming climate interactions. Shaded lines indicate the 95% credible intervals per climate interaction. The shaded grey areas illustrate the region of practical equivalence (ROPE), which covers a range of turnover ratio values generated from null models. (a) All observations assigned to bins with a varying width so that each bin covered approximately the same number of observations. (b) All observations assigned to bins with equal width.

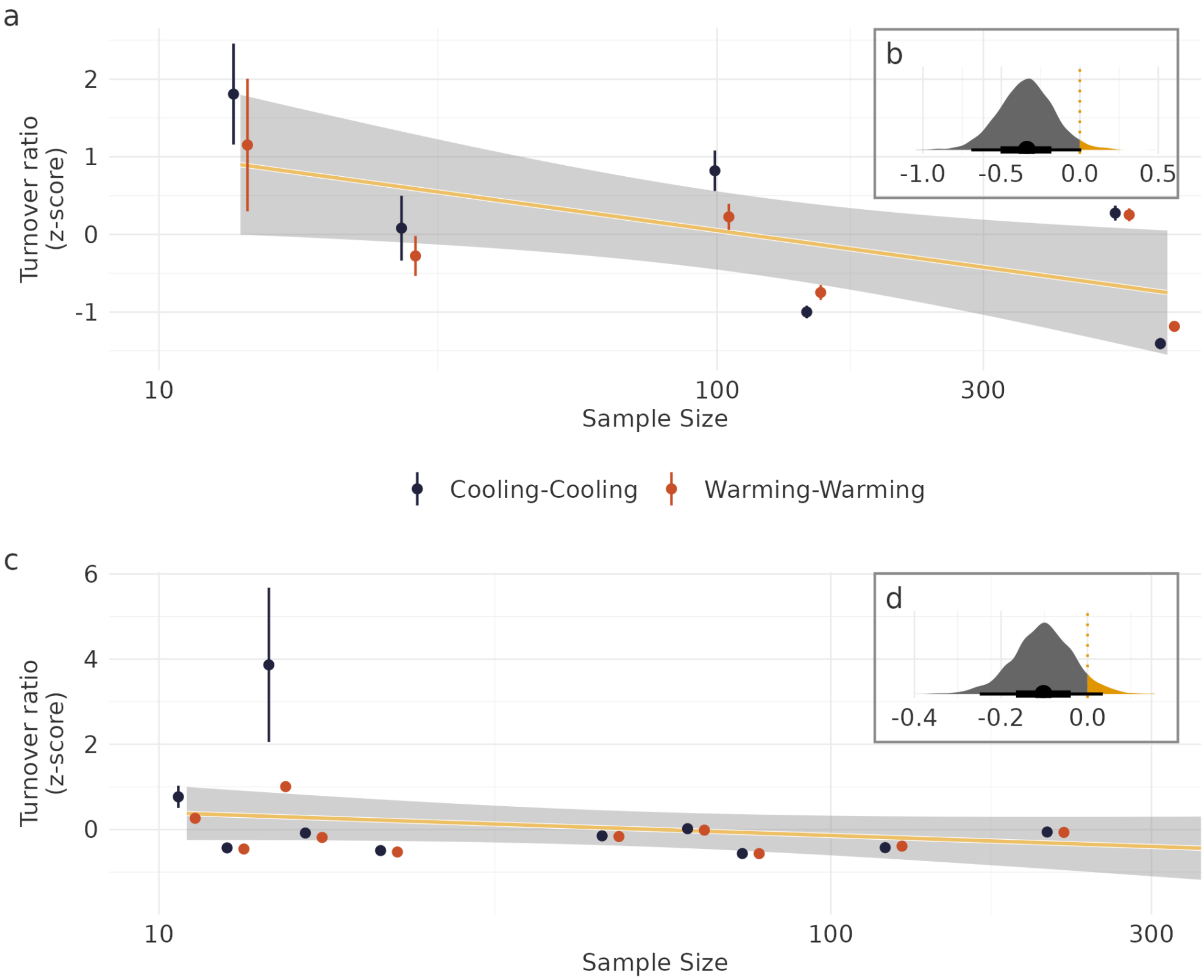

Extended Data Fig. 13: The estimated turnover ratio as a function of actual sample size. (a) The relationship between the turnover ratio per continent and the number of samples per continent. (b) The posterior estimate for the change in the turnover ratio per continent if the sample size is increased by one magnitude. (c) The relationship between the turnover ratio per climate class and the number of samples per climate class. (b) The posterior estimate for the change in the turnover ratio per climate class if the sample size is increased by one magnitude.

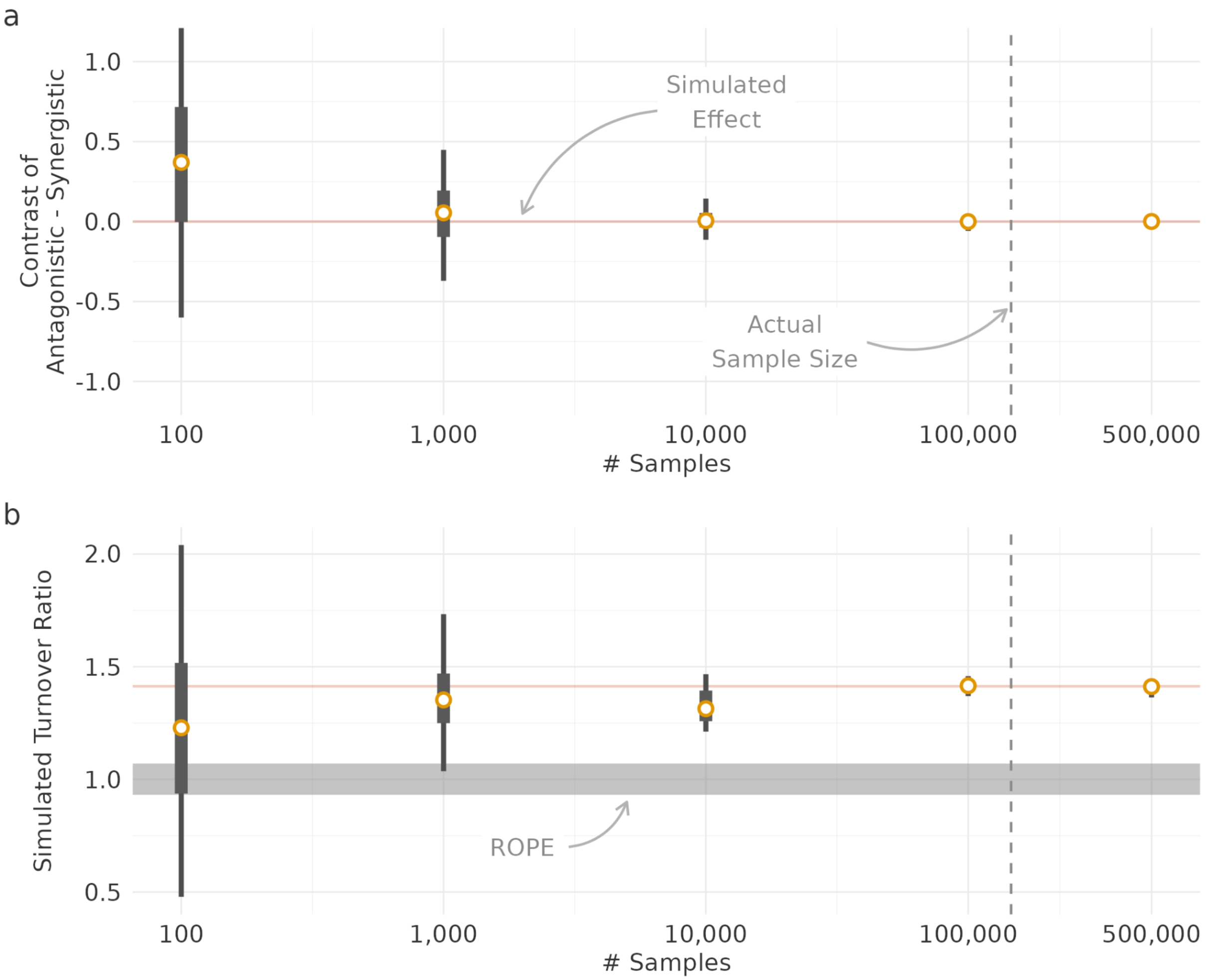

Extended Data Fig. 14: Power simulation as a function of sample size. Points show the median estimate for the effect based on models, and the thick grey line the 55% credible interval, and the thin grey line the 95% credible interval. (a) The simulated null effect is shown as the red line. Using simulated data based on this null effect, we fitted distributional models on a subset of the data and estimated the effect post hoc. This enabled us to quantify the minimum number of samples required to correctly assess an effect of zero, as well as the type I error rate (concluding a substantial difference when there is actually none, false positives) for our actual sample size (depicted by the dashed grey line). (b) We then simulated an effect similar to our actual results (a turnover ratio around 1.34 for synergistic climate interactions compared to antagonistic interactions, depicted by the red line). Again, we then subsampled the data and fitted distributional models. Comparing the range of the credible intervals based on model estimates to a range of values with practical equivalence (ROPE, shaded grey area) enabled us to assess the minimum number of samples to correctly assess the alternative effect. This similarly shows the type II error rate (concluding no difference when there is actually one, false positives) as a function of sample size.

Extended Data Table 1: Number of pollen sequences used in this work within continents and within climate classes.

Continent	**# Sequences**	**Climate Class**	**# Sequences**
Africa	28	Arid Desert	2
		Arid Steppe	4
		Polar Tundra	2
		Temperate Dry Summer	10
		Temperate Dry Winter	6
		Temperate Without dry season	1
		Tropical Savannah	3
Asia	149	Arid Desert	5
		Arid Steppe	13
		Cold Dry Summer	9
		Cold Dry Winter	22
		Cold Without dry season	76
		Polar Tundra	9
		Temperate Dry Summer	5
		Temperate Dry Winter	4
		Temperate Without dry season	6
Europe	532	Arid Steppe	13
		Cold Dry Summer	5
		Cold Without dry season	323
		Polar Tundra	38
		Temperate Dry Summer	18
		Temperate Without dry season	135

Continent	# Sequences	Climate Class	# Sequences
Latin America	102	Arid Desert	3
		Arid Steppe	3
		Cold Dry Summer	3
		Polar Tundra	32
		Temperate Dry Summer	11
		Temperate Dry Winter	7
		Temperate Without dry season	20
		Tropical Monsoon	6
		Tropical Rainforest	10
		Tropical Savannah	7
North America	641	Arid Desert	3
		Arid Steppe	14
		Cold Dry Summer	59
		Cold Without dry season	456
		Polar Tundra	41
		Temperate Dry Summer	19
		Temperate Without dry season	48
		Tropical Savannah	1
Oceania	14	Cold Without dry season	1
		Polar Tundra	2
		Temperate Without dry season	6
		Tropical Rainforest	5

Extended Data Table 2: All turnover risk metrics for all long-term trends compared to the region of practical equivalence (ROPE). The table shows the median risk estimate with the range of the 95% credible interval in square brackets. The grey values show the range of the ROPE for the focal risk metric.

	Absolute Risk [%]		**Risk Difference [%]**		**Risk Ratio**	
Overall	57 [52, 63]	[48, 52]	15 [3, 25]	[-4, 3]	1.25 [1.07, 1.67]	[0.93, 1.07]
Long-Term 100	54 [51, 56]	[48, 52]	8 [2, 12]	[-4, 3]	1.18 [1.05, 1.28]	[0.93, 1.07]
Long-Term 250	61 [52, 63]	[48, 52]	22 [5, 25]	[-4, 3]	1.57 [1.1, 1.69]	[0.93, 1.07]
Long-Term 500	59 [54, 59]	[48, 52]	17 [8, 18]	[-4, 3]	1.42 [1.18, 1.45]	[0.93, 1.07]
Long-Term 1000	57 [54, 57]	[48, 52]	15 [8, 15]	[-4, 3]	1.34 [1.18, 1.35]	[0.93, 1.07]

Extended Data Table 3: R-hat values for all full models. R-hat indicates the convergence of the Monte Carlo Markov Chains of a model. Values below 1.01 indicate complete convergence (good), values between 1.01 and 1.05 indicate partial convergence (mediocre), and values above 1.05 indicate that some parameters potentially did not converge (bad). All models converged successfully based on these metrics. No R-hat values were above 1.1 (R-hat$_{max}$), supporting the interpretation of good convergence.

	$\hat{R}_{good}$	$\hat{R}_{mediocre}$	$\hat{R}_{bad}$	$\hat{R}_{max}$
Long-Term 100	99.3%	0.7%	0%	1.013
Long-Term 250	99.9%	0.1%	0%	1.013
Long-Term 500	100%	0%	0%	1.01
Long-Term 1000	99.4%	0.6%	0%	1.012

6. Publication record

Record of all publications presented in this thesis:

Flantua, S.G.A., Mottl, O., Felde, V.A., Giesecke, T., Hooghiemstra, H., Irl, S., Lenoir, J., Mathes, G.H., McMichael, C., Seddon, A., Steinbauer, M.J., Tovar, C., Vetaas, O., Birks, H.J.B. & Grytnes, J.A. (2022) The joint world of macroecology and terrestrial palaeoecology. *Global Ecology and Biogeography*, in review

Joachimski, M. M., Müller, J., Gallagher, T. M., Mathes, G.H., Chu, D. L., Mouraviev, F., Silantiev, V., Sun, Y. D., & Tong, J. N. (2022). Five million years of high atmospheric CO2 in the aftermath of the Permian-Triassic mass extinction. *Geology*, *50*(6), 650–654. https://doi.org/10.1130/G49714.1

Mathes, G.H., Kiessling, W., Mottl, O., Flantua, S.G.A., Birks, H.J.B., Grytnes, J.A. & Steinbauer M.J. (2022) Climate legacies accelerated global rates of change in plant assemblages over the last 21000 years. *Nature Communications*, in review

Mathes, G. H., Kiessling, W., & Steinbauer, M. J. (2021). Deep-time climate legacies affect origination rates of marine genera. *Proceedings of the National Academy of Sciences*, *118*(36), e2105769118. https://doi.org/10.1073/pnas.2105769118

Mathes, G.H., Reddin, C.J., Kiessling, W., Antell, G.S., Saupe, E.E. & Steinbauer, M.J. (2022) Nowhere to run: Lagged responses of tropical and polar planktonic foraminifera over 700,000 years of climate change. *Global Ecology and Biogeography*, in submission

Mathes, G. H., van Dijk, J., Kiessling, W., & Steinbauer, M. J. (2021). Extinction risk controlled by interaction of long-term and short-term climate change. *Nature Ecology & Evolution*, *5*(3), 304–310. https://doi.org/10.1038/s41559-020-01377-w

Record of further own publications not used in this thesis:

Mathes, G. H., Steinbauer, M. J., & Cotton, L. (2022). Benthic foraminifera as bioindicators for assessing reef condition in Kāneʻohe Bay, Oʻahu, Hawaiʻi. *Pacific Conservation Biology*. https://doi.org/10.1071/PC21027

Schweizer, A.-M., Leiderer, A., Mitterwallner, V., Walentowitz, A., Mathes, G. H., & Steinbauer, M. J. (2021). Outdoor cycling activity affected by COVID-19 related epidemic-control-decisions. *Plos One*, 16(5), e0249268.

7. Conclusion

> **“Anything that happens, happens.**
> **Anything that, in happening, causes something else to happen, causes something else to happen.**
> **Anything that, in happening, causes itself to happen again, happens again.**
> **It doesn’t necessarily do it in chronological order, though.”**
> *– Douglas Adams*

Understanding the mechanisms that drive taxa into extinction or extirpation is among the most fundamental objectives of ecological research and conservation science (Brook & Alroy, 2017; Dietl & Flessa, 2011; Kerr et al., 2007). One of the fundamental issues for extinction studies using contemporary data is that this data is always dependent on past conditions (Ogle et al., 2015). These climate legacies and their causal effects on biotic systems can only be resolved by means of time series (Sugihara et al., 2012). The fossil record, together with palaeoclimatic data, provides such time series of ecological responses. Studying the fossil record comprises the potential to understand how the biosphere has responded to past climate changes, as well as to quantify the adaptive capacity and vulnerability of ecosystems (Pörtner et al., 2022). Developing macroevolutionary models that integrate those aspects in a single framework is an important goal of conservation science (Lawing & Matzke, 2014; Svenning et al., 2015).

Taking advantage of the fossil record, I was able to develop and test a heuristic framework for the quantification of the effects of climate legacies on ecosystems. In the introduction of this thesis, I identified general mechanisms that cause climate legacies. While these mechanisms are well-known (Svenning et al., 2015), they are rarely integrated in studies on the relationship between extinction risk and climate, as shown by a systematic review of the existing literature. A meta-analysis based on this systematic review, however, has shown that when these effects are included and quantified, large effect sizes were found. To facilitate the quantification of these effects in future research, I therefore developed the concept of climate interactions as a unifying framework. Under this framework, more deleterious extinction dynamics are expected when a short-term change adds to a long-term trend in the same direction (synergistic interaction), in stark contrast to a short-term change opposing the preceding long-term trend (antagonistic interaction). I tested this hypothesis and found evidence for the expected effect in extinction and origination events throughout the Phanerozoic (Manuscript 1 and 3), in migration lags throughout the Quaternary (Manuscript 4), and in compositional turnover of plant assemblages throughout the Holocene (Manuscript 6). To this evidence, I added baseline climate data for the most severe mass extinction event in Earth’s history (Manuscript 2), and provided a framework to combine and integrate contemporary data with past dynamics within ecological systems (Manuscript 5).

In the introduction, I further showed that there exists a conundrum of temperature-induced extinction events throughout the Quaternary (Botkin et al., 2007), where high rates of temperature change caused mass extinctions at most time intervals but not at all intervals. For example, moderate extinction events occurred during the Paleocene-Eocene Thermal Maximum (PETM), despite very high rates of warming (Foster et al., 2018). During the Late Eocene-Oligocene Cooling (LEOC), on the other hand, major biotic turnovers were found despite only a modest cooling trend (Coxall & Pearson, 2007). The framework of climate interactions might provide an explanation to this conundrum. The PETM warming follows a long-term cooling trend throughout the Cretaceous, which is an antagonistic climate interaction with lower extinction risk under the climate interaction framework. The LEOC, however, is added to a long-term cooling trend throughout the Paleogene, which represents a synergistic climate interaction with higher expected extinction risk.

Besides providing insights for past extinction events, the proposed framework of climate interaction can also shed light on future extinction dynamics under anthropogenic climate change. The accelerating warming trend, and therefore increased synergistic climate interactions, might hereby lead to unprecedented impacts on ecosystems (Manuscript 6). Not accounting for climate interactions could blur or even reverse apparent extinction patterns and prevent useful predictions for future scenarios (Manuscript 1). The findings reported in this thesis can thus pave the way for improved assessments of future extinction risk of taxa. Climate interactions comprise a scale-independent framework for the quantification of climate legacies in a variety of biotic systems. Bringing together the findings of the individual research projects of this thesis, with climate interactions covering timescales from 100 to a few million years, can form the basis for future research on extinction dynamics throughout Earth’s history.

“Let the past hold on to itself and let the present move forward into the future.”
– Douglas Adams

8. Acknowledgements

First of all, I would like to thank Manuel Steinbauer for his excellent supervision and mentoring, and his fantastic support throughout the past 5 years. You shaped the way I think about “Life, the Universe, and Everything”, and you equipped me with the necessary tools for an autonomous academic career. You further added another goal to my “bucket list”, as I am aspiring to beat you someday at the donkey-race in Hersbruck.

I am also very grateful to Wolfgang Kießling, similarly for his amazing support and supervision and for many valuable discussions about statistics, research, and science. I have improved my table soccer skills in secret and I am very much looking forward to a re-match in Waischenfeld.

I thank Axel Munnecke for guiding me through my first steps in academic research during my B.Sc. thesis, for sparking my interest in palaeontology, and for being a role model for aspiring scientists.

Rachel Warnock, for her tremendous help during my transition from a PhD student to a PostDoc. My move to Zurich would not have been possible without your advice.

Laura Cotton for guiding me through my first own research project and for helping me through my first academic conference.

I would like to thank the sport ecology team in Bayreuth for integrating a palaeobiologist in their research team, and for many fundamental discussions about the impact of humans in ecological systems.

Similarly, I would like to thank the paleobiology team in Erlangen for integrating a Bayreuth researcher in their team, and for their critical discussion of my research ideas, work, and manuscripts.

I would like to express my gratitude to Jens-Christian Svenning and John Birks and their research teams for being great hosts during my stay in Denmark and Norway.

I thank my whole family for their constant support. Beate and Herbert have allowed me to follow my own career path and I will always be grateful for that.

Above all, I thank my wife Anna Mathes for being the most wonderful person. Nothing of this would have been possible without your support and love.

9. References

AghaKouchak, A., Chiang, F., Huning, L. S., Love, C. A., Mallakpour, I., Mazdiyasni, O., Moftakhari, H., Papalexiou, S. M., Ragno, E., & Sadegh, M. (2020). Climate extremes and compound hazards in a warming world. *Annual Review of Earth and Planetary Sciences*, *48*(1), 519–548. https://doi.org/10.1146/annurev-earth-071719-055228

Anderegg, W. R. L., Plavcova, L., Anderegg, L. D. L., Hacke, U. G., Berry, J. A., & Field, C. B. (2013). Drought's legacy: Hydraulic deterioration underlies widespread aspen die-off and portends increased future vulnerability. *Global Change Biology*, *19*, 1188–1196.

Antell, G. S., Fenton, I. S., Valdes, P. J., & Saupe, E. E. (2021). Thermal niches of planktonic foraminifera are static throughout glacial–interglacial climate change. *Proceedings of the National Academy of Sciences*, *118*(18), e2017105118. https://doi.org/10.1073/pnas.2017105118

Barnosky, A. D., Matzke, N., Tomiya, S., Wogan, G. O., Swartz, B., Quental, T. B., Marshall, C., McGuire, J. L., Lindsey, E. L., & Maguire, K. C. (2011). Has the Earth's sixth mass extinction already arrived? *Nature*, *471*(7336), 51–57.

Beaugrand, G. (2015). Theoretical basis for predicting climate-induced abrupt shifts in the oceans. *Philosophical Transactions of the Royal Society B: Biological Sciences*, *370*(1659), 20130264.

Bence, J. R. (1995). Analysis of short time series: Correcting for autocorrelation. *Ecology*, *76*(2), 628–639.

Benito, B. M., Gil‐Romera, G., & Birks, H. J. B. (2020). Ecological memory at millennial time‐scales: The importance of data constraints, species longevity and niche features. *Ecography*, *43*(1), 1–10. https://doi.org/10.1111/ecog.04772

Benton, M. J. (2018). Hyperthermal-driven mass extinctions: Killing models during the Permian–Triassic mass extinction. *Philosophical Transactions of the Royal Society A: Mathematical, Physical and Engineering Sciences*, *376*(2130), 20170076.

Bolker, B. M., Brooks, M. E., Clark, C. J., Geange, S. W., Poulsen, J. R., Stevens, M. H. H., & White, J.-S. S. (2009). Generalized linear mixed models: A practical guide for ecology and evolution. *Trends in Ecology & Evolution*, *24*(3), 127–135.

Bond, D. P., & Grasby, S. E. (2017). On the causes of mass extinctions. *Palaeogeography, Palaeoclimatology, Palaeoecology*, *478*, 3–29.

Botkin, D. B., Saxe, H., Araujo, M. B., Betts, R., Bradshaw, R. H., Cedhagen, T., Chesson, P., Dawson, T. P., Etterson, J. R., & Faith, D. P. (2007). Forecasting the effects of global warming on biodiversity. *Bioscience*, *57*(3), 227–236.

Brook, B. W., & Alroy, J. (2017). Pattern, process, inference and prediction in extinction biology. In *Biology letters* (Vol. 13, Issue 1, p. 20160828). The Royal Society.

Bunting, E. L., Munson, S. M., & Villarreal, M. L. (2017). Climate legacy and lag effects on dryland plant communities in the southwestern U.S. *Ecological Indicators*, *74*, 216–229. https://doi.org/10.1016/j.ecolind.2016.10.024

Burnham, K. P. (1998). Model selection and multimodel inference. *A Practical Information-Theoretic Approach*.

Butler, M. J., Metzger, K. L., & Harris, G. M. (2017). Are whooping cranes destined for extinction? Climate change imperils recruitment and population growth. *Ecology and Evolution*, *7*(8), 2821–2834.

Button, D. J. (2017). Mass extinctions drove increased global faunal cosmopolitanism on the supercontinent Pangaea. *NATURE COMMUNICATIONS*, 8. https://doi.org/10.1038/s41467-017-00827-7

Cahill, A. E., Aiello-Lammens, M. E., Fisher-Reid, M. C., Hua, X., Karanewsky, C. J., Yeong

Ryu, H., Sbeglia, G. C., Spagnolo, F., Waldron, J. B., & Warsi, O. (2013). How does climate change cause extinction? *Proceedings of the Royal Society B: Biological Sciences*, *280*(1750), 20121890.

Calosi, P., Putnam, H. M., Twitchett, R. J., & Vermandele, F. (2019). Marine metazoan modern mass extinction: Improving predictions by integrating fossil, modern, and physiological data. *Annual Review of Marine Science*, *11*, 369–390.

Carlson, S. M., Cunningham, C. J., & Westley, P. A. (2014). Evolutionary rescue in a changing world. *Trends in Ecology & Evolution*, *29*(9), 521–530.

Chapin, F. S., & Starfield, A. M. (1997). Time lags and novel ecosystems in response to transient climatic change in arctic Alaska. *Climatic Change*, *35*(4), 449–461.

Chase, J. M. (2003). Community assembly: When should history matter? *Oecologia*, *136*(4), 489–498.

Chave, J. (2013). The problem of pattern and scale in ecology: What have we learned in 20 years? *Ecology Letters*, *16*, 4–16.

Chen, I.-C., Hill, J. K., Ohlemüller, R., Roy, D. B., & Thomas, C. D. (2011). Rapid range shifts of species associated with high levels of climate warming. *Science*, *333*(6045), 1024–1026.

Coops, N. C., Jassal, R. S., Leuning, R., Black, A. T., & Morgenstern, K. (2007). Incorporation of a soil water modifier into MODIS predictions of temperate Douglas-fir gross primary productivity: Initial model development. *Agricultural and Forest Meteorology*, *147*(3–4), 99–109.

Couvreur, T. L., Kissling, W. D., Condamine, F. L., Svenning, J.-C., Rowe, N. P., & Baker, W. J. (2015). Global diversification of a tropical plant growth form: Environmental correlates and historical contingencies in climbing palms. *Frontiers in Genetics*, *5*, 452.

Coxall, H. K., & Pearson, P. N. (2007). The Eocene-Oligocene transition. *Deep Time Perspectives on Climate Change: Marrying the Signal from Computer Models and Biological Proxies*, 351–387.

Devictor, V., Van Swaay, C., Brereton, T., Brotons, L., Chamberlain, D., Heliölä, J., Herrando, S., Julliard, R., Kuussaari, M., & Lindström, Å. (2012). Differences in the climatic debts of birds and butterflies at a continental scale. *Nature Climate Change*, *2*(2), 121–124.

Dietl, G. P., & Flessa, K. W. (2011). Conservation paleobiology: Putting the dead to work. *Trends in Ecology & Evolution*, *26*(1), 30–37.

Dormann, C. F., Bobrowski, M., Dehling, D. M., Harris, D. J., Hartig, F., Lischke, H., Moretti, M. D., Pagel, J., Pinkert, S., & Schleuning, M. (2018). Biotic interactions in species distribution modelling: 10 questions to guide interpretation and avoid false conclusions. *Global Ecology and Biogeography*, *27*(9), 1004–1016.

Dullinger, S., Willner, W., Plutzar, C., Englisch, T., Schratt-Ehrendorfer, L., Moser, D., Ertl, S., Essl, F., & Niklfeld, H. (2012). Post-glacial migration lag restricts range filling of plants in the European Alps. *Global Ecology and Biogeography*, *21*(8), 829–840.

Fine, P. V., & Ree, R. H. (2006). Evidence for a time-integrated species-area effect on the latitudinal gradient in tree diversity. *The American Naturalist*, *168*(6), 796–804.

Finnegan, S., Anderson, S. C., Harnik, P. G., Simpson, C., Tittensor, D. P., Byrnes, J. E., Finkel, Z. V., Lindberg, D. R., Liow, L. H., & Lockwood, R. (2015). Paleontological baselines for evaluating extinction risk in the modern oceans. *Science*, *348*(6234), 567–570.

Foote, M., Crampton, J. S., Beu, A. G., & Cooper, R. A. (2008). On the bidirectional relationship between geographic range and taxonomic duration. *Paleobiology*, *34*(4), 421–433.

Foster, G. L., Hull, P., Lunt, D. J., & Zachos, J. C. (2018). Placing our current 'hyperthermal'in the context of rapid climate change in our geological past. *Philosophical Transactions of the Royal Society A: Mathematical, Physical and Engineering Sciences*, *376*(2130), 20170086.

Friedlingstein, P., Bopp, L., Ciais, P., Dufresne, J.-L., Fairhead, L., LeTreut, H., Monfray, P., & Orr, J. (2001). Positive feedback between future climate change and the carbon cycle.

Geophysical Research Letters, *28*(8), 1543–1546.

Fukami, T. (2015). Historical contingency in community assembly: Integrating niches, species pools, and priority effects. *Annual Review of Ecology, Evolution, and Systematics*, *46*, 1–23.

Fukami, T., & Nakajima, M. (2011). Community assembly: Alternative stable states or alternative transient states? *Ecology Letters*, *14*(10), 973–984.

García Molinos, J., Halpern, B. S., Schoeman, D. S., Brown, C. J., Kiessling, W., Moore, P. J., Pandolfi, J. M., Poloczanska, E. S., Richardson, A. J., & Burrows, M. T. (2016). Climate velocity and the future global redistribution of marine biodiversity. *Nature Climate Change*, *6*(1), 83–88. https://doi.org/10.1038/nclimate2769

García‐Valdés, R., Bugmann, H., & Morin, X. (2018). Climate change‐driven extinctions of tree species affect forest functioning more than random extinctions. *Diversity and Distributions*, *24*(7), 906–918.

Gavin, D. G., Fitzpatrick, M. C., Gugger, P. F., Heath, K. D., Rodríguez‐Sánchez, F., Dobrowski, S. Z., Hampe, A., Hu, F. S., Ashcroft, M. B., & Bartlein, P. J. (2014). Climate refugia: Joint inference from fossil records, species distribution models and phylogeography. *New Phytologist*, *204*(1), 37–54.

Giesecke, T., Brewer, S., Finsinger, W., Leydet, M., & Bradshaw, R. H. (2017). Patterns and dynamics of European vegetation change over the last 15,000 years. *Journal of Biogeography*, *44*(7), 1441–1456.

Gilman, S. E., Urban, M. C., Tewksbury, J., Gilchrist, G. W., & Holt, R. D. (2010). A framework for community interactions under climate change. *Trends in Ecology & Evolution*, *25*(6), 325–331. https://doi.org/10.1016/j.tree.2010.03.002

Graham, R. W., Lundelius Jr, E. L., Graham, M. A., Schroeder, E. K., Toomey III, R. S., Anderson, E., Barnosky, A. D., Burns, J. A., Churcher, C. S., & Grayson, D. K. (1996). Spatial response of mammals to late Quaternary environmental fluctuations. *Science*, *272*(5268), 1601–1606.

Greenstein, B. J., & Pandolfi, J. M. (2008). Escaping the heat: Range shifts of reef coral taxa in coastal Western Australia. *Global Change Biology*, *14*(3), 513–528.

Griebeler, E. M., & Gottschalk, E. (2000). The influence of temperature model assumptions on the prognosis accuracy of extinction risk. *Ecological Modelling*, *134*(2–3), 343–356.

Harnik, P. G. (2011). Direct and indirect effects of biological factors on extinction risk in fossil bivalves. *Proceedings of the National Academy of Sciences*, *108*(33), 13594–13599.

Harnik, P. G., Lotze, H. K., Anderson, S. C., Finkel, Z. V., Finnegan, S., Lindberg, D. R., Liow, L. H., Lockwood, R., McClain, C. R., & McGuire, J. L. (2012). Extinctions in ancient and modern seas. *Trends in Ecology & Evolution*, *27*(11), 608–617.

Harnik, P. G., Simpson, C., & Payne, J. L. (2012). Long-term differences in extinction risk among the seven forms of rarity. *Proceedings of the Royal Society B: Biological Sciences*, *279*(1749), 4969–4976.

Hastings, A. (2004). Transients: The key to long-term ecological understanding? *Trends in Ecology & Evolution*, *19*(1), 39–45.

Hawkins, B. A., Rueda, M., Rangel, T. F., Field, R., & Diniz‐Filho, J. A. F. (2014). Community phylogenetics at the biogeographical scale: Cold tolerance, niche conservatism and the structure of N orth A merican forests. *Journal of Biogeography*, *41*(1), 23–38.

Hofmann, G. E., & Todgham, A. E. (2010). Living in the now: Physiological mechanisms to tolerate a rapidly changing environment. *Annu Rev Physiol*, *72*(1), 127–145.

Holling, C. S. (1973). Resilience and stability of ecological systems. *Annual Review of Ecology and Systematics*, 1–23.

Hopkins, M. J., Simpson, C., & Kiessling, W. (2014). Differential niche dynamics among major marine invertebrate clades. *Ecology Letters*, *17*(3), 314–323. https://doi.org/10.1111/ele.12232

Hurlbert, S. H. (1984). Pseudoreplication and the design of ecological field experiments. *Ecological Monographs*, *54*(2), 187–211.

Imperio, S., Bionda, R., Viterbi, R., & Provenzale, A. (2013). Climate change and human disturbance can lead to local extinction of Alpine rock ptarmigan: New insight from the Western Italian Alps. *PloS One*, *8*(11), e81598.

IUCN. (2022). *The IUCN red list of threatened species*.

Jetz, W., & Fine, P. V. (2012). Global gradients in vertebrate diversity predicted by historical area-productivity dynamics and contemporary environment. *PLoS Biology*, *10*(3), e1001292.

Joachimski, M. M., Alekseev, A. S., Grigoryan, A., & Gatovsky, Y. A. (2020). Siberian Trap volcanism, global warming and the Permian-Triassic mass extinction: New insights from Armenian Permian-Triassic sections. *GSA Bulletin*, *132*(1–2), 427–443.

Johnson, L. L., Anulacion, B. F., Arkoosh, M. R., Burrows, D. G., da Silva, D. A., Dietrich, J. P., Myers, M. S., Spromberg, J., & Ylitalo, G. M. (2013). Effects of legacy persistent organic pollutants (POPs) in fish—Current and future challenges. *Fish Physiology*, *33*, 53–140.

Jump, A. S., & Peñuelas, J. (2005). Running to stand still: Adaptation and the response of plants to rapid climate change. *Ecology Letters*, *8*(9), 1010–1020. https://doi.org/10.1111/j.1461-0248.2005.00796.x

Keith, D. A., Mahony, M., Hines, H., Elith, J., Regan, T. J., Baumgartner, J. B., Hunter, D., Heard, G. W., Mitchell, N. J., & Parris, K. M. (2014). Detecting extinction risk from climate change by IUCN Red List criteria. *Conservation Biology*, *28*(3), 810–819.

Keppel, G., Van Niel, K. P., Wardell-Johnson, G. W., Yates, C. J., Byrne, M., Mucina, L., Schut, A. G., Hopper, S. D., & Franklin, S. E. (2012). Refugia: Identifying and understanding safe havens for biodiversity under climate change. *Global Ecology and Biogeography*, *21*(4), 393–404.

Kerr, J. T., Kharouba, H. M., & Currie, D. J. (2007). The macroecological contribution to global change solutions. *Science*, *316*(5831), 1581–1584.

Kiessling, W., Simpson, C., Beck, B., Mewis, H., & Pandolfi, J. M. (2012). Equatorial decline of reef corals during the last Pleistocene interglacial. *Proceedings of the National Academy of Sciences*, *109*(52), 21378–21383.

Kinzig, A. P., Ryan, P., Etienne, M., Allison, H., Elmqvist, T., & Walker, B. H. (2006). Resilience and regime shifts: Assessing cascading effects. *Ecology and Society*, *11*(1).

Knoll, A. H., Bambach, R. K., Payne, J. L., Pruss, S., & Fischer, W. W. (2007). Paleophysiology and end-Permian mass extinction. *Earth and Planetary Science Letters*, *256*(3–4), 295–313.

Kocsis, Á. T., Reddin, C. J., & Kiessling, W. (2018). The stability of coastal benthic biogeography over the last 10 million years: XXXX. *Global Ecology and Biogeography*, *27*(9), 1106–1120. https://doi.org/10.1111/geb.12771

Kuneš, P., Svobodová-Svitavská, H., Kolář, J., Hajnalová, M., Abraham, V., Macek, M., Tkáč, P., & Szabó, P. (2015). The origin of grasslands in the temperate forest zone of east-central Europe: Long-term legacy of climate and human impact. *Quaternary Science Reviews*, *116*, 15–27.

Kuussaari, M., Bommarco, R., Heikkinen, R. K., Helm, A., Krauss, J., Lindborg, R., Öckinger, E., Pärtel, M., Pino, J., & Rodà, F. (2009). Extinction debt: A challenge for biodiversity conservation. *Trends in Ecology & Evolution*, *24*(10), 564–571.

Lavergne, S., Evans, M. E., Burfield, I. J., Jiguet, F., & Thuiller, W. (2013). Are species' responses to global change predicted by past niche evolution? *Philosophical Transactions of the Royal Society B: Biological Sciences*, *368*(1610), 20120091.

Lawing, A. M., & Matzke, N. J. (2014). Conservation paleobiology needs phylogenetic methods. *Ecography*, *37*(11), 1109–1122.

Lenihan, J. M., Drapek, R., Bachelet, D., & Neilson, R. P. (2003). Climate change effects on vegetation distribution, carbon, and fire in California. *Ecological Applications*, *13*(6), 1667–1681.

Leuning, R., Cleugh, H. A., Zegelin, S. J., & Hughes, D. (2005). Carbon and water fluxes over a temperate Eucalyptus forest and a tropical wet/dry savanna in Australia: Measurements and comparison with MODIS remote sensing estimates. *Agricultural and Forest Meteorology*, *129*(3–4), 151–173.

Li, X., Jousset, A., de Boer, W., Carrión, V. J., Zhang, T., Wang, X., & Kuramae, E. E. (2019). Legacy of land use history determines reprogramming of plant physiology by soil microbiome. *The ISME Journal*, *13*(3), 738–751.

Lieberman, B. S., & Saupe, E. E. (2016). Palaeoniches get stitches: Analyses of niches informing macroevolutionary theory. *Lethaia*, *49*(2), 145–149.

Lipsey, M. W., & Wilson, D. B. (2001). *Practical meta-analysis*. Sage Publications.

Lord, J. P., Barry, J. P., & Graves, D. (2017). Impact of climate change on direct and indirect species interactions. *Marine Ecology Progress Series*, *571*, 1–11.

Lunney, D., Stalenberg, E., Santika, T., & Rhodes, J. R. (2014). Extinction in Eden: Identifying the role of climate change in the decline of the koala in south-eastern NSW. *Wildlife Research*, *41*(1), 22–34.

Martin-Garin, B., Lathuilière, B., & Geister, J. (2012). The shifting biogeography of reef corals during the Oxfordian (Late Jurassic). A climatic control? *Palaeogeography, Palaeoclimatology, Palaeoecology*, *365*, 136–153.

Masson-Delmotte, V., Zhai, P., Pirani, A., Connors, S. L., Péan, C., Berger, S., Caud, N., Chen, Y., Goldfarb, L., & Gomis, M. I. (2021). Climate change 2021: The physical science basis. *Contribution of Working Group I to the Sixth Assessment Report of the Intergovernmental Panel on Climate Change*, 2.

Mathes, G. H., Kiessling, W., & Steinbauer, M. J. (2021). Deep-time climate legacies affect origination rates of marine genera. *Proceedings of the National Academy of Sciences*, *118*(36), e2105769118. https://doi.org/10.1073/pnas.2105769118

Mathes, G. H., van Dijk, J., Kiessling, W., & Steinbauer, M. J. (2021). Extinction risk controlled by interaction of long-term and short-term climate change. *Nature Ecology & Evolution*, *5*(3), 304–310. https://doi.org/10.1038/s41559-020-01377-w

Mayhew, P. J., Jenkins, G. B., & Benton, T. G. (2008). A long-term association between global temperature and biodiversity, origination and extinction in the fossil record. *Proceedings of the Royal Society B: Biological Sciences*, *275*(1630), 47–53. https://doi.org/10.1098/rspb.2007.1302

Mayr, E. (1963). Animal species and evolution. *Animal Species and Evolution.*

McElreath, R. (2020). *Statistical Rethinking, 2nd Edition*. https://learning.oreilly.com/library/view/-/9780429639142/?ar

McKinney, M. L. (1997). Extinction vulnerability and selectivity: Combining ecological and paleontological views. *Annual Review of Ecology and Systematics*, 495–516.

Menéndez, R., Megías, A. G., Hill, J. K., Braschler, B., Willis, S. G., Collingham, Y., Fox, R., Roy, D. B., & Thomas, C. D. (2006). Species richness changes lag behind climate change. *Proceedings of the Royal Society B: Biological Sciences*, *273*(1593), 1465–1470. https://doi.org/10.1098/rspb.2006.3484

Merilä, J. (2012). Evolution in response to climate change: In pursuit of the missing evidence. *BioEssays*, *34*(9), 811–818.

Miller, E. T., Zanne, A. E., & Ricklefs, R. E. (2013). Niche conservatism constrains Australian honeyeater assemblages in stressful environments. *Ecology Letters*, *16*(9), 1186–1194.

Mittelbach, G. G., Schemske, D. W., Cornell, H. V., Allen, A. P., Brown, J. M., Bush, M. B., Harrison, S. P., Hurlbert, A. H., Knowlton, N., & Lessios, H. A. (2007). Evolution and the latitudinal diversity gradient: Speciation, extinction and biogeography. *Ecology Letters*, *10*(4), 315–331.

Munday, P. L., Warner, R. R., Monro, K., Pandolfi, J. M., & Marshall, D. J. (2013). Predicting evolutionary responses to climate change in the sea. *Ecology Letters*, *16*(12), 1488–1500.

Murphy, G. E., Romanuk, T. N., & Worm, B. (2020). Cascading effects of climate change on plankton community structure. *Ecology and Evolution*, *10*(4), 2170–2181.

Normand, S., Randin, C., Ohlemüller, R., Bay, C., Høye, T. T., Kjær, E. D., Körner, C., Lischke, H., Maiorano, L., Paulsen, J., Pearman, P. B., Psomas, A., Treier, U. A., Zimmermann, N. E., & Svenning, J.-C. (2013). A greener Greenland? Climatic potential and long-term constraints on future expansions of trees and shrubs. *Philosophical Transactions of the Royal Society B: Biological Sciences*, *368*(1624), 20120479. https://doi.org/10.1098/rstb.2012.0479

Normand, S., Ricklefs, R. E., Skov, F., Bladt, J., Tackenberg, O., & Svenning, J.-C. (2011). Postglacial migration supplements climate in determining plant species ranges in Europe. *Proceedings of the Royal Society B: Biological Sciences*, *278*(1725), 3644–3653.

Ogle, K., Barber, J. J., Barron‐Gafford, G. A., Bentley, L. P., Young, J. M., Huxman, T. E., Loik, M. E., & Tissue, D. T. (2015). Quantifying ecological memory in plant and ecosystem processes. *Ecology Letters*, *18*(3), 221–235. https://doi.org/10.1111/ele.12399

Parmesan, C. (2006). Ecological and evolutionary responses to recent climate change. *Annual Review of Ecology, Evolution, and Systematics*, 637–669.

Payne, J. L., & Clapham, M. E. (2012). End-Permian mass extinction in the oceans: An ancient analog for the twenty-first century? *Annual Review of Earth and Planetary Sciences*, *40*(89), 2012.

Payne, J. L., Truebe, S., Nützel, A., & Chang, E. T. (2011). Local and global abundance associated with extinction risk in late Paleozoic and early Mesozoic gastropods. *Paleobiology*, *37*(4), 616–632.

Pecl, G. T., Araújo, M. B., Bell, J. D., Blanchard, J., Bonebrake, T. C., Chen, I.-C., Clark, T. D., Colwell, R. K., Danielsen, F., & Evengård, B. (2017). Biodiversity redistribution under climate change: Impacts on ecosystems and human well-being. *Science*, *355*(6332), eaai9214.

Penn, J. L., Deutsch, C., Payne, J. L., & Sperling, E. A. (2018). Temperature-dependent hypoxia explains biogeography and severity of end-Permian marine mass extinction. *Science*, *362*(6419), eaat1327.

Peters, S. E. (2005). Geologic constraints on the macroevolutionary history of marine animals. *Proceedings of the National Academy of Sciences*, *102*(35), 12326–12331. https://doi.org/10.1073/pnas.0502616102

Peterson, A. T. (2011). Ecological niche conservatism: A time‐structured review of evidence. *Journal of Biogeography*, *38*(5), 817–827.

Petryshyn, V. A., Greene, S. E., Farnsworth, A., Lunt, D. J., Kelley, A., Gammariello, R., Ibarra, Y., Bottjer, D. J., Tripati, A., & Corsetti, F. A. (2020). The role of temperature in the initiation of the end-Triassic mass extinction. *Earth-Science Reviews*, *208*, 103266.

Pinsky, M. L., Worm, B., Fogarty, M. J., Sarmiento, J. L., & Levin, S. A. (2013). Marine taxa track local climate velocities. *Science*, *341*(6151), 1239–1242.

Poloczanska, E. S., Brown, C. J., Sydeman, W. J., Kiessling, W., Schoeman, D. S., Moore, P. J., Brander, K., Bruno, J. F., Buckley, L. B., & Burrows, M. T. (2013). Global imprint of climate change on marine life. *Nature Climate Change*, *3*(10), 919–925.

Pomara, L. Y., LeDee, O. E., Martin, K. J., & Zuckerberg, B. (2014). Demographic consequences of climate change and land cover help explain a history of extirpations and range contraction in a declining snake species. *Global Change Biology*, *20*(7), 2087–2099.

Pörtner, H. O., Roberts, D. C., Adams, H., Adler, C., Aldunce, P., Ali, E., Begum, R. A., Betts, R., Kerr, R. B., & Biesbroek, R. (2022). *Climate change 2022: Impacts, adaptation and vulnerability*.

R Core Team. (2021). *R: A Language and Environment for Statistical Computing* (4.1.2) [R]. R Foundation for Statistical Computing. https://www.R-project.org/

Raup, D. M. (1979). Size of the Permo-Triassic Bottleneck and Its Evolutionary Implications. *Science*, *206*(4415), 217–218. https://doi.org/10.1126/science.206.4415.217

Reddin, C. J., Aberhan, M., Raja, N. B., & Kocsis, Á. T. (2022). Global warming generates predictable extinctions of warm- and cold-water marine benthic invertebrates via thermal habitat loss. *Global Change Biology*, gcb.16333. https://doi.org/10.1111/gcb.16333

Reddin, C. J., Kocsis, Á. T., & Kiessling, W. (2018). Marine invertebrate migrations trace climate change over 450 million years. *Global Ecology and Biogeography*, *27*(6), 704–713. https://doi.org/10.1111/geb.12732

Reddin, C. J., Nätscher, P. S., Kocsis, Á. T., Pörtner, H.-O., & Kiessling, W. (2020). Marine clade sensitivities to climate change conform across timescales. *Nature Climate Change*, *10*(3), 249–253. https://doi.org/10.1038/s41558-020-0690-7

Reichmann, L. G., Sala, O. E., & Peters, D. P. (2013). Precipitation legacies in desert grassland primary production occur through previous-year tiller density. *Ecology*, *94*(2), 435–443.

Ren, D., & Leslie, L. M. (2011). Three positive feedback mechanisms for ice-sheet melting in a warming climate. *Journal of Glaciology*, *57*(206), 1057–1066.

Riquelme, C., Estay, S. A., Contreras, R., & Corti, P. (2020). Extinction risk assessment of a Patagonian ungulate using population dynamics models under climate change scenarios. *International Journal of Biometeorology*, *64*(11), 1847–1855.

Rocha, J., Yletyinen, J., Biggs, R., Blenckner, T., & Peterson, G. (2015). Marine regime shifts: Drivers and impacts on ecosystems services. *Philosophical Transactions of the Royal Society B: Biological Sciences*, *370*(1659), 20130273.

Rosenzweig, M. L. (1995). *Species diversity in space and time*. Cambridge University Press.

Sala, O. E., Gherardi, L. A., Reichmann, L., Jobbagy, E., & Peters, D. (2012). Legacies of precipitation fluctuations on primary production: Theory and data synthesis. *Philosophical Transactions of the Royal Society B: Biological Sciences*, *367*(1606), 3135–3144.

Saltré, F., Rodríguez-Rey, M., Brook, B. W., Johnson, C. N., Turney, C. S., Alroy, J., Cooper, A., Beeton, N., Bird, M. I., & Fordham, D. A. (2016). Climate change not to blame for late Quaternary megafauna extinctions in Australia. *Nature Communications*, *7*(1), 1–7.

Sawilowsky, S. S. (2009). New effect size rules of thumb. *Journal of Modern Applied Statistical Methods*, *8*(2), 26.

Sax, D. F., Early, R., & Bellemare, J. (2013). Niche syndromes, species extinction risks, and management under climate change. *Trends in Ecology & Evolution*, *28*(9), 517–523.

Schueth, J. D., Bralower, T. J., Jiang, S., & Patzkowsky, M. E. (2015). The role of regional survivor incumbency in the evolutionary recovery of calcareous nannoplankton from the Cretaceous/Paleogene (K/Pg) mass extinction. *Paleobiology*, *41*(4), 661–679.

Sepkoski, J. J. (1981). A factor analytic description of the Phanerozoic marine fossil record. *Paleobiology*, 7(1), 36–53.

Sinervo, B., Miles, D. B., Wu, Y., MÉNDEZ-DE LA CRUZ, F. R., Kirchhof, S., & Qi, Y. (2018). Climate change, thermal niches, extinction risk and maternal-effect rescue of toad-headed lizards, Phrynocephalus, in thermal extremes of the Arabian Peninsula to the Qinghai—Tibetan Plateau. *Integrative Zoology*, *13*(4), 450–470.

Solé, R., & Levin, S. (2022). Ecological complexity and the biosphere: The next 30 years. In *Philosophical Transactions of the Royal Society B* (Vol. 377, Issue 1857, p. 20210376). The Royal Society.

Somero, G. N. (2012). The physiology of global change: Linking patterns to mechanisms.

Annual Review of Marine Science, *4*, 39–61.

Song, H., Kemp, D. B., Tian, L., Chu, D., Song, H., & Dai, X. (2021). Thresholds of temperature change for mass extinctions. *Nature Communications*, *12*(1), 1–8.

Souther, S., & McGraw, J. B. (2014). Synergistic effects of climate change and harvest on extinction risk of American ginseng. *Ecological Applications*, *24*(6), 1463–1477.

Stanley, S. M. (2016). Estimates of the magnitudes of major marine mass extinctions in earth history. *Proceedings of the National Academy of Sciences*, *113*(42), E6325–E6334.

Steinbauer, M. (2013). *The Effect of Spatial and Environmental Drivers on Patterns in Species Richness and Composition*. Universität Bayreuth, Fakultät für Biologie, Chemie und Geowissenschaften.

Stephens, L., Fuller, D., Boivin, N., Rick, T., Gauthier, N., Kay, A., Marwick, B., Armstrong, C. G., Barton, C. M., Denham, T., Douglass, K., Driver, J., Janz, L., Roberts, P., Rogers, J. D., Thakar, H., Altaweel, M., Johnson, A. L., Sampietro Vattuone, M. M., … Ellis, E. (2019). Archaeological assessment reveals Earth's early transformation through land use. *Science*, *365*(6456), 897–902. https://doi.org/10.1126/science.aax1192

Stigall, A. L. (2013). Analysing links between biogeography, niche stability and speciation: The impact of complex feedbacks on macroevolutionary patterns: Biotic and environmental impacts on speciation. *Palaeontology*, *56*(6), 1225–1238. https://doi.org/10.1111/pala.12003

Stigall, A. L. (2014). When and how do species achieve niche stability over long time scales? *Ecography*, *37*(11), 1123–1132. https://doi.org/10.1111/ecog.00719

Sugihara, G., May, R., Ye, H., Hsieh, C., Deyle, E., Fogarty, M., & Munch, S. (2012). Detecting causality in complex ecosystems. *Science*, *338*(6106), 496–500.

Sun, Y., Joachimski, M. M., Wignall, P. B., Yan, C., Chen, Y., Jiang, H., Wang, L., & Lai, X. (2012). Lethally hot temperatures during the Early Triassic greenhouse. *Science*, *338*(6105), 366–370.

Sunday, J. M., Bates, A. E., & Dulvy, N. K. (2012). Thermal tolerance and the global redistribution of animals. *Nature Climate Change*, *2*(9), 686–690. https://doi.org/10.1038/nclimate1539

Svenning, J.-C., Eiserhardt, W. L., Normand, S., Ordonez, A., & Sandel, B. (2015). The influence of paleoclimate on present-day patterns in biodiversity and ecosystems. *Annual Review of Ecology, Evolution, and Systematics*, *46*(1), 551–572. https://doi.org/10.1146/annurev-ecolsys-112414-054314

Svenning, J.-C., & Sandel, B. (2013). Disequilibrium vegetation dynamics under future climate change. *American Journal of Botany*, *100*(7), 1266–1286.

Svenning, J.-C., & Skov, F. (2004). Limited filling of the potential range in European tree species. *Ecology Letters*, *7*(7), 565–573.

Templeton, A. R. (2008). The reality and importance of founder speciation in evolution. *BioEssays*, *30*(5), 470–479. https://doi.org/10.1002/bies.20745

Thackeray, S. J., Sparks, T. H., Frederiksen, M., Burthe, S., Bacon, P. J., Bell, J. R., Botham, M. S., Brereton, T. M., Bright, P. W., & Carvalho, L. (2010). Trophic level asynchrony in rates of phenological change for marine, freshwater and terrestrial environments. *Global Change Biology*, *16*(12), 3304–3313.

Tzedakis, P. C., Lawson, I. T., Frogley, M. R., Hewitt, G. M., & Preece, R. C. (2002). Buffered tree population changes in a Quaternary refugium: Evolutionary implications. *Science*, *297*(5589), 2044–2047.

Urban, M. C. (2015). Accelerating extinction risk from climate change. *Science*, *348*(6234), 571–573. https://doi.org/10.1126/science.aaa4984

Urban, M. C., Tewksbury, J. J., & Sheldon, K. S. (2012). On a collision course: Competition and dispersal differences create no-analogue communities and cause extinctions during climate change. *Proceedings of the Royal Society B: Biological Sciences*, *279*(1735), 2072–2080.

Varela, S., Lima‐Ribeiro, M. S., Diniz‐Filho, J. A. F., & Storch, D. (2015). Differential effects of temperature change and human impact on European Late Quaternary mammalian extinctions. *Global Change Biology*, *21*(4), 1475–1481.

Vehtari, A., Gelman, A., & Gabry, J. (2017). Practical Bayesian model evaluation using leave-one-out cross-validation and WAIC. *Statistics and Computing*, *27*(5), 1413–1432. https://doi.org/10.1007/s11222-016-9696-4

Wahl, L. M., Gerrish, P. J., & Saika-Voivod, I. (2002). Evaluating the Impact of Population Bottlenecks in Experimental Evolution. *Genetics Society of America*, *162*, 12.

Walther, G.-R., Post, E., Convey, P., Menzel, A., Parmesan, C., Beebee, T. J., Fromentin, J.-M., Hoegh-Guldberg, O., & Bairlein, F. (2002). Ecological responses to recent climate change. *Nature*, *416*(6879), 389–395.

Warren, R., VanDerWal, J., Price, J., Welbergen, J. A., Atkinson, I., Ramirez-Villegas, J., Osborn, T. J., Jarvis, A., Shoo, L. P., Williams, S. E., & Lowe, J. (2013). Quantifying the benefit of early climate change mitigation in avoiding biodiversity loss. *Nature Climate Change*, *3*(7), 678–682. https://doi.org/10.1038/nclimate1887

Wickham, H., Averick, M., Bryan, J., Chang, W., McGowan, L. D., François, R., Grolemund, G., Hayes, A., Henry, L., & Hester, J. (2019). Welcome to the Tidyverse. *Journal of Open Source Software*, *4*(43), 1686.

Wiens, J. J., Camacho, A., Goldberg, A., Jezkova, T., Kaplan, M. E., Lambert, S. M., Miller, E. C., Streicher, J. W., & Walls, R. L. (2019). Climate change, extinction, and Sky Island biogeography in a montane lizard. *Molecular Ecology*, *28*(10), 2610–2624.

Wiens, J. J., & Donoghue, M. J. (2004). Historical biogeography, ecology and species richness. *Trends in Ecology & Evolution*, *19*(12), 639–644.

Wiens, J. J., & Graham, C. H. (2005). Niche conservatism: Integrating evolution, ecology, and conservation biology. *Annual Review of Ecology, Evolution, and Systematics*, *36*(1), 519–539. https://doi.org/10.1146/annurev.ecolsys.36.102803.095431

Williams, J. W., Shuman, B. N., Webb III, T., Bartlein, P. J., & Leduc, P. L. (2004). Late‐Quaternary vegetation dynamics in North America: Scaling from taxa to biomes. *Ecological Monographs*, *74*(2), 309–334.

Wright, I. J., Reich, P. B., Cornelissen, J. H., Falster, D. S., Groom, P. K., Hikosaka, K., Lee, W., Lusk, C. H., Niinemets, Ü., & Oleksyn, J. (2005). Modulation of leaf economic traits and trait relationships by climate. *Global Ecology and Biogeography*, *14*(5), 411–421.

Xenopoulos, M. A., Lodge, D. M., Alcamo, J., Märker, M., Schulze, K., & Van Vuuren, D. P. (2005). Scenarios of freshwater fish extinctions from climate change and water withdrawal. *Global Change Biology*, *11*(10), 1557–1564.

Yalcin, S., & Leroux, S. J. (2018). An empirical test of the relative and combined effects of land‐cover and climate change on local colonization and extinction. *Global Change Biology*, *24*(8), 3849–3861.

Zhang, L., Wang, C., Wignall, P. B., Kluge, T., Wan, X., Wang, Q., & Gao, Y. (2018). Deccan volcanism caused coupled pCO2 and terrestrial temperature rises, and pre-impact extinctions in northern China. *Geology*, *46*(3), 271–274.

10. Statutory declarations

(§ 8 Satz 2 Nr. 3 PromO Fakultät)

Hiermit versichere ich eidesstattlich, dass ich die Arbeit selbstständig verfasst und keine anderen als die von mir angegebenen Quellen und Hilfsmittel benutzt habe (vgl. Art. 64 Abs. 1 Satz 6 BayHSchG).

(§ 8 Satz 2 Nr. 3 PromO Fakultät)

Hiermit erkläre ich, dass ich die Dissertation nicht bereits zur Erlangung eines akademischen Grades eingereicht habe und dass ich nicht bereits diese oder eine gleichartige Doktorprüfung endgültig nicht bestanden habe.

(§ 8 Satz 2 Nr. 4 PromO Fakultät)

Hiermit erkläre ich, dass ich Hilfe von gewerblichen Promotionsberatern bzw. –vermittlern oder ähnlichen Dienstleistern weder bisher in Anspruch genommen habe noch künftig in Anspruch nehmen werde.

(§ 8 Satz 2 Nr. 7 PromO Fakultät)

Hiermit erkläre ich mein Einverständnis, dass die elektronische Fassung der Dissertation unter Wahrung meiner Urheberrechte und des Datenschutzes einer gesonderten Überprüfung unterzogen werden kann.

(§ 8 Satz 2 Nr. 8 PromO Fakultät)

Hiermit erkläre ich mein Einverständnis, dass bei Verdacht wissenschaftlichen Fehlverhaltens Ermittlungen durch universitätsinterne Organe der wissenschaftlichen Selbstkontrolle stattfinden können.

Bayreuth, 05.06.2023,

……………………………………………………………………………………….

Ort, Datum, Unterschrift